Lappeenrannan teknillinen yliopisto
Lappeenranta University of Technology

Mohammad Ahmed

SLIDING MODE CONTROL FOR SWITCHED MODE POWER SUPPLIES

Thesis for the degree of Doctor of Science (Technology) to be presented with due permission for public examination and criticism in the auditorium 1382 at Lappeenranta University of Technology, Lappeenranta, Finland on the 14th of December 2004, at noon.

Acta Universitatis
Lappeenrantaensis
196

Supervisor Professor Pertti Silventoinen
Department of Electrical Engineering
Lappeenranta University of Technology
Finland

Reviewers Professor Tore Undeland
Department of Electrical Power Engineering
Norwegian University of Science and Technology
Trondheim, Norway

D.Sc. Jukka Kaukonen
ABB Oy
Electrical Machines Automation Technology
Helsinki, Finland

Opponent Professor Tore Undeland
Department of Electrical Power Engineering
Norwegian University of Science and Technology
Trondheim, Norway

ISBN 951-764-979-7
ISBN 951-764-980-0 (PDF)
ISSN 1456-4491

Lappeenrannan teknillinen yliopisto
Digipaino 2004

Abstract

Mohammad Ahmed

SLIDING MODE CONTROL FOR SWITCHED MODE POWER SUPPLIES

Lappeenranta 2004

97 p.

Acta Universitatis Lappeenrantaensis 196

Diss. Lappeenranta University of Technology

ISBN 951-764-979-7, ISBN 951-764-980-0 (PDF), ISSN 1456-4491

Control applications of switched mode power supplies have been widely investigated. The main objective of research and development (R&D) in this field is always to find the most suitable control method to be implemented in various DC/DC converter topologies. In other words, the goal is to select a control method capable of improving the efficiency of the converter, reducing the effect of disturbances (line and load variation), lessening the effect of EMI (electro magnetic interference), and being less effected by component variation.

The main objective of this research work is to study different control methods implemented in switched mode power supplies namely (PID control, hysteresis control, adaptive control, current programmed control, variable structure control (VSC), and sliding mode control (SMC). The advantages and drawbacks of each control method are given.

Two control methods, the PID and the SMC are selected and their effects on DC/DC (Buck, Boost, and Buck-Boost) converters are examined. Matlab/Simulink™ is used to implement PID control method in DC/DC Buck converter and SMC in DC/DC (Buck, and Buck Boost) converters. For the prototype, operational amplifiers (op-amps) are used to implement PID control in DC/DC Buck converter. For SMC op-amps are implemented in DC/DC Buck converter and dSPACE™ is used to control the DC/DC Buck-Boost converter. The SMC can be applied to the DC/DC (Buck, Boost, and Buck-Boost) converters.

A comparison of the effects of the PID control and the SMC on the DC/DC Buck converter response in steady state, under line variations, load variations, and different component variations is performed. Also the Conducted RF-Emissions between the PID and SMC DC/DC Buck Converter are compared.

The thesis shows that, in comparison with the PID control, the SMC provides better steady-state response, better dynamic response, less EMI, inherent order reduction, robustness against system uncertainty disturbances, and an implicit stability proof.

Giving a better steady-state and dynamic response, the SMC is implemented in a DC/DC resonant converter. The half-wave zero current switching (HWZCS) DC/DC Buck converter is selected as a converter topology. A general guideline to select the tank component values, needed for the designing of a HWZCS DC/DC Buck, is obtained.

The implementation of the SMC to a HWZCS DC/DC Buck converter is analysed. The converter response is investigated in the steady-state region and in the dynamic region.

Keywords: DC/DC power conversion, variable structure system, resonant power conversion.

UDC 621.314.1 : 621.311.6 : 681.515.8

Acknowledgements

This research work has been carried out between January 2002 and December 2004 in the Department of Electrical Engineering of Lappeenranta University of Technology. Many people have helped me in the realization of this work and I would like to take this opportunity to express my gratitude to all of them.

I am deeply grateful to my supervisor professor Pertti Silventoinen for his support and guidance. I also express my sincere thanks to professor Juha Pyrhönen for giving me the opportunity to go further in my academic studies and professor Olli Pyrhönen for broadening my knowledge about Sliding Mode Control.

I wish to express my gratitude to official pre-examiners of the work D.Sc. Jukka Kaukonen from ABB Finland and professor Tore Undeland from the Norwegian University of Science and Technology for their valuable corrections and comments.

I would like to thank my colleague D.Sc. Mikko Kuisma for fruitful technical discussions that improved the publications related to this research work. I also would like to acknowledge D.Sc. Janne Nerg for his valuable advises. Many thanks to Lic.Tech. Kimmo Tolsa for building up the prototypes and helping with the measurements.

I am grateful to M.Sc. Pia Salminen for coordinating part of my theoretical studies. Many thanks to Piipa Virkki for organizing my participation in international conferences.

Financial support of the Department of Electrical Engineering at Lappeenranta University of Technology, Nokia Foundation, rector of Lappeenranta University of Technology (LTY) professor Markku Lukka, the Research Foundation of Lappeenranta University of Technology and NorFA is gratefully appreciated.

I am obliged to Mrs. Julia Vauterin for language revision.

Special thanks to my family and friends for supporting and encouraging me during the research and writing of the thesis.

This work is dedicated to the memory of my father Abdullah Ahmed.

Lappeenranta, December 2004

Mohammad Ahmed

Content

Abstract
Acknowledgements
List of Symbols and Abbreviations 7
Acronyms 9
List of Publications 11
1. INTRODUCTION 13
1.1 Objective of the Research Work 13
2. DC/DC POWER SUPPLIES 16
2.1 Introduction 16
2.2 Linear Power Supply 16
2.3 Switched Mode Power Supply 18
2.4 Switched-Mode Power Supply Topologies 19
2.4.1 Non-isolated Topologies 19
2.4.2 Isolated Topologies 20
2.4.3 Multiple Switch Topologies 21
2.5. DC/DC Resonant Converters 22
2.5.1 DC/DC Resonant Converter Topologies 22
2.6 Continuous Conduction Mode and Discontinuous Conduction Mode 23
2.7 Switched-Mode Topology Applications and Classifications 26
2.8 Summary 28
3. CONTROL METHODS 29
3.1 Introduction 29
3.2 Stability of Linear and Nonlinear Control Systems 29
3.3 Control Methods 31
3.4 PID Control 32
3.5 Hysteresis Control 34
3.6 Adaptive Control 37
3.6.1 Model-Reference Adaptive Control Method 38
3.6.2 Self-Tuning Controller 39
3.7 Current Programmed Control 40
3.8 Variable Structure Control System (VSCS) 43
3.9 Sliding Mode Control (SMC) 45
3.9.1 Principle of Sliding Mode Control 45
3.10 Summary 47
4. SLIDING MODE CONTROL 49
4.1 Introduction 49
4.2 Sliding Mode Control Researches and Applications in Electrical and Mechanical Systems 51
4.3 Review of the Theory of Sliding Mode Control 52
4.3.1 Existence Condition 52
4.3.2 Reaching Condition 53
4.3.3 System Description in Sliding Mode 53
4.3.4 Chattering 54
4.4 Sliding Mode Control for DC/DC Converters 55
4.4.1 Phase plane Description of SMC for DC/DC Buck Converter 56
4.4.2 Existence Condition of SMC for DC/DC Buck Converter 58
4.5 Sliding Mode Control Researches and Applications in DC/DC Converters 60
4.6 Summary 63

5. RESEARCH WORK 64
5.1 Summary of the Research Work 64
5.2 Summary of the Publications 66
5.2.1 Publication P [1] 66
5.2.2 Publication P [2] 66
5.2.3 Publication P [3] 68
5.2.4 Publication P [4] 68
5.2.5 Publication P [5] 68
5.2.6 Publication P [6] 69
5.2.7 Publication P [7] 69
5.2.8 Publication P [8] 69
5.2.9 Publication P [9] 70
6. CONCLUSIONS AND FUTURE WORKS 71
6.1 Conclusions 71
6.2 Suggestions for Future Researches 72
REFERENCES 74
APPENDICES 82

List of Symbols and Abbreviations

C	Capacitance
c	Constant of integration and is positive
C_d	Tank capacitance in parallel with the diode
C_r	Tank capacitance
C_t	Tank capacitance in parallel with the switch
D	Average duty cycle
$d(t)$	Duty cycle
$\hat{d}(t)$	Duty cycle variation
$\boldsymbol{f}$	Function vector with n dimension
$\boldsymbol{f}^+$	State velocity vector
$\boldsymbol{f}^-$	State velocity vector
f_c	Crossover frequency
f_L	Inverted zero frequency of the integral control
f_P	Pole frequency of the derivative control
f_o	Tank resonant frequency
$f_{s(max)}$	Maximum switching frequency
f_s	Switching frequency
$f_{s(nominal)}$	Nominal switching frequency
f_z	Zero frequency of the derivative control
$\boldsymbol{G}$	One by *n* matrix whose element are the derivative of the sliding surface
G_c	PID compensator gain
$G_c(s)$	Transfer function PID compensator
$G_{c1}(s)$	Transfer function of the derivative compensator
$G_{c2}(s)$	Transfer function of the integral compensator
$G_{vd}(s)$	Control to output transfer function
$G_{vg}(s)$	Line to output transfer function
H	Hysteresis width
$\boldsymbol{I}$	Identity matrix
I^*	Current Reference signal
$I_a(t)$	Artificial ramp waveform
I_b	Base current
I_c	Collector current
$i_c(t)$	Actual capacitor current
$i_{control}(t)$	Actual compensator current
I_{in}	Average input current
$i_{in}(t)$	Actual input current
$i_L(t)$	Actual inductor current
i_{L0}	Minimum inductor current
I_{load}	Average load current
i_n	Discrete inductor current
I_o	Average output current
$i_o(t)$	Actual output current
$i_s(t)$	Actual switch current
k	Positive scalar
K_D	Derivative gain

K_I	Integral gain
L	Inductance
$L_{critical}$	Critical Inductance
L_d	Tank inductance in series with the diode
L_m	Magnetizing inductance
L_r	Tank inductance
L_t	Tank inductance in series with the switch
m_1	Inductor current waveform when the switch is on
m_2	Inductor current waveform when the switch is off
N	Component of the state velocity vector
N_1	Number of turns in the primary side of a transformer
N_2	Number of turns in the secondary side of a transformer
n	Number of switching periods
P_{in}	Average input power
$P_{in(max)}$	Maximum output power
$P_{in(min)}$	Minimum input power
P_{loss}	Power loss
P_o	Average output power
$P_{o\,(max)}$	Maximum output power
$P_{o\,(min)}$	Minimum output power
Q	Quality factor
Q	Symbol for BJT transistor
R_c	Collector resistor
R_f	Scale multiplied by the compensator signal and the switching signal
R_L	Load resistor
$s(y,\dot{y})$	Switching function
$S_i(\boldsymbol{x},t)$	Individual switching surface
1/S	Integrator
t	Time
T_s	Average switching time
T_{uo}	DC gain of a unity closed loop system for a DC/DC converter
U	Past plant input
u	Discontinuous input control
u_{eq}	Equivalent control
$u(t)$	Control signal
V_c	Average capacitor voltage
$v_c(t)$	Actual capacitor voltage
V_{contol}	Control voltage
V_{in}	Average DC input current
$V_{in\,(min)}$	Minimum DC input voltage
$V_{o\,(max)}$	Maximum DC input voltage
$v_{in}(t)$	Actual input voltage
$\hat{v}_{in}(t)$	Small signal variation of the input voltage
V_L	Average inductor voltage
$v_L(t)$	Actual inductor voltage
V_n	Discrete output voltage
V_o	Average output voltage
$v_o(t)$	Actual output voltage
$\hat{v}_o(t)$	Small signal variation of the output voltage
V_{ref}	Reference voltage

$v_{ripple}(t)$	Voltage ripple
$\boldsymbol{x}$	Column vector with n dimension
x_1	Output voltage error
x_2	Derivative of x_1
$[\boldsymbol{x}^+]$	Representive point corresponding to the control input u^+
$[\boldsymbol{x}^-]$	Representive point corresponding to the control input u^-
$y(t)$	Output of the double integrator
$\dot{y}(t)$	Output of the first integrator and is the input to the second integrator
$\ddot{y}(t)$	Input to the double integrator
Z_o	Tank characteristic impedance
ω	Angular frequency
β	Beta, which is the ratio of the DC collector current to the DC base current
μ	DC conversion ratio for resonant converter
η	Efficiency
ω_L	Inverted zero angular frequency of the of the integral action
$\lambda_1(\boldsymbol{x})$,	Line equations that define the first sliding region boundary
$\lambda_2(\boldsymbol{x})$	Line equations that define the second sliding region boundary
μ_P	Maximum overshoot
φ_m	Phase margin
ω_p	Pole angular frequency of the derivative control
$\sigma(\boldsymbol{s})$	Sliding surface
$\sigma(\boldsymbol{x},t)$	Sliding surface with respect to time
τ	Time constant
ω_z	Zero angular frequency of the derivative control
Δi_L	Peak-to-peak inductor current
Δt	Change in time
Δv_c	Peak-to-peak capacitor voltage

Acronyms

AC	Alternating current
ASIC	Application specific integrated circuit
BJT	Bipolar junction transistor
BW	Bandwidth
CCM	Continuous conduction mode
CMOS	Complementary Metal Oxide Semiconductor
D	Derivative control
dB	Decibel
DC	Direct current
DCM	Discontinuous conduction mode
Den	Denominator of DC/DC Buck converter
Den1	Denominator of the derivative transfer function
Den2	Denominator of the Integral transfer function
EL2244/EL	Differentiator, integrator, subtractor
EMC	Electromagnetic compatibility
EMI	Electromagnetic interference
FET	Field effect transistor

H.P.F	High pass filter
HWZCS	half-wave zero current switching
I	Integral control
IC	Integrated circuit
IFBW	Intermediate frequency bandwidth
IGBT	Insulated gate bipolar transistor
I/O	Input output
IR2117	Derive circuit for the switch MOSFET
IRF530	Switch MOSFET
LM111	Comparator (Op-amp)
MIMO	Multi input-multi output
MOSFET	Metal-oxide field effect transistor
Num	Nominator of DC/DC Buck converter
Num1	Nominator of derivative transfer function
Num2	Nominator of the Integral transfer function
Op-amp	Operational amplifier
P	Proportional control
PD	Proportional derivative control
PFC	Power factor correction
PI	Proportional integral control
PID	Proportional integral derivative control
PWM	Pulse width modulator
Q	Output of the latch (S-R flip-flop)
R	Reset of the flip-flop
R&D	Research and development
RF	Radio frequency
RP	Representive point
S	Set of the flip-flop
SISO	Serial input serial output
SMC	Sliding mode control
SMPSs	Switched mode power supplies
SOSMC	Second-order sliding mode controller
Sys	Transfer function of DC/DC Buck converter
Sys1	Transfer function of the derivative
Sys2	Transfer function of the integral
Sys3	Transfer function of the DC/DC Buck converter plus the PID control
TTL	Transistor-transistor logic
VSCS	Variable structure control system
VSS	Variable structure system
ZCS	Zero current switching
ZVS	Zero voltage switching

List of Publications

This thesis consists of an overview and the following publications

P[1] M. Ahmed, M. Kuisma, K. Tolsa, P. Silventoinen. Standard Procedure for Modelling the Basic Three Converters (Buck, Boost, and Buck-boost) With PID Algorithm Applied. *Proceedings of XIII-th International Symposium on Electrical Apparatus and Technologies, SIELA 2003, 29-30 May, 2003*. Plovdive, Bulgaria.

P [2] M. Ahmed, M. Kuisma, P. Silventoinen. Implementing Simple Procedure for Controlling Switch Mode Power Supply Using Sliding Mode Control as a Control Technique. *Proceedings of XIII-th International Symposium on Electrical Apparatus and Technologies, SIELA 2003, 29-30 May, 2003*. Plovdive, Bulgaria.

P [3] M. Ahmed, M. Kuisma, K. Tolsa, P. Silventoinen. Implementing Sliding Mode Control for Buck Converter. *Proceedings of the Power Electronic Specialist Conference, PESC2003,* Acapulco, Mexico, June 2003. Provisionally accepted for publication in *IEEE Transactions on Power Electronics*.

P [4] M. Ahmed, M.Kuisma, P. Silventoinen, O. Pyrhonen. Effect of Implementing Sliding Mode Control on the Dynamic Behaviour and Robustness of Switch Mode Power Supply (Buck Converter). *Proceedings of the International Conference on Power Electronics and Drive systems* (*PEDS2003*). 17-20 November 2003, Singapore. Provisionally accepted for publication in *IEEE Transactions on Power Electronics*.

P[5] M. Ahmed, M. Kuisma, O. Pyrhonen, P. Silventoinen. Sliding Mode Control for Buck-Boost Converter Using Control Desk dSPACE^{TM}. *Proceedings of the International Conference on Power Electronics and Drive systems (PEDS2003)*. 17-20 November 2003, Singapore. Provisionally accepted for publication in *IEEE Transactions on Power Electronics*.

P [6] M. Ahmed, M. Kuisma, P. Silventoinen. Comparison between PID Control and Sliding Mode Control for Buck Converter. *Proceedings of the Symposium on Power Electronics, Electrical Drives, Automation and Motion. SPEEDAM 2004*. CAPRI – ITALY, 16-18 June, 2004.

P [7] M. Kuisma, M. Ahmed, P. Silventoinen. Comparison of Conducted RF-Emissions between PID and Sliding Mode Controlled DC-DC Converter. *Proceedings of the European Conference on Power Electronics and Applications EPE03*, September2003. Toulouse, France.

P [8] M. Ahmed, M. Kuisma, P. Silventoinen. Sliding Mode Control for Half-Wave Zero Current Switching Quasi-Resonant Buck Converter. *Proceedings of Nordic Workshop on Power Industrial Electronics, NORPIE/2004,* Trondheim, Norway. June 2004.

P [9] M. Ahmed, M. Kuisma, P. Silventoinen, J. Nerg, On the Design of Half-wave zero current switching DC/DC Buck converter. Submitted to the Power Electronic Specialist Conference (PESC 2005). Waiting for notification of acceptance by February 2005.

The research reported in publications was mainly done by the author of this thesis, Mohammad Ahmed. The authors' main contribution consisted of:

- Studying the theories and applications of different control methods,
- Concentrating in detail on the theory of PID and sliding mode control to switched mode power supplies,
- Studying the switched mode power supply topologies,
- Deriving mathematical analysis to non-isolated DC/DC converter,
- Deriving mathematical analysis of the control methods implemented in DC/DC converters,
- Designing the simulation models for the DC/DC converters with their control circuits in Matlab/Simulink™,
- Constructing the prototype of the simulated models,
- Testing the simulated model and the prototype, and taking measurements, and
- Writing regular reports to the supervisor.

All the publications in this thesis were done mainly by Mohammad Ahmed being the first author, except for P [7], the first author of which is Dr. Mikko Kuisma.

Professor Pertti Silventoinen had a constructive ability to direct the thesis. His analytical way of thinking helped the author to keep the research work in a defined boundary and not to deviate from the main idea. He read the publications and his valuable comments contributed to the speed-up of the research work.

Dr. Mikko Kuisma had a significant influence on the research work. Previously to each of the publications comprehensive technical discussions were held on the subject. These discussions proved to be very useful to get the best possible results. Each publication was reviewed several times and necessary corrections were made during the process of preparing the publications.

1. INTRODUCTION

1.1 Objective of the Research Work

Switched mode power supplies (SMPSs) are needed to convert electrical energy from one form to another. SMPSs are widely used in DC/DC conversions, where the input is a DC voltage that can be, for example, a rectified line voltage, an output voltage of a power factor correction (PFC) circuit, a battery or fuel cell voltage.

In such power conversions, DC/DC converters operate at relatively high switching frequencies, and this enables the use of small inductive components which improve the dynamic behaviour and reduce the size of the converter.

Despite the above-mentioned benefits of SMPSs, there are several parameters, which are not desired and have a strong influence on the converters behaviour, being mainly:

- Non-linear components in the converter structure,
- Line and load variations, and
- Electro-magnetic interferences (EMI).

The DC/DC converter has non-linear components (capacitors, inductors, and resistors), the value of which changes non-linearly if the converter is disturbed or may change within time. The effects of these converter parameters variations are given in P [6].

For the design of a DC/DC converter, a nominal input voltage and load values are suggested. In practice, these nominal values may deviate. For example, 20% line variation is expected or the nominal load may deviate to no-load or full load. These phenomena are studied in P [1], P [2], P [3], P [4], and P [6].

The purpose of electro-magnetic interference (EMC) is to ensure that an electronic system can operate in its electromagnetic environment without responding to electrical noise or generating unwanted electrical interference. For example, in DC/DC power supply EMI has an influence on the converter component. The EMI effects on the DC/DC converter are studied in P [7].

These parameters force the converter to deviate from the desired operating condition. If the parameter deviation increases, this will cause the converter not to operate in steady state. Many control methods are used to control SMPSs and solve the problem mentioned above. Each control method has its own advantages and drawbacks due to which that particular control method appears to be the most suitable control method under specific conditions, compared to other control methods. It is always demanded to obtain a control method that has the best performances under any conditions.

The thesis defines the causes by which the selecting of a specific control method is influenced, i.e. the sliding mode control (SMC), over other control methods. A detailed research analysis is done of the SMC implemented in some DC/DC converter topologies.

In order to record the benefits of the SMC, another control method is selected. The response of the converter is compared in steady state and in dynamic regions, which is controlled by the two different control methods (the PID and SMC).

The research work is done in following logical sequence:

- Study of the DC/DC converter topologies,
- Study of the control methods used to control the DC/DC converters,
- Selection of the DC/DC (Buck, Boost, and Buck-Boost) converters as the converter topologies, where the tests are done on them,
- Selection of the traditional PID control as one control method,
- Selection of the SMC as a second control method,
- Study of the behaviour of DC/DC converters under steady state and under dynamic conditions when the two control methods are implemented, and
- Comparison of the results and determining which control method is more suitable.

It is noticed that the influence of the SMC on the behaviour of the converter in steady state and under dynamic conditions is better than that of the PID control.

In order to reduce the switching losses (during the turn on-off), a DC/DC resonant converter is examined. The SMC is applied to the DC/DC resonant converter and the response of the converter is analysed in steady state and under dynamic conditions.

The research work process can be described as follows:

In chapter two, linear power supply is analysed and its advantages and drawbacks are discussed. In the next section, SMPSs are studied in detail and their benefits and drawbacks over linear regulators are shown. A classification of SMPSs into isolated and non-isolated DC/DC converters is given. The DC/DC resonant converter is studied and its advantages over hard switching DC/DC converter are shown. The DC/DC converters operate in either continuous conduction mode (CCM) or discontinuous conduction mode (DCM). Analyses for selecting the critical inductor value that forces the converter to operate in either CCM or DCM, for the basic three DC/DC (Buck, Boost, and Buck-Boost) converters are given. A look-up table is given to select the optimum critical inductor value. At the end of the chapter, a classification of the DC/DC power supply family is shown.

In chapter three, six control methods used to control DC/DC converters, namely the PID control, hysteresis control, adaptive control, current programmed control, variable structure control (VSC), and sliding mode control (SMC), are studied and each case is analysed individually in detail. The control analysis of each control method is given, its advantages and drawbacks are shown. The reasons for selecting SMC as the main control method for SMPSs in this research work are given. The principle of SMC is shown by means of mathematical equations.

Chapter four describes in detail SMC and a briefly reviews the history of SMC. The introductory part of the chapter introduces Prof. Utkin who is considered to be one of the first scientists having dealt with the subject of SMC, and briefly describes his most important researches in the field of SMC. In the next section, a review of the theory of SMC is given, more particularly; the existence condition, the reaching condition, the system description in sliding mode, the chattering. These mathematical equations are used to prove the analysis. The researches on and applications of SMC in electrical and mechanical systems are shown in a diagram.

In the next section of chapter four, the SMC is implemented to the DC/DC Buck converter and the above-mentioned SMC theories are proven. The results are verified with the

simulation results. Finally, the researches on and applications of the SMC for DC/DC converters are given in details.

In chapter five, a summary of the research work is given. The control methods used and the DC/DC converter topologies used are defined. The structure of the work is explained briefly. A research chart is given, which helps the reader the follow the main idea and the scope of the work. A summary of the publications is given. The publication summaries include nine publications and a brief explanation of each publication is given.

In chapter six, the conclusions obtained from the research work are given and the publications are explained. The main contribution of this thesis is summarized and suggestions for future research work are given.

2. DC/DC POWER SUPPLIES

2.1 Introduction

With the introduction of the transistor in the early 1950's and, especially, with the development of integrated circuits from the early 1960's onwards (Josephson 1967), designers of electronic equipment, computers and instrumentation increasingly have brought up the demand for smaller, more efficient power sources to supply their equipment. Therefore, to meet these demands, the power supply itself has become more and more sophisticated. In fact, the development in power supply technology can be directly linked to the introduction of various power semiconductor devices, even though the theory, in many cases, was already well known.

The regulated power supply technology can be divided into two distinct forms: firstly, the linear regulator which can be either a series or parallel regulator and, secondly, the switched-mode conversion technique. Switched-mode technology is multi-facetted with a wide variety of topologies achieving the result of providing a regulated DC voltage.

The main difference between the linear and switched-mode regulator is in efficiency. The linear regulator utilises simple techniques of controlled energy dissipation to achieve a regulated output voltage independent of line and load variations. It is, therefore, inherently inefficient, especially when a wide input voltage range has to be applied. When linear techniques are applied to regulate a low voltage from the mains (110V or 240V AC source) then the disadvantages of the technique become apparent.

2.2 Linear Power Supply

Linear power supplies provide significant advantages over switching regulators in:

- Simplicity,
- Cost, and
- Output noise.

A typical linear power supply is shown in Figure 2.1, which has the following disadvantages:

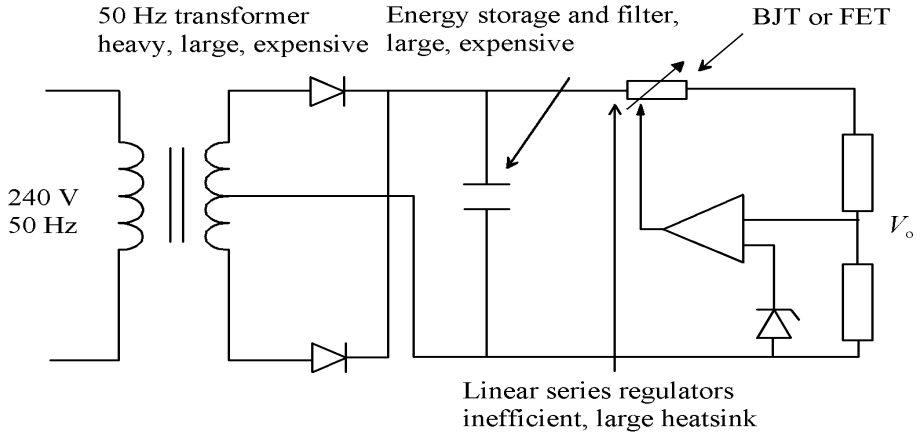

Figure 2.1. Practical linear series regulator circuit. The efficiency is lower compared to the switched mode power supply.

- The main transformer operating at a low frequency is heavy, large and expensive,
- Large heat-sinking is required to dissipate the heat generated by the regulating element, and
- The efficiency is low.

Two major types of linear regulators are considered and shown in Figure 2.2. The simple series regulator in Figure 2.2.a) is a transistor connected as an emitter follower (or source follower in FET). The transistor operates in its linear active region rather than a switch. The emitter voltage V_o becomes a function of $V_{control}$ rather than the input voltage or the load current and the term linear regulator is appropriate to describe the circuit. The power loss and efficiency are

$$P_{loss} = (V_{in} - V_o) I_{load}, \tag{2.1}$$

$$\eta = \frac{V_o I_{load}}{V_{in} I_{load}} = \frac{V_o}{V_{in}}. \tag{2.2}$$

The shunt regulator shown in Figure 2.2.b) resembles a common emitter amplifier circuit. The transistor, once again, is used in the linear active region. The collector current will be βI_b rather than the function of the load current. Again, the output is a linear function of the control, and the circuit is another example of a linear regulator. The losses and efficiency for the shunt regulator are

$$P_{loss} = V_o I_c + (I_{load} + I_c)^2 R_c, \tag{2.3}$$

$$\eta = \frac{V_o I_{load}}{V_{in} (I_{load} + I_c)}. \tag{2.4}$$

With no load there is a significant loss because $I_c \neq 0$, and, in best the case where $I_{load} >> I_c$, the efficiency becomes V_o/V_{in}.

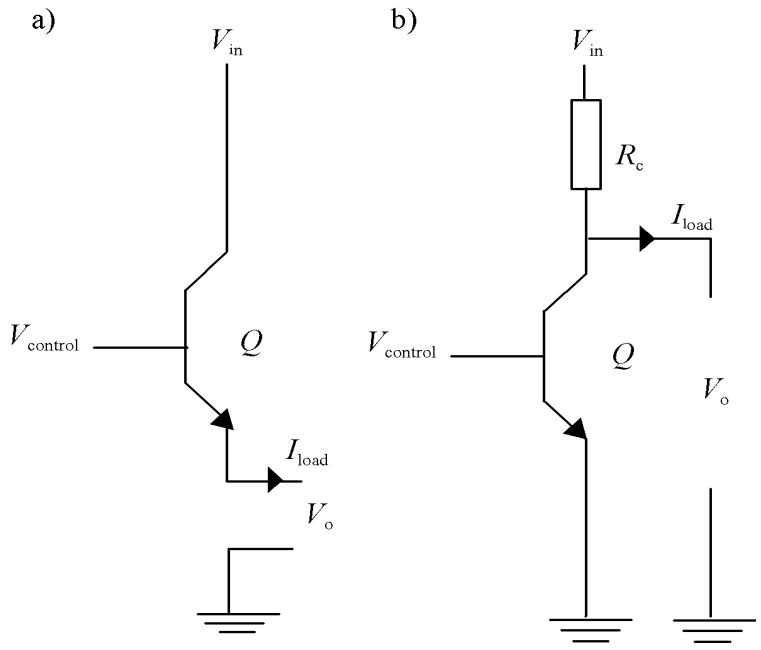

Figure 2.2. Basic circuits for linear regulators. a) Series regulator, b) shunt regulator.

Linear regulators acting as converters limit the efficiency. However, since they bring the possibility of perfect regulation, linear regulators are often used as elements of larger conversion systems.

2.3 Switched Mode Power Supply

Switched-mode power supply shown in Figure 2.3 offers the possibility of theoretically loss-less power conversion, which is not true in reality. The switched-mode regulator employs duty cycle control of a switching element to block the flow of energy and thus achieve regulation.

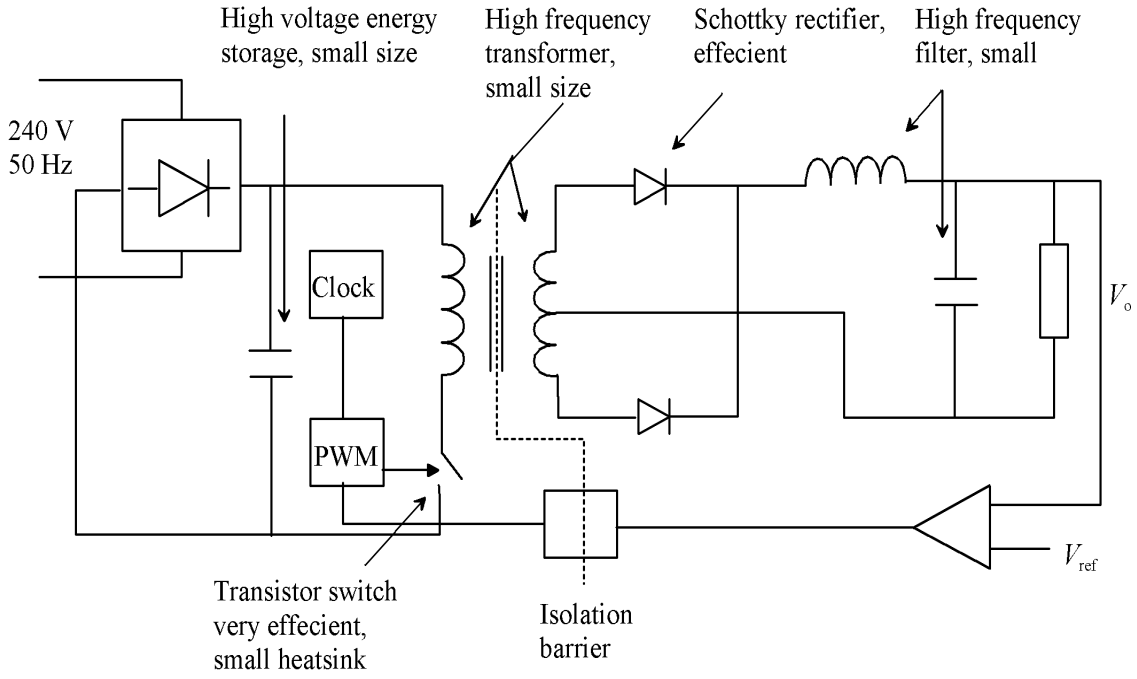

Figure 2.3. Practical circuit of switch mode regulator. This topology has more advantages compared to linear regulators.

The switched mode power supply has the following advantages compared to the linear regulator:

- High switching frequency enables the use of a small ferrite transformer core,
- Since the rectified mains voltage is chopped, the energy storage for hold-up can be accomplished on the primary side of the step-down transformer, and smaller but high voltage capacitors than in the linear counterpart can be used,
- It can step the voltage up/down and reverse its polarity,
- It may operate in a much larger DC input voltage range than the linear regulators, and
- It often has a higher efficiency.

Although the benefits of switched-mode techniques are significant, there are some drawbacks:

- Both the input and output present increased noise of the supply due to the power switching techniques, and
- The associated control circuitry is more complicated compared to the linear counterpart, e.g. an isolated feedback signal is needed for the control.

Historically, the linear regulators were very common during the late 1950's and early 1960's when power supplies using switching techniques were very rare. The prevailing use of switched-mode power supplies is linked to the development of fast, high-voltage switching power transistors and, to a smaller extent, to the developments of ceramic ferrite materials and capacitor technology. Nowadays, switched mode power supplies are widely used.

However, linear regulators are still in use in applications for the following reasons:

- Linear regulators are simple,
- It is possible in some cases to reach a high efficiency with linear power supplies too. This is accurate if the current that powers the regulator is a small percentage of the current drawn from the output of the regulator. Thus, when the voltage of the source powering the linear regulator is near the output voltage of the regulator, the efficiency is high. In that case, the linear regulator may be a better alternative than the switching regulator, and
- They have been available for tens of years.

2.4 Switched-Mode Power Supply Topologies

2.4.1 Non-isolated Topologies

With the upcoming commercial switched-mode power supply manufacturing industry during the 1970s, the theory and technology of switched-mode conversion was being re-nationalised as part of the academic discipline of power electronics.

The greatest contribution made within the discipline is by R.D. Middlebrook and his colleagues of the Power Electronics Group of Caltech in California, USA. The initial work of the Caltech Group, started in 1970 was performed with the aim of developing models for the three DC/DC switching regulator topologies, the Buck, Boost and Buck-Boost converters (Haver 1974), which were already developed in the 1960s.

From this work, the modelling and analysis method called state-space averaging was created (Pressman 1977). The state-space averaging allowed a theoretical prediction of the frequency response of a converter and, therefore, enabled a better understanding of the feedback loop and stability criteria of a switched-mode regulator.

Further work at Caltech, especially by Cuk in his PhD Thesis, produced a fourth topology of the basic DC/DC switching regulator, which the author described as an optimum topology (Cuk 1977) because of its symmetrical structure and non-pulsating input and output currents.

The new optimum topology DC/DC switching regulator is now commonly known as the Cuk converter, named after its inventor, and completes the family of single-switch non-isolated switching regulators.

The non-isolated DC/DC converters family shown in Figure 2.4 can be classified as follows:

- Buck converter (step down DC/DC converter),
- Boost converter (step up DC/DC converter),
- Buck-Boost converter (step up/down DC/DC converter, opposite polarity), and
- Cuk converter (step up/down DC/DC converter).

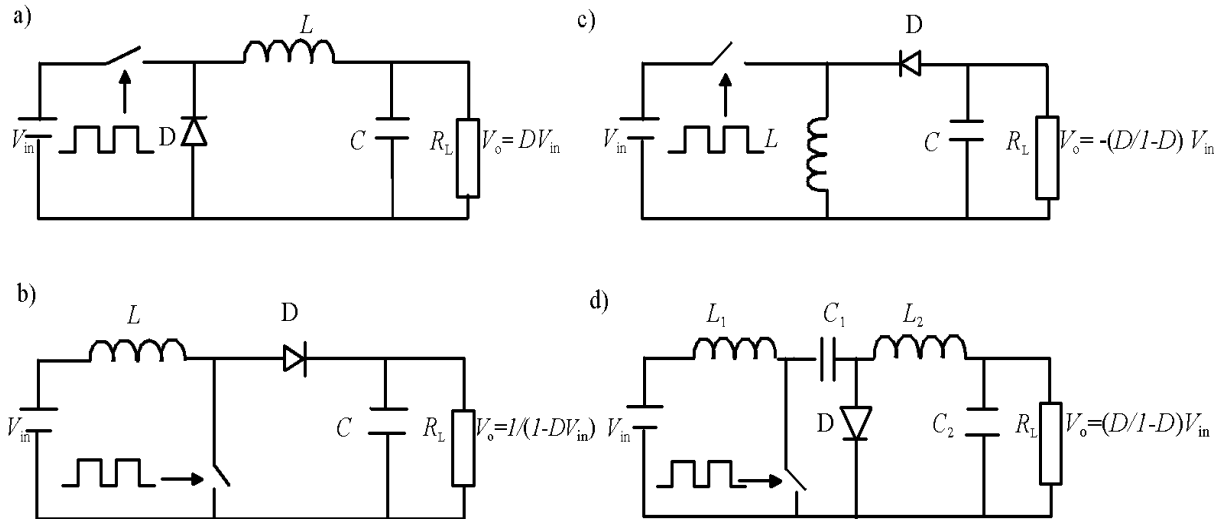

Figure 2.4. Non-isolated DC/DC converter topologies a) Buck converter, b) Boost converter, c) Buck-Boost converter, and d) Cuk converter. The equations for the output voltage in the figure are valid only in the case of continuous conduction mode converters.

2.4.2 Isolated Topologies

In many applications, isolation is a necessary requirement within the converter between input and output. By inserting isolation transformers into the four basic non-isolated switching regulator topologies, four single-ended isolated switching DC/DC converters can be obtained, shown in Figure 2.5:

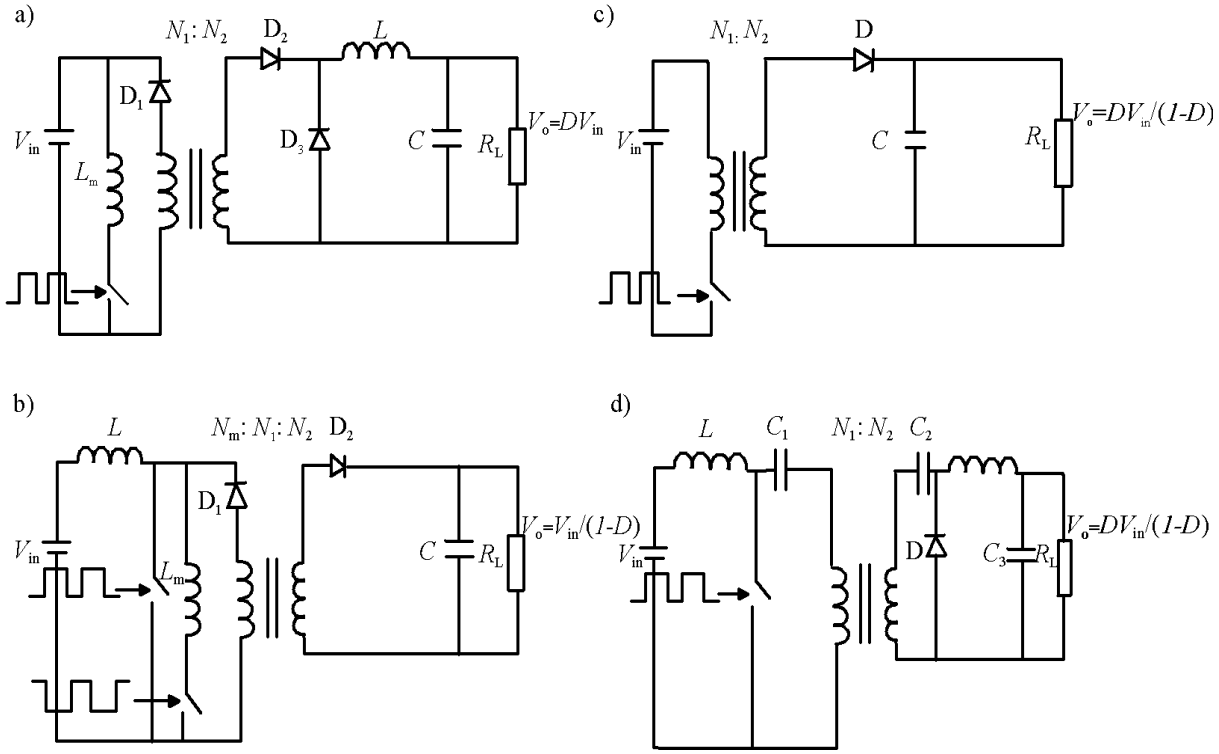

Figure 2.5. Isolated DC/DC converter topologies a) Forward converter, b) Isolated Boost converter, c) Flyback converter, and d) Isolated Cuk converter. N_1 is the number of turns in the primary, and N_2 is the number of turns in the secondary side of the transformer.

- The Forward converter (step down DC/DC converter),
- The Isolated Boost converter (step up DC/DC converter),
- The Flyback converter (step up/down DC/DC converter), and
- The Isolated Cuk converter (step up/down DC/DC converter).

The isolated DC/DC Buck and Buck-Boost topologies are more commonly referred to as the Forward and Flyback DC/DC converter respectively, and are the most used topologies in commercially manufactured switched-mode power supplies.

2.4.3 Multiple Switch Topologies

The main disadvantage of single switch topologies is that the transistor switch should be capable of high-voltage blocking (twice the DC input voltage), especially when operating from a rectified AC mains supply. The single switch topology is not an ideal solution for higher power converters either, since these converters need a higher current rating of the transistor switch. Therefore, another group of isolated DC/DC converters utilising more than one switch can be identified. Figure 2.6 illustrates three multiple switch topologies:

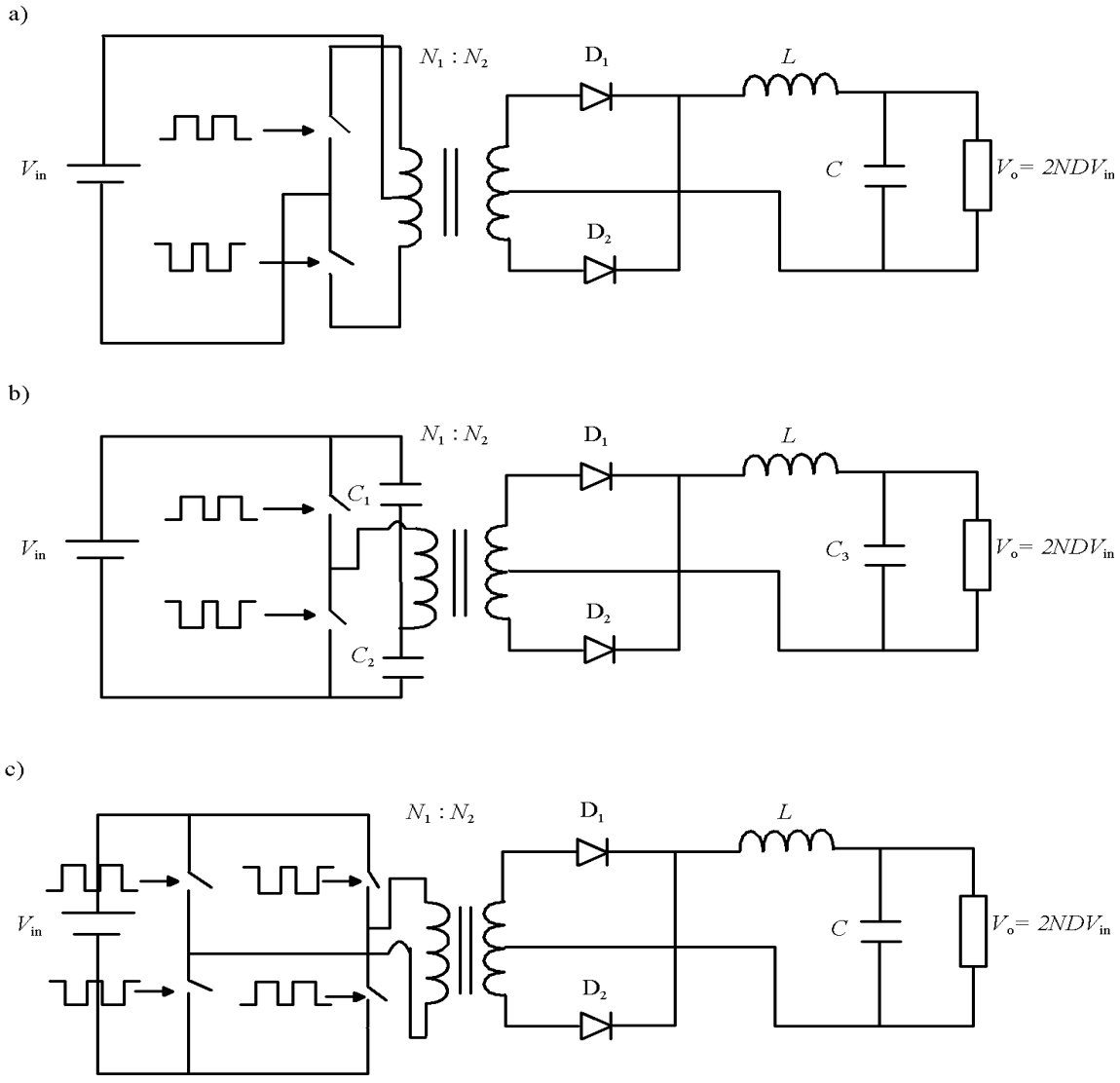

Figure 2.6. Multiple switches topologies DC/DC converters a) Push-pull converter, b) Half-bridge converter, and c) Full-bridge converter. N_1 and N_2 are the number of turns on primary and the secondary side of the transformer.

- The Half-bridge DC/DC converter,
- The Full-bridge DC/DC converter, and
- The Push-pull DC/DC converter.

These topologies have the additional advantage over the single-ended Forward and Flyback DC/DC converters that a full flux excitation of the transformer core occurs instead of only a half core flux capability. This makes these multiple switch topologies more suited for higher power operation.

2.5. DC/DC Resonant Converters

In all basic switched-mode topologies, the finite duration of the switching transitions will cause high peak pulse power dissipation in the device. This, again, produces degradation of the converter efficiency and, in the worst case, can lead to transistor damage during the turn-off transition. Therefore, research has been done on resonant converters, which are an alternative switched-mode topologies and one means to avoid switching losses (Ho 1993), (Erickson 1995), (Chen 1995), (Bevrani 2002), and (Chakraborty 2002). These converters have tuning circuits as part of the power conversion stage and exhibit sinusoidal voltages and/or currents, which leads to transistor switching transitions under the ideal conditions of zero stress.

If the current can be held near to zero during the transition, turn-on and turn-off losses will be minimized. A switching transition that takes place with low current is called zero-current switching (ZCS).

In the low voltage alternative, the voltage drop across the switch is held close to zero during the turn-on transition. The current increases while the voltage is low, so the losses during transition are low as well. This action is called zero-voltage switching (ZVS).

In DC/DC converters, the resonance can be used to create the conditions for ZCS or ZVS. This approach is called *soft switching*.

2.5.1 DC/DC Resonant Converter Topologies

The circuit of Figure 2.7 provides an arrangement for resonant DC/DC conversion. In this case, both an inductor and a capacitor have been added to alter the switch action. A similar *LC* pair is added to the diode. In any of these soft switching cases, switch action at a zero crossing cuts off the ringing resonant waveform.

This technique is often called *quasi-resonance*. Converters based on the circuit shown in Figure 2.7 can be called DC/DC resonant converter or DC/DC quasi-resonant converter.

The combinations offer several possibilities for resonant action as follows:

- If the parts are chosen so that C_t and L_d are very small and have minimal effect on the circuit action, the L_t and C_d form a series *LC* combination. The transistor can take advantages of current zero crossing for ZCS,
- If the values of C_t and L_d are significant while L_t and C_d values are small, then the transistor supports ZVS, and

• It is possible, in principle, to use all four parts to support ZVS and ZCS action together. This technique, called multi-resonance, is not common because it tends to constrain the converter control.

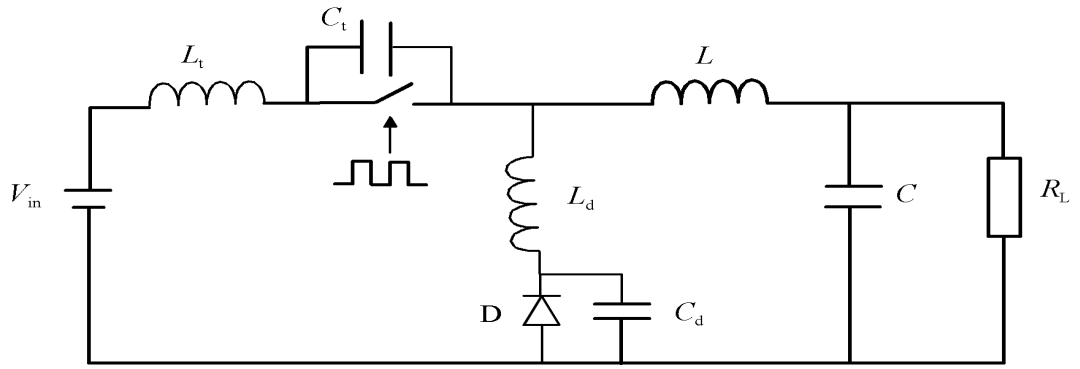

Figure 2.7. Resonant components added to DC/DC converters performing soft switching. This figure is the general structure of resonant converter, where ZVS or ZCS can be obtained by re-arranging the resonant components.

2.6 Continuous Conduction Mode and Discontinuous Conduction Mode

Switch mode power supply operates in following modes:

- Continuous conduction mode (CCM), and
- Discontinuous conduction mode (DCM).

This section shows by means of mathematical equations how to select the critical inductor value ($L_{critical}$) for the three non isolated DC/DC (Buck, Boost, Buck-Boost) converters, before going on to the analysis of the publications.

In the case of the CCM; $L_{critical}$ is the smallest inductor value for which the inductor current is greater than zero at all times and under all allowed operating conditions of the converter. For the DCM; $L_{critical}$ is the biggest inductor value for which the inductor current should reach zero for some instant of time.

The DCM occurs with large inductor current ripple in a converter operating at light load, and the properties of the DC/DC converter changes rapidly. The DC/DC converter ratio becomes load dependent and the output impedance is increased.

In some applications, it is required that the DC/DC converter operates in CCM, while for some other applications the DC/DC converter is needed to operate in DCM. The designer of SMPSs can select and design the converter to operate in DCM if it is required to:

- Obtain a fast response. The converter starts each cycle with no stored inductor energy, and makes its full current transition immediately, and
- Have a small inductor value which implies a lower cost.

On the other hand, DCM operation for SMPSs converters has the following disadvantages

- Load regulation problems. The converter ratio becomes load dependent, and
- High current variation in an inductor will increase the losses in its magnetic parts, and can lead to magnetic saturation.

When selecting the inductor value for a given operation mode, the boundary is defined as

$$\begin{array}{ll} L \geq L_{\text{critical}} & \text{(CCM)} \\ L < L_{\text{critical}} & \text{(DCM)} \end{array}. \tag{2.5}$$

The following equations show how to find L_{critical} for a DC/DC Buck converter operating in:

- A defined DC input voltage range ($V_{\text{in (min)}}$ to $V_{\text{in (max)}}$),
- A defined output power range ($P_{\text{o (min)}}$ to $P_{\text{o (max)}}$),
- A known DC output voltage (V_{o}), and
- A nominal switching frequency $f_{\text{s(nominal)}}$.

At the end of this section, a look-up table shows the L_{critical} for the three non isolated DC/DC (Buck, Boost, and Buck-Boost) converters. For the DC/DC Buck converter shown in Figure 2.8, assuming zero inductor resistance, the inductor voltage is defined as

$$V_{\text{L}} = L\frac{\Delta i_{\text{L}}}{\Delta t}, \tag{2.6}$$

where Δi_{L} is the peak-to-peak inductor current variation, and Δt is the period of the switch being in the condition (on or off). For the case when the switch is on

$$V_{\text{in}} - V_{\text{o}} = L\frac{\Delta i_{\text{L}}}{DT_{\text{s}}}, \tag{2.7}$$

where D denotes the average duty cycle when the switch is on, and T_{s} represents the nominal switching period and is equal to $1/f_{\text{s(nominal)}}$.

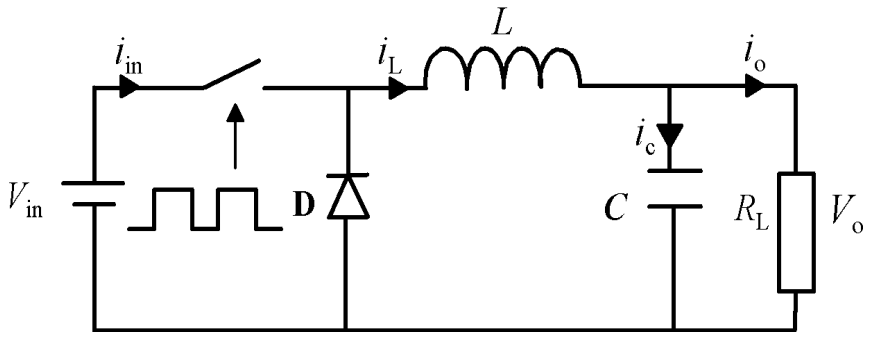

Figure 2.8. DC/DC Buck converter topology used as a step down converter. The figure helps to drive equation to find the critical inductor value (L_{critical}).

Under a particular condition, when the inductor $L = L_{\text{critical}}$, it will produce the familiar triangle wave with a minimum at zero and a maximum at 2 i_{o}. Equation (2.7) can be written as follow

$$V_{\text{in}} - V_{\text{o}} = L\frac{2i_{\text{o}}}{DT_{\text{s}}}, \tag{2.8}$$

where i_{o} is the load current and is equal to i_{L} in this case. For DC/DC Buck converter, the average duty cycle is

$$D = \frac{V_o}{V_{in}}, \tag{2.9}$$

and

$$i_o = \frac{P_o}{V_o}, \tag{2.10}$$

where P_o is the average output power. Substituting equations (2.9) (2.10) into (2.8), and for the case $L = L_{critical}$, it can be written

$$V_{in} - V_o = L_{critical} \frac{2\left(\frac{P_o}{V_o}\right)}{\left(\frac{V_o}{V_{in}}\right) T_s}. \tag{2.11}$$

Re-arranging the terms leads to a general equation for the DC/DC Buck converter, where $L_{critical}$ is defined as

$$L_{critical} = \frac{(V_{in} - V_o)(V_o)^2 T_s}{2 P_o V_{in}}. \tag{2.12}$$

If the design requires the converter operates in CCM under all conditions, then the condition $L > L_{critical}$ should be satisfied to operate in CCM under all conditions and the worst case occurs at a minimum output power and a maximum input voltage (refer to Appendix A.1).

On the other hand, if it is required that the converter operates in DCM under all conditions, then the condition $L < L_{critical}$ should be satisfied to operate in DCM under all conditions. The worst case appears then at a maximum output power and a minimum input voltage, (Appendix A.1).

Table 2-1 lists the critical inductor values for the three non-isolated DC/DC (Buck, Boost, and Buck,-Boost) converters, operating in both CCM and DCM (see Appendix A.2) for the Boost converter, and (refer to Appendix A.3) for the Buck-Boost converter.

Table 2-1. The critical inductor values for the three non-isolated DC/DC (Buck, Boost, and Buck-Boost) converters. The table shows how to select a suitable inductor value in CCM or DCM for a DC/DC converter. Assuming that the converter operates in: a defined input range, a defined output power range, a defined output voltage value, and a known switching frequency.

Converter type	$L_{critical}$	CCM	DCM
DC/DC Buck	$L_{critical} = \frac{(V_{in} - V_o)(V_o)^2 T_s}{2 P_o V_{in}}$	$L > \frac{(V_{in(max)} - V_o)(V_o)^2 T_s}{2 P_{o(min)} V_{in(max)}}$	$L < \frac{(V_{in(min)} - V_o)(V_o)^2 T_s}{2 P_{o(max)} V_{in(min)}}$
DC/DC Boost	$L_{critical} = \frac{(V_o - V_{in})(V_{in})^2 T_s}{2 P_{in} V_o}$	$L > \frac{(V_o - V_{in(max)})(V_{in(max)})^2 T_s}{2 P_{in(min)} V_o}$	$L < \frac{(V_o - V_{in(min)})(V_{in(min)})^2 T_s}{2 P_{in(max)} V_o}$
DC/DC Buck-Boost	$L_{critical} = \frac{V_o (V_{in})^2 T_s}{2 P_{in} (V_o + V_{in})}$	$L > \frac{V_o (V_{in(max)})^2 T_s}{2 P_{in(min)} (V_o + V_{in(max)})}$	$L < \frac{V_o (V_{in(min)})^2 T_s}{2 P_{in(max)} (V_o + V_{in(min)})}$

The table helps the designer to select an inductor value that enables the converter to work in any desired mode of CCM and DCM, even when the worst case is given in the design specification.

2.7 Switched-Mode Topology Applications and Classifications

Within the electronics sector, the switched-mode power supply market is now well established with a large number of power supply manufacturers world-widely providing a wide set of units to be used for commercial and military purposes.

The main end-user systems for switched-mode supplies are computers, large mainframe as well as smaller, personal and word processors, and the various telecommunication systems.

The topologies and control methods used to achieve the desired output voltages in the various power ranges tend to vary from manufacturer to manufacturer. In general, switching regulators are usually used as secondary regulators in multiple-output units, isolated single-ended configurations are used in low power single or multiple outputs AC/DC converters and multiple switch topologies are used for higher output power applications.

Combining linear and switch-mode regulators is a common technique for generating multiple supply voltages.

The linear regulator in Figure 2.9 converts battery voltage to a logic supply, and one or more switch regulators generate the other voltages required for analog circuitry and LCD-display bias.

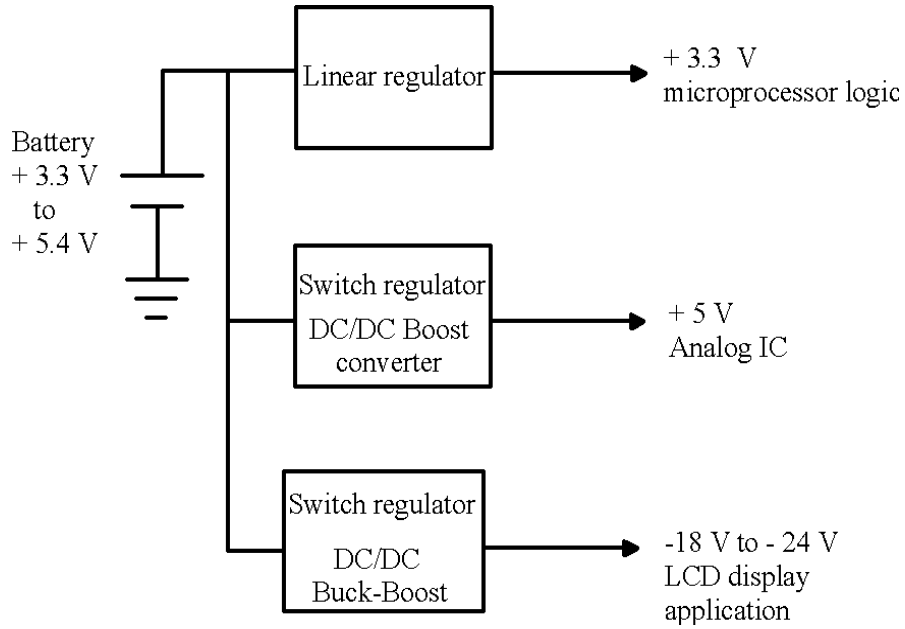

Figure 2.9. Combining linear regulator and switch regulators for various applications.

Figure 2.10 shows a different approach that achieves noise and ripple rejection with the combination of linear and switch-mode regulators. Because the power drawn by these regulators is not a major portion of the total load in a portable system, their effect on the battery life is minimal.

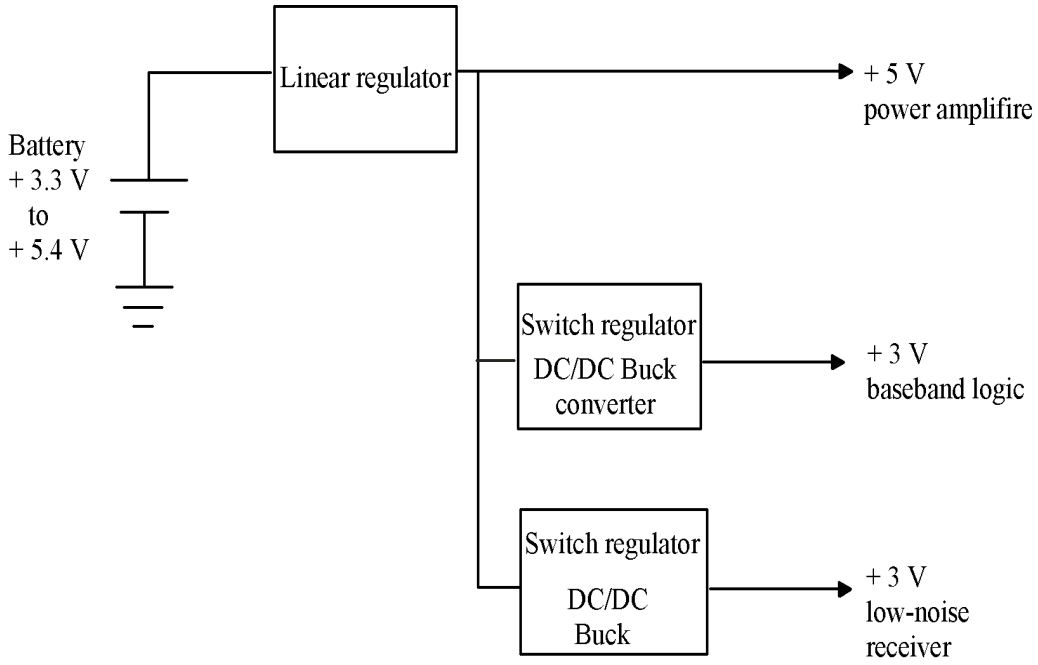

Figure 2.10. Combining linear regulator and switch regulators to achieve noise and ripple rejection.

The various converter topologies can be arranged in a family tree as illustrated in Figure 2.11.

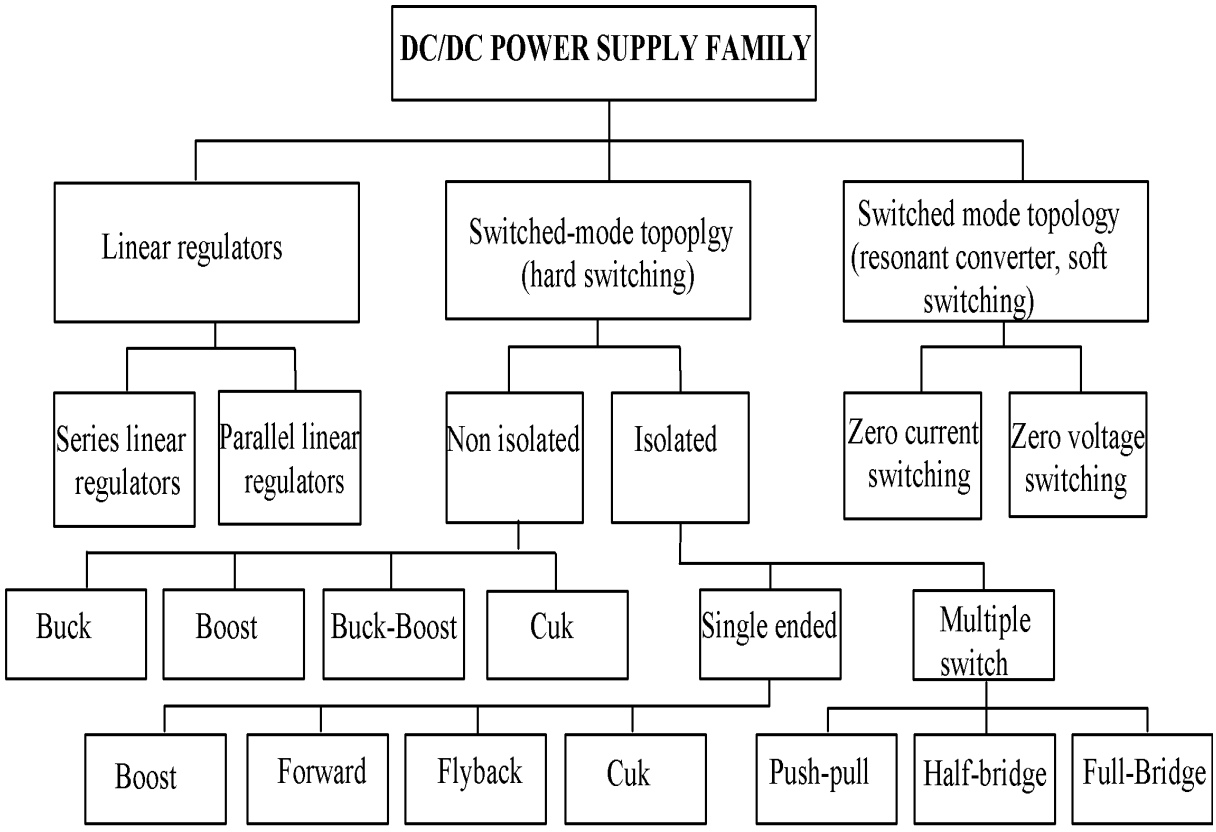

Figure 2.11. DC/DC power converter family tree. The DC/DC converter family is divided into three branches, which are the Linear regulator, switched mode topology (hard switching), and resonant converter (soft switching). These branches are divided into sub-branches, shown in the Figure.

2.8 Summary

The regulated power supply technology was divided into: linear power supplies, and switch mode power supplies. In each category an analysis of the converter structure is done. The advantages and drawbacks of each category are shown. Table 2-2 summarize these differences.

Table 2-2. A comparison between the advantage and disadvantage of linear regulator and switch regulators.

	Linear regulator	Switching regulator
Function	Only steps down	Steps up or down, or inverts
Efficiency	Low to medium and high if V_{in}-V_{out} difference is small.	High
Power loss	High if the average load or the input/output voltage differences are high	Low, where components usually run cool
Complexity	Low. Usually requires only the regulator and low-value bypass capacitors.	Medium to high**.** Usually requires inductor, diode, and filter caps in addition to IC.
Total Cost	Low.	Medium to high**,** due to external components
Ripple/Noise	Low. No ripple, low noise. Better noise rejection.	Medium to high**,** due to ripple at switching rate

A mathematical analysis was given, by means of which it can be made sure that the non-isolated DC/DC (Buck, Boost, and Buck-Boost) converters operate in either CCM or DCM under all conditions. The DC/DC resonant converter was analyzed. Finally, a chart showing the DC/DC power supply family was given.

3. CONTROL METHODS

3.1 Introduction

Feedback control is the basic mechanism through which systems, whether mechanical, electrical, or biological, maintain their equilibrium. Feedback control may be defined as the use of different signals that are determined by comparing the actual values of the system variables to their desired values, as a means of a control system.

In recent years, control theories and their applications to controlling electrical and mechanical systems have developed in a notable way. Research in the interesting field of switch mode power supply control is done with the objective of improving the stability, reducing the sensitivity to disturbances, improving the efficiency and also with the objective of developing control methods to improve the system performances (Boudreaux 1997), (Forsyth 1998), (Charaabi 2002), (Adell 2003), (Lee 2003), and (Peng 2004).

The challenge behind this wide interest is the need of finding the most suitable control method to overcome the main problems arising and affecting the performance of the circuit. These problems are:

- Non-linearity due to the non-linear components in the structure of the converter,
- Stability in steady-state and under line and load variations,
- Achieving large-signal stability often calls for reduction of the useful bandwidth, which, again, affects the converter performances,
- Application of these techniques to high-order DC/DC converters, such as Cuk and Sepic topologies, may cause a very critical design of the control parameters and a difficult stabilization,
- Reduction of the costs by reducing the components used in the control prototype, and
- Reduction of the EMI.

3.2 Stability of Linear and Nonlinear Control Systems

Classical control design is used for linear systems and can also be used successfully in some cases of nonlinear systems. A control system can be designed to be such that is robust to variations in the system parameters as well as to measurement errors and external disturbances. Thus, the classical techniques can be used for linear systems and for the linarized version of a nonlinear system. The classical control methods give good results at an equilibrium point near which the system behaviour is approximately linear.

Below, some classical control methods to measure the stability are given:

- Routh-Hurwitz stability criterion,
- Nyquist stability criterion,
- Bode-plot diagram approach,
- The root-locus method, and
- Nichols chart.

Although the Routh-Hurwitz gives a relatively quick determination of the absolute stability, it does not show how to improve the design. In addition, it does not give an indication of the relative system performance.

When using the methods of Nyquist and Bode, the system description needed for the control design is the magnitude and phase of the frequency response. This is advantageous, since the frequency response can be experimentally measured and the transfer function can then be computed. Frequency-domain techniques can also be applied to systems with simple types of non-linearities using the describing function approach, which relies on the Nyquist criterion.

As for the root locus design, the transfer function is needed. The block diagram is heavily used to determine the transfer functions of the composite systems. An exact description of the internal system dynamics is not needed for classical design, only the input/output (I/O) behaviour of the system is important.

The Nichols chart is a very useful technique for checking the stability and the closed-loop frequency response of a feedback system. The stability is determined from a plot of an open loop gain phase characteristic. At the same time, the closed-loop frequency response of the system is determined by utilizing the contours of the constant closed-loop amplitude and phase shift, which are overlaid on the gain-phase plot.

Unfortunately, it is not possible to design control systems for advanced nonlinear multivariable systems, such as those arising in aerospace applications, using the assumption of linearity and treating the single-input/single-output transmission pairs one at a time.

The modern control techniques were first established for linear systems. Extensions to nonlinear systems can be made using the Lyapunov approach, which can be easily extended to multi input multi output (MIMO) systems, dynamic programming and other techniques.

The subject of nonlinear control deals with the analysis and design of nonlinear control systems, i.e. of control systems containing at least one nonlinear component. In the analysis, a nonlinear closed-loop system is assumed to be designed and the determination of the characteristic of the system behaviour is done.

In the design of a nonlinear control, a nonlinear plant to be controlled and certain specifications of the closed-loop system behaviour are given. The task is to construct a controller so that the closed-loop system meets the desired characteristics.

The analysis of nonlinear systems studies the effect of limit-cycle, soft and hard self-excitation, hysteresis, jump resonance and sub harmonic generation. In addition, the response to a specific input function must be determined.

Several tools are available for the analysis of nonlinear systems. It may be mentioned:

- The Linearization approximation,
- The Describing function concept,
- The Piecewise-linear approximation,
- The phase plane,
- The Lyapunov's stability criterion,
- Popov's method, and
- The Sliding mode control (SMC).

If the deviation from linearity is not large, the linear approximation may permit the extension of an ordinary linear concept. A describing function is defined as: the ratio of the fundamental component of the output of a nonlinear device to the amplitude of a sinusoidal input signal.

Approximating nonlinearity by means of piecewise-linear segmentation is a useful tool for analysis. The method has the advantage of yielding a solution for the nonlinearity of any order. For the phase plane, the variation of the displacement is plotted against the velocity on a graph known as the phase-plane, and the curve for a specific step input is known as the trajectory.

Lyapunov's fundamental method of determining the stability of a dynamic system is based on the generalization of energy consideration. An important feature of Popov's approach is that it is applicable to a system of higher order. Once the frequency response of the linear element is known, very little additional calculations are required to determine the stability of the nonlinear control systems.

One of the most intriguing aspects of sliding mode control is the discontinuous nature of the control action. The primary function of each of the feedback channels is to switch between the two different system structures, so that a new type of system motion called sliding mode exists in a manifold $s = 0$.

3.3 Control Methods

In this chapter an explanation of some common methods used to control switch mode power supplies are given, and the reasons for selecting the sliding mode control (SMC) to be used in this research are given. There are many control methods to control DC/DC converters. Figure 3.1 shows some of the most common and simpler control methods, which are studied in this thesis and are given below:

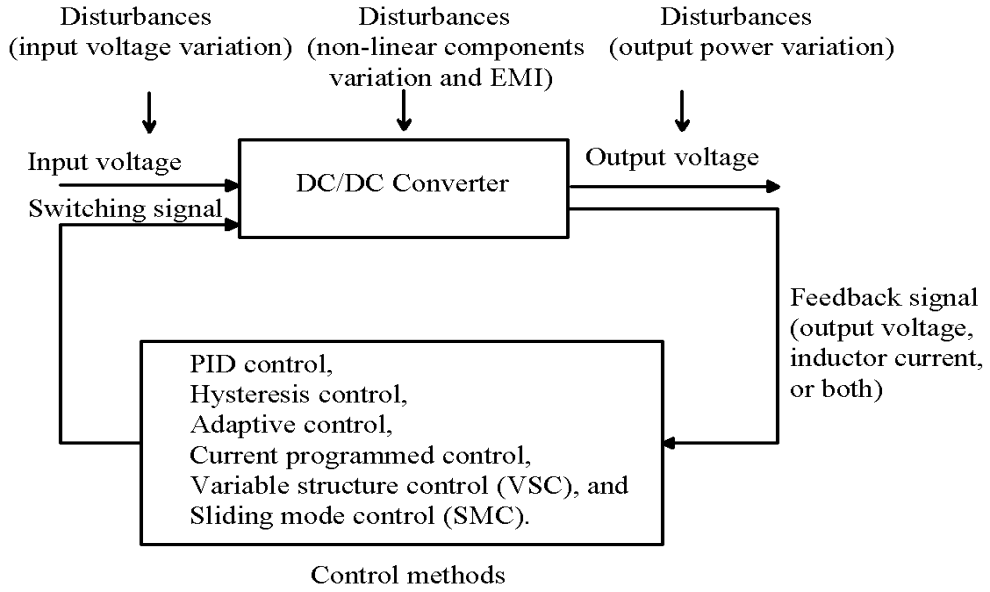

Figure 3.1. A block diagram showing some methods used to control DC/DC converters and the disturbances that have influence on the behaviour of the converter and its stability. The feedback signal may be the output voltage, the inductor current, or both. The feedback control can be either analog or digital control.

- PID control,
- Hysteresis control,
- Adaptive control,
- Current programmed control,

- Variable structure control (VSC), and
- Sliding mode control (SMC).

3.4 PID Control

In the proportional control, (P) control, only gain adjustment is available to improve the system performance. The limitations of its ability to achieve both satisfactory accuracy and acceptable relative stability are understandable. If a P controller can not meet the performance specifications, it should be replaced by a dynamic controller or a dynamic compensator to provide more flexibility.

The focus is on series compensation using proportional plus integral plus derivative (PID) controllers as a dynamic compensator. Among the control methods the PID controller is traditionally used to control DC/DC converters (Forsyth 1998), (Philip 1998), (Erickson 1997), and (Prodic 2002).

A good understanding of the P, I, and D actions, in both analytical and physical terms, is therefore important to evaluate how a dynamic compensation can change the system behaviour.

The lead compensator or derivative action (D) has an effect on the converter response at high frequencies and is used to improve the phase margin (φ_m). In the derivative control a zero is added to the loop gain, at frequency (f_z) sufficiently far below the crossover frequency (f_c), so that the φ_m of the closed-loop system is increased by the desired amount.

A side effect of adding f_z is that, it causes the compensator gain to increase with frequency that causes the compensator to differentiate the error signal. So a step must be taken to ensure that the closed loop system remains equal to unity at the desired f_c. The D transfer function $G_{c1}(s)$ must contain high frequency poles (f_p).

The pole has also the beneficial effect of attenuating the high frequency noise. If the compensator gain at the switching frequency is high, then the switching harmonics are amplified by the compensator and can disrupt the operation of the pulse width modulator (PWM). So, at a frequency less than the switching frequency, the compensator network should contain poles. Equation (3.1) shows the transfer function of the D compensator.

$$G_{c1}(s) = K_D \frac{\left(1 + \frac{s}{\omega_z}\right)}{\left(1 + \frac{s}{\omega_p}\right)}, \tag{3.1}$$

where K_D is the derivative gain, $\omega_z = 2\pi f_{z,}$ and $\omega_p = 2\pi f_{p.}$

The converter response can be further improved by adding a lag compensator. This is known as the integral action (I) which produces a high gain at low frequencies, thus reducing the error in steady state.

An inverted zero (f_L) is added to the loop gain. If f_L is sufficiently lower than f_c, then the φ_m is unchanged. The transfer function of the lag compensator is

$$G_{c2}(s) = K_I\left(1 + \frac{\omega_L}{s}\right), \tag{3.2}$$

where K_I is the integral gain, and $\omega_L = 2\pi f_L$.

The advantages of lead and lag compensators can be combined in order to obtain both a wide bandwidth and a zero steady-state error. At low frequencies, the compensator integrates the error signal, which causes a large low-frequency loop gain and an accurate regulation of the low-frequency components of the output voltage. At high frequencies, the compensator introduces the phase lead into the loop gain, which improves the phase margin. This type of compensator is called PID controller.

Figure 3.2 shows a simple block diagram for a general DC/DC converter topology with implemented PID control.

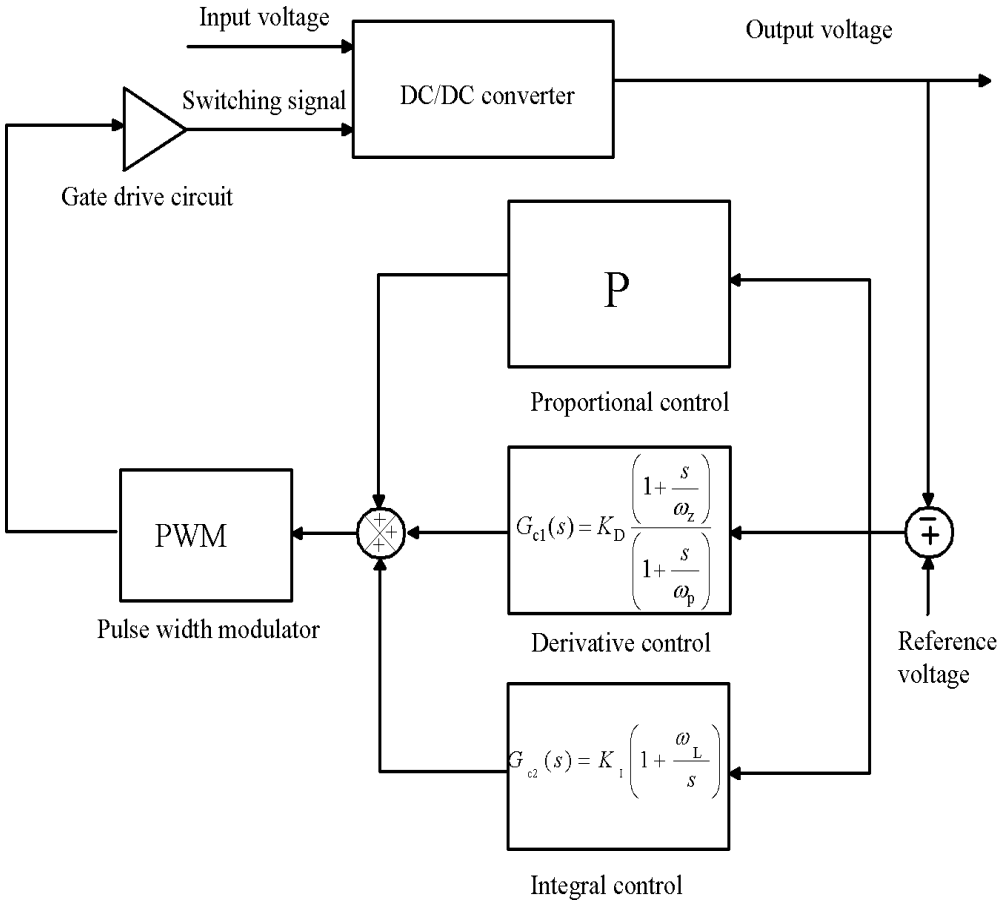

Figure 3.2. A simplified block diagram for a DC/DC converter with PID control showing the transfer functions of the derivative and integral control in separate blocks. A gate drive circuit is used to provide isolation for the transistor switch.

Figure 3.3 a) show a bodeplot of a DC/DC Buck converter with a unity gain feedback, while Figure 3.3 b) shows the converter response when a PID control is added. The phase margin has improved and the gain is higher with the PID compensator.

The DC/DC Buck converter has an input voltage V_{in} = 24 volts, an output voltage V_o = 12 volts, the nominal switching frequency $f_{s(nominal)}$ = 100 kHz, L = 69 µH, and C = 220 µF.

Publication P [1] shows how to design a PID control for the three non-isolated DC/DC (Buck, Boost, and Buck-Boost) converters, using a look-up table. The Simulation model and the prototype of the system (converter plus PID control) are designed. The output voltage and inductor current are studied in steady-state and under dynamic conditions.

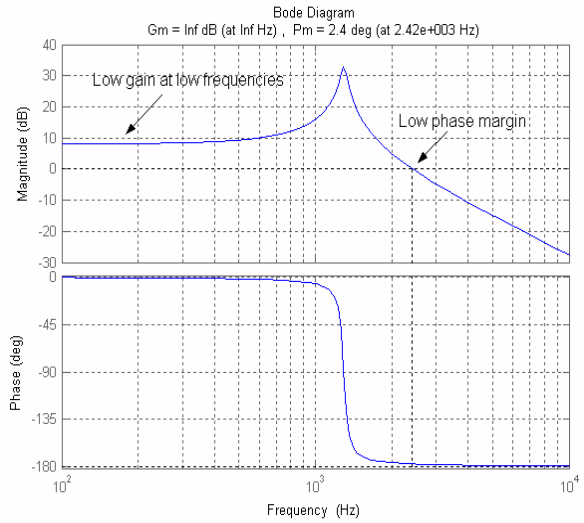

Figure 3.3 a). Bode plot of DC/DC Buck converter with unity gain feedback. The converter has a low gain at low frequencies and low φ_m = 2.4 degree at 2.42 kHz. So, a PID compensator is needed to improve the converter response.

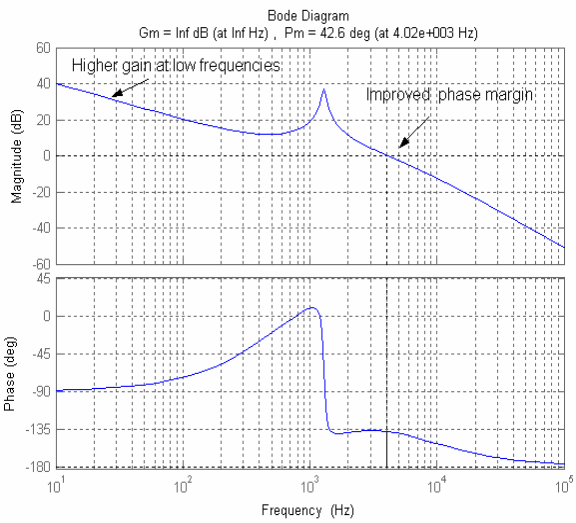

Figure 3.3 b). Bode plot of DC/DC Buck converter with PID control. The converter has a higher gain than without PID at low frequencies and an acceptable φ_m = 42.6 degree at 4 kHz. The converter response has improved.

The voltage feedback control has good static regulation properties and tends to be stable when reasonable values of gain are used. The dynamic performance is limited because a PID voltage control can not react to a disturbance until the effects have appeared in the converter output.

As PID is applied to DC/DC converters, the operating point dependency can become a challenge. Extra φ_m at one operating point does not guarantee extra φ_m at all points.

The PID control in P [1] depends on the small signal AC model, the controller can follow variations with a frequency smaller then the switching frequency.

3.5 Hysteresis Control

Hysteresis control has been applied to SMPSs (Mascarenhas 1992), (Leung 2003), and (Philip 1998). In this section, an explanation of the implementation of the hysteresis control in DC/DC converters is explained. Before that, a physical explanation of hysteresis control is given in terms of switching boundaries. Figure 3.4 describes that, as long as the output value remains within the boundary ($Output_{high}$, $Output_{low}$), then it can be said that the output is in normal steady-state condition. The high and low settings can be associated with the switching boundaries that determine the control action, and the switch action takes place when the state trajectory crosses the boundary.

When both high and low boundaries are used, the space between the two boundaries defines a *dead band* in which no control action takes place. If the system has one state variable and

both (on-off) levels of the system are the same, then the system might chatter and the (on-off) switching will be fast in an attempt to keep the operating state at the desired level.

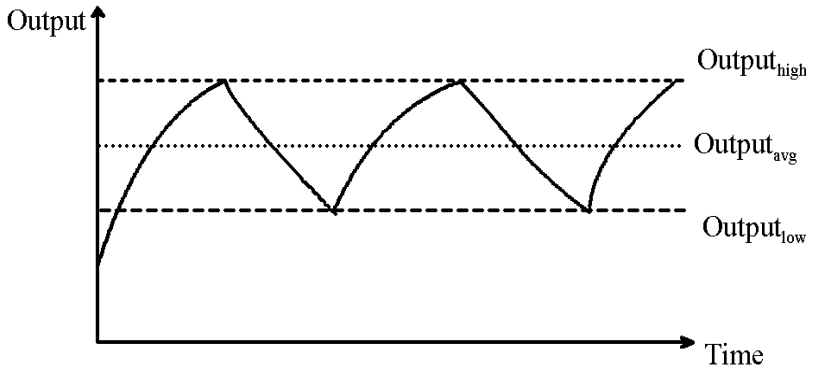

Figure 3.4. Boundaries of the output value with respect to time. The upper and lower boundaries are represented by the Output$_{high}$, and Output$_{low}$. The control action takes place when the state trajectory crosses the boundary.

In systems with two or more states, the extra dynamics of other states might prevent chattering. In power converters, however, the fast switching associated with chattering is destructive, and it is essential to avoid the behaviour. Therefore, the dead band is a typical feature of power electronic boundary control (Philip 1998).

As an example, it is given in Figure 3.5 a DC/DC Buck converter with a hysteresis control shown. The converter parameters are: input voltage V_{in} = 24 volts, output voltage V_o = 12 volts, output voltage ripple is set to be 1%, the nominal switching frequency $f_{s(nominal)}$ = 100 kHz, L = 69 μH, and C = 220 μF.

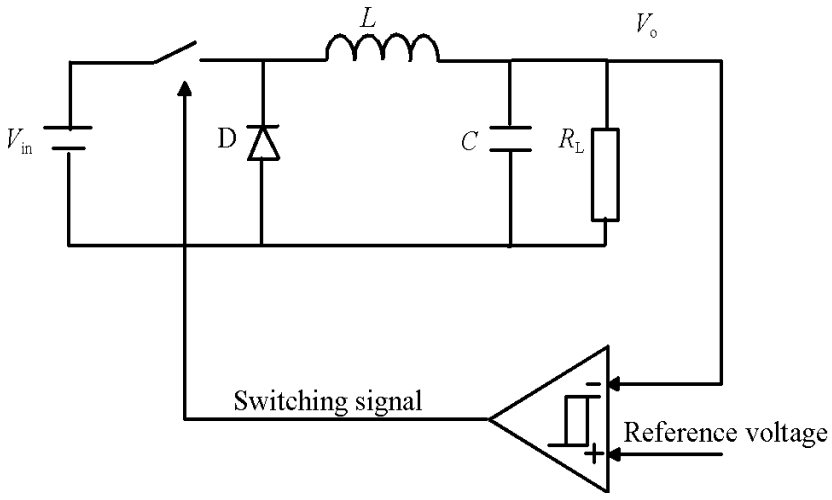

Figure 3.5. Hysteresis control of DC/DC Buck converter based on the output voltage.

Regardless of the voltage starts, the switch action pick up as soon as a boundary is encountered. The voltage rises from 0 to 12.12 volts at a rate limited by the L and C values. The transistor then turns off and remains off until the voltage falls to 11.88 volts. The specific switching times and state values are determined slowly by the action of the linear circuit.

Once the output voltage is between the boundaries, the switch action keeps it in the vicinity of the boundaries under all conditions. The general operation becomes independent of the line,

load, inductor, and capacitor values. The hysteresis control eliminates the output variations other than the ripple and this is called *robustness*. Figure 3.6 shows the behaviour of the DC/DC Buck converter under hysteresis control with the parameters given above.

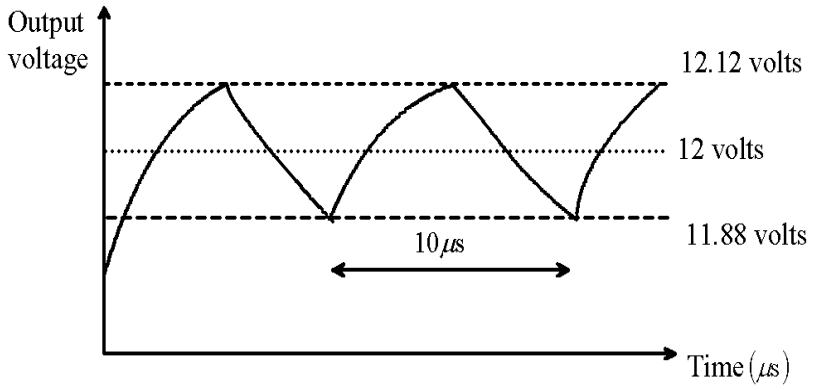

Figure 3.6. Time behaviour of DC/DC Buck converter under hysteresis control. The converter parameters are given above. The output voltage operates in the boundaries of 1% of the output voltage.

One disadvantage of this type of controller based on the output voltage is that it does not work with all kinds of converters. For example, in the case of the DC/DC Boost converter shown in Figure 3.7, starting from the zero voltage condition, the switch turns on and remains on since there is no energy flow to raise the output voltage.

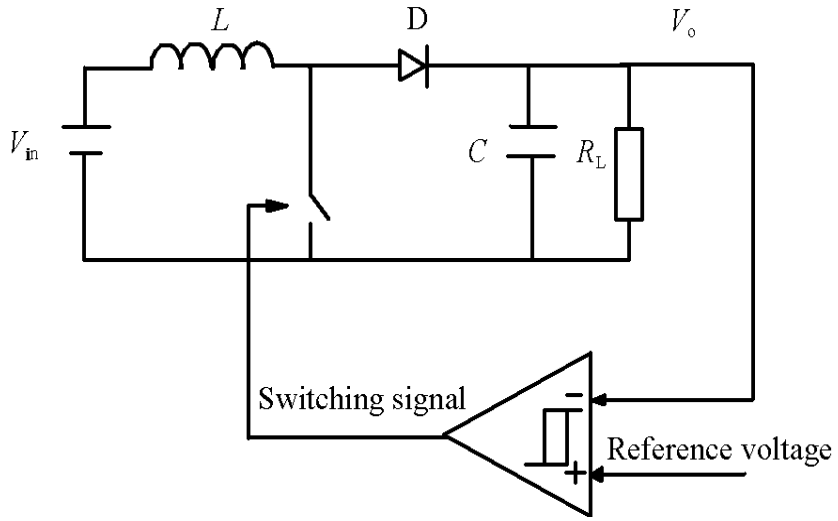

Figure 3.7. Hysteresis control for DC/DC Boost converter based on output voltage. From initial zero voltage condition, the switch turns on and remains on. Finally, there is no energy flow to raise the output voltage.

From the above discussion it can be stated that the switch should have a straight influence on the state variables so that the hysteresis control can operate correctly. For example, the DC/DC Buck converter: $V_L = V_{in} - V_o$ when the switch is on, and $V_L = -V_o$ when the switch is off, and it can be seen that V_o is involved in both cases.

For the DC/DC Boost converter: $V_L = -V_{in}$ when the switch on and $V_L = V_{in} - V_o$ when the switch is off, and it shown that the switch, being on, has no direct influence on V_o. Therefore, the hysteresis controller based on the output voltage implemented in a DC/DC Boost converter can not operate correctly.

In the case of the DC/DC Buck-Boost converter shown in Figure 3.8, the same problem arises since: $V_L = -V_{in}$ when the switch is on and: $V_L = -V_o$ when the switch is off, and again V_o is not involved when the switch is on.

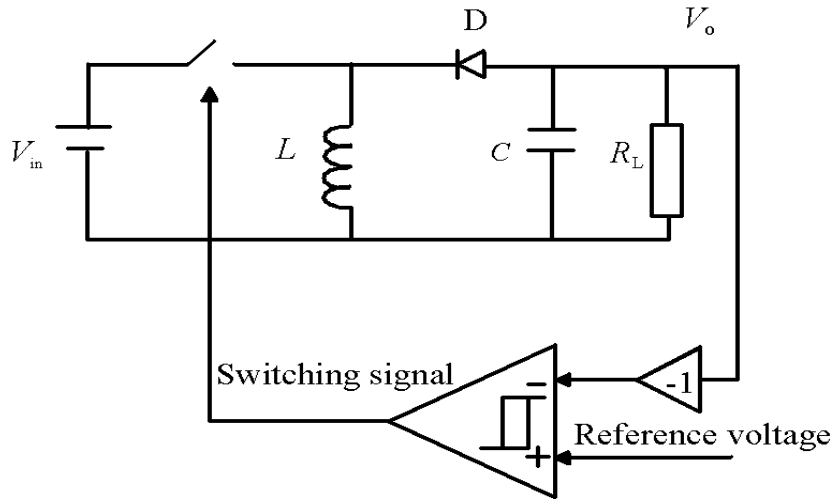

Figure 3.8. Hysteresis control for DC/DC Buck-Boost converter based on output voltage. From the initial zero voltage condition the switch turns on and remains on. Finally, there is no energy flow to raise the output voltage.

The hysteresis control can involve variables other than the output voltage; the inductor current is another variable that can be also controlled. The problem with this kind of control approach is that the control settings become load dependent. An analysis of the case of the DC/DC Buck converter parameters given above gives: $V_o = 12$ volts and a load value $R_L = 10\ \Omega$, the current settings is 1.2 A, while for $R_L = 1.2\ \Omega$ the current settings is 10 A.

The control performance is different when the inductor current is used as a feedback; the current reaches the boundary and then slides along it to the operating point. Many boundary controls have the attributes of the sliding mode control (SMC) (Philip 1998), in which the system dynamics are effectively governed by the boundary rather than the trajectory.

The current mode hysteresis control can be implemented using the two loops method. The error between the actual and desired voltage gives an additional current that must be delivered to the load. A PI block can use the voltage error signal to provide a current value for the hysteresis control. This is also called sliding mode control for a DC/DC converter, which is the subject of this research and will be discussed later in detail.

3.6 Adaptive Control

In some control tasks the systems to be controlled have parameter uncertainty at the beginning of the control operation. Unless such parameter uncertainty is gradually reduced by an adaptation or estimation mechanism, it may cause inaccuracy or instability for the control systems. In many other tasks, such as those in power systems, the system dynamics may have a well-known behaviour at the beginning, but it experiences unpredictable parameter variations as the control operation goes on.

Without a continuous re-design of the controller, the initially appropriate controller design may not be able to effectively control the changing plant. Generally, the basic objective of

adaptive control is to maintain the consistent performance of a system in the presence of uncertainty or unknown variation in plant parameters.

Two main means to approach the constructing of adaptive controllers can be mentioned:

- The Model-reference adaptive control method, and
- The Self-tuning method.

3.6.1 Model-Reference Adaptive Control Method

The model-reference adaptive control method shown in Figure 3.9 consists of four parts:

- A plant containing unknown parameters,
- A reference model for compactly specifying the desired output of the control system,
- A feedback control law containing adjustable parameters, and
- An adaptation mechanism for updating the adjustable parameters.

The plant is assumed to have a known structure, although the parameters are unknown. For linear plants, this means that the number of poles and the number of zeros are assumed to be known, but their location is unknown. For nonlinear plants, this implies that the structure of the dynamic equations is known, but that some parameters are unknown.

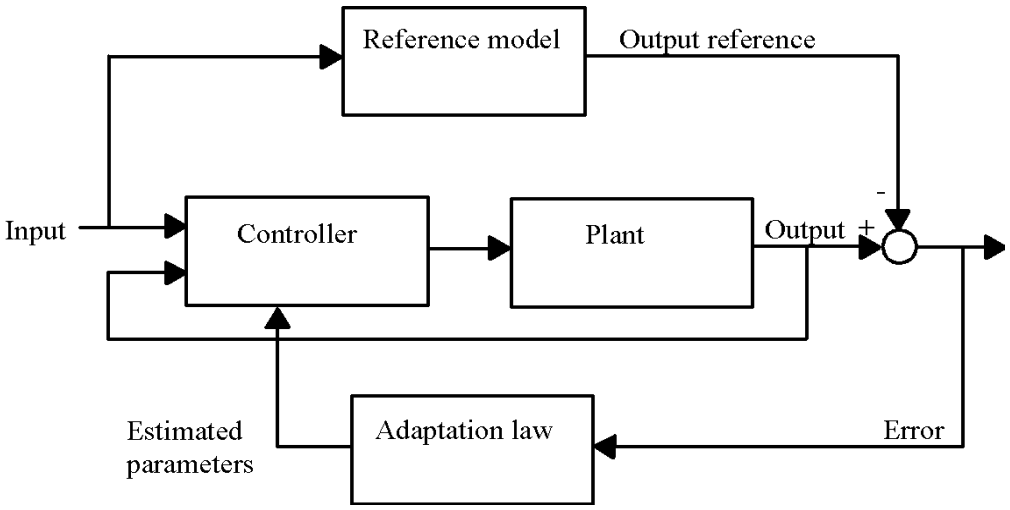

Figure 3.9. A model-reference adaptive control system showing the four main parts used in this model.

A reference model is used to specify the ideal response of the adaptive control system to the external command. It provides the ideal plant response which the adaptation mechanism should seek in adjusting the parameters. The choice of the reference model is part of the adaptive control design.

The controller is usually parameterized by a number of adjustable parameters. The controller should have perfect tracking capacity in order to allow the possibility of tracking convergence. That means that, when the plant parameters are exactly known, the corresponding controller parameters should make the plant output identical to that of the reference model.

When the plant parameters are unknown, the adaptation mechanism will adjust the controller parameters so that perfect tracking is asymptotically achieved. The adaptation mechanism is

used to adjust parameters in the control law. The main difference with the conventional control lies in the existence of this adaptation mechanism.

3.6.2 Self-Tuning Controller

A controller obtained by coupling a controller with an on-line (recursive) parameters estimator is called self-tuning controller. Figure 3.10 illustrates the schematic structure of such a controller.

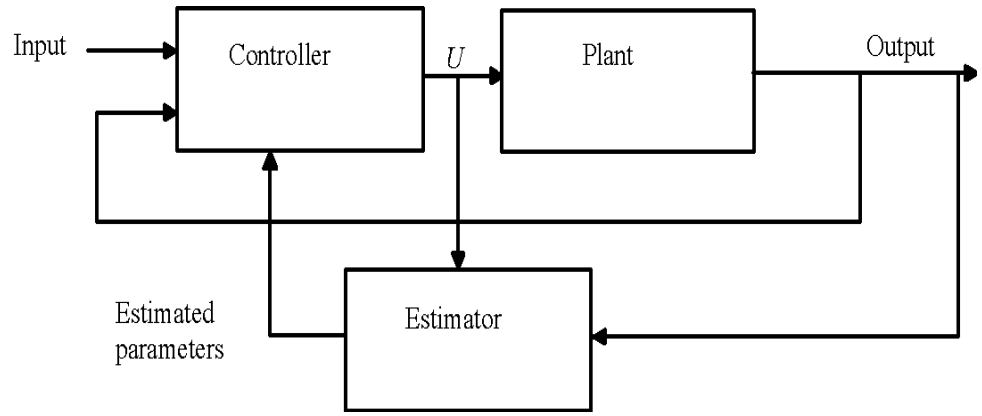

Figure 3.10. A self-tuning controller. The computer finds the corresponding controller parameters, and then computes *U* based on the controller parameters and measured signals.

The operation of a self-tuning controller proceeds as follows: at each time instant, the estimator sends to the controller a set of estimated plant parameters, which is computed based on the past plant input (*U*) and the output. The computer finds the corresponding controller parameters, and then computes *U* based on the controller parameters and measured signals. This *U* causes a new plant output to be generated, and the whole cycle of parameters and input updates is repeated.

In the basic approach to self-tuning control, estimation to the plant parameters is assumed then computing the controller parameters is done. Such a scheme is often called *indirect adaptive control*, because of the need to translate the estimated parameters into controller parameters. It is possible to eliminate this part of the computation. To do this, it can be noticed that the control law parameters and plant parameters are related to each other for a specific control method.

This implies the re-parameterising of the plant model using controller parameters that are also known, then applying standard estimation techniques to the model concerned. Since no translation is needed in this scheme, it is called direct adaptive control.

The essential function of the adaptation design is to synthesize an adaptation mechanism, which will guarantee that the control system remains stable and the tracking error converges to zero as the parameters are varied.

The general adaptive control provide an accurate way to control systems, but the complexity of the control method and its high cost makes this method not very suitable for switched mode power supply.

3.7 Current Programmed Control

Another control method used for SMPSs is the current programmed control (Peng 2004), (Erickson 1997). In this method the converter output is controlled by choosing a reference value for the peak transistor switch current $i_s(t)$. The control input signal is a current $i_{control}(t)$. The control circuit turns the switch on and off, so that the peak transistor current follows $i_{control}(t)$.

The switch duty cycle $d(t)$ is not directly controlled, but depends on $i_{control}(t)$, the inductor current, capacitor voltage, and power input voltage.

Figure 3.11 shows a block diagram of the current programmed control with the three non-isolated DC/DC (Buck, Boost, and buck-Boost) converters and the way they are connected.

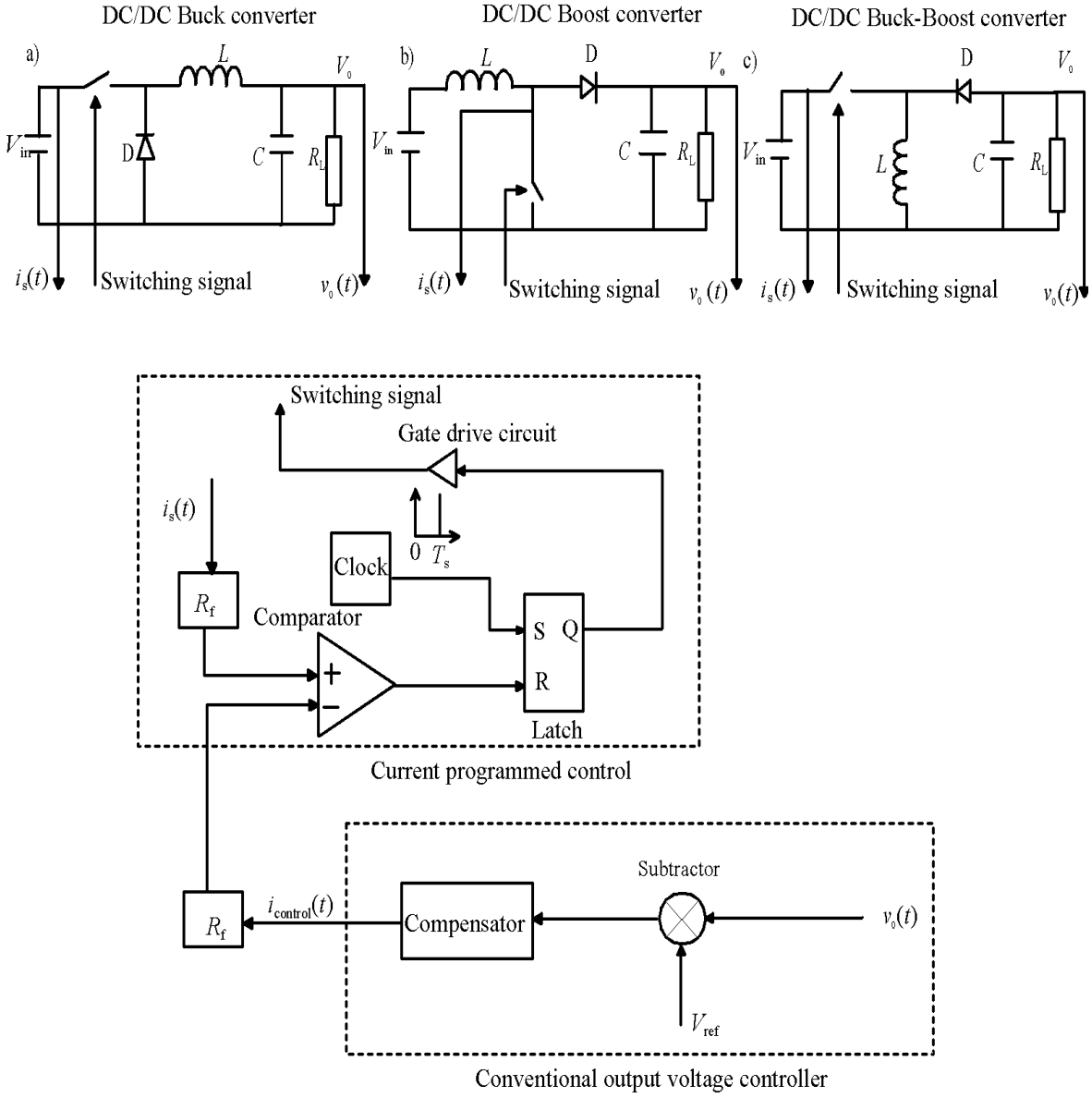

Figure 3.11. Block diagram showing the structure of the current programmed control for the three non-isolated DC/DC converters a) Buck, b) Boost, and c) Buck-Boost. The arrows show how each converter is connected to the controller. The peak transistor current replaces the duty cycle as the control input.

The controller functions in the following way: A clock pulse at the set input of a latch (S-R flip-flop) initiates the switching period. This causes the latch output Q to be high and to turn on the switch. While the switch is on the switch current, $i_s(t)$, which is equal to the inductor current $i_L(t)$, increases with a positive slope m_1. When $i_s(t)$ equals $i_{control}(t)$, the controller turns the switch off and $i_L(t)$ decreases for the remaining the switching period.

The controller must measure the switch current $i_s(t)$ with a current sensor circuit and compare $i_s(t)$ to $i_{control}(t)$ using an analog comparator. This can be done by multiplying both $i_s(t)$ and $i_{control}(t)$ by a scale, which is R_f. When $i_s(t) \geq i_{control}(t)$, the compensator resets the latch, turning the switch off for the remaining of the switching period.

The output voltage $V_o(t)$ is compared to the reference voltage V_{ref} to generate an error signal. This error signal is applied to the compensator circuit and the output of the compensator is multiplied by the scale (R_f). Figure 3.12 shows the control signal $i_{control}(t)$ and the switching current $i_s(t)$ waveforms.

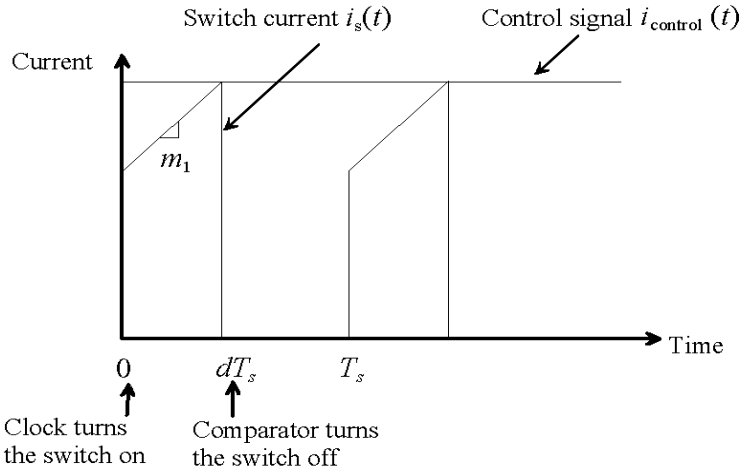

Figure 3.12. The switch current $i_s(t)$ and control input $i_{control}(t)$ waveforms for the current programmed control circuit. The switch turns off whenever $i_s(t) \geq i_{control}(t)$.

The advantage of this control method is that the control to output transfer function $v_o(s)/i_{control}(t)$ contains one less pole than $v_o(s)/d(s)$, regardless of the converter topology (Erickson 1997). Nonetheless, a wide bandwidth output voltage control can be obtained without needing a lead compensator network.

The disadvantages of the current programmed control are: firstly, its susceptibility to noise in $i_s(t)$ or $i_{control}(t)$ signals. This noise can reset the latch, which disrupts the operation of the controller. A filtering is necessary for the sensed switch current waveform to remove the turn-on current spikes caused by the stored charge of the diode.

Secondly, the current programmed control loses its stability when the average duty cycle $D > 0.5$. Equation (3.3) (Erickson 1997) shows that after a finite switching cycle the perturbation in the inductor current will increase. This growing oscillation saturates the current programmed controller after a finite switching period. If $D < 0.5$, then the disturbance in the inductor current waveform becomes small in magnitude after few switching periods.

Figures 3.13.a) and b) show the inductor current waveform controlled by current programmed control with $D = 0.7$ and $D = 0.3$, respectively. When $D = 0.7$ the perturbation increases by a

factor of $(D/1\text{-}D)^n$ every switching cycle, while for $D = 0.3$ the perturbation decreases by the same factor every switching cycle.

$$i_{\mathrm{L}}(nT_{\mathrm{s}}) = i_{\mathrm{L}}(0)\left(-\frac{D}{1-D}\right)^{n}, \tag{3.3}$$

where n: is the number of switching periods.

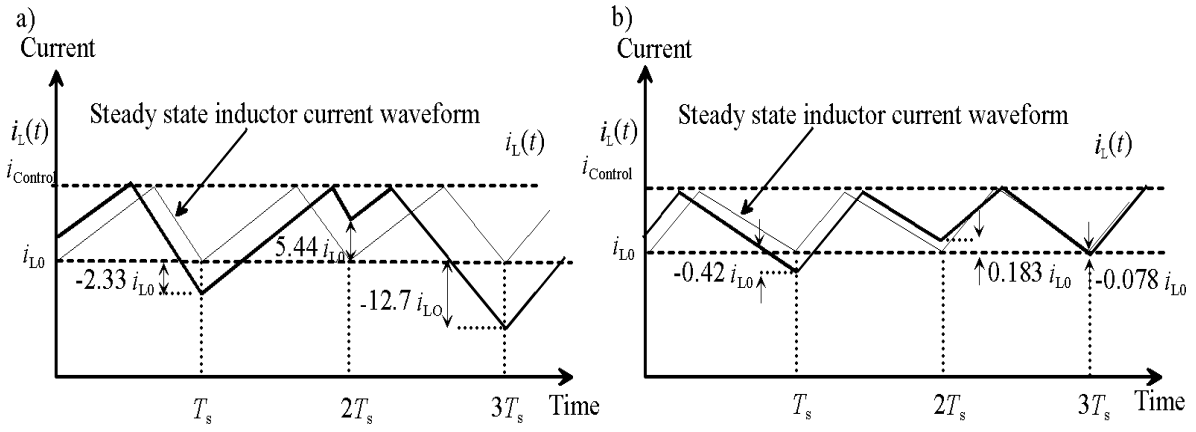

Figure 3.13. a) Unstable oscillation when $D = 0.7$, it can be seen that the perturbation increases by a factor of $(D/1\text{-}D)^n$ every switching cycle. b) Stable oscillation when $D = 0.3$, in this case the perturbation decreases by a factor of $(D/1\text{-}D)^n$ every switching cycle.

The instability problem for $D > 0.5$ is a common problem in the current programmed control for all DC/DC converter topologies. The problem of instability can be solved for all duty cycles by adding an artificial ramp to the sensed switched current waveform. This is shown in Figure 3.14, where the controller turns the switch off when

$$i_{\mathrm{a}}(dT_{\mathrm{s}}) + i_{\mathrm{s}}(dT_{\mathrm{s}}) = i_{\mathrm{control}}\,. \tag{3.4}$$

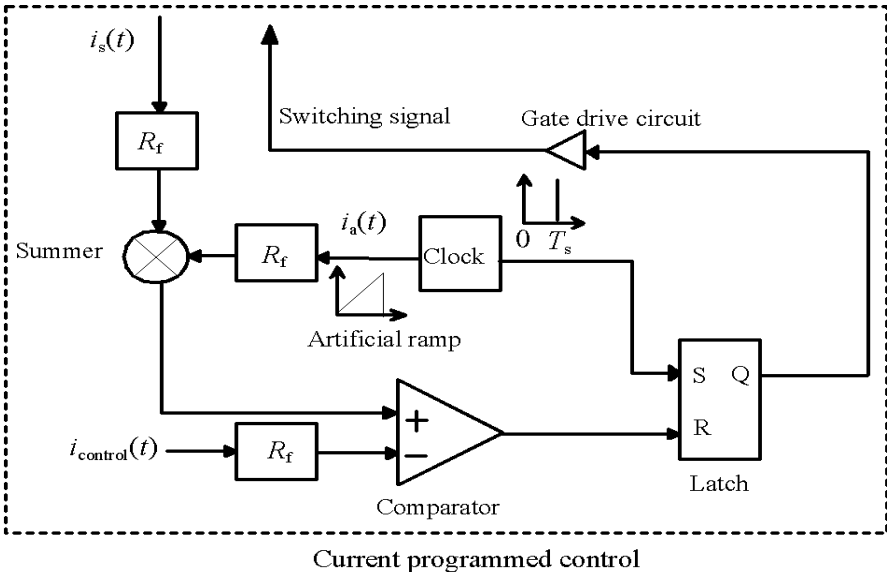

Figure 3.14. Stabilization of the current programmed control by an addition of an artificial ramp to the measured switch current. The switch turns off when equation (3.4) is satisfied.

3.8 Variable Structure Control System (VSCS)

The Variable Structure Control System **(**VSCS), as the name suggests, is a class of systems whereby the control law is deliberately changed during the control process according to some defined rules that depend on the state of the system. Researches and applications of VSCS to converters have been considered (Nicolas 1995), (Jacobina 2001), and (Soumitro 2001).

For the purpose of illustration, a double integrator system with feedback loop is shown in Figure 3.15 and given by equation (3.5).

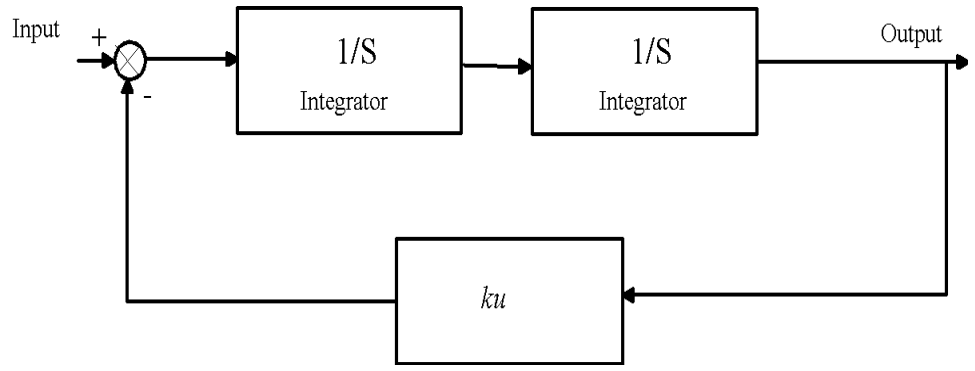

Figure 3.15. A simplified block diagram of a second order system (double integrator) with feedback control used for the purpose of explaining the principle of the variable structure control system (VSCS).

$$\ddot{y}(t) = u(t), \tag{3.5}$$

where *u(t)* is the control signal. Initially considering the effect of using the feedback control law

$$u(t) = -k\, y(t), \tag{3.6}$$

where *k* is strictly a positive scalar, and *y(t)* is the output. One way of analyzing the resulting closed-loop motion is the use of a phase portrait, which is essentially a plot of velocity against position. Substituting equation (3.6) into (3.5) and multiplying the result by $\dot{y}$ leads to

$$\dot{y}\ddot{y} = -k\, y\dot{y}. \tag{3.7}$$

Integrating equation (3.7) gives the following relationship between velocity and position

$$\dot{y}^2 + ky^2 = c, \tag{3.8}$$

where *c* represents a constant of integration resulting from the initial conditions and is strictly positive. Importantly, time does not appear explicitly in equation (3.8). A plot of $\dot{y}$ against y is an ellipse that depends on the initial conditions; this is shown in Figure 3.16.

It can be said that the control law in equation (3.6) is not appropriate since, as shown in Figure 3.16, the $\dot{y}$ and y variables do not move toward the origin (the closed-loop is stable, it is not, however, asymptotically stable).

To obtain an asymptotically stable system, the following control law can be considered

$$u(t) = \begin{cases} -k_1\, y(t) & \text{if } y\dot{y} < 0 \\ -k_2\, y(t) & \text{otherwise} \end{cases}, \qquad (3.9)$$

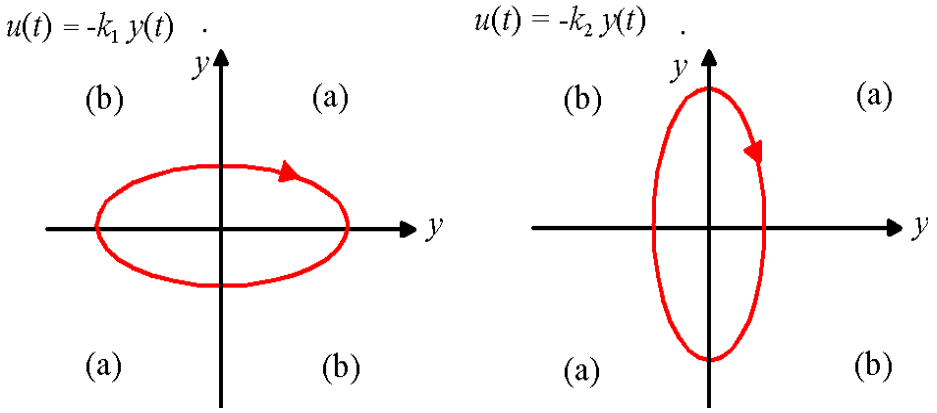

Figure 3.16. Phase property of simple harmonic motion, the trajectories are stable but not asymptotically stable.

where $0 < k_1 < 1 < k_2$. The phase plane (y, $\dot{y}$) is partitioned by the switching rule into four quadrants separated by the axis as shown in Figure 3.16. The control law $u = -k_2\, y$ will be in effect in the quadrants of the phase plane labeled (a). In this region, the distance from the origin of the points in the phase portrait decreases along the system trajectory.

Likewise, in region (b), when the control law $u = -k_1\, y$ is in operation, the distance from the origin of the points in the phase portrait also decreases. This system clearly fits the description of a VSCS mentioned earlier.

For the phase portrait of the closed-loop system under the VSC law, u is obtained by splicing together the appropriate regions from the two phase portrait in Figure 3.16. In this way the phase portrait must spiral in towards the origin and an asymptotically stable motion results, as it is shown in Figure 3.17.

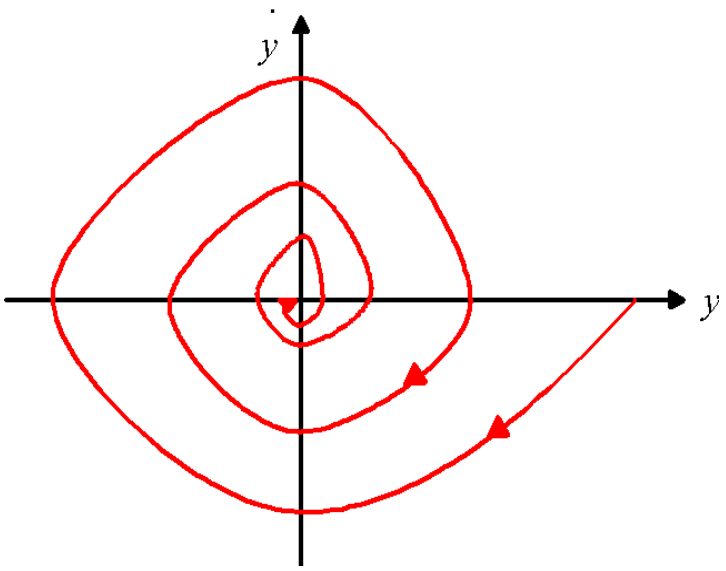

Figure 3.17. Phase portrait of the system under the VSCS, the trajectory is moving toward the origin and is asymptotically stable.

3.9 Sliding Mode Control (SMC)

An approach that complies with the non-linear nature of switch-mode power supplies is represented by the SMC, which is derived from the VSCS theory. This control method offers several advantages over the other control methods (Mattavelli 1993), (Rossetto 1994), (Spiazzi 1997), (Forsyth 1998), (Utkin 1999 a), (Castilla 2000), (Alarcon 2001), which are:

- Stability even for large line and load variations,
- Robustness,
- Good dynamic response, and
- Simple implementation.

Variable structure systems (VSS) are systems the physical structures of which are changed intentionally during time with respect to the structure control law. The instances at which the changing of the structure occurs are determined by the current state of the system. From this point of view, switch-mode power supplies represent a particular class of the VSS, since their structure is periodically changed by the action of controlled switches and diodes.

The SMC for VSS offers an alternative way to implement a control action, which exploits the inherent variable structure nature of DC/DC converters. In practice, the converter switches are driven as a function of the instantaneous values of the state variables in a way that forces the system trajectory to stay on a suitable selected surface in the state space called the *sliding surface*. The most remarkable feature of the SMC is its ability to result in a robust control system.

3.9.1 Principle of Sliding Mode Control

A more significant example results using the variable structure law of equation (3.9) is given by

$$u(t) = \begin{cases} -1 & \text{if } s(y, \dot{y}) > 0 \\ +1 & \text{if } s(y, \dot{y}) < 0 \end{cases}, \tag{3.10}$$

where the switching function is defined by

$$s(y, \dot{y}) = k\, y + \dot{y}\,, \tag{3.11}$$

where k is a positive design scalar. The reason for the use of the term 'switching function' is clear, since the function given in equation (3.11) is used to decide which control structure is in use at any point $(y, \dot{y})$ in the phase plane.

Equation (3.10) is usually written more concisely as

$$u(t) = -\text{sig}(s(t))\,, \tag{3.12}$$

where sgn(.) is the *signum*, or more colloquially, the sign function.

Equation (3.10) is used to control the double integrator. For large values of $\dot{y}$ the phase portrait is shown in Figure 3.18. The dotted line in the figure represents the set of points for

which $s(y,\dot{y})=0$; in this case a straight line through the origin of gradient –k. However, for values of $\dot{y}$ satisfying the inquiry $k|\dot{y}|<1$ then

$$\begin{cases} \lim_{s\to o^+} \dot{s} < 0 \\ \lim_{s\to o^-} \dot{s} > 0 \end{cases}. \tag{3.13}$$

When $k|\dot{y}|<1$ the system trajectories on either side of the line point towards the line

$$\sigma(s)=\{(y,\dot{y}) \ : \ s(y,\dot{y})=0\}. \tag{3.14}$$

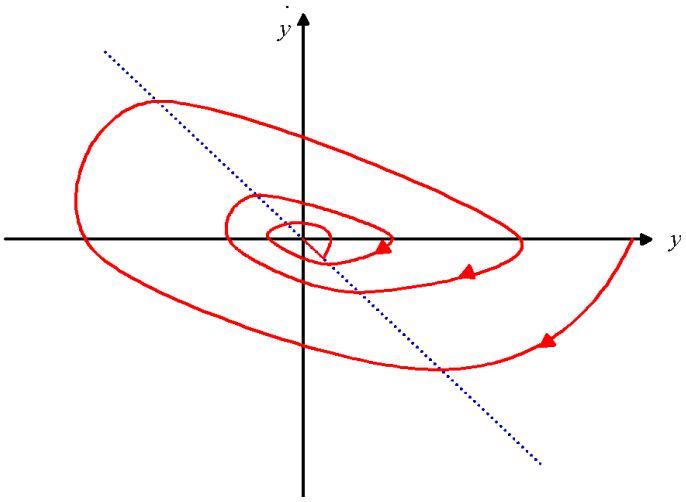

Figure 3.18. Phase portrait of the system for large $\dot{y}$. The dot line represents the sliding line and the trajectory moves toward the sliding line.

This is demonstrated in Figure 3.19, which shows different phase portraits intercepting the same point on the line σ(s) from different initial conditions.

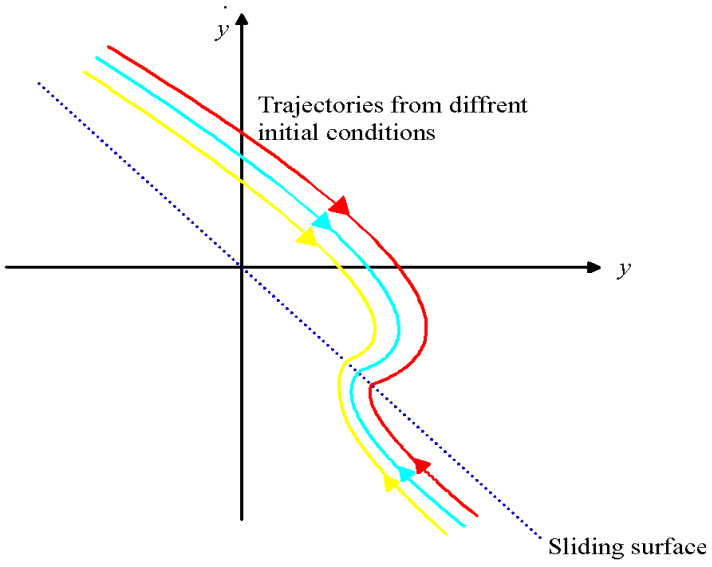

Figure 3.19. Phase portrait of the system under VSC near the origin. Different trajectories move toward the sliding line from different initial conditions.

If infinite switching frequency were possible, the motion would be trapped or constrained to remain on the line σ(*s*). The motion, when confined to the line σ(*s*) satisfies the differential equation obtained from re-arranging $s(y, \dot{y}) = 0$, namely

$$\dot{y}(t) = -k\, y(t) \ . \tag{3.15}$$

This represents first-order decay and the trajectory will slide along the line σ(*s*) to the origin, this is shown in Figure 3.20. Such a dynamical behaviour is described as an ideal sliding mode or an ideal sliding motion, and the line σ(*s*) is termed the *sliding surface*.

During sliding motion, the system behaves as a reduced-order system that is apparently independent of the control. The control action ensures instead that the conditions in equation (3.14) are satisfied, this guarantees that $s(y, \dot{y}) = 0$.

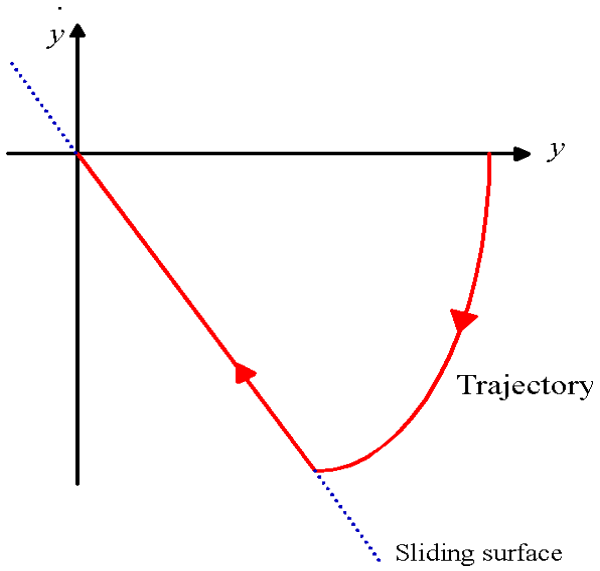

Figure 3.20. Phase portrait of a sliding motion. The control law in equation (3.14) ensures that the trajectory moves toward the sliding surface σ(*s*).

3.10 Summary

This chapter focused on different control methods (PID control, Hysteresis control, Adaptive control, Current programme control, VSC, and SMC) used to control DC/DC converters. An explanation of each control methods with its advantages and disadvantages was given. In general, the control methods can be classified into linear and non-linear control methods.

A comparison between the characteristics of linear and non –linear control methods are given below:

- Linear control methods rely on the key assumption of small range operation for the linear model to be valid. When the required operation range is large, a linear controller is likely to perform very poorly or to be unstable, because the non-linearities in the system can not be properly compensated for non-linear controllers, on the other hand, may handle the non-linearity in large range operation directly,
- In designing linear controllers, it is usually necessary to assume that the parameters of the system model are reasonably well known. However, many control problems involve uncertainties in the model parameters; this may be due to a slow time variation

of the parameters. A linear controller based on inaccurate or obsolete values of the model parameters may exhibit significant performance degradation or even instability. Non-linearities can be intentionally introduced into the controller part of a control system so that model uncertainties can be tolerated,

• Linear control may require high quality actuators and sensors to produce linear behaviour in the specified operation range, while non-linearities may permit the use of less expensive components with non-linear characteristics, and

• Good non-linear control designs may be simpler and more intuitive than their linear control parts. This result comes from the fact that non-linear controller designs are often rooted in the physics of the plant.

The SMC was discussed in the final section and the reason of selecting the SMC as a control method in this research was explained.

4. SLIDING MODE CONTROL

4.1 Introduction

In the formulation of any control problem there will, typically, be discrepancies between the actual plant and the mathematical model developed for controller design. This mismatch may be due to the variation in system parameters or the approximation of complex plant behaviour by a straightforward model.

It must be carefully ensured that the resulting controller has the ability to produce the required performance levels in practice despite of the plant/model mismatches. This aroused intense interest in the development of robust control methods, which seeks to solve this problem. The SMC methodology gives one particular approach to robust controller design.

The SMC is a particular type of the VSCS, which is characterized by a suite of feedback control laws and a decision rule. The decision rule, termed the switching function, has at its input some measure of the current system behaviour and produces as an output the particular feedback controller, which should be used at that instant of time. A VSS may be regarded as a combination of subsystems, where each subsystem has a fixed control structure and is valid for specified regions of the system behaviour.

Introducing this additional complexity into the system renders the ability to combine useful properties of each of the composite structures of the system. Furthermore, the system may be designed to possess new properties not present in any of the composite structures alone.

The utilization and development of these ideas began in the Soviet Union in the late 1950's. The VSCS evolved out of the pioneering work done in Russia by Emel'yanov and Barbashin in the early 1960s. The idea did not appear outside Russia until the mid 1970s, as Itkis' book and Utkin's survey paper were published in English.

In the SMC, the VSCS is designed to drive and then constrain the system state to lie within the neighborhood of the switching function. This approach has two advantages:

- The dynamic behaviour of the system may be tolerated by the particular value reference chosen for the switching function, and
- The closed-loop response becomes totally insensitive to a particular class of uncertainty.

The latter invariance property clearly makes the methodology an appropriate candidate concept for robust control. In addition, the ability to directly specify the performance makes the SMC attractive from the design perspective.

Prof. Utkin is one of the originators of the concepts of VSS and SMC. He is an author of five books and more than 280 technical papers. His current research interests are control of infinite-dimensional plants including flexible manipulators, sliding modes in discrete time systems and microprocessor implementation of SMC, control of electric drives and alternators, robotics and automotive control. Some of his most interested researches are:

(Utkin 1992) presented a new control approach based on discrete-time sliding modes. The ideal case in which the parameters are known was first analyzed and a new definition of the

equivalent control was obtained, which is defined as the continuous control that reduces to zero, in finite time, the distance of the system state from the sliding manifold in correspondence with the sampling interval. Then, under the assumption of the bounded parametric uncertainties, an adaptive control scheme that guarantees the asymptotic satisfaction of the same control objective was designed and coupled with the variable structure control strategy.

(Utkin 1994) developed sliding mode based design methods for the control of manipulators, mobile robots operating in workspace with obstacles, railway wheel-set and flexible shaft. The core idea of the design rested upon the utilization of a state sub-vector as an intermediate control.

(Utkin 1996) presented a model based approach to the problem of automobile power-train monitoring. A model for a discrete crank-angle domain model was derived. A procedure for designing discrete sliding mode observers, for state and input estimation was presented and applied to the power-train estimation problem. The sliding observers were used in the nonlinear parity equation residual generation scheme for fault detection and isolation. Experimental results were provided to demonstrate that the designed observers estimated the power-train states with good accuracy, and that the monitoring scheme was effective in isolating both actuator and sensor faults.

(Utkin 1999 b) presented a SMC guideline for practicing control engineers. The guideline offered an accurate assessment of the chattering phenomenon, and a catalogs implementable SMC design solutions. It also provided a frame of reference for future SMC researches.

(Utkin 2000) developed the ideas of speed- and flux-sensorless SMC for an induction motor illustrated in the previous work by one of the authors. A sliding-mode observer/controller was proposed in this paper. The convergence of the nonlinear time-varying observer along with the asymptotic stability of the controller was analyzed. PWM implementation using sliding mode concepts was also discussed. Major attention was paid to the torque control and then the developed approach was utilized for speed control. Computer simulations and experiments were carried out to test the proposed estimation and control algorithm. The experimental results demonstrated high efficiency of the estimated and control method.

(Utkin 2001) described a new closed-loop approach to estimate the induction machine speed and rotor time constant from the measured terminal voltages and currents for the speed/torque sensorless control. For this purpose, a new state estimator, which eliminates the flux information of the machine, was defined and a Lyapunov function was derived to determine the speed and rotor resistance. The proposed algorithm was analyzed and verified experimentally.

(Utkin 2002) stated that in the practical electric machine control it is not desirable or possible to measure all the state variables needed for control implementation. A good observer-based method to obtain state variables to be used in the control law is always pursued by researchers. Observation algorithms make use of the machine model equations and allow the estimation of the rotor speed and/or flux from the motor terminal measurement of the current and voltage. He stated that, among different observation methods, the sliding mode observer is a promising approach. The paper attempted to provide a status review and synopsis of the main approaches used in the sliding mode observer design for electric machines. Both the induction machine and permanent magnet synchronous machine were treated in this paper.

The research work expanded from flux estimation and machine parameter estimation to the issue of sensorless control.

(Utkin 2004) designed a sliding mode stabilizing controller for synchronous generators based on the complete model of the plant. He used the block control approach in order to derive a nonlinear sliding surface on which the mechanical dynamics were linarized. The combined approach enabled to compensate the inherent non-linearities of the generator and to reject high-level external disturbances. A nonlinear observer was designed for the estimation of the rotor fluxes and mechanical torque.

4.2 Sliding Mode Control Researches and Applications in Electrical and Mechanical Systems

As the field of SMC applications is increasing, researchers are working to prove the efficiency of the SMC in electrical and mechanical systems. Lately, many researches have done research on the implementing of the SMC in electrical and mechanical systems. Some of the main fields of research on the subject are shown in Figure 4.1.

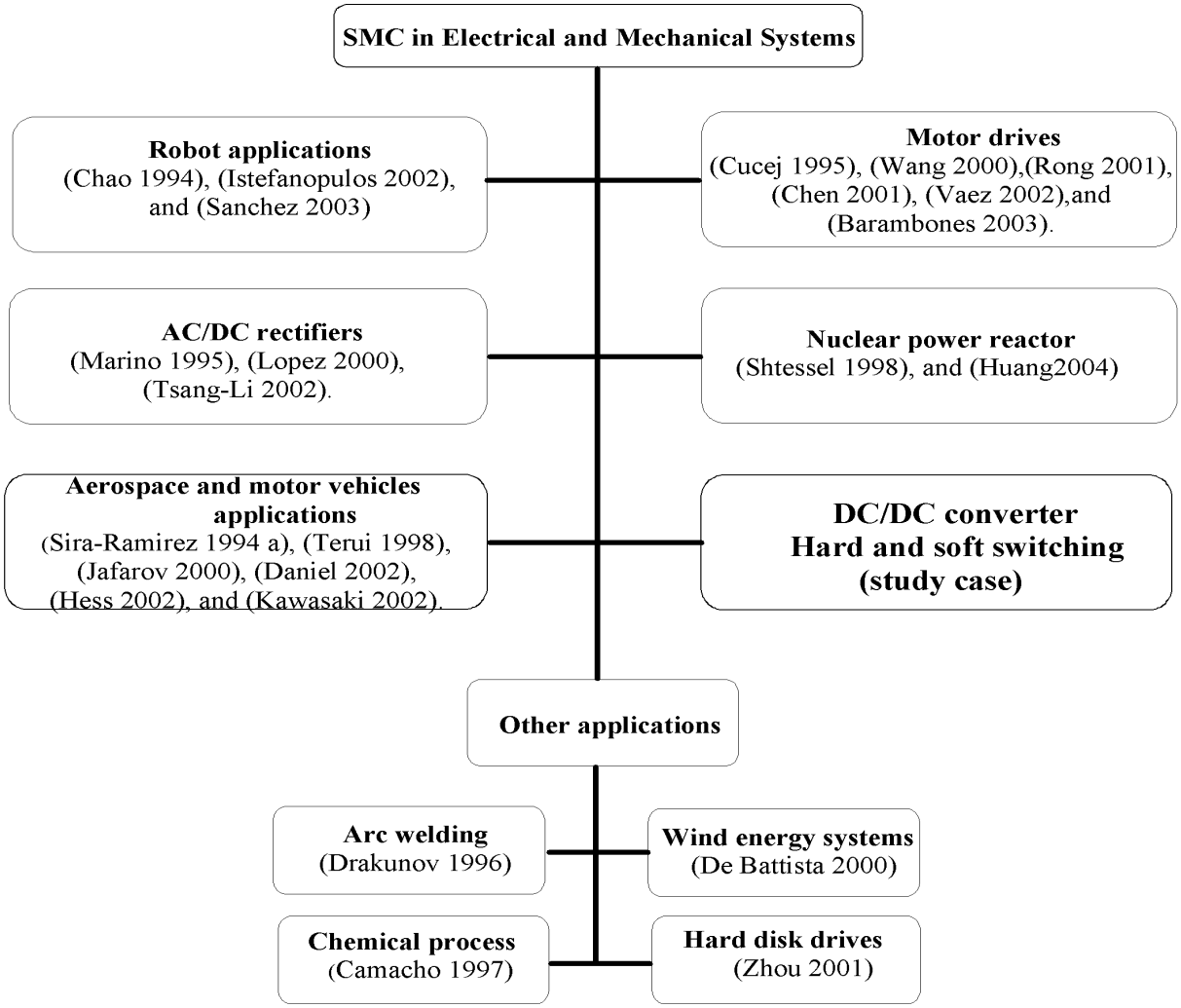

Figure 4.1. Applications of SMC in electrical and mechanical systems. The figure describes the six main areas where the SMC has been applied and widely investigated and also some other areas where less applications and researches can be shown, but which have a promising future.

4.3 Review of the Theory of Sliding Mode Control

The sliding mode design approach consists of two components. The first involves the design of a switching function so that the sliding motion satisfies the design specifications. The second is concerned with the selection of a control law, which will make the switching function attractive to the system state.

It can be seen that this control law is not necessarily discontinuous. Considering the following general system with scalar control

$$\dot{\boldsymbol{x}} = \boldsymbol{f}(\boldsymbol{x},t,u), \tag{4.1}$$

where $\boldsymbol{x}$ is the column vector, $\boldsymbol{f}$ is a function vector with n dimension, and u represents an element that can influence the system motion (control input).

Considering that the function vector $\boldsymbol{f}$ is discontinuous on the surface $\sigma(\boldsymbol{x}, t) = 0$, thus

$$\boldsymbol{f}(\boldsymbol{x},t,u) = \begin{cases} \boldsymbol{f}^{+}(\boldsymbol{x},t,u^{+}) & \text{for } \sigma \to 0^{+} \\ \boldsymbol{f}^{-}(\boldsymbol{x},t,u^{-}) & \text{for } \sigma \to 0^{-} \end{cases}. \tag{4.2}$$

The system is in sliding mode if its representative point (RP) moves on the sliding surface $\sigma(\boldsymbol{x}, t) = 0$.

4.3.1 Existence Condition

As stated previously, in order that the sliding mode can exist, the phase trajectories of the two substructures corresponding to the two different values of the vector function $\boldsymbol{f}$ must be directed toward the sliding surface $\sigma(\boldsymbol{x}, t) = 0$.

In other words, while approaching the sliding surface from the points which satisfy ($\sigma < 0$), the corresponding state velocity vector $\boldsymbol{f}^{-}$ must be directed toward the sliding surface, and the same happens for the points above the surface ($\sigma > 0$) for which the corresponding state velocity vector is $\boldsymbol{f}^{+}$.

Indicating with subscript N the components of the state velocity vectors $\boldsymbol{f}^{+}$ and $\boldsymbol{f}^{-}$ orthogonal to the sliding surface, the following equation can be written

$$\begin{aligned} \lim_{\sigma \to 0^{+}} \boldsymbol{f}_{\mathrm{N}}^{+} < 0 \quad &\Rightarrow \quad \lim_{\sigma \to 0^{+}} \nabla\sigma\, \boldsymbol{f}^{+} < 0 \\ \lim_{\sigma \to 0^{-}} \boldsymbol{f}_{\mathrm{N}}^{-} > 0 \quad &\Rightarrow \quad \lim_{\sigma \to 0^{-}} \nabla\sigma\, \boldsymbol{f}^{-} > 0 \end{aligned}. \tag{4.3}$$

Since

$$\frac{d\sigma}{dt} = \sum_{i=1}^{n} \frac{\partial\sigma}{\partial x_{\mathrm{i}}} \frac{dx_{\mathrm{i}}}{dt} = \nabla\sigma\, \boldsymbol{f}. \tag{4.4}$$

The existence condition of the sliding mode becomes

$$\begin{matrix} \lim\limits_{\sigma\to 0^+} \dfrac{d\sigma}{dt} < 0 \\ \lim\limits_{\sigma\to 0^-} \dfrac{d\sigma}{dt} > 0 \end{matrix} \quad \Rightarrow \quad \lim_{\sigma\to 0} \sigma \frac{d\sigma}{dt} < 0 \,. \tag{4.5}$$

When the inequality given in equation (4.5) holds in the entire state space and not only in the region around the sliding surface, then this condition is also sufficient condition for the system to reach the sliding surface.

4.3.2 Reaching Condition

In this section, an illustration on a simple sufficient condition for the system to reach the sliding regime, which will be used later with respect to the application of the SMC to switching power supplies, is given. Considering again the system $\dot{\boldsymbol{x}} = \boldsymbol{f}(\boldsymbol{x}, t, u)$ for which the scalar discontinuous input u is given by

$$u = \begin{cases} u^+ & \text{for} \quad \sigma(\boldsymbol{x}) > 0 \\ u^- & \text{for} \quad \sigma(\boldsymbol{x}) < 0 \end{cases}. \tag{4.6}$$

Let $[\boldsymbol{x}^+]$ and $[\boldsymbol{x}^-]$ be the steady-state RP corresponding to the inputs u^+ and u^-, where $\mathbf{x}$ is a column vector. Then, a sufficient condition for the system to reach the sliding surface is given by

$$\begin{matrix} \left[\boldsymbol{x}^+\right] \in \sigma(\boldsymbol{x}) < 0 \\ \left[\boldsymbol{x}^-\right] \in \sigma(\boldsymbol{x}) > 0 \end{matrix}. \tag{4.7}$$

In other words, if the steady-state point for one substructure belongs to the region of the phase space reserved to the other substructure, then sooner or later the system RP will hit the sliding surface.

4.3.3 System Description in Sliding Mode

In making an analysis of the VSS, it is next focused on the behaviour of the system operating in sliding regime. Equation (4.8) defines a particular class of systems that are linear with the control input, i.e.

$$\dot{\boldsymbol{x}} = \boldsymbol{f}(\boldsymbol{x}, t) + \boldsymbol{B}(\boldsymbol{x}, t)u \,. \tag{4.8}$$

The scalar control input u is discontinuous on the sliding surface $\sigma(x, t) = 0$, while f and B are continuous function vectors. Under SMC, the system trajectories stay on the sliding surface

$$\sigma(\boldsymbol{x}, t) = 0 \quad \Rightarrow \quad \dot{\sigma}(\boldsymbol{x}, t) = 0 \,, \tag{4.9}$$

$$\dot{\sigma}(\boldsymbol{x},t) = \frac{d\sigma}{dt} = \sum_{i=1}^{n} \frac{\partial \sigma}{\partial x_i} \frac{dx_i}{dt} = \nabla \sigma \, \dot{\boldsymbol{x}} = \boldsymbol{G} \, \dot{\boldsymbol{x}} \,, \tag{4.10}$$

where $\boldsymbol{G}$ is a 1 by n matrix, the elements of which are the derivatives of the sliding surface with respect to the state variables (gradient vector). Using equations (4.8) and (4.10) leads to

$$\boldsymbol{G}\,\dot{\boldsymbol{x}} = \boldsymbol{G}\,\boldsymbol{f}(\boldsymbol{x},t) + \boldsymbol{G}\,\boldsymbol{B}(\boldsymbol{x},t) u_{\text{eq}} = 0 \,, \tag{4.11}$$

where the control input u was substituted by an equivalent control u_{eq} that represents an equivalent continuous control input, which maintains the system evolution on the sliding surface.

Substituting equation (4.11) into equation (4.8) gives (see Appendix A.4)

$$\dot{\boldsymbol{x}} = \left[\boldsymbol{I} - \boldsymbol{B}(\boldsymbol{G}\boldsymbol{B})^{-1}\boldsymbol{G}\right] \boldsymbol{f}(\boldsymbol{x},t) \,. \tag{4.12}$$

Equation (4.12) describes the system motion under SMC. It is important to note that the matrix $\boldsymbol{I} - \boldsymbol{B}(\boldsymbol{G}\,\boldsymbol{B})^{-1}\boldsymbol{G}$ is less than the full rank. This is because, under sliding regime, the system motion is constrained to be on the sliding surface. As a consequence, the equivalent system described by equation (4.12) is of the order n-1.

This equivalent control description of the VSS in sliding regime is valid also for multiple control inputs. In this case, the system motion is constrained on the hyper surface obtained by the intersection of the individual switching surface S_{i} ($\boldsymbol{x}$, t) = 0 i.e.

$$\sigma = \left[S_1, S_2, ..., S_{\text{m}}\right]^T = 0 \,. \tag{4.13}$$

In this case equations (4.11) and (4.12) are still valid provided that u_{eq} is now an equivalent vector and $\boldsymbol{G}$ is an m by n matrix.

4.3.4 Chattering

The chattering phenomenon is understood to be an oscillatory motion in the neighbourhood of the sliding manifold. Possible mechanisms that cause chattering include non- idealities of switching devices for control realization or the existence of parasitic dynamics in series with the plant. The chattering phenomenon shown in Figure 4.2 is unavoidable in the real application of the SMC.

(Bondarev 1985) showed that chattering caused by un-modeled dynamics may be eliminated in systems with asymptotic observers, in which the observers serve as a bypass for high frequency components.

An alternative approach suggestion is a continuous approximation of discontinues control. In many cases, this is not a remedy for the problem since the slop in linear approximations must be adjusted to avoid excitation of the un-modeled dynamics. In addition to that, continuous approximation is unpractical in switching converters related systems, in which the on-off operation is the particular way of operating.

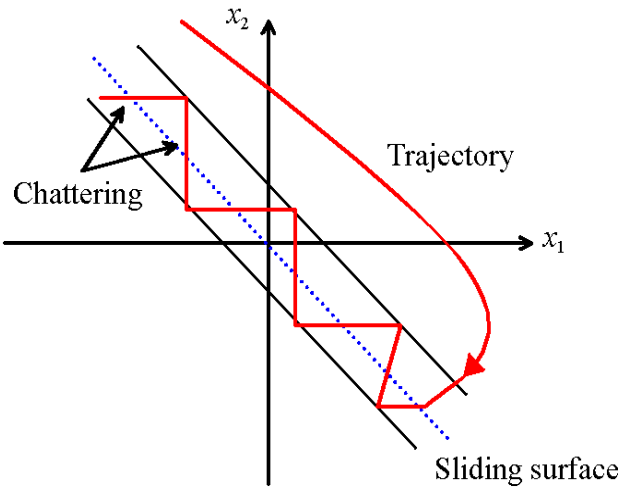

Figure 4.2. Chattering phenomenon in SMC due to non-linearity of the system. The trajectory moves toward the sliding line and oscillates in a defined boundary.

4.4 Sliding Mode Control for DC/DC Converters

As it was mentioned, one of the most important features of the sliding mode regime in the VSS is the ability to achieve response that is independent of the system parameters. From this point of view, the DC/DC converter is particularly suitable for the application of the SMC, because of its controllable state ‘‘the system is controllable if every state variable can be affected by an input signal’’. The output voltage and its derivative are both continuous and accessible for measurement.

For DC/DC converters used in practice, the motion rate of the current is much faster than the motion rate of the output voltage. The control problem can be solved by using cascaded control structure with two control loops: an inner current control loop, and an outer voltage control loop. The combined loops represent the SMC.

The voltage control is usually realized with standard linear control techniques, while the current control is implemented using either PWM or hysteresis control. Here the sliding mode approach is used for the control of inductor current. Figure 4.3 shows the general structure of SMC for DC/DC converters.

This general approach can be implemented to any of the three non-isolated DC/DC (Buck, Boost, and Buck –Boost converters). This can be proved with the publications in this research work, where:

- P [2] implements this method in DC/DC (Buck, and Buck-Boost) converters using Matlab/Simulink™,
- P [3] Implements analog SMC with op-amp to control DC/DC Buck converter, and
- P [5] Implements a digital SMC represented by dSPACE™ to control the DC/DC Buck Boost converter.

This SMC approach can also be extended to be implemented in DC/DC resonant converters. This can be found in P [8], and P [9], where the SMC was implemented in half-wave zero current switching (HWZCS) DC/DC Buck converter. The implementation was proved by both simulation and prototype.

The main problem of this control method is that there is no direct way to measure the gain of linear part, which can be considered as a drawback and this can be found in P [2]. One possible way is to apply a step response and select a suitable gain to the specified application.

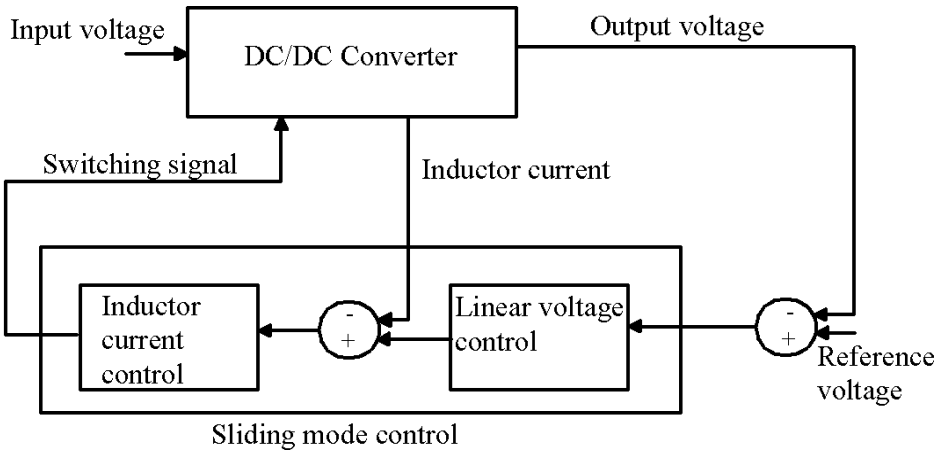

Figure 4.3. A block diagram showing the structure of SMC for DC/DC converters. The control structure consists of two control loops: a linear voltage loop, and a non-linear current loop. The combined loops are the SMC.

4.4.1 Phase plane Description of SMC for DC/DC Buck Converter

For DC/DC converters, the inductor current and the capacitor voltage are selected as the state variables. For the DC/DC Buck converter shown in Figure 4.4, it is more convenient to use a system description, which involves the output error and its derivative (Mattavelli 1997), i.e.

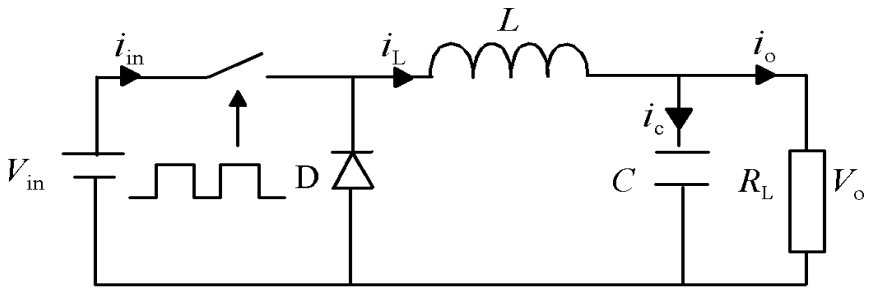

Figure 4.4. The DC/DC Buck converter topology, showing the component used in the structure and the way they are connected.

$$\begin{cases} x_1 = V_o - V_{ref} \\ x_2 = \dfrac{dx_1}{dt} = \dfrac{dv}{dt} = \dfrac{i_c}{C} \end{cases}, \tag{4.14}$$

where V_{ref} represents the reference voltage, V_o is the output voltage, and i_c denotes the capacitor current. Considering the CCM operation, the system equations in terms of the state variables x_1 and x_2 can be written as follow (see Appendix A.5)

$$\begin{cases} \dot{x}_1 = x_2 \\ \dot{x}_2 = -\dfrac{x_1}{LC} - \dfrac{x_2}{R_L C} + \dfrac{V_{in}}{LC}u - \dfrac{V_{ref}}{LC} \end{cases}. \tag{4.15}$$

In matrix form

$$\dot{\boldsymbol{x}} = \boldsymbol{A}\boldsymbol{x} + \boldsymbol{B}\boldsymbol{u} + \boldsymbol{D}\,, \tag{4.16}$$

where u is the discontinuous input that can assume the value 0 or 1. In matrix form

$$\boldsymbol{A} = \begin{bmatrix} 0 & 1 \\ -\dfrac{1}{LC} & -\dfrac{1}{R_{\mathrm{L}}C} \end{bmatrix}, \qquad \boldsymbol{B} = \begin{bmatrix} 0 \\ \dfrac{V_{\mathrm{in}}}{LC} \end{bmatrix}, \qquad \boldsymbol{D} = \begin{bmatrix} 0 \\ -\dfrac{V_{\mathrm{ref}}}{LC} \end{bmatrix}. \tag{4.17}$$

The phase trajectories corresponding to the substructures u = 0, 1 are shown in Figure 4.5 for different values of initial conditions.

It is convenient to select the sliding surface as a linear combination of the state variables since it results in simple-to-implement control systems and it allows the use of the equivalent control method to describe the system dynamics in the sliding mode, thus

$$\sigma(\boldsymbol{x}) = c_1 x_1 + x_2 = \boldsymbol{C}^{\mathrm{T}}\boldsymbol{x} = 0\,, \tag{4.18}$$

where $\boldsymbol{C}^{\mathrm{T}} = [c_1, 1]$ is the vector of the sliding surface coefficient that corresponds to $\boldsymbol{G}$ in equation (4.10). The coefficient c_2 was set to 1 without loss of generality. Equation (4.18) describes a line in the phase plane passing through the origin, which represents a stable operating point for this converter (zero output voltage error and its zero derivative).

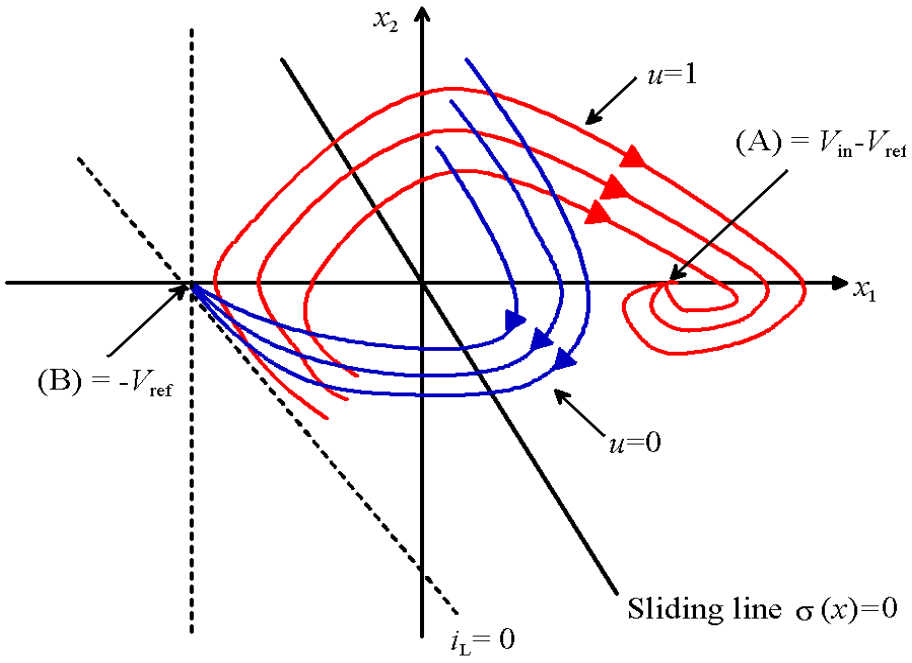

Figure 4.5. System trajectory and sliding line in the phase plane of a DC/DC Buck converter. Point (A) shows where the trajectories terminate when the switch is on, while point (B) shows where the trajectories terminate when the switch is off. From equation (4.14) $x_1 = V_0$-V_{ref}, while $x_2 = i_c/C$.

Substituting equations (4.15) into (4.18) leads to

$$\sigma(\boldsymbol{x}) = c_1 x_1 + \dot{x}_1 = 0\,, \tag{4.19}$$

which describes the system dynamics in the sliding mode. Thus if the existence and the reaching condition of the SMC are satisfied, a stable system is obtained by choosing a positive value of c_1.

According to equations (4.5), and (4.7) and by choosing the following control law

$$u = \begin{cases} 0 & \text{for } \sigma(\boldsymbol{x}) > 0 \\ 1 & \text{for } \sigma(\boldsymbol{x}) < 0 \end{cases}, \tag{4.20}$$

then both the existence and the reaching conditions are satisfied. In fact, it can be easily seen that in this control law, for both sides of the sliding line, the phase trajectories of the corresponding substructures are directed toward the sliding line (at least in small region around it).

It is shown in Figure 4.5 that the real structure has a physical limitation due to the rectifying characteristic of the free-wheeling diode. In fact, when the switch is off the inductor current (i_L) can only assume a nonnegative value.

In practice, when i_L goes to zero it remains zero and the output capacitor discharges exponentially to zero. This situation corresponds to the DCM and poses a constraint to the state variable. The boundary of this region can be derived from the constraint $i_L = 0$ and is given as (see Appendix A.6)

$$x_2 = -\frac{1}{R_L C} x_1 - \frac{V_{ref}}{R_L C}, \tag{4.21}$$

which corresponds to the straight line with a negative slope equal to $-1/R_L C$ and passing through the point ($-V_{ref}$, 0), as it is shown in Figure 4.5. It is also shown that the line $x_1 = -V_{ref}$ defines another not physically accessible region of the phase plane, i.e. $V_o < 0$.

4.4.2 Existence Condition of SMC for DC/DC Buck Converter

To give a more precise demonstration of the existence of the sliding regime for DC/DC Buck converter, and by taking the derivative of equation (4.18)

$$\dot{\sigma}(\boldsymbol{x}) = \boldsymbol{C}^{\mathrm{T}} \dot{\boldsymbol{x}} = 0. \tag{4.22}$$

Substituting equation (4.16) into (4.22) results in

$$\dot{\sigma}(\boldsymbol{x}) = \boldsymbol{C}^{\mathrm{T}} \boldsymbol{A}\boldsymbol{x} + \boldsymbol{C}^{\mathrm{T}} \boldsymbol{B}u + \boldsymbol{C}^{\mathrm{T}} \boldsymbol{D}. \tag{4.23}$$

From equation (4.5) the condition for the sliding regime to exist results in

$$\dot{\sigma}(\boldsymbol{x}) = \begin{cases} \boldsymbol{C}^{\mathrm{T}} \boldsymbol{A}\boldsymbol{x} + \boldsymbol{C}^{\mathrm{T}} \boldsymbol{B}\boldsymbol{u}^{+} + \boldsymbol{C}^{\mathrm{T}} \boldsymbol{D} < 0 & \text{for } \sigma(\boldsymbol{x}) > 0 \\ \boldsymbol{C}^{\mathrm{T}} \boldsymbol{A}\boldsymbol{x} + \boldsymbol{C}^{\mathrm{T}} \boldsymbol{B}\boldsymbol{u}^{-} + \boldsymbol{C}^{\mathrm{T}} \boldsymbol{D} > 0 & \text{for } \sigma(\boldsymbol{x}) < 0 \end{cases}. \tag{4.24}$$

Using equations (4.16), (4.19) and (4.20) leads to (refer to Appendix A.7)

$$\begin{cases} \lambda_1(\boldsymbol{x}) = (c_1 - \dfrac{1}{R_L C})x_2 - \dfrac{1}{LC}x_1 - \dfrac{V_{ref}}{LC} < 0 & \text{for } \sigma(\boldsymbol{x}) > 0 \\ \lambda_2(\boldsymbol{x}) = (c_1 - \dfrac{1}{R_L C})x_2 - \dfrac{1}{LC}x_1 + \dfrac{V_{in} - V_{ref}}{LC} > 0 & \text{for } \sigma(\boldsymbol{x}) < 0 \end{cases} . \qquad (4.25)$$

Equations $\lambda_1(\boldsymbol{x}) = 0$ and $\lambda_2(\boldsymbol{x}) = 0$ define the two lines in the phase plane with the same slope passing through points ($-V_{ref}$, 0) and ($V_{in} - V_{ref}$) respectively.

The regions of existence of the sliding mode are depicted in Figure 4.6 for $c_1 > 1/ R_L C$ and in Figure 4.7 for $c_1 < 1/ R_L C$.

It can be seen that the increase of the c_1 value causes a reduction of the sliding mode existence region (the sliding line coefficient c_1 determines also the system dynamic response in the sliding mode). From equation (4.19) the system dynamic response results in a first order with time constant $\tau = 1/ c_1$. Thus, high response speed i.e. $\tau < R_L C$ limits the existence region of the sliding mode and can cause overshoot and ringing during transient.

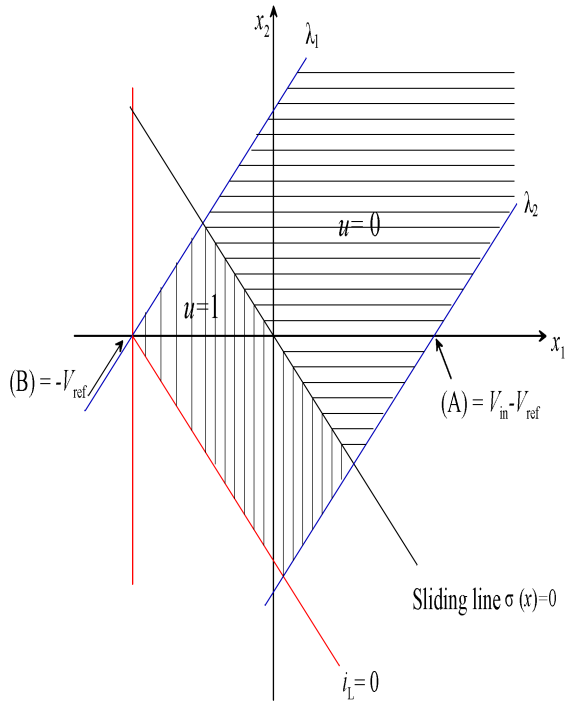

Figure 4.6. Region of existence of the sliding mode in the phase plane when $c_1 > 1/ R_L C$. The boundaries of the region are defined by equation (4.25). Point (A) shows the termination of the trajectories when the switch is on, while point (B) shows the termination of the trajectories when the switch is off.

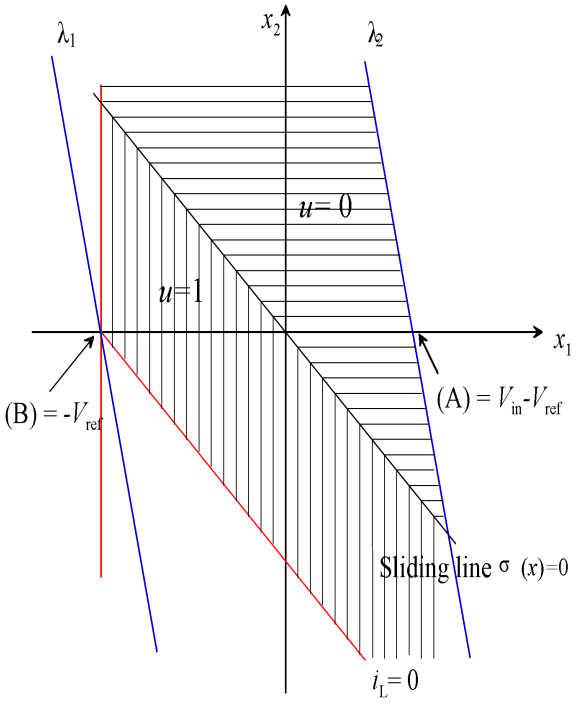

Figure 4.7. Region of existence of the sliding mode in the phase plane when $c_1 < 1/ R_L C$. The boundaries of the region are defined by equation (4.25). Point (A) shows the termination of the trajectories when the switch is on, while point (B) shows the termination of the trajectories when the switch is off.

The time responses of the output voltage and the inductor current for different c_1 values are shown in Figure 4.8 and Figure 4.9 respectively, where $k = c_1 R_L C$. The simulation model is

given in Appendix B.3. It can be seen that with $k = 1$ neither the output voltage nor the inductor current have overshoot during the start-up.

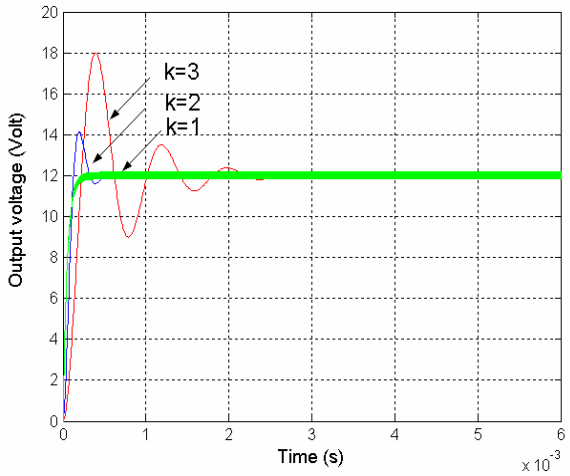

Figure 4.8. Time responses of the output voltage at different k values, where $k = c_1 R_L C$. It can be seen that as the value of k increases, more ringing and overshoot occur.

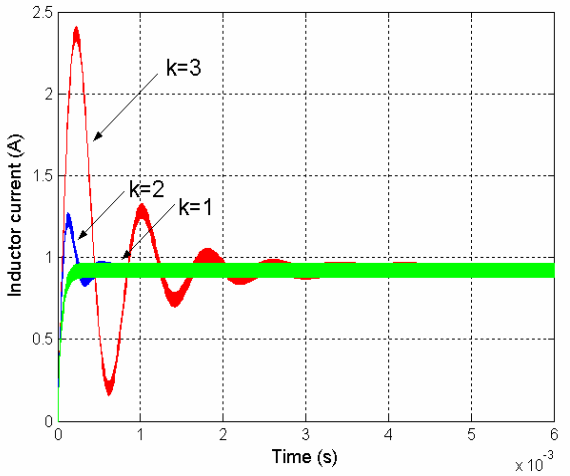

Figure 4.9. Time responses of the inductor current at different k values, where $k = c_1 R_L C$. Again as in the output voltage response, as the value of k increases, more ringing and overshoot occur.

4.5 Sliding Mode Control Researches and Applications in DC/DC Converters

The applications of the SMC in DC/DC converters have been widely investigated; many researches on SMC applied to switch mode power supplies have been done. Some of the most important researches and achievements are mentioned below.

(Malesani 1992) published a novel approach to the design of SMC for Cuk power converters, which is valid for both complete status feedback (fourth-order controller) and reduced status feedback (second-order controller). According to the proposed design criteria, both control techniques ensure excellent static and dynamic performances, and this, as a result, allows a simple control implementation and a minimum size of the energy transfer capacitor. Experimental results were reported and compared with those obtained with other popular control techniques. The main advantages of the proposed approach are: a simple control implementation, large-signal stability, nonoscillatory response of all state variables and short settling time are ensured in any operating condition, and the transfer capacitor can become small, since decoupling of the input and output stages is not required.

(Mattavelli 1993) described a general-purpose SMC, which can be applied to most DC/DC power converter topologies. The paper shows that the control circuit has the same circuit complexity as standard current-mode controllers, but provides an extreme robustness and speed of response against supply, load, and parameter variations. Moreover, contrary to other sliding-mode techniques, the proposed solution features constant switching frequency in steady state, synchronization to external triggers, and absence of steady-state errors in the output voltage.

(Im 1994) introduced a closed-loop output voltage control method for ZCS using the SMC. Because the closed-loop system can be reduced from 3rd order to 2nd order, the system design becomes simplified. It is shown that the dynamic ranges of the output voltage and load

resistance are very large, and that the dynamic behaviour of the SMC is not affected by input voltage, which shows the robustness of the SMC technique. These features were verified by computer simulations and experiments, with good agreement.

(Rossetto 1994) described a PWM rectifier including an uncontrolled rectifier and a Cuk converter stage driven by a SMC. He states that, alike the other high-quality rectifiers, this solution allows low-distorted and in-phase line current. Moreover, due to the SMC, fast and stable response is achieved, in spite of the large output filter. The control complexity is the same as that of standard current-mode controls. Converter analysis, design criteria, and experimental results are reported. The converter provides excellent stability, robustness and dynamic response.

(Sira-Ramirez 1994 b) proposed the method of extended linearization for the systematic solution of SMC design for DC/DC power converters of the Boost and the Buck-Boost types. A nonlinear sliding surface with suitable stabilizing properties is synthesized on the basis of the extension of a linear sliding design carried out for the parameterized average linear incremental model of the converter. The obtained feedback strategies lead to asymptotically stable sliding modes with remarkable self-scheduling properties. Simulation examples are presented for illustrative purposes.

(Spiazzi 1997) dealt with small-signal analysis of DC/DC converters with SMC. He developed a suitable small signal model, which allows the selection of control coefficients, the analysis of parameter variation effects, the characterization of the closed loop behaviour in terms of audio susceptibility, output and input impedances, and reference to output transfer function. The model includes effects of the filters used to evaluate state variable errors. Simulated and experimental results demonstrate the model potentialities and show the validity of the approach.

(Lopez 1998) introduced a new approach to interleaving parallel power converters using a multi-input SMC scheme. The control approach is based on sliding surfaces that naturally provide interleaving between the cells of a modular power supply system. Moreover, the sliding surfaces provide equal current distribution among the power converter modules and a regulated voltage in the output. The technique shows to be also effective if there are a varying number of cells in the system. Simulation and experimental results are presented for a parallel structure based on Buck power converters.

(Castilla 2000) created a novel design methodology of SMC schemes for quantum resonant converters. The method is based on the imposition of a specified output-voltage dynamic response, and it provides a set of sliding surfaces guaranteeing high robustness and large-signal stability. From among these schemes and taking into account a simple practical implementation, the final configuration is selected. Simulation and experimental results, confirming the validity of the proposed solution, were reported.

(Orosco 2000) gave a complete analysis of discrete SMC for DC/DC power converters in general. The analysis includes the reaching condition, the proof of the existence condition of the sliding mode and stability condition. In addition, a design example for the Buck converter is presented. The control schemes propose the elimination of the main problems of the SMC. The presence of a digital filter reduces the settling time. Some simulation results show the digital filter effect and an over voltage reduction at start up with a ramp reference instead of step reference.

(Alarcon 2001), in his paper, described the design and implementation of a microelectronic CMOS analog integrated circuit providing versatile SMC laws for switching DC/DC power converters. In addition to its ability to perform general linear-surface state control laws, the controller circuit includes compensating dynamics. The proposal of this analog IC design, which operates in current-mode processing, exhibits a good performance as far as the operation speed, power consumption, suitability for low-voltage operation and robustness in front of the interference are concerned. The main circuit allowing modular connection is composed of externally linarized transconductors based on current conveyors, current-mode amplifiers, filtering stages, and a trans-impedance high-speed hysteretic comparator. Full-transistor-level post-layout simulations for a CMOS 0.8 μm technology and experimental results validate the high-speed functionality of the proposed SMC ASIC implementation.

(Cortes 2002) revisited the SMC of the Boost converter. He presented and analyzed several sliding surfaces. Some of the surfaces presented do not depend on the circuit load, and this eliminates the necessity to measure the current measurement. The proposed analysis is based on the switching model of the circuit instead of the average model typically used. Practical aspects of implementing SMC with the proposed surfaces are discussed.

(Fossas 2002), in his researches, applied the results obtained from second-order sliding mode controller (SOSMC) algorithms to a linear Buck converter in regulation tasks. As usual in SOSMC, the chattering, an undesired consequence of SMC is highly reduced. A basic requirement for the method to be applicable is to find appropriate bounds for the state variables (current and voltage) as well as for the input control. The proposed method proves to be robust in face of line and load perturbations.

(Morel 2002) first studied the behavior of a current-mode-controlled Boost converter and exhibited its chaotic behaviour (when the duty cycle exceeds 50%). Then, he introduced a practical SMC method aiming to eliminate chaos and keep the desired current-controlled property. Indeed, the standard method (slope compensation) only partly cures this major drawback and, even though it eliminates chaos, the converter is not current-controlled any more. The proposed SMC method does not only provide stability, it also increases the input voltage variation domain for which the system remained stable. The SMC converter always remains current-controlled, i.e. independently of the duty cycle. Finally, a mathematical modeling of the whole circuit (close-loop) is established and its performance is studied in detail.

(Lopez 2004) showed the analysis and design of a parallel-connected converter system using SMC techniques. The design is particularized for a system that consists of Boost converters and a current feedback loop based on a proportional–integral (PI) compensator of the output voltage error. The paper emphasizes the advantages of the SMC over the classic design method based on small-signal models. It is shown that the SMVC provides an effective and robust means of controlling nonlinear multi-input converters. The design is based on the Utkin conditions, which permit us to know the regions under which a sliding mode exists. This fact allows to design the compensator and to introduce some modifications in the control loop that avoided input-current overshoots during the system startup. Simple design expressions are obtained and verified with simulation and experimental results, thus showing the improvements achieved with the proposed modifications.

4.6 Summary

A brief history of SMC was given with a short summary of the first researches done in this field. The theory of SMC was given in details. SMC researches and applications in electrical and mechanical system were reported in brief. The theoretical study of SMC applied to the DC/DC Buck converter was given in detail. The researches done on SMC for switch mode power supplies and the achievements obtained were given in a separate section.

5. RESEARCH WORK

5.1 Summary of the Research Work

As mentioned before, switch mode power supplies can be controlled with various control methods. Each control method has its own advantages and drawbacks with respect to dynamic performances, cost, efficiency, and EMI.

This research focused on two control methods described in the previous chapters, which are

- The PID control, and
- The SMC.

The PID control was implemented in DC/DC Buck converter, and the SMC was implemented in the DC/DC (Buck, and Buck-Boost) converters. These methods can be verified to the three DC/DC (Buck, Boost, and Buck-Boost) converters. The effects of these two control methods on the behaviour of the converter in steady state, under line variation, under load variation, under components variation, in EMI, and in stability were studied and analyzed.

The proceeding of the work can be structured as follows:

- Designing the converter using mathematical evaluations,
- Designing a control circuit,
- Building-up the Simulink model of the system (converter plus controller),
- Constructing the prototype,
- Measuring the results,
- Comparing the results obtained from the two control methods,
- Improving the converter structure using resonant converter,
- Designing the HWZCS DC/DC Buck converter,
- Implementing SMC on the HWZCS DC/DC Buck converter, and
- Measuring the results.

The first step of the work was to design and implement the PID control for three non-isolated DC/DC converters. A mathematical procedure using a look-up table was implemented. This procedure helps the designer to select the optimum values when designing one of the non-isolated DC/DC converters with PID control.

In order to prove the mathematical analysis, a simulation model for the DC/DC (Buck, and Boost) converters was designed. A prototype based on the simulation model was constructed, and comparisons between the simulated and the prototype results for the output voltage and inductor current were done in steady state, under line and load variations, under full load, under no-load, and under component variations.

This research and previous researches discussed in chapter three showed that the SMC can manipulate efficiently the nonlinear phenomena that appear in switched mode power supplies. Furthermore, the SMC is less affected by disturbances compared to the other control techniques, and it is not operating at a constant switching frequency.

The next step was to design the SMC for the three non-isolated DC/DC (Buck, Boost, and Buck-Boost) converters. A simulation and a prototype model for DC/DC (Buck, Boost, and Buck-Boost) converters were designed and built-up. The research showed in detail the control

loops structure of the SMC. This was identified both with the simulation model and the prototype.

The selection of the SMC to be used for this work is explained based on previous researches, and a complete analysis with an example to define the theories of SMC was given.

For the prototype model of the SMC, both the analog control using op-amps, and the digital control using dSPACE™ were implemented. The DC/DC Buck converter and the HWZCS DC/DC Buck converter were controlled using op-amps, while DC/DC Buck-Boost converter was controlled using dSPACE™.

The main focus was on the effect of SMC on the behaviour of the converter. The output voltage and inductor current were studied for both the simulation and prototype models in the following regions:

- Steady state,
- Line voltage variation,
- Load variation,
- Full load,
- No-load, and
- Component variations.

The research work at this point showed that SMC can control the three non-isolated DC/DC (Buck, Boost, and Buck-Boost) converters not only by means of simulation models, but also by using the prototype control circuits.

A comparison was done in order to verify and confirm that the steady-state and dynamic response of SMC is good, compared to the other control methods. The simulation and prototype results obtained from the PID and SMC for the DC/DC Buck converter were compared.

The output voltage and inductor current in both cases were studied, analyzed, and compared in steady state and under different dynamic conditions. The SMC showed to have a better dynamic response. Also the effects of both control methods on the EMI were studied and compared, and the results showed that the EMI is reduced when using the SMC.

The research work was extended to improve the non-isolated DC/DC converter structure. The DC/DC resonant converter was studied and analyzed. Resonant converters are used to convert DC-to-DC through an additional conversion stage: the resonant stage in which a DC signal is converted to a high-frequency AC signal. The potential advantage of the resonant converter includes the natural commutation of power switches, in which causes a low switching power dissipation and reduced component stresses, which, in turn, results in an increased power efficiency and increased switching frequency.

The HWZCS DC/DC Buck converter was selected as a DC/DC resonant converter topology and a guideline to select the tank component values was made, assuming that the converter operates in a defined input voltage range, a defined output power range, and a defined maximum switching frequency.

The research work and previous researches showed that the HWZCS DC/DC Buck converter is not operating at a constant switching frequency and it is sensitive to dynamic variation.

Since the SMC showed to have a good steady-state and dynamic response and to not operate at a constant switching frequency, it was used as a control method for the HWZCS DC/DC Buck converter. The tank inductor current waveform, tank capacitor voltage waveform, output voltage waveform, and main inductor current waveform were studied and analyzed:

- In steady state,
- Under dynamic disturbances, and
- Under different tank component values.

The prototype was constructed using op-amps, and the simulation and the prototype results showed that the SMC is a good control method for the HWZCS DC/DC Buck converter. The mathematical algorithm obtained agrees with the simulation and the prototype results that define a boundary for the ZCS, provided that the input voltage, output power, and the maximum switching frequency are known. Figure 5.1 summarizes the research work explained above.

5.2 Summary of the Publications

5.2.1 Publication P [1]

Publication P [1] focuses on a simple algorithm that can be used to analyze the three non-isolated DC/DC (Buck, Boost, and Buck-Boost) converters. The Buck converter is chosen as an example. The analyzed method uses the AC equivalent circuit modeling, where one equation is used for all the converters mentioned earlier, comparing it with look-up table, calculating the transfer function of the converter with unity loop gain where. The PID control is added to the circuit with some simple procedure to improve the dynamic behaviour and the stability. Both simulation and prototype models are build-up and a comparison between the two models is given.

The output voltage and the inductor current of the DC/DC Buck converter with the PID control are tested in steady state, under line variation and under load variation. The results show that the steady-state and the dynamic responses of both the simulated and the prototype model are close to each other and this proves efficiency of the mathematical design.

5.2.2 Publication P [2]

Publication P [2] focuses on the SMC as a control method for the switch mode power supply. A simple procedure is used to control the non-isolated DC/DC converters using Matlab/Simulink™ in the design. The design procedure is explained in detail and the Buck converter is taken as an example. The output voltage and the inductor current are tested in steady state and under line and load variations. To show that this control algorithm can be implemented in the basic three non-isolated DC/DC (Buck, Boost, and Buck-Boost) converters, the DC/DC Buck-Boost converter is selected with different parameters and the same tests are applied to it.

The SMC is gaining increasing importance as a control design tool in Matlab/Simulink™ for the robust control of linear and non-linear systems. Its strength results from the ease and flexibility of the methodology for its design and implementation.

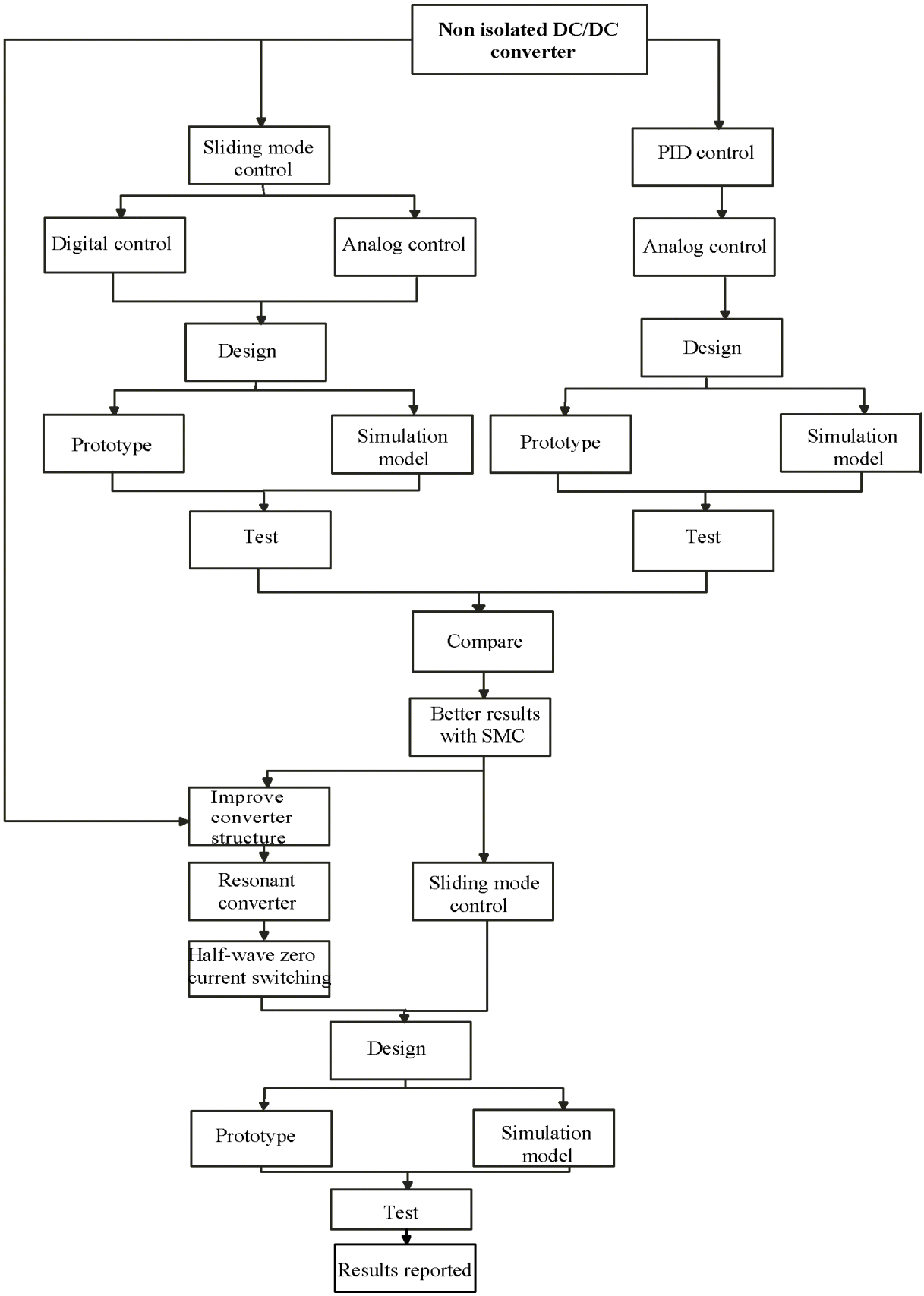

Figure 5.1. A research chart showing the sequence of the research work. The work starts by applying two control methods (PID, and SCM) for hard switching non-isolated DC/DC converters. The SMC showed to have better results. The SMC was applied to a soft switching HWZCS DC/DC Buck converter and the results gave a good steady-state and dynamic response.

5.2.3 Publication P [3]

Publication P [3] links the theory of SMC to the control of switched mode power supply. A practical implementation of SMC is done. An analysis and experimental study of the DC/DC Buck converter are reported, and nonlinear state feedback control is derived to achieve a desired output voltage. The publication focuses on the modelling of a SMC circuit in Matlab/Simulink™ and on its implementation in the DC/DC Buck converter. Next, a prototype with SMC is build up. The output voltage and inductor current of both models are compared in steady-state mode and under line and load variations.

The simulation model and the prototype showed that the SMC can stabilize the DC/DC Buck converter, and that the output voltage and the inductor current can return to steady state even when the converter is affected by line and load variations with a small overshoot and settling time.

5.2.4 Publication P [4]

In this publication a brief analysis of the SMC structure is given followed by a block diagram showing the internal structure of the control loops and the way they are connected to the converter. The DC/DC Buck converter was chosen as an example and the simulation model of the converter with its control circuit is build-up in Matlab/Simulink™.

The output voltage, inductor current and the instant switching frequency are analyzed and studied in the following three regions: turn-on region, line and load variation region, and finally components variation region. In the third part, considering the robustness, a wide range of changes of the DC/DC Buck converter component parameters (inductor, capacitor, and resistor) values are applied each variation individually, and the effects of the SMC on the converter response due to these variations are analyzed.

The publication shows that the SMC for switch mode power supply has a good immunity against component variations, and each component has a different level of effect on the converter response, when implementing SMC. The effect of these components can be found in the publication.

5.2.5 Publication P [5]

This publication focuses on the use of a new control tool, known as dSPACE™, to control the switch mode power supply, where the control circuit can be programmed through MATLAB/Simulink™. The prototype of the three non-isolated DC/DC (Buck, Boost and Buck-Boost) converters can be controlled by the simulation model by means of real time hardware. The DC/DC Buck-Boost converter is chosen as the prototype converter. The SMC is chosen as a control method in MATLAB/Simulink™ to control the DC/DC Buck-Boost prototype model.

The publication shows that the SMC algorithm may be realized by using dSPACE™ to control the prototype.

The publication shows also that one main disadvantage of using dSPACE™ as a control tool for switch mode power supply is the limitation of the I/O sampling frequency of dSPACE™,

which is limited to 100 kHz. As a result, an assumption for the switching frequency to not exceed one forth of 100 kHz is done. This disadvantage leads to a high inductor value (in value and size) and more parasitic losses. The processor technology is improving fast so that it may be possible in near future to achieve calculation time steps even less than 1 μs, and so to overcome these disadvantages.

5.2.6 Publication P [6]

This publication studies the DC/DC Buck converter response controlled with two different control methods. The first control method is the PID control and the second control method is the SMC.

The output voltage and the inductor current of both models are studied and compared in the transient region (turn-on), steady-state region, under line variation, and under load variation. It is shown that the SMC for the DC/DC Buck converter is more effective than the PID control, especially when dynamic tests are applied.

It is obvious that the future use of SMC is promising as its application in switch mode power supply is concerned, because, firstly, it is a non linear control and can evaluate the non linearity of the converter components and, secondly, it is not operating at a constant switching frequency.

5.2.7 Publication P [7]

In this publication, a comparison between the EMI-noise effects of a fixed-frequency, PID-controlled PWM and SMC converter was done. Both simulation and experimental results are reported.

The paper shows that the proper selection of the control strategy has an effect on the EMI performance of the switch mode power converter. With a non-linear control circuit, it is possible to achieve the same results as achieved with more complicated spread spectrum modulation techniques proposed in the literature.

5.2.8 Publication P [8]

This publication focuses on the practical implementation of the SMC in a HWZCS DC/DC Buck converter. A detailed mathematical analysis is performed in order to select the appropriate tank component values. The tank inductor value is assumed to be small and constant and a range of tank capacitor values is obtained. The prototype of an analog SMC for the HWZCS DC/DC Buck converter is constructed.

In order to study the effect of SMC on the behaviour of the converter, the system is tested in steady state and under different load value conditions. The obtained graphs show that the performance of the SMC is good, even under the worst load conditions, i.e. at no load and full load.

5.2.9 Publication P [9]

The main goal of this paper is to define the range of the tank component values for a HWZCS DC/DC Buck converter. Two mathematical conditions are applied and ranges for the tank inductor value and the tank capacitor value, where ZCS occurs, are defined. The analysis is proved with both simulation and prototype results.

The simulation and the prototype results are close to each other and coincide with the mathematical analysis. The design algorithm is a good guideline to select the tank component values in the design of a HWZCS DC/DC Buck converter. The publication simplifies a mathematical procedure obtained from previous studies to define the range of tank component values for a HWZCS DC/DC Buck converter.

6. CONCLUSIONS AND FUTURE WORKS

6.1 Conclusions

This chapter summarizes the major contributions and the main results of this thesis. The main objective of the work was to implement two different control methods, the PID control and the SMC, in the three non-isolated DC/DC (Buck, Boost, and Buck-Boost) converters.

Chapter 1 defined the main frame of the work, explained and analyzed briefly the work done in each chapter. In chapter 2 a detailed explanation and classification of switched mode power supply were given. The chapter also defined and summarized, with the aid of mathematical equations, the value of the critical inductance for the three non-isolated DC/DC (Buck, Boost, and Buck-Boost) converters.

Chapter 3 analyzed six different control methods used to control switched mode power supplies. The advantages and drawbacks of each control method are shown. In chapter 4 a detailed analysis of the theory of SMC and a survey of the previous researches on the electrical and mechanical application of SMC were given. The reason for selecting the SMC as a control method for switched mode power supply was given. The SMC was applied to the DC/DC Buck converter and a detailed mathematical analysis was shown.

Chapter 5 summarized the research process. A brief explanation of the research work was given and a chart explaining the sequence of the work was shown. The chapter also gave a summary of the publications with a short explanation of each publication.

The main contributions of this thesis can be summarized as follows:

- **Definition of six control methods to control switched mode power supplies:** Six control methods for switched mode power supplies were presented, namely: the PID control, the hysteresis control, the adaptive control, the current mode programmed control, the VSC and the SMC. Their operation was explained in detail, the advantages and drawbacks of each control method when implemented in switched mode power supplies are shown.
- **Study of the SMC and its implementation in DC/DC converters:** The analysis and the theories of SMC were given in details. The DC/DC Buck converter was taken as an example. The example showed in detail the satisfying of the theories of SMC and the implementation of SMC in the converter.
- **Implementation of PID control in the basic three non-isolated DC/DC (Buck, Boost, and Buck-Boost) converters:** The PID control was implemented in the DC/DC Buck converter using simulation and prototype models. The circuit was tested in steady state and under different dynamic variations. Both the simulation model and the prototype gave close results under different conditions. A look-up table was introduced to help the designer to implement the PID control in any of the above mentioned converters.
- **Implementation of SMC in the basic three non-isolated DC/DC (Buck, Boost, and Buck-Boost):** A detailed analysis of the internal structure of SMC to switched mode power supplies formed the main part of the contribution. The SMC was studied theoretically and the reason for selecting the SMC for switched mode power supplies was made clear. Simulation and prototype models of the SMC to be implemented in the three non-isolated DC/DC (Buck, Boost, and Buck-Boost) converters were built-

up. The models were tested under different conditions, and the output voltage and the inductor current were studied in steady state, line variations, load variations, full load, and no-load, component variations. For the prototype, an analog controller using op-amps and a digital controller using dSPACE™ were implemented.

• **Comparison of the effects of PID control and SMC on the DC/DC Buck converter response in steady state and in dynamic region:** In order to study and analyze the SMC effect on the converter behaviour and to compare it to another control method, a comparison was done for the output voltage and the inductor current responses of the DC/DC Buck converter controlled with the PID control and the SMC. Tests were done and the results were obtained in steady state and under dynamic conditions. The SMC showed to have a better response, especially under dynamic conditions.

• **Comparison of the Conducted RF-Emissions between a PID and SMC DC/DC Converter:** A comparison of the EMI-noise effects of a fixed-frequency, PID-controlled PWM and SMC converter has been done. The simulation and prototype results of both models were compared. It was shown that the proper selection of the control strategy has an effect on the EMI performance of the switch mode power converter. The tests and simulations also showed that a non-linearly controlled system can be parameter sensitive and, therefore, the designer should know and study the non-linear effects of the converter system before adopting the technique for production purposes.

• **The advantages of SMC over DC/DC converters:** the importance of the SMC as a design tool for the robust control of linear and non-linear systems is increasing. Its strength results from the ease and flexibility of the methodology to be used for design and implementation. The thesis showed that the SMC provides a better steady-state response, a better dynamic response, less EMI, inherent order reduction, robustness against system uncertainties disturbances and an implicit stability proof, compared to the PID control. So, it can be said that the SMC design for DC/DC converters allows a high-performance control system.

• **DC/DC resonant converter:** An improvement of the DC/DC converter structure was investigated by implementing a resonant converter, where it improves the efficiency by applying ZCS or ZVS. A general guideline to select the tank components values, when designing a HWZCS DC/DC Buck, were obtained, assuming that the converter operates in a defined input voltage range, a defined output power range and at a known maximum switching frequency. The guideline helps the designer to select the optimum values, which ensures the ZCS.

• **SMC for HWZCS DC/DC Buck converter:** The implementation of SMC to a HWZCS DC/DC Buck converter was studied. The output voltage, main inductor current, tank capacitor voltage, and tank inductor current waveforms were studied in steady-state region and in dynamic region.

6.2 Suggestions for Future Researches

In the past years, the SMC for switched mode power supplies has been widely investigated. In many researches, it is shown that the SMC is a good control method, compared to the other control methods. In most of these researches, the statements are proven with simulation evidence and without clear comparisons to the other control methods. This research implemented the SMC by means of both a simulation model and a prototype in the three non isolated DC/DC (Buck, Boost, and Buck-Boost) converters. A comparison for the DC/DC Buck converter controlled by PID and SMC was done.

It is important to extend the investigation and to do further comparing research on the SMC and other controlled methods, as it is done in this thesis for the three non-isolated DC/DC (Buck, Boost, and Buck-Boost) converters, by using simulation and prototype models.

An interesting research area is the comparative study of the SMC and other control methods, when SMC is implemented in more complicated DC/DC converters. The comparison can be carried out in simulation and prototype tests.

More investigations of the implementation of the SMC in DC/DC resonant converters, including ZCS and ZVS, can be done. Another research field is the comparative study of the efficiency of the DC/DC converter and the resonant converter, when SMC is implemented.

REFERENCES

Adell, P., Schrimpf, R., Holman, W., Boch, J., Stacey, J., Ribero, P., Sternberg, A. 2003. *Total-dose and single-event effects in DC/DC converter control circuitry.* IEEE Transactions on Nuclear Science, Volume: 50 ,Issue: 6 ,Dec. 2003, pp: 1867 – 1872.

Alarcon, E., Romero, A., Poveda, A., Porta, S., Martinez-Salamero, L. 2001. *Sliding-mode control analog integrated circuit for switching DC-DC power converters*. Proceeding of the IEEE International Symposium on Circuits and Systems, (ISCAS 2001). , Volume: 1, 6-9 May 2001 pp: 500 - 503 vol. 1.

Barambones, O., Garrido, A., Maseda, F. 2003. *A robust field oriented control of induction motor with flux observer and speed adaptation*. Proceedings of IEEE Conference on Emerging Technologies and Factory Automation, ETFA 03, Volume: 1, 16-19 Sept. 2003. pp: 245 - 252 vol.1.

Bevrani, H., Mitani, Y. Tsuji, K. 2002. *Robust control design for a ZCS converter*. ECON 02, Proceedings of the IEEE Industrial Electronics Society conference, 28th Annual Conference, Volume: 1, 5- 8 Nov. 2002 pp: 609 - 614 Vol.1.

Bondarev, A., Kostileva, N., Utkin, V. 1985. *Sliding modes in systems with asymptotic state observer*. Journal of Automation and Remote Control,1985.

Boudreaux, R., Nelms, R., Hung, J. 1997. *Simulation and modeling of a DC-DC converter controlled by an 8-bit microcontroller*. Proceedings of the IEEE Applied Power Electronics Conference and Exposition. APEC 97, Twelfth Annual, Volume: 2, 23-27 Feb. 1997, pp: 963 - 969 vol.2.

Calvente, J., Guinjoan, F., Martinez, L., Poveda, A. 1996. *Subharmonics, bifurcations and chaos in a sliding-mode controlled boost switching regulator*. Proceedings of the IEEE International Symposium on Circuits and Systems. ISCAS 96. vol. 1, 12-15 May 1996.

Camacho, O., Smith, C., Chacon, E. 1997. *Toward an implementation of sliding mode control to chemical processes*. Proceedings of the IEEE International Symposium on Industrial Electronics. ISIE 97, 7-11 July 1997 pp: 1101 - 1105 vol.3.

Castilla, M., Garcia de Vicuna, L., Lopez, M., Lopez, O., Matas, J. 2000. *Dynamic response optimization of quantum series-parallel resonant converters using sliding mode control*. Proceeding of the IEEE 31st Annual Power Electronics Specialists Conference, (PESC 00), Volume: 2, 18-23 June 2000, pp: 702 - 707 vol.2.

Chakraborty, C., Mukhopadhyay, S. 2002. *A novel compound type resonant rectifier topology*. Proceedings of the First IEEE International Workshop on Electronic Design, Test and Applications, 29-31 Jan. 2002 pp: 428 – 430.

Chao, L., Jian, C., Yu-Wein, W. 1994. *Control of robot manipulator using a fuzzy model-based sliding mode control scheme*. Proceedings of the 33rd IEEE Conference on Decision and Control, Volume: 4, 14-16 Dec. 1994 pp: 3506 - 3511 Vol.4.

Charaabi, L., Monmasson, E., Slama-Belkhodja, I. 2002. *Presentation of an efficient design methodology for FPGA implementation of control systems. Application to the design of an anti-windup PI controller*. IEEE proceedings on 28th Annual Conference of the Industrial Electronics Society, IECON 02, Volume: 3, 5-8 Nov. 2002 pp: 1942 - 1947 vol.3.

Chen, J., Ioinovici, A. 1995. "*Switched-capacitor-based quasi-resonant converter operating at constant switching frequency*''. Proceedings of the International Telecommunications Energy Conference. INTELEC 95, 29 Oct.-1 Nov. 1995 pp: 315 –321.

Chen Z., Zhang J., Zeng, J. 2001. *A new method of sliding mode control and application to AC servo system.* Proceedings of the Fifth International Conference on Electrical Machines and Systems. ICEMS 2001, Volume: 2, 18-20 Aug. 2001. pp: 759 - 762 vol.2.

Cortes, D., Alvarez, J. 2002. *Robust sliding mode control for the boost converter*. Proceedings of VIII IEEE International Power Electronics Congress, (CIEP 2002), 20-24 Oct. 2002 pp: 208 – 212.

Cucej, Z., Planinsic, P., Golob, M., Donlagic, D. 1995. *Modulator based on fuzzy controllers in sliding mode control of AC motor drive*. Proceedings of 1995 International Conference on Power Electronics and Drive Systems, 21-24 Feb. 1995 pp: 774 - 779 vol.2.

Cuk, S., Middlebrook, R. 1977. *A New optimum topology switching DC/DC converter*. IEEE Power Electronics Specialists Conference (PESC)*,* 1977 Record, pp 160-179.

Daniel, D, Shtessel, Y.; Zhu, J. 2002. *Reusable launch vehicle attitude control using a time-varying sliding mode control technique*. Proceedings of the Thirty-Fourth Southeastern Symposium on System Theory, 18-19 March 2002 pp: 81 – 85.

Deane, J., Hamill, D. 1990. *Instability, Subharmonics, and Chaos in Power Electronic Systems*. IEEE Transactions on power electronics, vol. 5. No. 3. July, 1990.

De Battista, H., Puleston, P., Mantz, R., Christiansen, C. 2000. *Sliding mode control of wind energy systems with DOIG-power efficiency and torsional dynamics optimization*. IEEE Transactions on Power Systems, Volume: 15, Issue: 2, May 2000 pp: 728 – 734.

Drakunov, S., Barbieri, E., Silver, D. 1996. *Sliding mode control of a heat equation with application to arc welding*. Proceedings of the 1996 IEEE International Conference on Control Applications, 15-18 Sept. 1996 pp: 668 – 672.

Erickson, R. 1997. *Fundamental of Power Electronics*. Kluwer Academic Publishers. ISBN 0-412-08541-0. 773 pages.

Forsyth, A., Mollov, S. 1998. *Modelling and control of DC-DC converters.* Power Engineering Journal , Volume: 12 ,issue: 5 ,Oct. 1998 pp: 229 – 236.

Forsyth, A., War, G., Mollov*,* V. 2003. *Extended fundamental frequency analysis of the LCC resonant converter,* Proceeding of IEEE Power Electronics Transactions, Volume: 18, Issue: 6, Nov. 2003pp: 1286 – 1292.

Fossas, E., Ras, A. 2002. *Second-order sliding-mode control of a Buck converter*. Proceedings of the 41st IEEE Conference on Decision and Control, Volume: 1, 10-13 Dec. 2002 pp: 346 - 347 Vol.1.

Haver, R. 1974. *A new approach to switching regulators*. Motorola Application Note AN-719, May 1974.

Hess, R., Wells, S., Vetter, T. 2002. *MIMO sliding mode control as an alternative to reconfigurable flight control designs*. American Control Conference, Proceedings of the 2002, Volume: 5, 8-10 May 2002 pp: 3637 - 3643 vol.5.

Hsiao-Dong Chiang, Chih-Wen Liu, Varaiya, P., Wu, F., Lauby, M. 1993. *Chaos in a simple power system*. IEEE Transactions on Power Systems, vol. 8 Issues: 4, November 1993.

Ho, W., Pong, M. 1993. *Power loss and efficiency analysis of quasi-resonant converters*. Proceedings of the IEEE Industrial Electronics, Control, and Instrumentation conference. IECON 93, 15-19Nov.1993, pp 842 -847, vol.2.

Huang, Z., Edwards, R., Lee, K. 2004. *Fuzzy-Adapted Recursive Sliding-Mode Controller Design for a Nuclear Power Plant Control*. IEEE Transactions on Nuclear Science, Volume: 51, Issue: 1, Feb. 2004 pp: 256 – 266.

Im, S., Kwon, W., Cho, G. 1994. *Sliding mode control of a zero-current switching resonant converter*. IEEE Electronics Letters, Volume: 30, Issue: 5, 3 March 1994 pp: 381 – 382.

Istefanopulos, Y., Jafarov, E., Parlakci, M. 2002. *A new robust continuous sliding mode control for robot manipulators with parameter perturbations*. American Control Conference. Proceedings of the 2002, Volume: 4, 8-10 May 2002 pp: 3202 - 3206 vol.4.

Jacobina, C., de Rossiter Correa, M., Pinheiro, R., da Silva, E., Lima, A., 2001. *Modeling and control of unbalanced three-phase systems containing PWM converters*. Proceedings of the IEEE Transactions on Industry Applications, Volume: 37, Issue: 6, Nov.-Dec. 2001 pp: 1807 – 1816.

Jafarov, E., Tasaltin, R. 2000. *Robust sliding-mode control for the uncertain MIMO aircraft model F-18*. IEEE Transactions on Aerospace and Electronic Systems, Volume: 36, Issue: 4, Oct. 2000 pp: 1127 – 1141.

JEAN_JACQUES, E, SLOTINE WEIPING, LI. 1991 *Applied Non-linear Control*. Prentice-Hall International Edition, ISBN 0-13-040049-1 1991, USA.

Jefferies, D., Deane, J., Johnstone, G. 1989. *An Introduction to Chaos*. Electronics & Communication Engineering Journal. May/June, 1989.

Josephson, E. 1967. *Satellite power supply has variable pulse-width*. Electronics, Feb 1967.

Kawasaki, S., Ouchi, S. 2002. *Traction control for automobiles by model-following sliding mode control*. SICE 2002. Proceedings of the 41st SICE Annual Conference, Volume: 2, 5-7 Aug. 2002 pp: 1175 - 1180 Vol.2.

Lazar, J., Martinelli, R. 2001. *Steady-state analysis of the LLC series resonant converter*, Proceeding of the IEEE Applied Power Electronics Conference and Exposition,. APEC 2001, Volume: 2, 4-8 March 2001 pp: 728 - 735 vol.2.

Lee, D., Noh, H., Hyun, D., Choy, I. 2003. *Sensorless control scheme using simple duty feedback technique in DC/DC converters*. IEE Proceedings on Electric Power Applications, Volume: 150, Issue: 6, 7 Nov. 2003, pp: 695 – 702.

Leung, K., Chung, H.., Hui, R. 2003. *Use of state trajectory prediction in hysteresis control for achieving fast transient response of the buck converter*. Proceedings of International Symposium on Circuits and Systems,. ISCAS '03, Volume: 3, 25-28 May 2003 pp: III-439 - III-442 vol.3.

Lin, R., Lee. F. 1996. *Novel zero-current-switching-zero-voltage-switching converters*. Proceedings of the IEEE Power Electronics Specialists Conference, 1996. PESC '96 Record, 27thAnnual IEEE, Vol.: 1, 23-27 June 1996 pp: 438 - 442 vol.1.

Lopez, M., de Vacuna, L., Castilla, M., Gaya, P., Lopez, O. 2004. *Current Distribution Control Design for Paralleled DC/DC Converters Using Sliding-Mode Control*. Proceeding of IEEE Transactions on Industrial Electronics, Volume: 51, Issue: 2, April 2004 pp: 419 – 428.

Lopez, M., Garcia De Vicuna, J., Castilla, M., Lopez, O., Majo, J. 1998. *Interleaving of parallel DC-DC converters using sliding mode control*. Proceedings of the 24th Annual Conference of the IEEE Industrial Electronics Society, (IECON 98), Volume: 2, 31 Aug.-4 Sept. 1998 pp: 1055 - 1059 vol.2.

Lopez, M., Garcia de Vicuna, J., Castilla, M., Matas, J.; Lopez, O. 2000. *Control design for parallel-connected DC/AC inverters using sliding mode control*. Power Electronics and Variable Speed Drives. 18-19 Sept. 2000. pp: 457 – 460.

Lyshevski, E. 2000. *Resonant converters: nonlinear analysis and control*. Proceeding on IEEE Industrial Electronics Transactions, Volume: 47, Issue: 4, Aug. 2000 pp: 751 – 758.

Malesani, L., Rossetto, L., Spiazzi, G., Tenti, P. 1992. *Performance optimization of Cuk converters by sliding-mode control*. Conference Proceedings on Applied Power Electronics Conference and Exposition (APEC), Seventh Annual, 23-27 Feb. 1992 pp: 395 – 402.

Marino, P., Vasca, F. 1995. *Sliding mode control for three phase rectifiers*. Power Electronics Specialists Conference. 1995. PESC '95 Record, 26th Annual IEEE, Volume: 2, 18-22 June 1995. pp: 1033 - 1039 vol.2.

Mascarenhas, P.1992. *Hysteresis control of a continuous boost regulator*. IEE Colloquium on Static Power Conversion, ,11 Nov 1992, pp:7/1 - 7/4.

Mattavelli, P., Rossetto, L., Spiazzi, G., Tenti, P. 1993. *General-purpose sliding-mode controller for DC/DC converter applications*. Proceeding of the IEEE Power Electronics Specialists Conference, (PESC 93) Records, 20-24 June 1993 pp: 609 – 615.

Mattavelli, P.,Spiazzi, G. , Rossetto, L. 1997. *Sliding mode control of DC-DC converters*. Congresso Brasileiro de Elettronica de Potencia (COBEP), Belo Horizonte, December 1997, pp. 59-68.

Mihalic, F., Milanovic, M. 1999. *EMI reduction in randomized boost rectifier*. Proceedings of the IEEE International Symposium on Industrial Electronics, vol. 2, ISIE '99. 1999.

Mohan, N, Undeland, T, Robbins, W. 1989. *Power Electronics: Converter, Applications, and Design*. JOHN WILEY & SONS, ISBN 0-471-61342-8, 1989, USA.

Morel, C. 2002. *Sliding mode control via current mode control in DC-DC converters*. Proceeding of IEEE International Conference on Systems, Man and Cybernetics, Volume: 5, 6-9 Oct. 2002 pp: 6 pp. vol.5.

Nicolas, B., Fadel, M., Cheron, Y. 1995. *Sliding mode control with DC-DC converters with input filter based on Lyapunove-function approach*. Proceeding of APEC Conf., 1995, pp. 1.338-1.343.

Orosco, R., Vazquez, N. 2000. *Discrete sliding mode control for DC/DC converters*. Proceeding of the VII IEEE International Power Electronics Congress, (CIEP 2000), 15-19 Oct. 2000, pp: 231 – 236.

Parker, T., Chua, L. 1987. *Chaos: A Tutorial for Engineers*. Proceedings of the IEEE, vol. 75, No. 8, August, 1987.

Peng, L., Lehman, B. 2004. *A design method for paralleling current mode controlled DC-DC converters*. IEEE Transactions on Power Electronics, Volume: 19, Issue: 3, May 2004, pp: 748 – 756.

Pereira, N., Borges, B., Anunciada, V. 1996. *Supra resonant fixed frequency full bridge DC-DC resonant converter with reduced switching losses*. Proceedings of the 18th International Telecommunications Energy Conference. INTELEC 96, 6-10 Oct. 1996.

Philip, T. 1998. *Elements of Power Electronics*. Oxford University press. ISBN 0-19-511701-8. 0-766 pages.

Pressman, A. 1977. *Switching and linear power supply, power converter design*. Hayden Book Co., Ltd., New York, 1977.

Prodic, A., Maksimovic, D. 2002. *Design of a digital PID regulator based on look-up tables for control of high-frequency DC-DC converters*. Proceedings Workshop on IEEE Computers in Power Electronics, 3-4 June 2002, pp: 18 – 22.

Rong, W. 2001. *Total sliding-mode controller for PM synchronous servo motor drive using recurrent fuzzy neural network.* IEEE Transactions on Industrial Electronics, Volume: 48, Issue: 5, Oct. 2001.pp:926 – 944.

Rossetto, L., Spiazzi, G., Tenti, P., Fabiano, B., Licitra, C. 1994. *Fast-response high-quality rectifier with sliding mode control*. IEEE Transactions on Power Electronics, Volume: 9, Issue: 2, March 1994 pp: 146 – 152.

Sanche, Z., Fierro, R. 2003. *Sliding mode control for robot formations*. IEEE International Symposium on Intelligent Control. 2003 pp:438 – 443.

Sarén, H., Parviainen, A. 2002 *Real Time Simulation and Measurement Environment of DC Converters for Educational Purposes*, proceeding of SIMS 2002. University of Oulu, Finland, ISBN 952-5183-18-1. 273, pp 133-138.

Shtessel, Y. 1998. *Sliding mode control of the space nuclear reactor system*. IEEE Transactions on Aerospace and Electronic Systems, Volume: 34, Issue: 2, April 1998. pp: 579 – 589.

Sira-Ramirez, H., Zribi, M., Ahmad, S. 1994 a. *Dynamical sliding mode control approach for vertical flight regulation in helicopters*. IEE Proceedings on Control Theory and Applications, Volume: 141, Issue: 1, Jan. 1994 pp: 19 – 24.

Sira-Ramirez, H.; Rios-Bolivar, M. 1994 b. *Sliding mode control of DC-to-DC power converters via extended linearization*. IEEE Transactions Circuits and Systems, Fundamental Theory and Applications, Volume: 41, Issue: 10, Oct. 1994 pp: 652 – 661.

Soumitro, B., George, C., Verghese. 2001. *Nonlinear phenomena in power electronics*'', ISBN 0-7803-5383-8. TK 7881.15B36 2001.

Spiazzi, G., Mattavelli, P., Rossetto, L., Malesani, L. 1995. *Application of Sliding Mode Control to Switch-Mode Power Supplies*," Proceeding of Journal of Circuits, Systems and Computers (JCSC), Vol.5, No.3, September 1995, pp.337-354.

Spiazzi, G., Mattavelli, P., Rossetto, L. 1997. *Small-signal analysis of DC-DC converters with sliding mode control*. IEEE Transactions on Power Electronics, Volume: 12, Issue: 1, Jan. 1997 pp: 96 – 102.

Stankovic, A., Verghese, G., Perreault, D. 1993. *Analysis and synthesis of random modulation schemes for power converters*. Proceedings of the IEEE Power Electronics Specialists Conference, PESC '93, 1993.

Stone, D., Chambers B., Howe D. 1995 a. *Random Carrier Frequency Modulation of PWM Waveforms to Ease EMC Problems in Switched Mode Power Supplies*. Proceedings of International Conference of Power Electronics and Drive Systems, PEDS 1995.

Stone, D. A, Chambers, B. 1995 b. *Easing radiated EMC problems with spread-spectrum modulation of computer clock signals*. Electronics Letters, vol. 31, No 24, 1995.

Tsang-Li, T., Jian-Shiang, C. 2002. *UPS inverter design using discrete-time sliding-mode control scheme*. IEEE Transactions on Industrial Electronics, Volume: 49, Issue: 1, Feb. 2002. pp: 67 – 75.

Teja, E. 1981. *Special report: switching power supplies.* EDN (USA), Vol.26, No.3, Feb 4th, 1981, pp 94-108.

Terui, F. 1998. *Position and attitude control of a spacecraft by sliding mode control*. American Control Conference, 1998. Proceedings of the 1998, Volume: 1, 24-26 June 1998 pp: 217 - 221 Vol.1.

Tse, K., Chung, H.S.-H., Huo, S., So, H. 2000. *Analysis and spectral characteristics of a spread-spectrum technique for conducted EMI suppression*. IEEE Transactions on Power Electronics, vol. 15 No 2, March 2000.

Utkin, V. 1993. *Sliding mode control design principles and applications to electric drives*. IEEE Transactions on Industrial Electronics, Volume: 40, Issue: 1, Feb. 1993 pp: 23 – 36.

Utkin, V. 1994. *Sliding mode control in mechanical systems*. Proceeding of 20th International Conference on Industrial Electronics, Control, and Instrumentation, IECON 94, Volume: 3, 5-9 Sept. 1994, pp: 1429 - 1431 Vol.3.

Utkin, V., Bartolini, G., Ferrara, A. 1992. *Design of discrete-time adaptive sliding mode control*. Proceedings of the 31st IEEE Conference on Decision and Control, 1992, 16-18 Dec. 1992, pp: 2387 - 2391 vol.2.

Utkin, V. Derdiyok, A., Zhang, Y., Guven, M. 2001. *A sliding mode speed and rotor time constant observer for induction machines*. Proceeding of the 27th IEEE Annual Conference on Industrial Electronics Society, 2001. IECON 01. Volume: 2, 29 Nov.-2 Dec. 2001 pp: 1400 - 1405 vol.2.

Utkin, V., Guldner, J., Shi, J.1999 a. *Sliding Mode Control in Electro-mechanical Systems*, ISBN0-7484-0116-4(cased). 0-265 pages, Taylor & Francis 1999.

Utkin, V., Krishnaswami, V., Siviero, C., Carbognani, F., Rizzoni, G., 1996. *Application of sliding mode observers to automobile power-train diagnostics*. Proceedings of the 1996 IEEE International Conference on Control Applications, 1996, 15-18 Sept. 1996 pp: 355 – 360.

Utkin, V., Loukianov, A., Canedo, J., Cabrera-Vazquez, J. 2004. *Discontinuous Controller for Power Systems: Sliding-Mode Block Control Approach*. IEEE Transactions on Industrial Electronics, Volume: 51, Issue: 2, April 2004 pp: 340 – 353.

Utkin, V., Young, K., Ozguner, U. 1999 b. *A control engineer's guide to sliding mode control*. IEEE Transactions on Control Systems Technology, Volume: 7, Issue: 3, May 1999 pp: 328 – 342.

Utkin, V. Zhang, Y., Changxi, J. 2000. *Sensorless sliding-mode control of induction motors*. IEEE Transactions on Industrial Electronics, Volume: 47, Issue: 6, Dec. 2000 pp: 1286 – 1297.

Utkin, V., Zhang, Y. 2002. *Sliding mode observers for electric machines-an overview*. IECON 02 [Proceeding of 28th IEEE 2002 Annual Conference of the Industrial Electronics Society], Volume: 3, 5-8 Nov. 2002, pp: 1842 - 1847 Vol.3.

Vaez, S., Bakhtvar, S. 2002. *Cascade sliding mode control of permanent magnet synchronous motors*. Industrial Electronics Society (IECON 02), IEEE 2002 28th Annual Conference. Volume: 3, 5-8 Nov. 2002 pp: 2051 - 2056 Vol.3.

Vazquez, N., Hernandez, C., Alvarez, J., Arau, J. 2003. *Sliding mode control for DC/DC converters: a new sliding surface*. Proceeding of the IEEE International Symposium on Industrial Electronics, ISIE 03, Volume: 1, June9-11, 2003, pp: 422 – 426.

Vilathgamuwa M., Deng J., Tseng, K.J. 1999. *EMI Suppression with Switching Frequency Modulated dc-dc Converters*. Proceedings of the IEEE Industry Applications Magazine, vol. 5, No. 6, 1999.

Wai, R. 2000. *Adaptive sliding-mode control for induction servomotor drive*. IEE Proceedings on Electric Power Applications, Volume: 147, Issue: 6, Nov. 2000, pp: 553 – 562.

Wang, J., Zhao, Z., Fei, X. 2000. *The application of optimal sliding mode control in DC motor*. Proceedings of the 3rd World Congress on Intelligent Control and Automation, Volume: 4, 28 June-2 July 2000, pp: 3001 - 3004 vol.4.

Weinberg, A. 1974. *Boost regulator with a new energy transfer principle*. Proceedings of the Spacecraft Power Conversion Electronics Seminar. Sept 1974, ESRO Publication SP-103.

Zhou, J., Zhou, R., Wang, Y., Guo, G. 2001. *Improved proximate time-optimal sliding-mode control of hard disk drives*. IEE Proceedings on Control Theory and Applications, Volume: 148, Issue: 6, Nov. 2001 pp: 516 – 522.

APPENDICES

APPENDIX A (Mathematical Equations)

APPENDIX A.1

To prove in CCM condition that the worst case, when selecting $L_{critical}$, occurs for a minimum output power and a maximum input voltage, refer to equation (2.12) that is re-written below:

$$L_{critical} = \frac{(V_{in} - V_o)(V_o)^2 T_s}{2P_o V_{in}}. \quad \text{(A.1.1)}$$

Re-arranging the terms

$$L_{critical} = \frac{(V_{in})(V_o)^2 T_s}{2P_o V_{in}} - \frac{(V_o)^3 T_s}{2P_o V_{in}}, \quad \text{(A.1.2)}$$

which leads to

$$L_{critical} = \frac{(V_o)^2 T_s}{2P_o}\left(1 - \frac{V_o}{V_{in}}\right). \quad \text{(A.1.3)}$$

From equation (2.5) and in order for the CCM condition to occur

$$L \geq L_{critical}. \quad \text{(A.1.4)}$$

From equation (A.1.3), the highest $L_{critical}$ value occurs when P_o is at its minimum value and V_{in} is at its maximum value, which is considered to be the worst case.

For the DCM condition to occur and from equation (2.5)

$$L < L_{critical}. \quad \text{(A.1.5)}$$

From equation (A.1.3), the lowest $L_{critical}$ value occurs when P_o is at its maximum value and V_{in} is at its minimum value, which are considered to be the worst case.

APPENDIX A.2

For the DC/DC Boost converter, shown in Figure A.1, assuming zero inductor resistance, the inductor voltage is defined as

$$V_L = L\frac{\Delta i_L}{\Delta t}, \quad \text{(A.2.1)}$$

where V_L is the voltage across the inductor, Δi_L is the peak-to-peak inductor current, and Δt is the period when the switch is in condition (on or off).

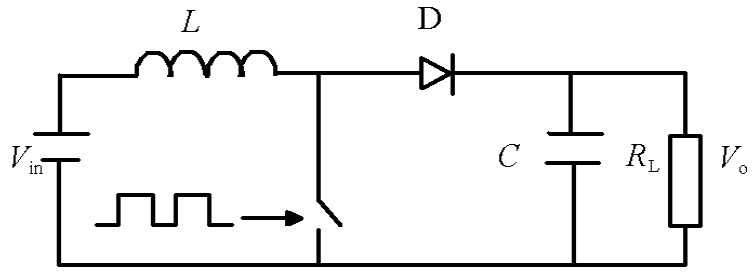

Figure A.1. DC/DC Boost converter topology used as a step up converter. The figure helps to derive the equation to find the critical inductor value.

For the case when the switch is on

$$V_{in} = L\frac{\Delta i_{in}}{DT_s}, \tag{A.2.2}$$

where i_{in} is the input current and is equal to i_L in this case, D denotes the average switching duty ratio, and T_s represents the nominal switching period and is equal to $1/f_{s(nominal)}$.

Under particular conditions, when the inductor $L = L_{critical}$, it will produce the familiar triangle wave with a minimum at zero and a maximum at 2 i_{in}. So equation (A.2.2) can be written as follows

$$V_{in} = L\frac{2\,i_{in}}{DT_s}. \tag{A.2.3}$$

For a DC/DC Boost converter, the average duty cycle is

$$D = \frac{V_o - V_{in}}{V_o}, \tag{A.2.4}$$

and

$$i_{in} = \frac{P_{in}}{V_{in}}. \tag{A.2.5}$$

For efficiency (η) = 100%

$$P_o = P_{in}, \tag{A.2.6}$$

where P_{in} is the average input power, and P_o is the average output power. Substituting equations (A.2.4), (A.2.5), (A.2.6) into (A.2.3) and for the case $L = L_{critical}$ leads to

$$V_{in} = L_{critical}\frac{2\left(\frac{P_{in}}{V_{in}}\right)}{\left(\frac{V_o - V_{in}}{V_o}\right)T_s}. \tag{A.2.7}$$

Re-arranging the terms lead to a general equation for the DC/DC Boost converter, where it defines the critical inductor value that is

$$L_{\text{critical}} = \frac{(V_{\text{o}} - V_{\text{in}})(V_{\text{in}})^2 T_{\text{s}}}{2P_{\text{in}}V_{\text{o}}}. \tag{A.2.8}$$

To prove in CCM condition that the worst case, when selecting L_{critical}, occurs for a minimum input power value and maximum input voltage value, the terms in equation (A.2.8) are re-arranged, which leads to

$$L_{\text{critical}} = \frac{(V_{\text{o}})(V_{\text{in}})^2 T_{\text{s}}}{2P_{\text{in}}V_{\text{o}}} - \frac{(V_{\text{in}})^3 T_{\text{s}}}{2P_{\text{in}}V_{\text{o}}}, \tag{A.2.9}$$

this leads to

$$L_{\text{critical}} = \frac{(V_{\text{in}})^2 T_{\text{s}}}{2P_{\text{in}}V_{\text{o}}}\left(1 - \frac{V_{\text{in}}}{V_{\text{o}}}\right). \tag{A.2.10}$$

From equation (2.5) and in order for the CCM condition to occur

$$L \geq L_{\text{critical}}. \tag{A.2.11}$$

From equation (A.2.10), the highest L_{critical} value occurs when P_{in} is at its minimum value and V_{in} is at its maximum value, which is considered to be the worst case.

For the DCM condition to occur and from equation (2.5)

$$L < L_{\text{critical}}. \tag{A.2.12}$$

From equation (A.2.10), the lowest L_{critical} value occurs when P_{in} is at its maximum value and V_{in} is at its minimum value, which are considered to be the worst case.

APPENDIX A.3

For the DC/DC Buck-Boost converter, shown in Figure A.2, assuming a zero inductor resistance, the inductor voltage is defined as

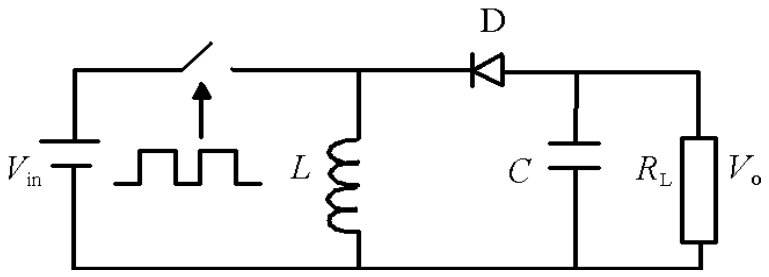

Figure A.2. DC/DC Buck-Boost converter topology used as a step up/down converter with opposite polarity. The figure helps to derive the equation to find the critical inductor value.

$$V_{\mathrm{L}} = L\frac{\Delta i_{\mathrm{L}}}{\Delta t}, \tag{A.3.1}$$

where V_{L} is the voltage across the inductor, Δi_{L} is the peak-to-peak inductor current, and Δt is the period when the switch is in condition (on or off). For the case when the switch is on

$$V_{\mathrm{in}} = L\frac{\Delta i_{\mathrm{in}}}{DT_{\mathrm{s}}}, \tag{A.3.2}$$

where i_{in} is the input current and is equal to i_{L} in this case, D denotes the average switching cycle when switch on, and T_{s} represents the nominal switching period and is equal to $1/f_{\mathrm{s(nominal)}}$.

Under particular conditions, when the inductor $L = L_{\mathrm{critical}}$, it will produce the familiar triangle wave with a minimum at zero and a maximum at 2 i_{in}. So, equation (A.3.2) can be written as

$$V_{\mathrm{in}} = L\frac{2\,i_{\mathrm{in}}}{DT_{\mathrm{s}}}. \tag{A.3.3}$$

For a DC/DC Buck-Boost converter, the average duty cycle is

$$D = \frac{V_{\mathrm{o}}}{V_{\mathrm{o}} + V_{\mathrm{in}}}, \tag{A.3.4}$$

and

$$i_{\mathrm{in}} = \frac{P_{\mathrm{in}}}{V_{\mathrm{in}}}. \tag{A.3.5}$$

For efficiency (η) = 100%

$$P_{\mathrm{o}} = P_{\mathrm{in}}, \tag{A.3.6}$$

where P_{in} is the average input power, and P_{o} is the average output power. Substituting equations (A.3.4), (A.3.5), (A.3.6) into (A.3.3) and for the case $L = L_{\mathrm{critical}}$ leads to

$$V_{\mathrm{in}} = L_{\mathrm{critical}}\frac{2\left(\frac{P_{\mathrm{in}}}{V_{\mathrm{in}}}\right)}{\left(\frac{V_{\mathrm{o}}}{V_{\mathrm{o}} + V_{\mathrm{in}}}\right)T_{\mathrm{s}}}. \tag{A.3.7}$$

Re-arranging the terms leads to a general equation for DC/DC Boost converter, where it defines the critical inductor value, that is

$$L_{\mathrm{critical}} = \frac{V_{\mathrm{o}}\left(V_{\mathrm{in}}\right)^2 T_{\mathrm{s}}}{2P_{\mathrm{in}}\left(V_{\mathrm{o}} + V_{\mathrm{in}}\right)}. \tag{A.3.8}$$

To prove in CCM condition that the worst case, when selecting L_{critical}, occurs for a minimum input power value and a maximum input voltage value, the terms in equation (A.3.8) are re-arranged, which leads to

$$L_{\text{critical}} = \frac{(V_{\text{o}})(V_{\text{in}})T_{\text{s}}}{2P_{\text{in}}}\left(\frac{V_{\text{in}}}{(V_{\text{o}}+V_{\text{in}})}\right). \tag{A.3.9}$$

From equation (2.5) and in order for the CCM condition to occur

$$L \geq L_{\text{critical}}. \tag{A.3.10}$$

From equation (A.3.9), the highest L_{critical} value occurs when P_{in} is at its minimum value and V_{in} is at its maximum value, which is considered to be the worst case.

For the DCM condition to occur and from equation (2.5)

$$L < L_{\text{critical}}\ . \tag{A.3.11}$$

From equation (A.3.9), the lowest L_{critical} value occurs when P_{in} is at its maximum value and V_{in} is at its minimum value, which are considered to be the worst case.

APPENDIX A.4

From equation (4.8)

$$\dot{\boldsymbol{x}} = \boldsymbol{f}(\boldsymbol{x},t) + \boldsymbol{B}(\boldsymbol{x},t)u\ . \tag{A.4.1}$$

And from (4.11)

$$\boldsymbol{G}\,\dot{\boldsymbol{x}} = \boldsymbol{G}\,\boldsymbol{f}(\boldsymbol{x},t) + \boldsymbol{G}\boldsymbol{B}(\boldsymbol{x},t)u_{\text{eq}}. \tag{A.4.2}$$

Rearranging the terms

$$u_{eq} = -(\boldsymbol{G}\,\boldsymbol{B})^{-1}\boldsymbol{G}\,\boldsymbol{f}(\boldsymbol{x},t). \tag{A.4.3}$$

Substituting equation (A.4.3) into equation (A.4.1) leads to

$$\dot{\boldsymbol{x}} = \boldsymbol{f}(\boldsymbol{x},t) - \boldsymbol{B}(\boldsymbol{x},t)(\boldsymbol{G}\,\boldsymbol{B})^{-1}\boldsymbol{G}\,\boldsymbol{f}(\boldsymbol{x},t), \tag{A.4.4}$$

which results in the same equation as in equation (4.12) and is written below

$$\dot{\boldsymbol{x}} = \left[\boldsymbol{I} - \boldsymbol{B}(\boldsymbol{x},t)(\boldsymbol{G}\,\boldsymbol{B})^{-1}\boldsymbol{G}\right]\boldsymbol{f}(\boldsymbol{x},t). \tag{A.4.5}$$

APPENDIX A.5

For the DC/DC Buck converter shown in Figure 4.4, it is more convenient to use a system description, which involves the output error and its derivative, i.e.

$$x_1 = V_{\mathrm{o}} - V_{\mathrm{ref}} . \tag{A.5.1}$$

$$x_2 = \frac{dx_1}{dt} = \frac{d\left(V_{\mathrm{o}} - V_{\mathrm{ref}}\right)}{dt} = \frac{i_c}{C} . \tag{A.5.2}$$

By taking the derivative

$$\dot{x}_1 = x_2 . \tag{A.5.3}$$

$$\dot{x}_2 = \frac{1}{C}\frac{d}{dt} i_{\mathrm{c}} . \tag{A.5.4}$$

Now considering the DC/DC Buck converter when the switch is on

$$i_{\mathrm{c}} = i_{\mathrm{L}} - i_{\mathrm{o}} . \tag{A.5.5}$$

Substituting equation (A.5.5) into (A.5.4) results in

$$\dot{x}_2 = \frac{1}{C}\left[\frac{d}{dt} i_{\mathrm{L}} - \frac{d}{dt} i_{\mathrm{o}}\right]. \tag{A.5.6}$$

But

$$V_{\mathrm{L}} = L\frac{d}{dt} i_{\mathrm{L}} ,$$

$$\frac{d}{dt} i_{\mathrm{L}} = \frac{V_{\mathrm{L}}}{L} . \tag{A.5.7}$$

For the DC/DC Buck converter when the switch is on

$$V_{\mathrm{L}} = V_{\mathrm{in}} - V_{\mathrm{o}} . \tag{A.5.8}$$

Substituting (A.5.8) into (A.5.7) leads to

$$\frac{d}{dt} i_{\mathrm{L}} = \frac{V_{\mathrm{in}} - V_{\mathrm{o}}}{L} . \tag{A.5.9}$$

Substituting (A.5.9) into (A.5.6) and for $i_{\mathrm{o}} = \frac{V_{\mathrm{o}}}{R_{\mathrm{L}}}$ results in

$$\dot{x}_2 = \frac{1}{C}\left[\frac{V_{\mathrm{in}} - V_{\mathrm{o}}}{L} - \frac{d}{dt}\frac{V_{\mathrm{o}}}{R_{\mathrm{L}}}\right]. \tag{A.5.10}$$

Re-arranging the terms

$$\dot{x}_2 = \frac{V_{\text{in}}}{LC} - \frac{V_{\text{o}}}{LC} - \frac{1}{R_{\text{L}}C}\frac{d}{dt}V_0 . \tag{A.5.11}$$

From equation (A.5.1)

$$V_{\text{o}} = x_1 + V_{\text{ref}} . \tag{A.5.12}$$

Substituting equation (A.5.12) into (A.5.11) leads to

$$\dot{x}_2 = \frac{V_{\text{in}}}{LC} - \frac{\left(x_1 + V_{\text{ref}}\right)}{LC} - \frac{1}{R_{\text{L}}C}\frac{d}{dt}V_0 . \tag{A.5.13}$$

Re-arranging the terms

$$\dot{x}_2 = \frac{V_{\text{in}}}{LC} - \frac{x_1}{LC} - \frac{V_{\text{ref}}}{LC} - \frac{1}{R_{\text{L}}C}\frac{d}{dt}V_0 . \tag{A.5.14}$$

From equation (A.5.2) $\frac{dV_{\text{ref}}}{dt} = 0$, then the equation becomes

$$x_2 = \frac{dV_{\text{o}}}{dt} . \tag{A.5.15}$$

Substituting equation (A.5.15) into (A.5.14) results in

$$\dot{x}_2 = \frac{V_{\text{in}}}{LC} - \frac{x_1}{LC} - \frac{V_{\text{ref}}}{LC} - \frac{x_2}{R_{\text{L}}C} . \tag{A.5.16}$$

For the DC/DC Buck converter, the control signal *u* is multiplied by the input voltage

$$\dot{x}_2 = \frac{V_{\text{in}}}{LC}u - \frac{x_1}{LC} - \frac{V_{\text{ref}}}{LC} - \frac{x_2}{R_{\text{L}}C} . \tag{A.5.17}$$

Equations (A.5.3) and (A.5.17) define the system equation for the DC/DC Buck converter controlled with the SMC.

APPENDIX A.6

For the DC/DC Buck converter shown in Figure 4.4, it is more convenient to use a system description, which involves the output error and its derivative, i.e.

$$x_1 = V_{\text{o}} - V_{\text{ref}} . \tag{A.6.1}$$

$$x_2 = \frac{dx_1}{dt} = \frac{d\left(V_{\text{o}} - V_{\text{ref}}\right)}{dt} = \frac{i_c}{C} . \tag{A.6.2}$$

By taking the derivative

$$\dot{x}_1 = x_2 \,. \tag{A.6.3}$$

$$\dot{x}_2 = \frac{1}{C}\frac{d}{dt} i_{\mathrm{c}} \,. \tag{A.6.4}$$

Now considering the DC/DC Buck converter when the switch off

$$i_{\mathrm{c}} = i_{\mathrm{L}} - i_{\mathrm{o}} \,. \tag{A.6.5}$$

Substituting equation (A.6.5) into (A.6.4) results in

$$\dot{x}_2 = \frac{1}{C}\left[\frac{d}{dt} i_{\mathrm{L}} - \frac{d}{dt} i_{\mathrm{o}}\right]. \tag{A.6.6}$$

But the inductor current is assumed to be zero

$$i_{\mathrm{L}} = 0 \,. \tag{A.6.7}$$

Substituting equation (A.6.7) into (A.6.6) leads to

$$\dot{x}_2 = \frac{1}{C}\left[-\frac{d}{dt} i_{\mathrm{o}}\right]. \tag{A.6.8}$$

It is known that

$$i_{\mathrm{o}} = \frac{V_{\mathrm{o}}}{R_{\mathrm{L}}} \,. \tag{A.6.9}$$

Substituting equation (A.6.9) into (A.6.8) leads to

$$\dot{x}_2 = -\frac{1}{R_{\mathrm{L}} C}\left[\frac{d}{dt} V_{\mathrm{o}}\right]. \tag{A.6.10}$$

From equation (A.6.1)

$$V_{\mathrm{o}} = x_1 + V_{\mathrm{ref}} \,. \tag{A.6.11}$$

Substituting equation (A.6.11) into (A.6.10) results in

$$\dot{x}_2 = -\frac{1}{R_{\mathrm{L}} C}\left[\frac{d}{dt}\left(x_1 + V_{\mathrm{ref}}\right)\right]. \tag{A.6.12}$$

Integrating both sides of equation (A.6.12) leads to equation (4.12) in the text, which is

$$x_2 = -\frac{1}{R_L C}\left(x_1 + V_{ref}\right). \tag{A.6.13}$$

APPENDIX A.7

From (4.16)

$$\dot{\boldsymbol{x}} = \boldsymbol{A}\boldsymbol{x} + \boldsymbol{B}\boldsymbol{u} + \boldsymbol{D}\,, \tag{A.7.1}$$

where

$$\boldsymbol{A} = \begin{bmatrix} 0 & 1 \\ -\frac{1}{LC} & -\frac{1}{R_L C} \end{bmatrix}, \qquad \boldsymbol{B} = \begin{bmatrix} 0 \\ \frac{V_{in}}{LC} \end{bmatrix}, \qquad \boldsymbol{D} = \begin{bmatrix} 0 \\ -\frac{V_{ref}}{LC} \end{bmatrix}. \tag{A.7.2}$$

And it is known from (4.19) that

$$\sigma(\boldsymbol{x}) = c_1 x_1 + \dot{x}_1 = 0\,. \tag{A.7.3}$$

Taking the derivative of equation (A.7.3)

$$\dot{\sigma}(\boldsymbol{x}) = \boldsymbol{C}^T \dot{\boldsymbol{x}} = 0\,. \tag{A.7.4}$$

Substituting equation (A.7.1) into equation (A.7.4) leads to

$$\dot{\sigma}(\boldsymbol{x}) = \boldsymbol{C}^{\mathrm{T}}\boldsymbol{A}\boldsymbol{x} + \boldsymbol{C}^{\mathrm{T}}\boldsymbol{B}\boldsymbol{u} + \boldsymbol{C}^{\mathrm{T}}\boldsymbol{D}\,. \tag{A.7.5}$$

From equation (4.20) and for the first condition when $u = 0$ and for $\sigma(x) > 0$

$$\dot{\sigma}(\boldsymbol{x}) = \begin{bmatrix} c_1 & 1 \end{bmatrix}\begin{bmatrix} 0 & 1 \\ -\frac{1}{LC} & -\frac{1}{R_L C} \end{bmatrix}\begin{bmatrix} x_1 \\ x_2 \end{bmatrix} + \begin{bmatrix} c_1 & 1 \end{bmatrix}\begin{bmatrix} 0 \\ \frac{V_{in}}{LC} \end{bmatrix} 0 + \begin{bmatrix} c_1 & 1 \end{bmatrix}\begin{bmatrix} 0 \\ -\frac{V_{ref}}{LC} \end{bmatrix}, \tag{A.7.6}$$

results in

$$\lambda_1(\boldsymbol{x}) = (c_1 - \frac{1}{R_L C})x_2 - \frac{1}{LC}x_1 - \frac{V_{ref}}{LC} < 0\,. \tag{A.7.7}$$

Similarly, for the second condition in (4.20) $u = 1$ for $\sigma(x) < 0$

$$\dot{\sigma}(\boldsymbol{x}) = \begin{bmatrix} c_1 & 1 \end{bmatrix}\begin{bmatrix} 0 & 1 \\ -\frac{1}{LC} & -\frac{1}{R_L C} \end{bmatrix}\begin{bmatrix} x_1 \\ x_2 \end{bmatrix} + \begin{bmatrix} 0 \\ \frac{v_{in}}{LC} \end{bmatrix} 1 + \begin{bmatrix} c_1 & 1 \end{bmatrix}\begin{bmatrix} 0 \\ -\frac{V_{ref}}{LC} \end{bmatrix}, \tag{A.7.8}$$

leads to

$$\lambda_2(\boldsymbol{x}) = (c_1 - \frac{1}{R_L C})x_2 - \frac{1}{LC}x_1 - \frac{V_{in} - V_{ref}}{LC} > 0 \quad . \tag{A.7.9}$$

APPENDIX B (Simulation Models and Matlab™ – Scripts)

APPENDIX B.1

Matlab™ -scripts for Figure 3.3 a) and b) in Chapter 3.

```
% This is the transfer function of an uncompensated loop for the DC/DC Buck converter

L = 69e-6
C = 220e-6
R_L = 10
Num = [0 0 2.5]
Den = [L*C L/R_L 1]
Sys = tf (Num, Den)

% This is the derivative transfer function

Num1 = 0.806*[1/5234.5  1]
Den1 = [1/44168  1]
Sys1 = tf (Num1,Den1)

% This is the Integral transfer function

f_L = 500
ω_L = 2*3.14*f_L
Num2 = [1 ωL]
Den2 = [1  0]
Sys2 = tf (Num2, Den2)

% This is the transfer function of the compensated loop (PID plus DC/DC Buck converter)

Sys3 = tf (Sys*Sys1*Sys2)

% This is the Bodeplot of the uncompensated loop for DC/DC Buck converter

Subplot (2, 1, 1)
Bode (Sys)
Margin (Sys)
Grid
Hold

% This is the Bodeplot of the compensated loop (PID plus for DC/DC Buck converter)

Subplot (2,1,2)
Bode (Sys3)
Margin (Sys3)
Grid
```

APPENDIX B.2

Simulation models of a DC/DC Buck converter with PID control used in the publications

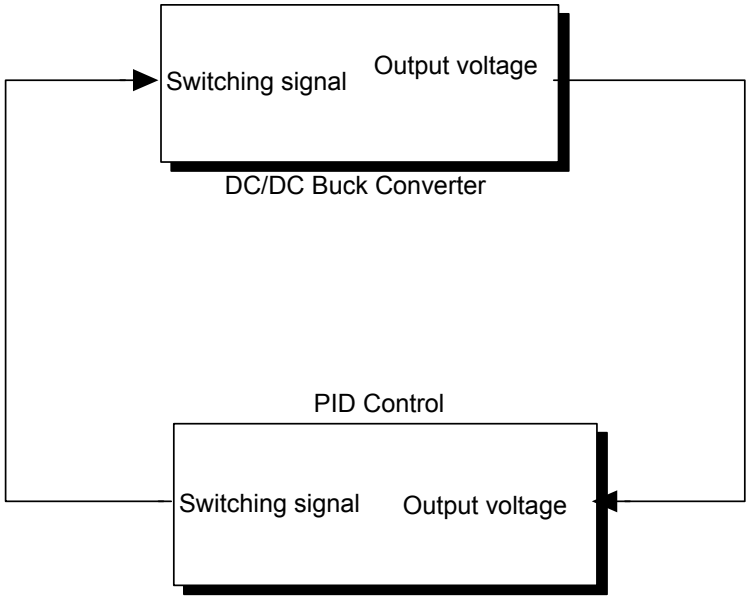

Figure B.1. Simulink™ model for DC/DC Buck converter with PID control, used as a simulation model in the publications of the thesis.

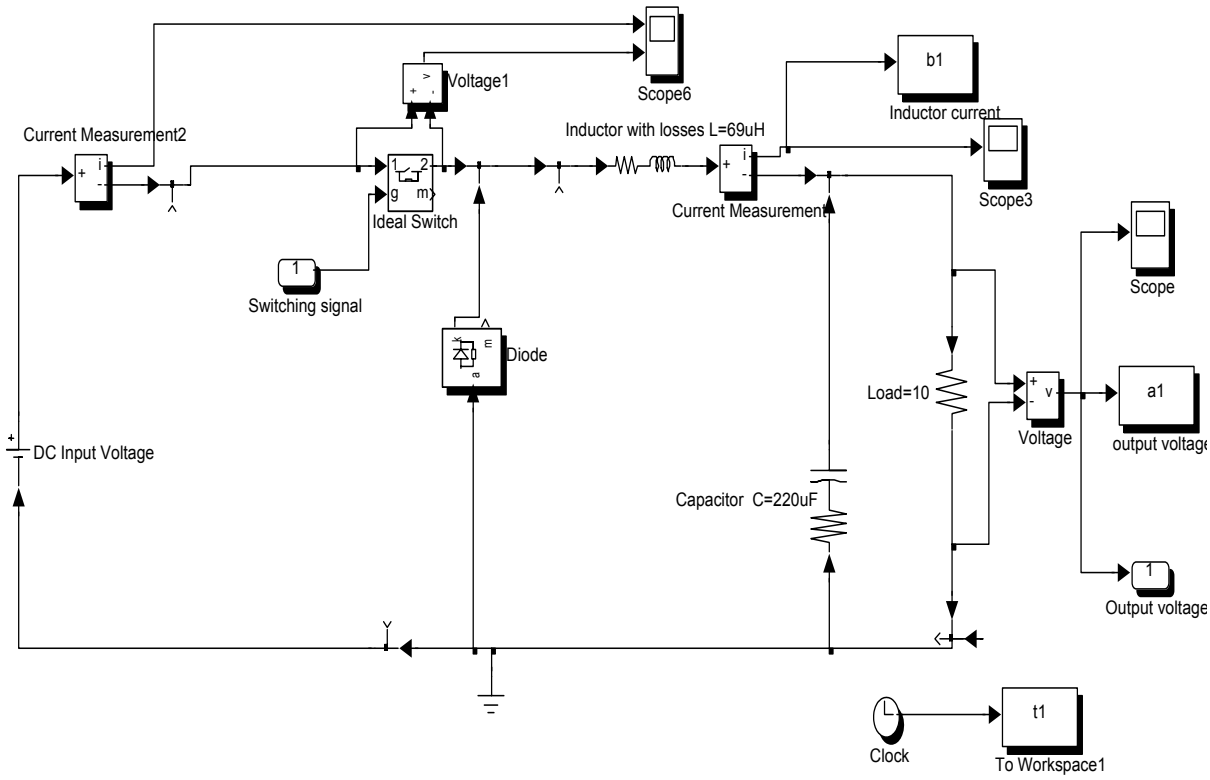

Figure B.2. Simulink™ model for the internal structure of the DC/DC Buck converter, given in Figure B.1. The inductor loss is set to minimum.

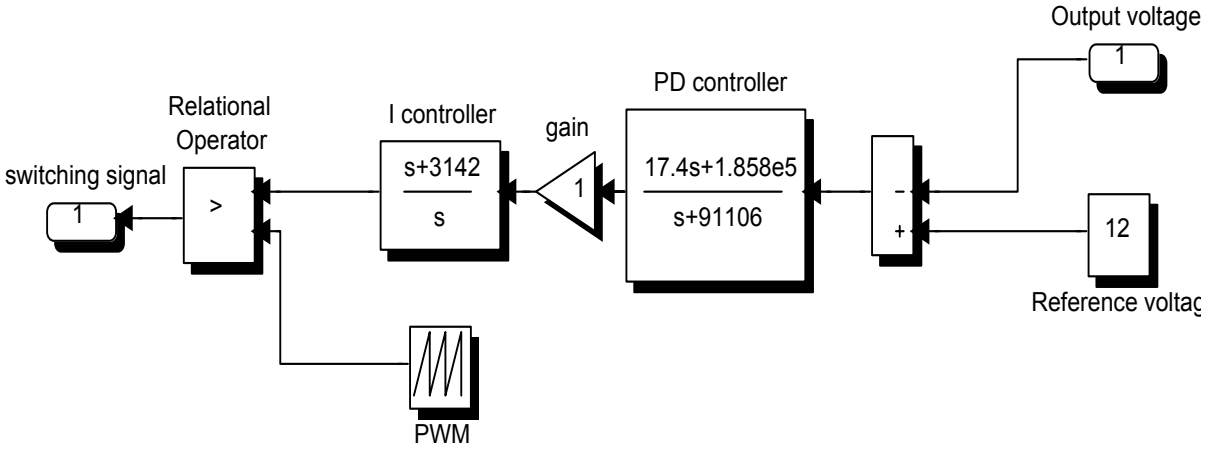

Figure B.3. Simulink^{TM} model for the internal structure of the PID, given in Figure B.1.

APPENDIX B.3

Simulation models of a DC/DC Buck converter with SMC of Figures 4.8, and 4.9

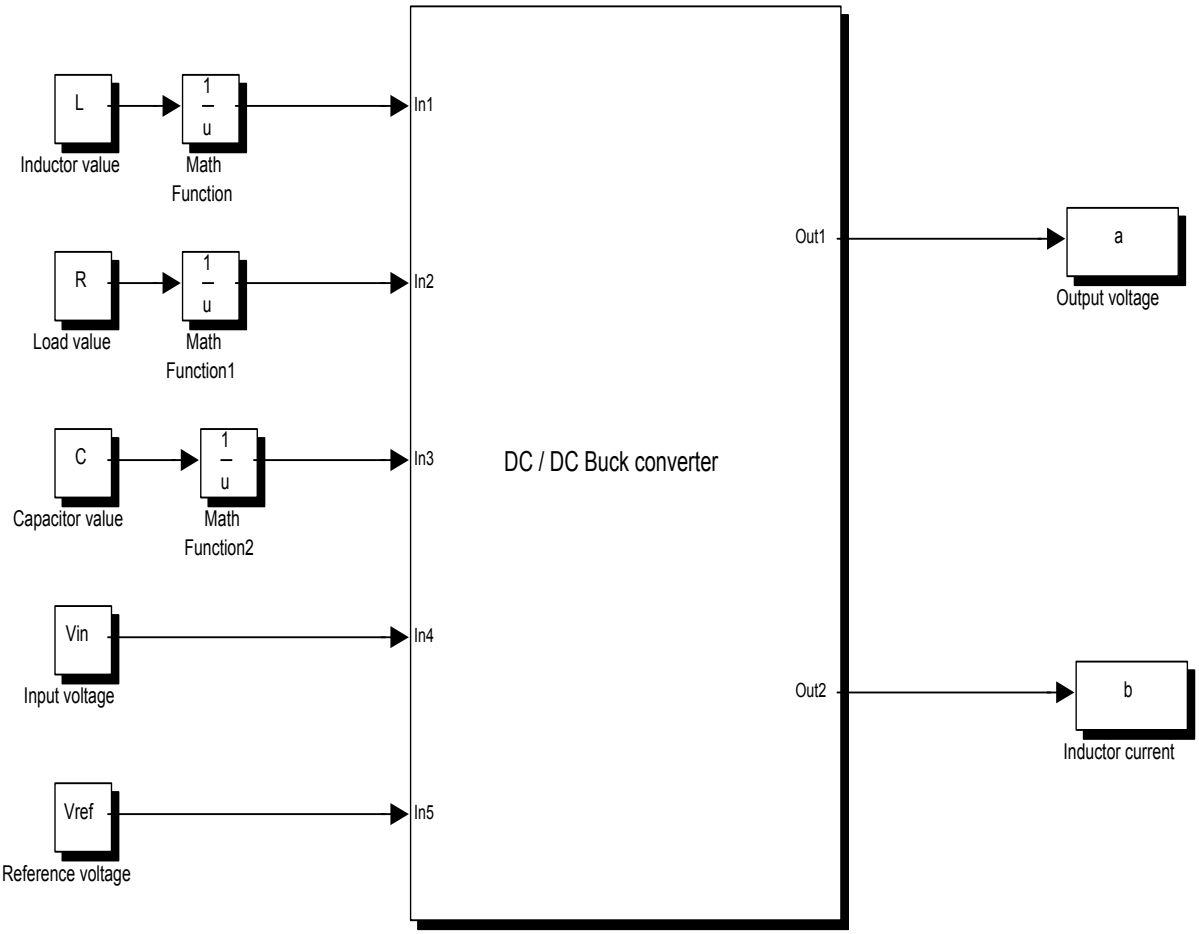

Figure B.4. Simulink^{TM} model for DC/DC Buck converter with SMC, the model is used to obtain Figures 4.8, and 4.9. The model is derived from equation (4.15).

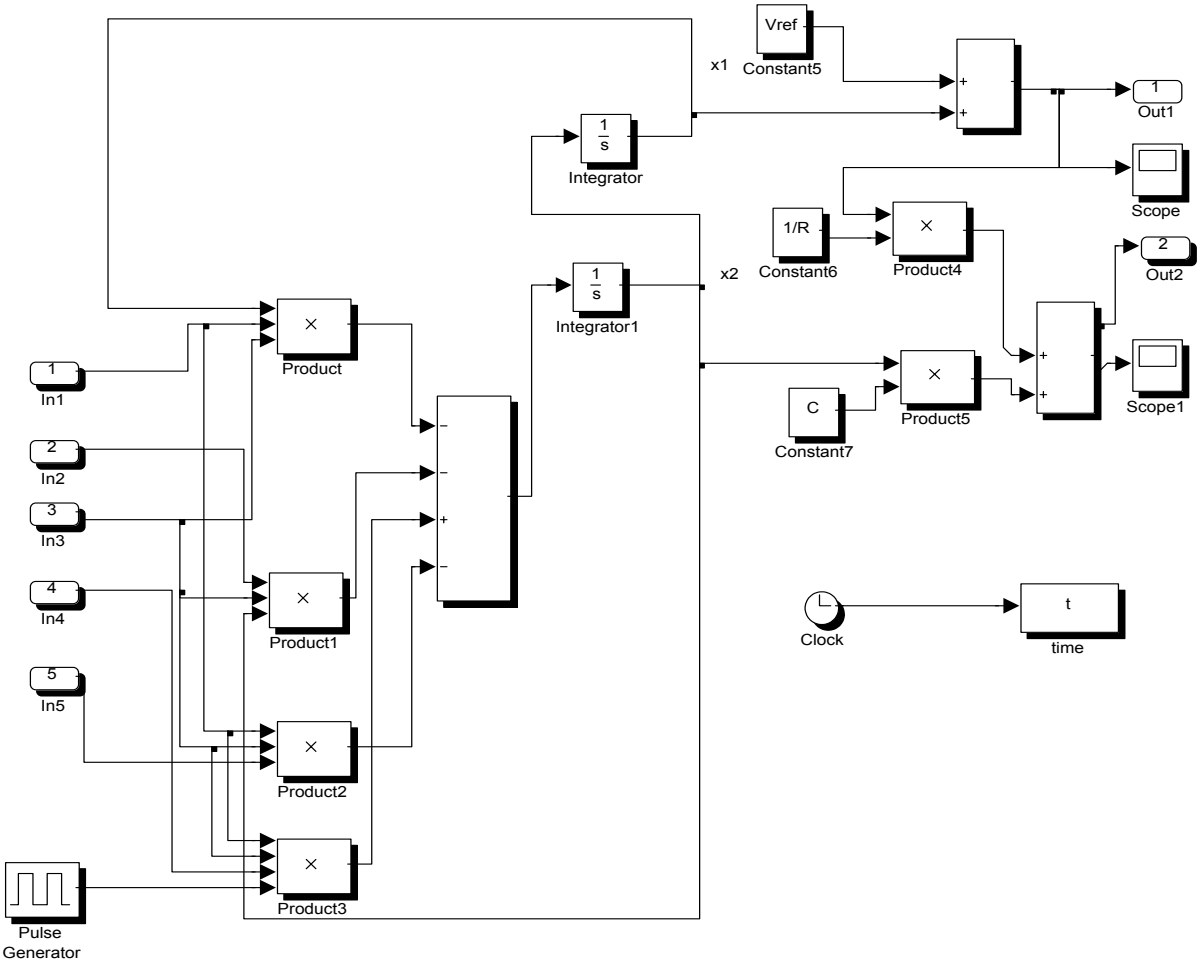

Figure B.5. Simulink^{TM} model for the internal structure of DC/DC Buck converter given in Figure B.4.

APPENDIX B.4

Simulation models of a DC/DC Buck converter with SMC used in the publications

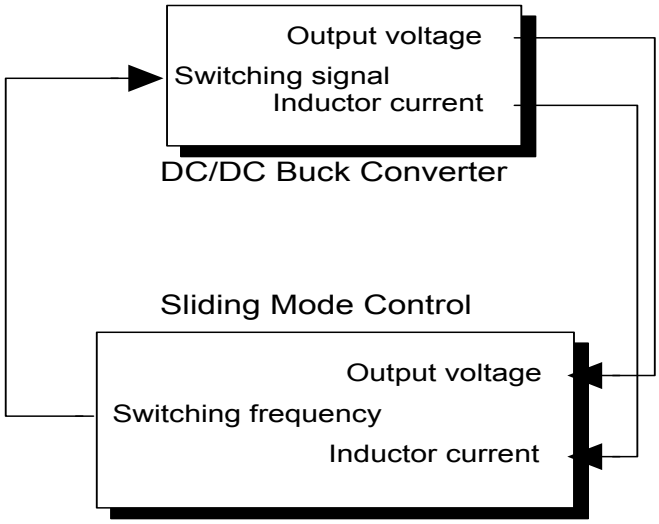

Figure B.6. Simulink^{TM} model for DC/DC Buck converter with SMC, used as a simulation model in the publications of the thesis.

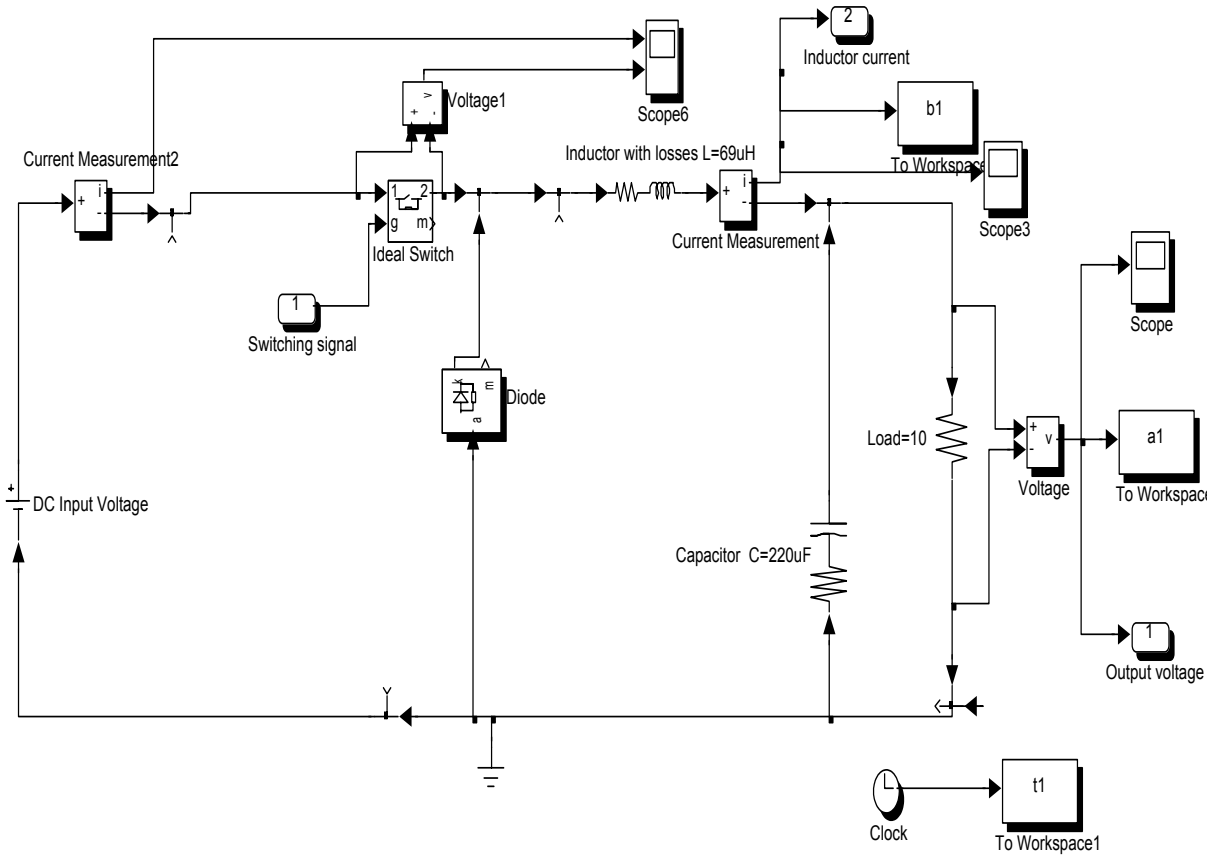

Figure B.7. Simulink™ model for the internal structure of the DC/DC Buck converter, given in Figure B.6. The inductor loss is set to minimum value.

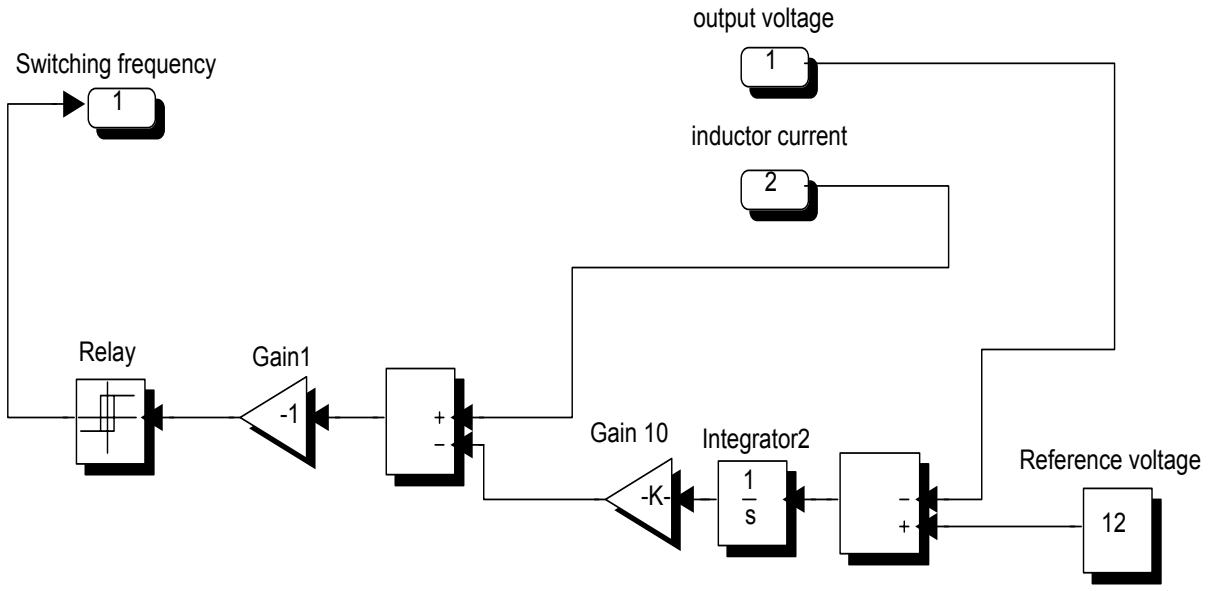

Figure B.8. Simulink™ model for the internal structure of the SMC, given in Figure B.6.

APPENDIX B.5

Simulation models of a HWZCS DC/DC Buck converter with SMC used in the publications

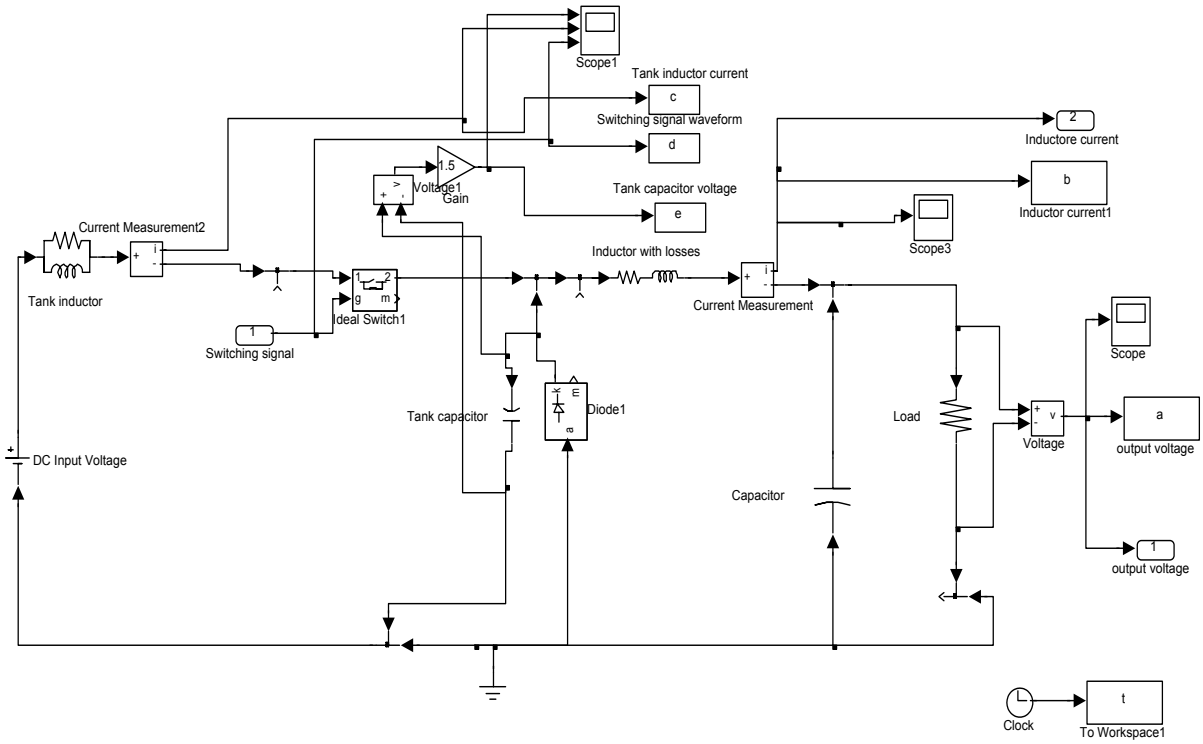

Figure B.9. Simulink^{TM} model for the internal structure of the HWZCS DC/DC Buck converter used for simulation.

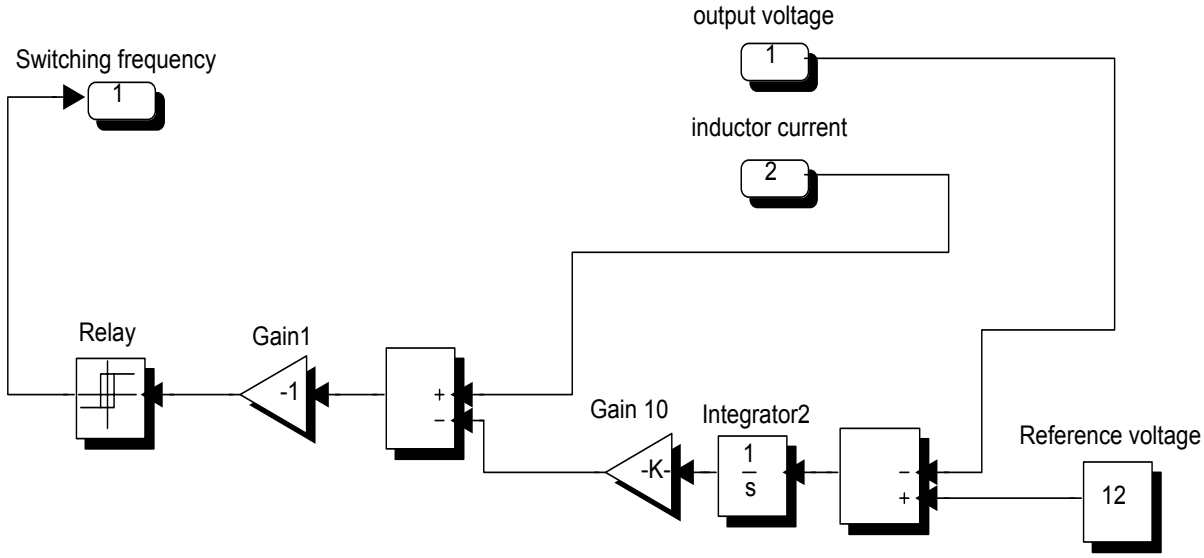

Figure B.10. Simulink^{TM} model for the internal structure of the SMC, used to control the circuit Figure B.9.

APPENDIX C (Schematic Diagram of the Prototype)

APPENDIX C.1

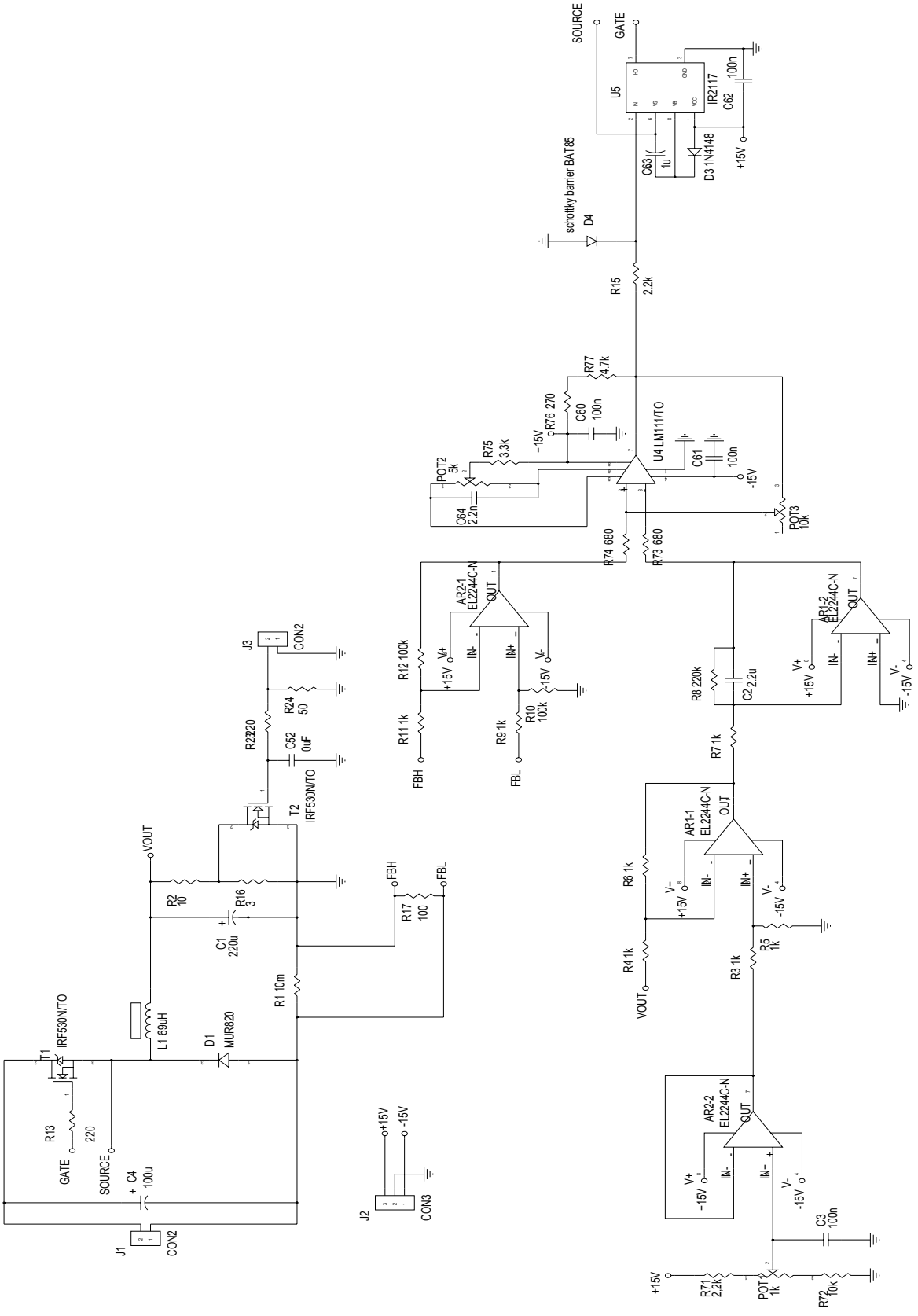

Figure C.1. Schematic diagram of the DC/DC Buck converter controlled by SMC.

Publication P [1]

M. Ahmed, M. Kuisma, K. Tolsa, P. Silventoinen. Standard Procedure for Modelling the Basic Three Converters (Buck, Boost, and Buck-boost) With PID Algorithm Applied. *Proceedings of XIII-th International Symposium on Electrical Apparatus and Technologies, SIELA 2003, 29-30 May, 2003*. Plovdive, Bulgaria.

STANDARD PROCEDURE FOR MODELING THE BASIC THREE CONVERTERS (BUCK, BOOST, AND BUCK-BOOST) WITH PID ALGORITHM APPLIED

M. Ahmed, M. Kuisma, K. Tolsa, P. Silventoinen

Lappeenranta University of Technology, P.O. Box 20, 53851 LPR, Finland
Department of Electrical Engineering
E-Mail: ahmed@lut.fi. E-Mail: kuisma@lut.fi. E-mail: kimmo.tolsa@lut.fi.
E-Mail: pertti.silventoinen@lut.fi

Abstract. During the last few decades switch mode power supplies have been widely investigated and analyzed in different ways. Designers are interested in finding the easiest method to analyze and model the DC/DC converter and then choose the suitable control technique that can get the best results. This paper focuses on a simple algorithm that could be used to analyze the basic three converters Buck, Boost, and Buck-Boost, choosing the Buck converter as an example. The analyzed method uses the AC equivalent circuit modelling where one equation is used for all the converters mentioned earlier, comparing it with look-up table, calculating the transfer function of the converter with unity loop gain where. At this stage Matlab™ is used to check the circuit performance. PID control could be added to the circuit also with some simple procedure to improve the stability. The overall system is built in Matlab/Simulink™. A prototype of the model is build-up based on the Simulink™ model. Comparison of the output voltage and inductor current between the simulated model and prototype model results are done in steady state and dynamic tests for line and load variation are presented. The efficiency of the prototype model is measured. The paper shows that a simple algorithm is used to reach our goal for teaching purposes and also for some industry applications.

KEYWORDS: Buck converter, PID control.

1. INTRODUCTION

The wide variety of circuit topologies ranges from the single transistor Buck, Boost, and Buck-Boost converters to complex configuration comprising two or four devices and employing soft-switching or resonant techniques to control the switching losses. However, similar methods of analysis and control are applied to many of these converters. The inherent switching operation of power electronic converters results in the circuit components being connected together in periodically changing configurations, each configuration being described by a separate set of equations. The transient analysis and control design of converters is therefore difficult since a number of equations must be solved in sequence.

The technique of averaging provides a solution of this problem. A single equation may be formed to describe the converter approximately over a number of switching cycles by simply taking linearly weighted average of the separate equations for each switched configuration of the converter. The basic AC modelling approach is a common averaging technique.

When the circuit is modelled, we go through the design of PID controller with the help of Matlab™ in a simple way to get an overall system with good quality performance. Simulink™ model of the converter is built up and the controller obtained is added to the model (the reason behind replacing the linarized model by the Simulink™ model is to make dynamic tests). A prototype of the system using op-amp for the control circuit is build-up in the laboratory. Comparison between simulated and prototype results are done.

2. THE BASIC AC MODELLING APPROACH

The inductor current and capacitor voltage of small-signal AC model of the Buck converter are given in equation (1) and (2)

$$L\frac{d\hat{i}(t)}{dt}=D\hat{v}_{in}(t)+\hat{d}(t)V_{in} \tag{1}$$

$$C\frac{d\hat{v}(t)}{dt}=-\frac{\hat{v}_o(t)}{R_L} \tag{2}$$

The AC output voltage variation $\hat{v}_0(t)$ can be expressed as the superposition of the terms arising from those two inputs

$$\hat{v}_o(s)=G_{vd}(s)\hat{d}(s)+G_{vg}(s)\hat{v}_{in}(s) \tag{3}$$

The first term represents the control to output transfer function while the second term represents the line to output transfer function. Hence the transfer function $G_{vd}(s)$ and $G_{vg}(s)$ can be defined as

$$G_{vd}(s)=\frac{\hat{v}_o(s)}{\hat{d}(s)}\ ,\ G_{vg}(s)=\frac{\hat{v}_o(s)}{\hat{v}_{in}(s)} \tag{4}$$

An algebraic approach to drive these transfer functions is by talking the Laplace transform and letting the initial condition be zero, we can find the *general transfer function*

$$\hat{v}_o(s)=G_{go}\frac{1}{1+\frac{s}{Q\omega_o}+\left(\frac{s}{\omega_o}\right)^2}\hat{v}_{in}(s)+G_{do}\frac{\left(1-\frac{s}{\omega_z}\right)}{1+\frac{s}{Q\omega_o}+\left(\frac{s}{\omega_o}\right)^2}\hat{d}(s) \tag{5}$$

The line to output transfer function contains DC gain G_{go}, while the control to output transfer function have a DC gain G_{do}. The salient features of the line to output and control to output transfer functions of the basic (Buck, Boost, and Buck-Boost) converters are summarized in table.1.

Table.1 Silent features of the small-signal CCM transfer function of some basic DC/DC converter [1].

Converter	G_{go}	G_{do}	W_o	Q(quality factor)	W_z
Buck	D	$\frac{V_o}{D'}$	$\frac{1}{\sqrt{LC}}$	$R_L\sqrt{\frac{C}{L}}$	∞
Boost	$\frac{1}{D'}$	$\frac{V_o}{D'}$	$\frac{D'}{\sqrt{LC}}$	$D'R\sqrt{\frac{C}{L}}$	$\frac{D'^2R_L}{L}$
Buck-Boost	$\frac{D}{D'}$	$\frac{V_o}{DD'^2}$	$\frac{D'}{\sqrt{LC}}$	$D'R\sqrt{\frac{C}{L}}$	$\frac{D'^2R_L}{DL}$

3. BUCK CONVERTER WITH PID CONTROL

At this stage and with the aid of equation (5) and table 1 it is possible to design any of the three basic converters with standard procedure focusing on the weak points of the converter like poor phase margin at high frequency, low DC gain at low frequency and improving these parameters by addition of PID control. The Buck converter has been chosen as an example with the following parameters shown in table 2.

Table 2.The converter main circuit parameters

Parameter name	Symbol	Value
Input voltage	V_{in}	24 volts
Output voltage	V_o	12 volts
Capacitor	C	220 µF
Inductor	L	69 µH
Load resistance	R_L	13 Ω
Switching frequency	$f_{s(nominal)}$	100 kHz

1. By simple comparison between equation (5) and table.1, we find that

$$G_{do}=\frac{V_o}{D}=24\,,\ f_o=\frac{\omega_o}{2.\pi}=\frac{1}{2.\pi.L.C}=1.292\ \text{kHz},Q=R_L\sqrt{\frac{C}{L}}=17.8$$

By substituting the control to output part of equation (5), we get

$$T(s)=\frac{G_cH(s)}{V_m}\frac{V_o}{D}\frac{1}{1+\frac{s}{\omega_oQ}+\left(\frac{s}{\omega_o}\right)^2} \tag{6}$$

2. With unity gain compensator and equating s = 0, we can find the DC gain of the loop system

T_{uo} = 2.502 = 7.9 dB

3. With Matlab™ help, bode diagram of the overall system is shown in figure 1.The overall system has a poor phase margin of 2.4 degree at a frequency equal 2.417 kHz.

4. Let us design a compensator to attain a crossover frequency f_c of one twentieth of the switching frequency (assumption)

(7) $$f_c = \frac{1}{20} f_s = 5\,\text{kHz}$$

5. The gain at f_c equal to-19 dB, to obtain a unity gain at f_c, the compensator should have a gain of 19 dB at f_c. This compensator should improve the phase margin, so a PD is needed. We choose the phase margin to be 47 degree (assumption), and the lead compensator will have the following pole and zero.

(8) $$f_z = (5\text{kHz})\sqrt{\frac{1-\sin(47^\circ)}{1+\sin(47^\circ)}} = 1.7\,\text{kHz}, f_p = (5\text{kHz})\sqrt{\frac{1+\sin(47^\circ)}{1-\sin(47^\circ)}} = 14.5\,\text{kHz}$$

6. The low-frequency compensator gain of 19 dB at 5 kHz is obtained as follow:

(9) $$G_{co} = \left(\frac{f_c}{f_o}\right)^2 \frac{1}{T_{uo}} \sqrt{\frac{f_z}{f_p}} = 2.04$$

7. The low frequency regulation could be further improved by an addition of inverted zero (lag compensator), so a PID compensator is build up, and to let the integral control not affect the phase margin we choose f_L to be one tenth of f_c.

(10) $$f_L = 500\text{Hz}$$

8. This lead compensator will increase the gain at frequency bellow the 500 Hz. From previous calculations the PID control will have the following transfer function (equation 11), and bode plot of the Buck converter with PID control is shown in figure 2.

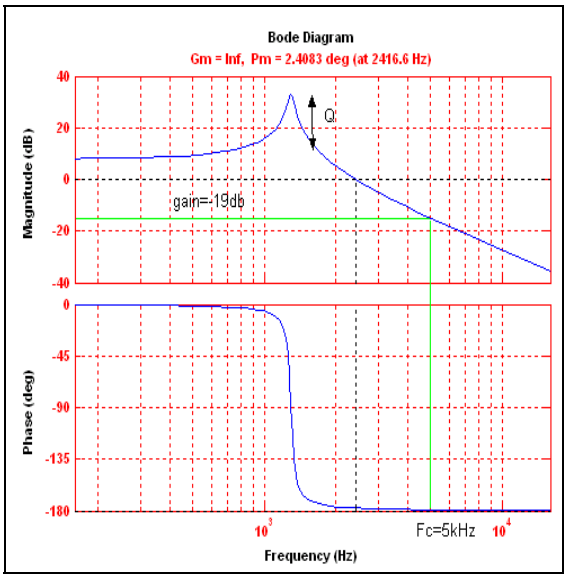

Figure 1. Bode plot of the overall system with unity compensator feedback.

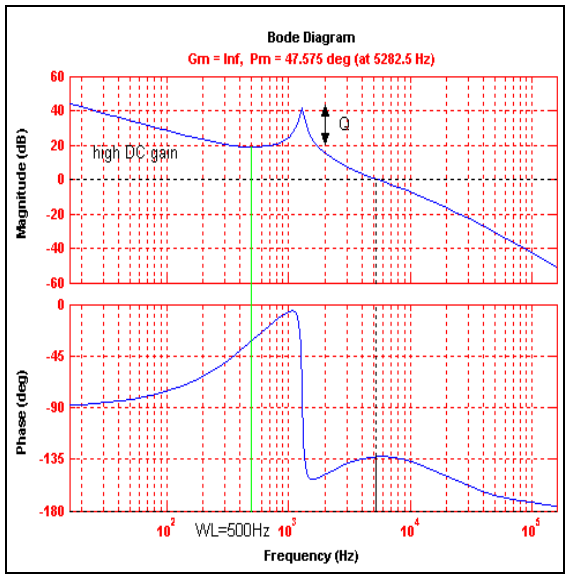

Figure 2. Bode plot of Buck converter with PID compensator it could be shown that the phase margin has improved and is 47.5 degree

$$G_c(s) = G_{co}\frac{\left(1+\frac{s}{\omega_Z}\right)\left(1+\frac{\omega_L}{s}\right)}{\left(1+\frac{s}{\omega_P}\right)} \quad (11)$$

3.1 Simulation model

Figure 3 shows the block diagram of the PID control loop that is used for design of the Buck converter in Matlab/Simulink™, and this application could be extended to the basic three converters simply by changing the parameters in the derivative and integral action by following the procedure explained earlier.

3.2 Prototype model

Straightforward prototype implementation of the Simulink™-model was constructed in the Laboratory of Applied Electronics, Lappeenranta University of Technology. Figure 4 shows the block diagram of the model and the main components used in the design. The operation of the prototype can be described as follow:

The output voltage is subtracted from the reference voltage using op-amp1. The voltage difference signal is passed through integrator (op-amp2). The integrated signal is passed through differentiator (op-amp3) generating signal 1. Signal 1 is compared with a saw tooth signal (signal 2) using LM111. The output level of the LM111 signal should be translated to a voltage difference between gate-source of the switching device IRF530. High side MOSFET/IGBT driver IR2117 is used for this purpose.

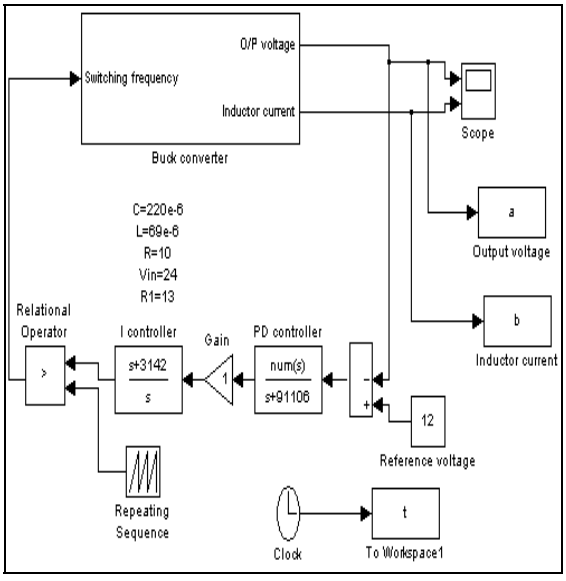

Figure 3. Buck converter with PID control implemented in Matlab/Simulink™.

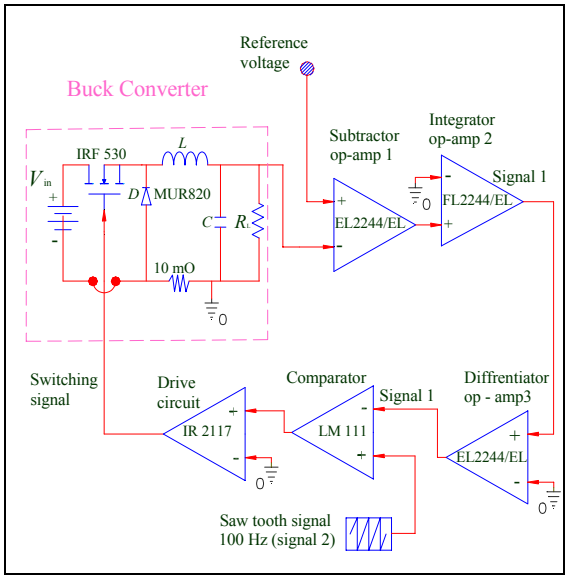

Figure 4. Simplified block diagram of the Buck converter with PID control. For simplicity the passive components are not shown.

4. TEST RESULTS

Figure 5 shows the output voltage and inductor current of the Simulink/Matlab™ model, where the mean output voltage is 12 volts and mean inductor current is 0.85 A and 1.1 A peak to peak. It is interesting to see that mean output voltage is 12.2 volt and mean inductor current is 0.78 A of the prototype model (Figure 6.) are approximately the same as in the simulated model (Figure 5.). This shows that the measured model could be used in the design of switch mode power supply and it gives acceptable results. Next for dynamic test the circuit was tested under line variation were the input voltage take a step change from 20 volt to 28 volt, figure 7 shows the output voltage of the simulated model with a very small overshoot and settling time that it could be said that it can be neglected. The same response was obtained for the prototype model in figure 8. For load variation the load value was changed from 10 Ω to 13 Ω, it could be seen that in both simulated and prototype results in figures 9 and 10 respectively that the system is not affected by the disturbance applied. The efficiency of the circuit was measured to check the power loss in the prototype model. The results showed that our non-optimized model had efficiency of 93%.

5. CONCLUSION

The paper focused on implementing a standard algorithm to analyze the basic three converters using small signal AC model. Any of these converters could be designed with unity feedback using the look-up table and comparing it with the general transfer function (the Buck converter was taken as an example in this paper). The overall system was tested where the stability can be assessed using phase margin test. Compensator is added in the forward path of feedback loop to shape the loop gain such that the desired performance is obtained. The system was improved using a PID control using again a standard procedure. The overall model was implemented using Matlab/Simulink™; a prototype of the simulated model was build-up. The output voltage and inductor current of both models were compared in steady state and dynamic response. The efficiency was also calculated and they all showed acceptable results. The paper shows that with standard mathematical procedure and a simple effective control technique, it is possible to design a switch power supply with good performance.

REFRENCES

[1] Robert W. Erickson. "*Fundamentals of Power Electronics*". ISBN 0-412-08541-0, Chapman & Hall 1997.

[2] Mohan, Undeland, and Robbins" *Power Electronics: Converter, Applications, and Design*". JOHN WILEY & SONS, ISBN 0-471-61342-8, 1989, USA.

[3] JEAN_JACQUES E.SLOTINE WEIPING LI "*Applied Non-linear Control*" Prentice-Hall International Edition, ISBN 0-13-040049-1 1991, 1991, USA.

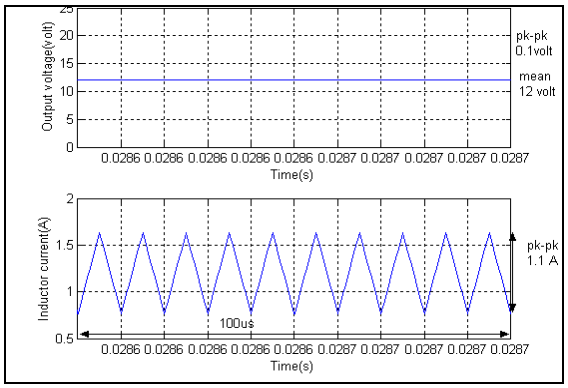

Figure 5. Output voltage and inductor current of Buck converter in steady state Matlab/Simulink™ model, the x-axis length is 100us and it's clear that the switching frequency is 100 kHz.

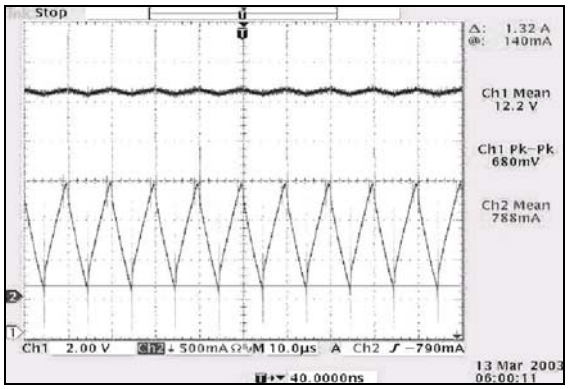

Figure 6. Output voltage and inductor current of Buck converter in steady state, the x-axis length is 10us/div. Channel 1 for output voltage, is 2v/div. Channel 2 for inductor current, is 0.5 A/div.

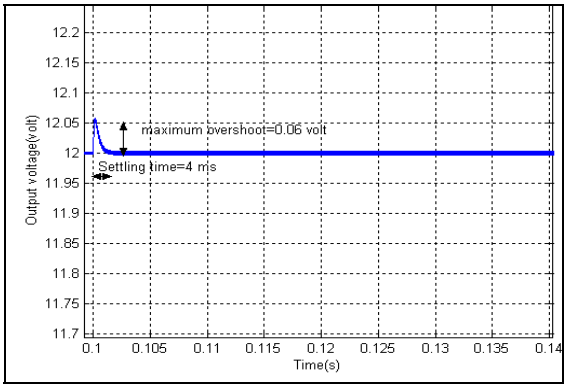

Figure 7. Output voltage of the Buck converter Matlab/Simulink™, where the input voltage takes a step change from 20 volt to 28 volt, the settling time is 4 ms and maximum overshoot is small.

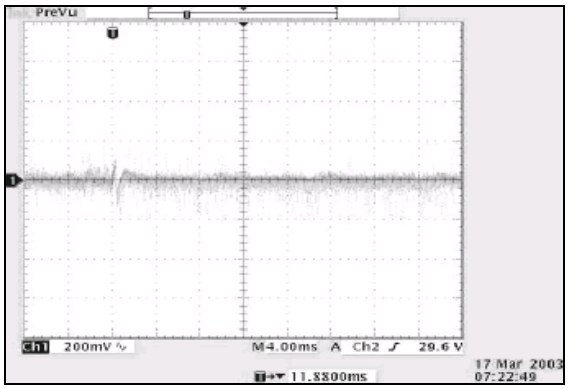

Figure 8. Output voltage of the Buck converter prototype model, where the input voltage take a step change from 20 volt to 28 volt, the settling time is 3 and small overshoot.

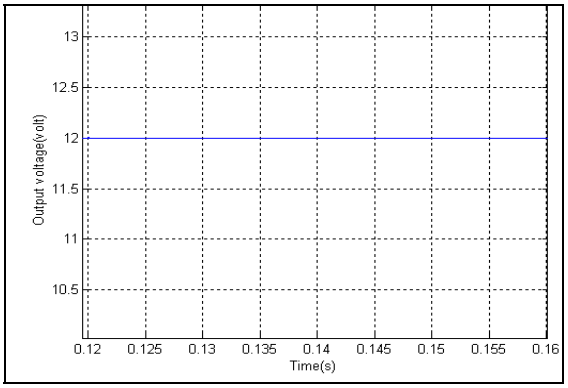

Figure 9. Output voltage of the Buck converter Matlab/Simulink™ model, the load take a step change from 10 Ω to 13 Ω, it can be shown that the converter is not effected by load variation.

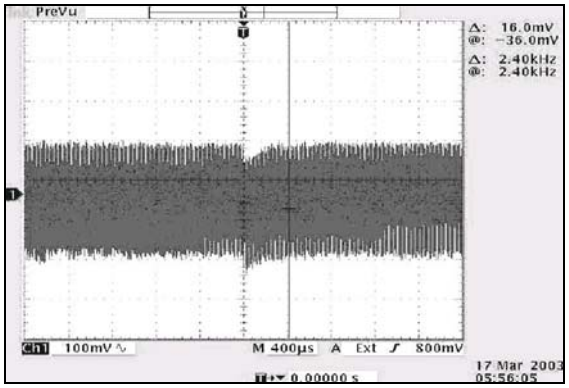

Figure 10. Output voltage of the Buck converter prototype model, the load takes a step from 10 to13 Ω, the settling time and the overshoot are small.

Publication P [2]

M. Ahmed, M. Kuisma, P. Silventoinen. Implementing Simple Procedure for Controlling Switch Mode Power Supply Using Sliding Mode Control as a Control Technique. *Proceedings of XIII-th International Symposium on Electrical Apparatus and Technologies, SIELA 2003, 29-30 May, 2003*. Plovdive, Bulgaria.

IMPLEMENTING SIMPLE PROCEDURE FOR CONTROLLING SWITCH MODE POWER SUPPLY USING SLIDING MODE CONTROL AS A CONTROL TECHNIQUE

Mohammad AHMED, Miko KUISMA and Pertti SILVENTOINEN

Lappeenranta University of Technology, P.O. Box 20, 53851 LPR, Finland
Department of Electrical Engineering
E-Mail: ahmed@lut.fi. E-Mail: kuisma@lut.fi. E-Mail: pertti.silventoinen@lut.fi

Abstract. This paper focuses on the sliding mode control (SMC) as a control technique for the switch mode power supply, where a simple procedure is used to control the converter using Matlab/Simulink™ in the design. The design procedure is explained in detail and the Buck converter is taken as an example. The circuit is tested in steady state where the output voltage, inductor current, and average switching frequency are shown in details. To ensure that SMC can work with disturbances, a dynamic test (line and load variations) is applied to the circuit. Finally to show that this control algorithm (design procedure plus simulation model) could be implemented for the basic three (Buck, Boost, and Buck-Boost) converters, the Buck-Boost converter is taken with different parameters as a second choice and the same previous tests are applied to it.

Keywords: Buck converter, Buck-Boost converter, sliding mode control.

1. INTRODUCTION

During the last few decades switch mode power supplies have been controlled in different manners, designers in this field are trying to find the easiest way to control converters with highest performance to be obtained. The biggest problem that face designers are the non-ideal component, line and load variation that cause non-linearity and let the converter deviate from its normal operating point. Another problem is the long design procedure for the controller that needs to be repeated each time we build a new converter or change its parameters. The sliding mode control (SMC) is a control approach, which complies with the non-linear nature of switch-mode power supplies. This control technique offers several advantages compared to traditional control methods: robustness, good dynamic response and simple implementation.

2. DESIGN PROCEDURE

The design starts with some easy mathematical calculations that could be explained in detail from the converter parameters given in table.1 to be designed.

Table 1.The Buck converter main circuit parameters

Parameter name	Symbol	Value
Input voltage	V_{in}	24 volts
Output voltage	V_o	12 volts
Capacitor	C	220 μF
Load resistance	R_L	13 Ω
Nominal switching frequency	F_s	100 kHz

The design procedure consist of six points that could be repeated easily to any of the basic three converters as follow:

1. Choose the duty cycle D and for Buck converter it is

(1) $$D = \frac{V_o}{V_{in}} = \frac{12}{24} = 0.5$$

2. Determine the average output current

(2) $$I_o = \frac{V_o}{R_L} = \frac{12}{13} = 0.92 \text{ A}$$

3. Find the output power P_o

(3) $$P_o = V_o I_o = 11.04 \text{ W}$$

4. Choose the efficiency of the circuit and let it be 92% in this example. From the efficiency we can determine the input power

(4) $$\eta = \frac{P_o}{P_{in}} \Rightarrow P_{in} = 12 \text{ W}$$

5. Determine the average input current

(5) $$I_{in} = \frac{P_{in}}{V_{in}} = \frac{12}{24} = 0.5 \text{ A}$$

6. We choose the current ripple Δi_L and let it be here 1 A, by using the specified nominal switching frequency given in table.1 to be implemented in the general equation (6) when the switch is on, we can find the inductor value needed.

(6) $$V_L = L\frac{\Delta i_L}{\Delta_t}$$

$$L = 60 \text{ μH}$$

At this point we are able to go further and implement the SMC to the Buck converter with the parameters above. It could be said that it is very necessary to determine the inductor value in this way to be sure that the model will operate in the desired switching frequency.

The procedure could be repeated easily if the converter parameters or the topology is changed without the need to make hard calculations.

3. IMPLEMENTING THE SYSTEM IN MATLAB/SIMULINK™

The converter could be implemented easily to Matlab/Simulink™, where many books explain how to implement the converter [1]. The SMC structure to switch mode power supply in Matlab/Simulink™ is as follow:

The control circuit consists of a linear part; usually for simplicity it is represented with proportional plus Integral (PI) control. The second part is the non-linear control, which is the SMC that includes a hysterisis used to drive the switch. The non-linear part represented by the hysterisis block could be implemented as follow:

Since we assumed the ripple current is 1 A, we activate the hysterisis block and there are the *switch off* and *switch on* points, here it is represented with (*0.5* and *–0.5*) respectively.

For the linear part, it is difficult to find a standard procedure to determine the proportional gain. The reason behind this difficulty is that the SMC is non-linear control and could not be linarized. It is not possible to choose the linear part parameters based on the non-linear part. Choosing a low integral gain could reduce the overshoot, but the steady state error increases. It is left for the designer to choose his parameters depending on the application.

To implement SMC to switch mode power supply, the circuit consist of an output voltage control loop were the output voltage is subtracted from the reference voltage; the difference is passed through an integral with a gain. This integrated signal is subtracted from the inductor current signal and the difference is passed through a hysteresis. Figure 1 shows the implementation of PI plus SMC to switch mode power supply in Matlab/Simulink™. The SMC and the PI control are in boxes.

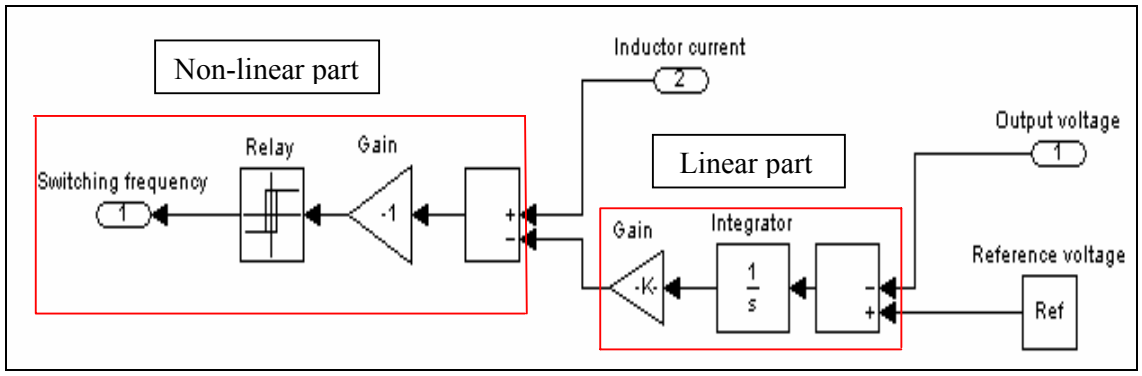

Figure 1. The simulation block diagram in Matlab/Simulink™; controller includes the sliding mode current controller (inner loop) and the voltage control loop (PI control).

It could be said each time we build a new converter all we need to do is to make the easy calculation explained above and change the following parameters without the need to modify the control circuit where these parameters could be written in a separate M-file in Matlab™ and are shown in table 2.

Table 2. The parameters that need to be considered in the design of SMC to power supply

Input voltage	Load value
Capacitor value	Reference voltage
Inductor value	Hysteresis
Proportional gain (optional)	

4. TEST RESULTS

With the parameters values given in table 1 and inductor value obtained for the Buck converter, the system (Buck converter plus SMC) is tested in steady state where the output voltage, inductor current, and average switching frequency are shown in figure 2. The graph shows that the theoretical results are close to the results in the graph.

To approve that the SMC has a good dynamic response a step change in the input voltage is applied where the input voltage change. Figure 3 shows the output voltage has no overshoot, which means that SMC is effective tool against disturbances (line variation).

Finally the circuit was tested under load variation where the load changes its value from 13 Ω to 10 Ω, and the results in figure 4 shows acceptable response with small overshoot and settling time.

To approve that this control algorithm could be implemented to any of the basic three converters (Buck, Boost, Buck-Boost), we choose the Buck-Boost converter as a second topology with the parameters given in table 3.

The same calculation is repeated (step 1 to step 6), and the inductor value was found to be 80 μH. The circuit was tested in the same environment of Buck converter and results are given from figure 5 to figure 7.

Table 3.The Buck-Boost converter main circuit parameters

Parameter name	Symbol	Value
Input voltage	V_{in}	12 volts
Output voltage	V_o	24 volts
Capacitor	C	220 μF
Load resistance	R_L	20 Ω
Nominal switching frequency	F_s	100 kHz

5. CONCLUSION

The SMC was implemented as a control tool for the Buck converter using Matlab/Simulink™ with some simple calculation to be done. This implementation could be extended to the basic three converters (Buck, Boost, Buck-Boost) so the Buck-Boost converter was choosing as a second topology. The structure of this control loop in Matlab/Simulink™ is similar for all types of power converters.

The SMC can be seen as an effective tool for controlling the switch mode power supply and the system behave in a stable mode in steady state, also it can force the converter to stay in the stable mode due to large line and load variation.

The SMC is an efficient and easy control algorithm that could be implemented in Matlab/Simulink™ and is gaining increasing importance as a control design tool in Matlab/Simulink™ for the robust control of linear and non-linear systems. Its strength results from the ease and flexibility of the methodology for its design and implementation.

The control topology consists of a linear and non-linear part, and its left to the designer to tune the linear part depending on the application.

REFERENCES

[1] Vadim Utkin, Jurgen Guldner, and Jingxin Shi "*Sliding Mode Control in Electromechanical Systems*", ISBN 0-7484-0116-4(cased), Taylor & Francis 1999.

[2] G. Spiazzi, P. Mattavelli, L. Rossetto, L. Malesani, "Application of Sliding Mode Control to Switch-Mode Power Supplies," Journal of Circuits, Systems and Computers (JCSC), Vol.5, No.3, September 1995, pp.337-354.

[3] G. Spiazzi, P. Mattavelli, L. Rossetto, "Sliding Mode Control of DC-DC Converters," 4 " Congresso Brasileiro de Elettronica de Potencia (COBEP), BeloHorizonte, December 1997, pp.59-68.

[4] Bondarev, A.G. and S.A.Bondarev, N.E. Kostileva and V.I.Utkin,"sliding modes in systems with asymptotic state observer", Automation and remote control, 1985.

[5] P. Mattavelli, L. Rossetto, G. Spiazzi, P. Tenti, "General-purpose sliding-mode controller for DC/DC converter applications", Proc. of IEEE Power. Electronics Specialists Conf. (PESC), Seattle, June 1993, pp.609-615.

[6] Soumitro Banerjee, George C. Verghese ''*Nonlinear phenomena in power electronics*'', ISBN 0-7803-5383-8. TK 7881.15B36 2001.

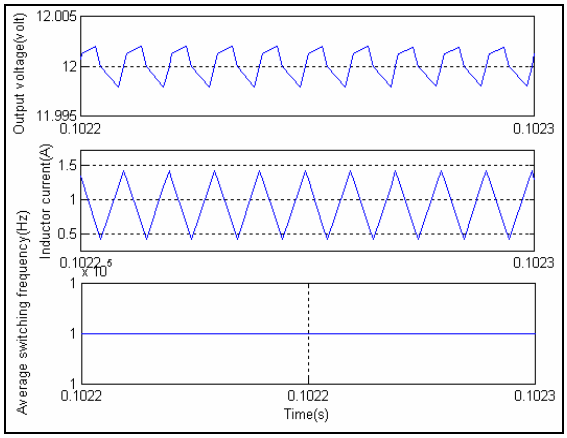

Figure 2. Output voltage, inductor current, and average switching frequency of Buck converter with SMC in steady state region. The voltage ripple is very small, peak-to-peak inductor current is 1 A, and the average switching frequency is 100 kHz.

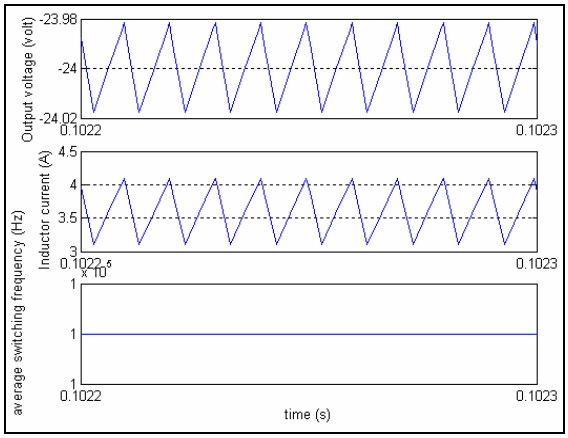

Figure 5. Output voltage, inductor current, and average switching frequency of Buck-Boost converter with SMC in steady state region. The voltage ripple is very small, peak-to-peak inductor current is 1 A, and the average switching frequency is 100 kHz.

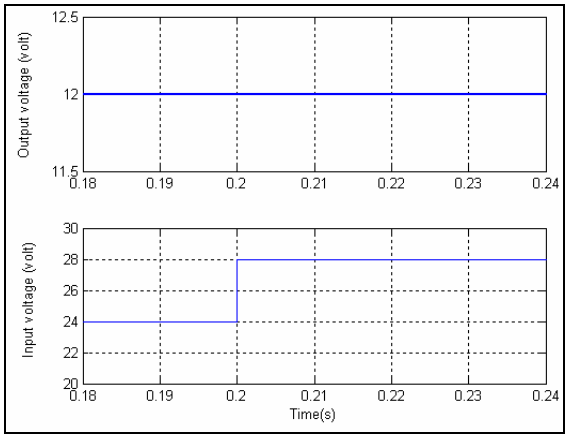

Figure 3. Output voltage of the Buck converter with SMC when the input take a step change from 24 volt to 28 volt. It can be seen that the converter is not affected by this change.

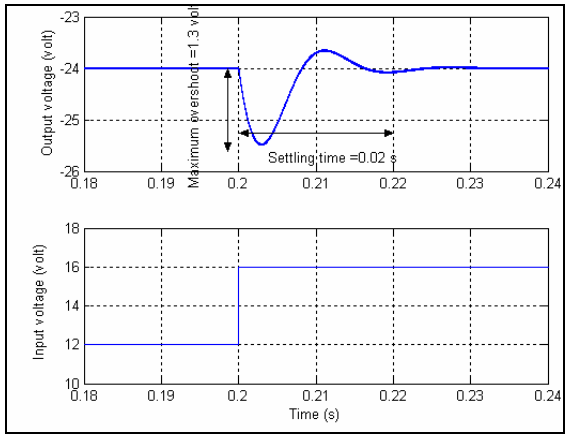

Figure 6. Output voltage of the Buck –Boost converter with SMC when the input take a step change from 12 volt to 16 volt. It can be seen that the converter output voltage has a maximum overshoot of 1.3 and 0.02s settling time but SMC force the system to return to its steady state.

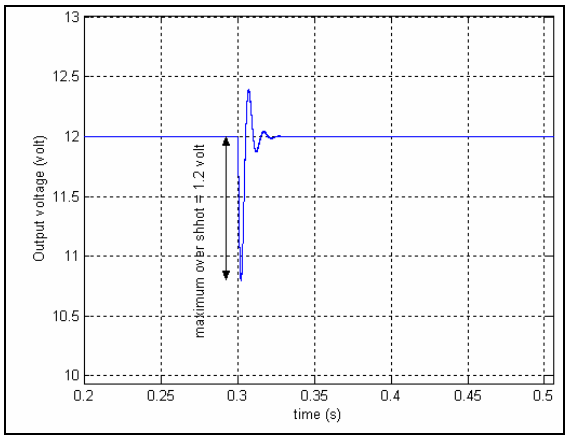

Figure 4. Output voltage of Buck converter when load value takes a step change from 13 Ω to 10 Ω. It could be seen that there is an overshoot but the SMC can overcome it and return the response to its steady state with a very small settling time.

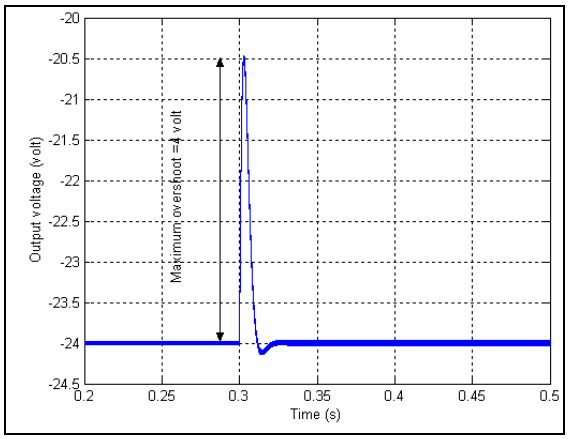

Figure 7. Output voltage of Buck-Boost converter when load value takes a step changes from 20 Ω to 13 Ω. It could be seen that there is a maximum overshoot of 4 volts but the SMC can overcome it and return the response to its steady state with a very small settling time.

Publication P [3]

M. Ahmed, M. Kuisma, K. Tolsa, P. Silventoinen. Implementing Sliding Mode Control for Buck Converter. *Proceedings of the Power Electronic Specialist Conference, PESC2003,* Acapulco, Mexico, June 2003. Provisionally accepted for publication in *IEEE Transactions on Power Electronics*.

Implementing Sliding Mode Control for Buck Converter

M. Ahmed, M. Kuisma, K. Tolsa, P. Silventoinen
Department of Electrical Engineering
Lappeenranta University of Technology, P.O. Box 20, 53851 LPR, Finland

Abstract – The theory of sliding mode control (SMC) to switch mode power supplies have been widely investigated in literature, but most of the papers have focused on the theoretical aspects of this control without any practical implementations.

This paper links the theory to practical power supply design. Analysis and experimental study of Buck converter is presented, and nonlinear state feedback control is derived to achieve desired output voltage. The paper focuses on modelling a control circuit in Matlab/Simulink™ and implementing it to the Buck converter. Next, a prototype with SMC is build up. The output voltage and inductor current of the both models are compared in steady state mode and under line and load variations.

The efficiency is also calculated from the measurements made with the prototype. All these measurements showed advantageous results.

Keywords-Buck converter, Sliding mode control (SMC)

I. Introduction

The sliding mode control (SMC) has been proposed to improve the robustness and the dynamic response in switch mode power supplies. The theory of SMC to switch mode power supply has been widely investigated in literature, but most of the papers have focused on the theoretical aspects of this control without any practical implementations. This paper links the theory to practical power supply design. The SMC is a control approach, which complies with the non-linear nature of switch-mode power supplies. This control technique offers several advantages compared to traditional control methods: Stability, even for large line and load variations, robustness, good dynamic response and simple implementation.

One of the most important features of the sliding mode regime in variable structure systems (VSS) is the ability to achieve responses that are independent of the system parameters, the only limit being the canonical form description of the system. From this point of view, the Buck DC/DC converter is suitable for the application of the SMC, since the Buck converter fulfils the statement: ‘‘the system is controllable if every state variable can be affected by an input signal’’.

The output voltage and its derivative are both continuous and accessible for measurement. Before going forward for applying SMC to switch mode power supply, let us take a brief look on the theory of SMC.

II. Sliding Mode Control

Let us define the following control law:

Region I: $(x_2 + cx_1) < 0 \Rightarrow u = -1$, and

Region II: $(x_2 + cx_1) > 0 \Rightarrow u = +1$,

Where c is lower than q (system eigenvalues). The switching boundaries are then $x_2$and the line x_2+cx_1.

The system structure changes whenever the system representative point (P) enters a region defined by the switching boundaries. The immediate consequence of this property is that, once (P) hits the switching line, the control law ensures that the (P) does not move away from the switching line $x_2+cx_1=0$, which is called the sliding line; the above discussion could be explained in Fig. 1.

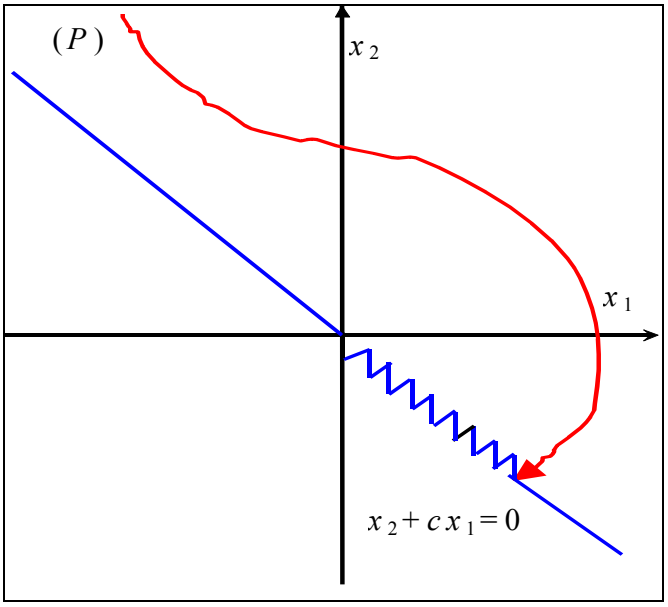

Fig. 1. Sliding regime in VSS (switching line with hysteresis).

When sliding mode exists, the resultant system performance is completely different from that dictated by any of the substructures of the VSS. Performance can be, under particular conditions, made independent of the properties of

the substructures employed and dependent only on the preset control law. (In this example the boundary $x_2+cx_1=0$).

If the switching boundary is not ideal, i.e. the commutation frequency between the two substructures is finite, and then the overall system trajectory is as shown again in Fig. 1.

If the width of the hysteresis around the switching line goes to zero, then the system behaviour returns to ideal. This phenomenon is called *chattering*. To have more detailed description of the properties of SMC, the reader should refer to [1], [3], and [5].

III. Sliding Mode Control of Buck DC/DC Converter

The question arises, how SMC could be implemented for switch mode power supplies? Fig. 2 shows a block diagram showing the implementation of this control for DC/DC converters. For most DC/DC converters used in practice, the motion rate of the current is much faster than the motion rate of the output voltage. Using cascaded control structure with two control loops can solve the control problem: an inner current control loop and an outer voltage control loop. The voltage control is usually realized with standard linear control techniques, where as the current control is implemented using either PWM or hysteresis control. Here we use the sliding mode approach for the control of inductor current.

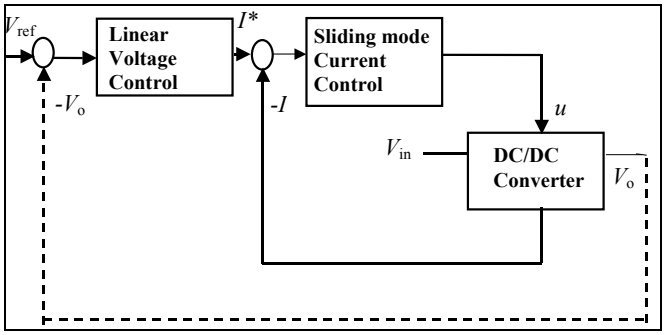

Fig. 2. Cascaded control structure of DC/DC converter.

A. Simulation Model

Fig. 3 explains in detail the internal structure of the control part in Fig. 2 used as a control for the three basic converters (Buck, Boost, Buck-Boost) in Matlab/Simulink™.

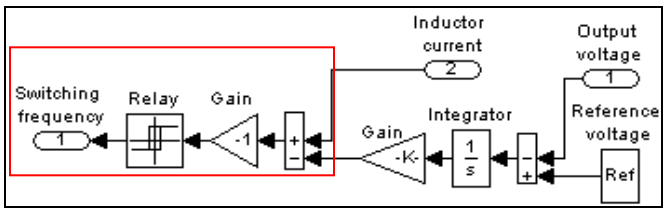

Fig. 3. The simulation block diagram for the controller, controller includes the sliding mode current controller (inner loop in block) and the voltage control loop (PI control).

To construct the simulation model for the sliding mode controlled Buck converter, system model for the main power circuit has to be made. For the Buck converter, it is convenient to use a system description, which involves the output error and its derivative [1], i.e.

$$\begin{cases} x_1 = v - v^* \\ x_2 = \dfrac{dx_1}{dt} = \dfrac{dv}{dt} = \dfrac{i_c}{C} \end{cases} \tag{1}$$

The system equations, in terms of state variables $x_1$and x_2, and considering a continuous conduction mode (CCM) operation can be written as:

$$\begin{cases} \dot{x}_1 = x_2 \\ \dot{x}_2 = -\dfrac{x_1}{LC} - \dfrac{x_2}{RC} + \dfrac{v_{in}}{LC}u - \dfrac{v^*}{LC} \end{cases} \tag{2}$$

Where v^* : O/P voltage of the linear control.

u : Is a discontinuous input, which can assume the values 0 (switch off) or 1(switch on).

Direct implementation of the simulation model of the SMC-Buck converter can be derived from equations (1) & (2) and the control block diagram presented in Fig. 3.

B. Prototype Model

Straightforward prototype implementation of the Simulink-model was constructed in the Laboratory of Applied Electronics, Lappeenranta. Fig. 4 shows the overall picture of the prototype build up in the laboratory.

Fig. 4. The prototype model of, the Buck converter with the sliding mode control build in the Electronics laboratory at Lappeenranta University of Technology.

The block diagram of the model and the main components used in the design are presented in Fig. 5, and the operation of the prototype can be described as follows:

The output voltage is subtracted from the reference voltage using op-amp1. The voltage difference signal is integrated using op-amp2. The output of this amplifier generate signal 1. Op-amp3 is used to detect the inductor current with a shunt resistor, generating signal 2. In next stage, signal 1 and 2 are compared using a comparator (LM111), where hysteresis is used to control the switching frequency. The output level of the LM111 signal should be translated to a voltage difference between gate-source of the switching device IRF530. High side MOSFET/IGBT driver IR2117 is used for this purpose.

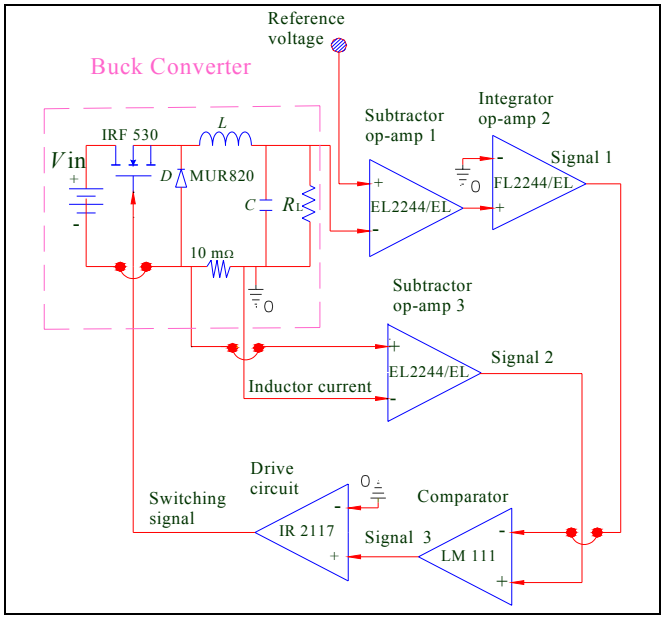

Fig. 5. Simplified block diagram of the Buck converter with sliding mode control showing the component used in the prototype design and how the signal is generated at each stage.

The converter main circuit had the following parameters shown in table 1.

TABLE 1.
THE CONVERTER MAIN CIRCUIT PARAMETERS

Parameter name	Symbol	Value
Input voltage	V_{in}	24 volts
Output voltage	V_o	12 volts
Capacitor	C	220 µF
Inductor	L	69 µH
Load resistance	R_L	13 Ω
Nominal switching frequency	$f_{s(nominal)}$	100 kHz

IV. TEST RESULTS

Fig. 6 shows the output voltage and inductor current of the Simulink/Matlab™ model, and Fig. 7 shows the same graph for the prototype model. Both models are in steady state. The voltage ripple is approximately 1 volt taking the spikes into account for the prototype model, while the actual ripple for both models is approximately 0.5 volt. The peak-to-peak inductor current is 1.75 A for Matlab/Simulink™ and 1.95 A for prototype model. The both models were tested under line variation as shown in Fig. 8 and 9 respectively; the input was changed from 20 volt to 28 volt. The settling time for both models is approximately 20 ms, which is the time, required to returns to steady state. The two models where tested under load variation where the load changes from 10 Ω to 13 Ω, and the maximum overshoot of the output voltage is 0.7 volt, this is shown in Fig. 10 and 11 respectively.

The efficiency of the circuit was also measured to check the power losses in the prototype model. The results showed that our non-optimized prototype had 93.5 % efficiency.

V. CONCLUSION

A general-purpose SMC for DC/DC converter is presented. The application of the SMC techniques to DC/DC converter is analyzed in detail with respect to Buck converter. The sliding motion is performed in the inner current loop. The structure of this loop is similar for all types of power converters.

A simulation model in Matlab/simulink™ for the system is build, and then implementation of this model in a prototype is explained. The simulation and prototype model showed, that this control can stabilize the power supply, and that the output voltage and inductor current can return to steady state even when it is effected by line and load variation, with a very small overshoot and settling time. The efficiency of the prototype model showed acceptable results. SMC is gaining increasing importance as a design tool for the robust control of linear and non-linear systems. Its strength results from the ease and flexibility of the methodology for its design and implementation. SMC provides inherent order reduction, robustness against system uncertainties disturbances, and an implicit stability proof, so it could be said that the design allows high performance control system at low cost.

REFRENCES

[1] V.Utkin, J.Guldner, and J. Shi, Sliding Mode Control in Electromechanical Systems,ISBN0-7484-0116-4(cased),Taylor & Francis 1999.

[2] G. Spiazzi, P. Mattavelli, L. Rossetto, L. Malesani, "Application of Sliding Mode Control to Switch-Mode Power Supplies," Journal of Circuits, Systems and Computers (JCSC), Vol.5, No.3, September 1995, pp.337-354.

[3] Mattavelli, L G. Spiazzi, P.. Rossetto, "Sliding Mode Control of DC-DC Converters," 4 " Congresso Brasileiro de Elettronica de Potencia (COBEP), BeloHorizonte, December 1997, pp.59-68.

[4] Bondarev, A. Kostileva, N., and Utkin, V. "sliding modes in systems with asymptotic state observer", Automation and remote control, 1985.

[5] P. Mattavelli, L. Rossetto, G. Spiazzi, P. Tenti, General-purpose sliding-mode controller for DC/DC converter applications, Proc. of IEEE Power. Electronics Specialists Conference, (PESC), Seattle. June1993, pp.609-610.

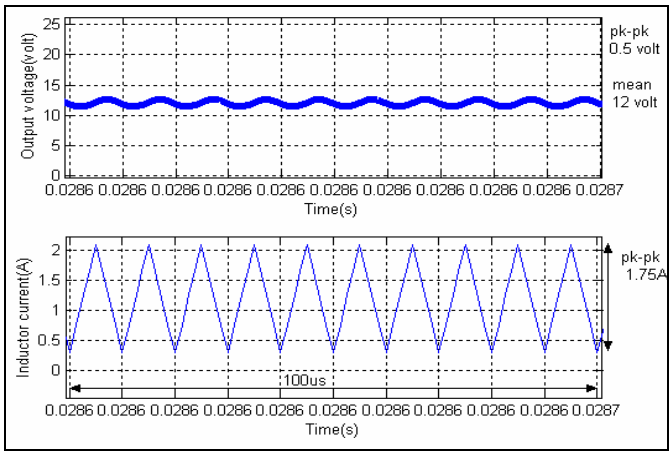

Fig. 6. Output voltage and inductor current of Buck converter in steady state Matlab/Simulink™ model, x-axis length is 100us and its clear there are ten switching cycle, and the switching frequency is 100kHz.

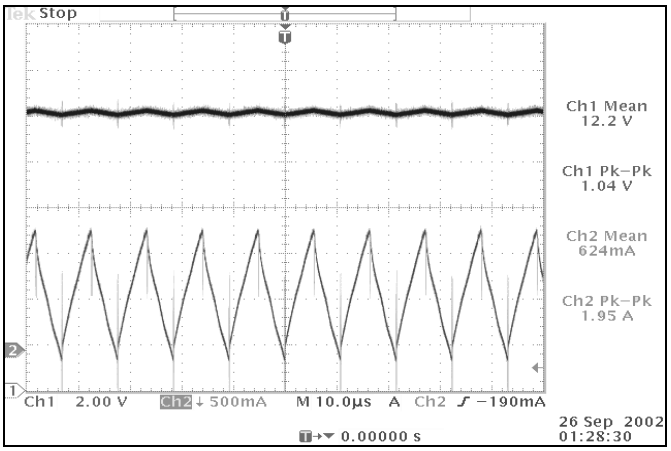

Fig. 7. Output voltage and inductor current of Buck converter in steady state prototype model, the x-axis length is 10us/div. Channel 1, which is for output voltage, is 2v/div. Channel 2, which is for inductor current, is 0.5 A/div.

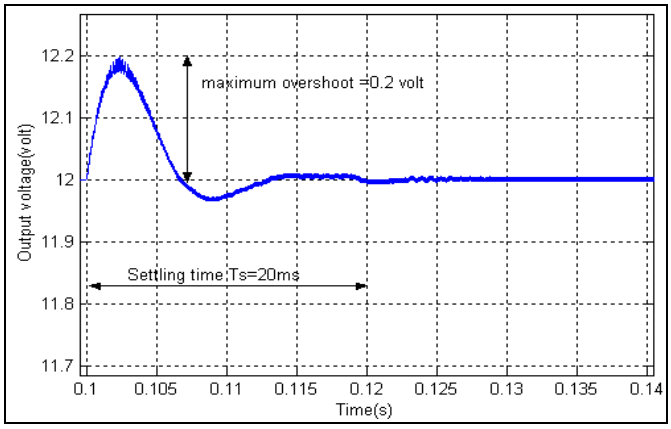

Fig. 8. Output voltage of the Buck converter Matlab/Simulink™ model, where the input voltage takes a step change from 20 volt to 28 volt, the settling time is 20 ms. The length of x-axis is 40 ms, which is the same length of Fig. 7.

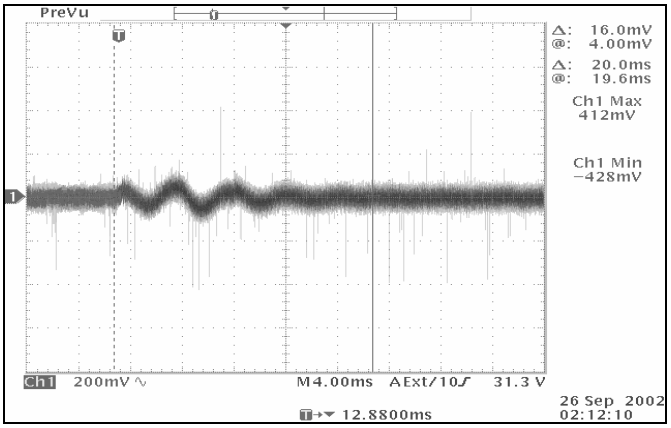

Fig. 9. Output voltage of the Buck converter prototype model, where the input voltage take a step change from 20 volt to 28 volt, the settling time is 20 ms and it is the same as for Matlab/Simulink™ model. The x-axis length is 4 ms/div.

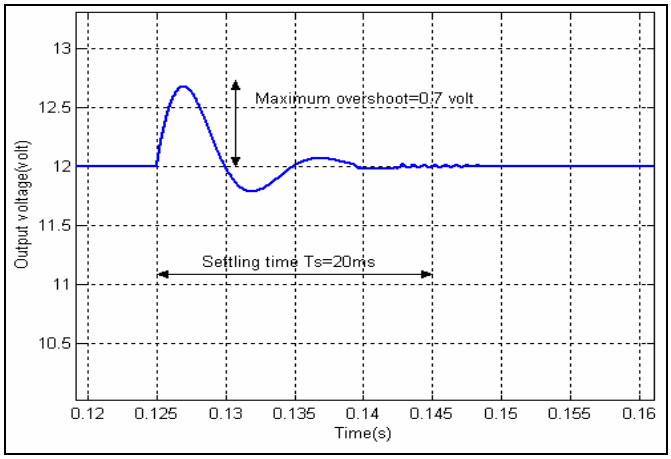

Fig. 10. Output voltage of the Buck converter Matlab/Simulink™ model, where the load take a step change from 10 Ω to 13 Ω, the settling time is 20ms, and a maximum overshoot of 0.7 volt. The length of x-axis is 40 ms.

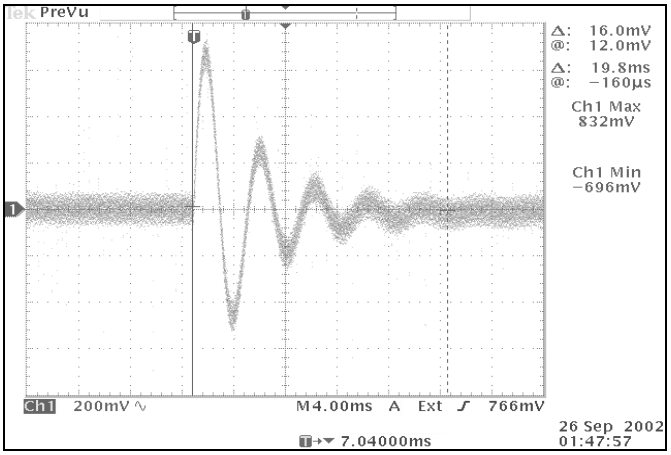

Fig. 11. Output voltage of the Buck converter prototype model, where the load take a step change from 10 Ω to 13 Ω, the x-axis is 4 ms/div and settling time is 19.8 ms. The x-axis length is 4ms/div, and y-axis is 200mv/div and maximum overshoot of 0.7 volt is recommended.

Publication P [4]

M. Ahmed, M.Kuisma, P. Silventoinen, O. Pyrhonen**.** Effect of Implementing Sliding Mode Control on the Dynamic Behaviour and Robustness of Switch Mode Power Supply (Buck Converter). *Proceedings of the International Conference on Power Electronics and Drive systems (PEDS2003)*. 17-20 November 2003, Singapore. Provisionally accepted for publication in *IEEE Transactions on Power Electronics*.

Effect of Implementing Sliding Mode Control on the Dynamic Behavior and Robustness of Switch Mode Power Supply (Buck Converter)

M. Ahmed, M.Kuisma, P. Silventoinen, O. Pyrhonen

Department of Electrical Engineering, Lappeenranta University of Technology, Finland
P.O.Box 20, FIN-53851 LPR, Finland

Abstract- **The focus of this paper is on the implementation of sliding mode control (SMC) for switch mode power supply. A brief analysis of the control structure is explained followed by a block diagram showing the internal structure of the control loops and the way they are connected to the converter. The Buck converter was chosen as an example and the simulation model of the converter with its control circuit was build-up in Matlab/Simulink™.**
Once the circuit was build-up, the study of the dynamic response of Buck converter controlled by SMC is done. The output voltage, inductor current, and the instant switching frequency are analyzed and studied in the following three regions: turn on region, line and load variation region, and finally components variation region. In the third part concerning robustness a wide range of change of the Buck converter component parameters values are applied individually, and the study of the effect of SMC on the converter response due to these variations are analyzed.

Keywords -**Buck converter, dynamic response, and sliding mode control.**

I. INTRODUCTION

The stability is an important aspect in the design of switch mode power supplies; a feedback control is used to achieve the required performance. Ideally the circuit is in steady state but actually the circuit is affected by line and load variations (disturbances), and variation of the circuit component (robustness). These parameters have a severe affect on the behavior of switch mode power supply and may cause instability. Many control techniques are used to reduce the influence of these factors. In this paper analysis of the sliding mode control (SMC) as a control tool for Buck converter is done. The reason behind our choice is that many theoretical studies [1], [2], and [3] promise that the SMC control algorithm, which is a non-linear control has a good immune against the dynamic change of the power supply.

This paper is an extension to a previous research [4], where linking the theoretical study of SMC to Buck converter and implemented in a prototype model was approved, and comparison between the simulated and prototype results was done. The approved paper [4] is further investigated in this research by re-presentation of the simulation model and study the effect of SMC on the converter (Buck) dynamic response with respect to turn-on region, disturbances, and robustness. Finally a conclusion is presented for the study.

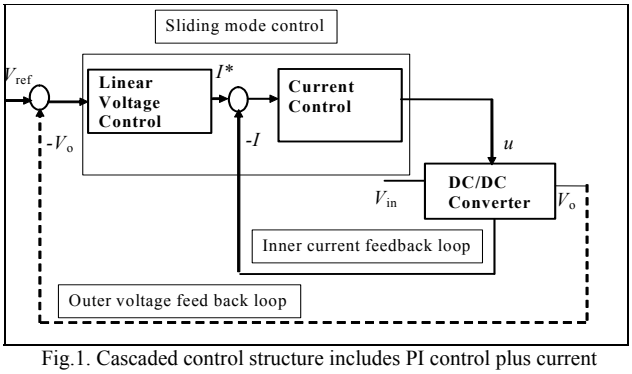

Fig.1. Cascaded control structure includes PI control plus current control, which compose together the SMC.

II. CIRCUIT DESIGN

The Buck converter with SMC is build-up in Matlab/Simulink™ [4] and is re-presented in this paper. A brief explanation of the implementation of SMC to switch mode power supply (the Buck converter in this paper) is explained. To study in detail the SMC for switch mode power supplies refer to [1], [2], [3], and [4].

Fig.1 shows a block diagram showing the implementation of this control to switch mode power supply. For DC/DC converters used in practice, the motion rate of the current is much faster than the motion rate of the output voltage. Using cascaded control structure with an inner current control loop and an outer voltage control loop can solve the control problem. The voltage control is usually realized with standard linear control technique, whereas the current control is implemented using hysteresis control. The combined loops compose the SMC.

The Buck converter for test set-up model used in this paper had the following parameter given in TABLE.1.

TABLE 1
THE BUCK CONVERTER MAIN CIRCUIT PARAMETERS

Parameter name	Symbol	Value
Input voltage	V_{in}	24 volts
Output voltage	V_o	12 volts
Capacitor	C	220 μF
Load resistance	R_L	10 Ω
Nominal switching frequency	F_s	100 kHz

0-7803-7885-7/03/$17.00 ©2003 IEEE

III CONTROLLER DESIGN IN MATLAB/SIMULINK™

The SMC circuit used in Matlab/Simulink™ for controlling switch mode power supply is shown in Fig.2. The hysteresis control is the inner loop while the outer loop is the PI control. Combination of these two loops composes the SMC.

Three parameters need to be changed when changing the topology or component parameters are: the reference voltage, the hysteresis block, and integral gain value. For more detail refer to [5].

The reference voltage is taken directly from the design parameters while the other two parameters could be chosen as follow:

For any converter to be designed an assumption of the inductor current ripple must be made. For this example it is assumed that the inductor current ripple is 1 A. In hysteresis block there are the *switch off* point and *switch on point* and here they are *0.5* and *–0.5* respectively.

Finally a high integral gain reduces the error in steady state, increases the overshoot and settling time. In this model we choose the integral gain to be 100, the reason behind this choice is that the SMC acts as a derivative action and will reduce the settling time and the overshoot [5].

Before deeply explaining the system behavior let us write the inductor voltage general law, which is very useful in our explanation

$$V_{\mathrm{L}} = L\frac{\Delta I}{\Delta T}, \tag{1}$$

where L indicates the inductor value, V_{L} is the voltage across the inductor, ΔI represent the inductor current ripple, and ΔT denotes the switching period.

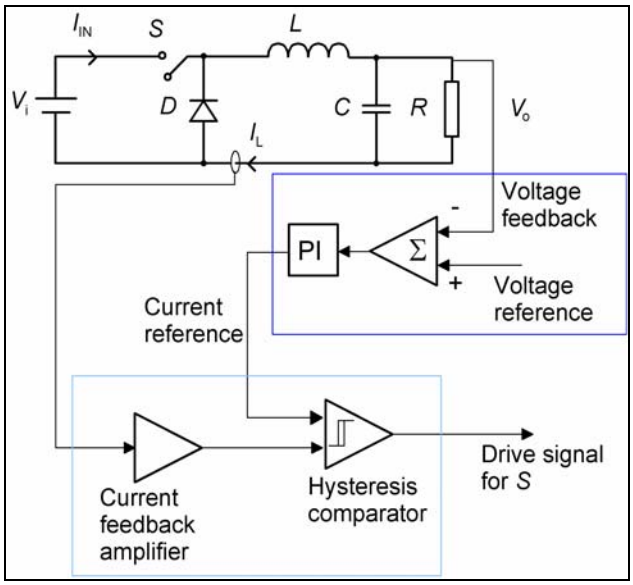

Fig.2. Buck converter circuit controlled by PI+ Current hysteresis control circuit in Simulink™, where together they compose SMC.

Since the switching period is inversely proportional to the instant switching frequency

$$\Delta T = \frac{1}{\Delta f}, \tag{2}$$

where Δf indicates the instant switching frequency.

Then by substituting equation (2) into equation (1) leads to

$$\Delta f = \frac{V_{\mathrm{L}}}{\Delta I \cdot L}. \tag{3}$$

Using the parameters from TABLE.1 to equation (1), and applying the condition when the switch is on, the following is obtained:

$$\begin{aligned} V_{\mathrm{L}} &= V_{\mathrm{in}} - V_{\mathrm{o}} = 12\ \mathrm{V} \\ \Delta I &= 1\ \mathrm{A} \\ L &= 60\ \mu\mathrm{H} \end{aligned} \tag{4}$$

IV SIMULATION RESULTS

In this section investigation of the effect of SMC on the output voltage, inductor current and instant switching frequency is studied in:

A. Transient region (turn on region),

B. Under line and load variations (disturbances), and

C. Component variation (robustness).

In the three regions the stability of the converter is examined in dynamic response, and a complete analysis of the affect of parameters mentioned above on the output voltage, inductor current, and the instant switching frequency is performed.

A. Transient region (turn on region)

By examining Fig.3 it could be seen that the output voltage has a maximum overshoot of 4 volts, while the inductor current has 1.5A overshoot. The settling time is about 28 ms.

From control point of view the maximum overshoot should not exceeds 10% of the steady state value but the maximum overshoot of the output voltage and inductor current is higher than the 10%. Reducing the integral gain could reduce this, but the steady state error increase [5]. It is recommended to choose a high gain to affect in the transient region. It is left for the designer to choose the parameters depending up on the application [5]. To be more specific there is no cretin rule for choosing the gain for the integral.

B. Under line and load variations

To study the effect of line variation, a step change in the input voltage was applied from 24 volt to 28 volt. It could be stated from Fig.4 that the hysteresis control with the integral action performing the SMC will force the output voltage and inductor current to stay in a stable mode with a very small change in the output voltage, which takes approximately 10 ms to overcome this slight change.

Due to this step input change, the instant switching frequency is changed to be higher and this is true if we consider equation (3) were $V_L = V_{in} - V_o$ for the switch is *on*. This means that the relation between the input voltage and instant frequency is proportional.

For load variation the load was changed from 10Ω to 15 Ω, it could be said as shown in Fig.5 that an oscillation with 28 ms settling time occur, but still the hysteresis control with PI control (SMC) forces the system to return to its steady state and stay in the manifold [4].

C) Component variation (resistor, inductor, capacitor)

Most of the references [1], [2], [3], and [7] mention that the SMC is robust, that mean less affected by component variation compared to other control technique. None of them had shown by means of simulation or prototype how SMC is immune against these variations. In this section explanation of the meaning of this statement is identified by means of simulation.

Resistor variation

Fig.6 shows the behavior of the output voltage, inductor current, and instant switching frequency when the load changes linearly from 5 Ω to 50 Ω. As the load value increase the converter will transfer its operation from continuous conduction mode (CCM) to discontinuous conduction mode (DCM). For this model the DCM starts at a load value of 23 Ω. In the DCM mode the output ripple voltage increase but it is still in an acceptable range, also the instant switching frequency changes. In general it could be said that the SMC still keeps the system stable while the load change for a wide range.

It is shown for higher load values the hysteresis current control with PI control will keep the output voltage stable but with more ripples in the output voltage and DCM inductor current rises.

Inductor variation

By examining Fig.7 and by changing the inductor value linearly from 10 μ to 1 mH, it is shown that the output ripple increases but still is small. From equation (3) it could be stated that the inductor value is inversely proportional to the instant switching frequency. This could be shown in Fig.7 were the inductor value changes linearly from 10 μ to 1 mH.

It is shown that the instant switching is very high at low inductor value and it goes down as the inductor value increase, while the inductor current stays in CCM.

Capacitor variation

Fig.8 shows that the capacitor variation linearly from 50 μF to 1 mF has no sufficient effect on converter behavior except that for a very small value the ripple voltage is higher but still small. The capacitor change has no severe affect on the value of the inductor current and the instant switching frequency.

V CONCLUSION

SMC is gaining increasing importance as a design tool for the robust control of linear and non-linear systems.

The SMC control was implemented as a control technique intended for controlling switch mode power supply choosing the Buck converter as an example. SMC is simple to implement in Matlab/Simulink™ for switch mode power supply with only few parameters need to be changed when changing the converter topology or the converter parameters. The simulated model was tested in transient region (turn on) and also with respect to line and load variations (disturbances).

SMC for switch mode power supply has a good immunity against component variations, and each component has a different level of effect on the converter response when implementing SMC and this could be classified as follows:

A. Load value has sever effect and when the load value deviates highly from the nominal load value the inductor current behavior change from CCM to DCM, and higher ripple voltage but with a stable mode.

B. Inductor value has medium effect, with a high switching frequency at small inductor value, and again a stable response is obtained with respect to a wide range of inductor values.

C. Capacitor value has little effect, and from the analysis it is obtained that it is not necessary to have a very large capacitor to smooth the output voltage. This is an advantage with respect to the size of the prototype.

REFERENCES

[1] V. Utkin, J. Guldner, and J. Shi "Sliding Mode Control in Electromechanical Systems", ISBN 0-7484-0116-4(cased), Taylor & Francis 1999

[2] G. Spiazzi, P. Mattavelli, L. Rossetto, L. Alesani, "Application of Sliding Mode Control to Switch-Mode Power Supplies," Journal of Circuits, Systems and Computers (JCSC), Vol.5, No.3, September 1995, pp.337-354

[3] G. Spiazzi, P. Mattavelli, L. Rossetto, "Sliding Mode Control of DC-DC Converters," 4 " Congresso Brasileiro de Elettronica de Potencia (COBEP), BeloHorizonte, December 1997, pp.59-68

[4] M. Ahmed, M. Kuisma, K. Tolsa, P. Silventoinen, " Implementing Sliding Mode Control for Buck Converter'', Power Electronic specialist conference (PESC) Proc. Mexico June, 2003, pp 634-637, Vol. 2.

[5] M. Ahmed, M. Kuisma, P. Silventoinen, "Implementing Simple Procedure for Controlling Switch Mode Power Supply Using Sliding Mode Control as a Control Technique'', XIII-th International Symposium on Electrical Apparatus and technologies (Siela). May 2003, pp 9-14, Vol. 1

[6] A.G. Bondarev, S.A. Bondarev. N.E. Kostileva and V. Utkin, "sliding modes in systems with asymptotic state observer", Automation and remote control, 1985

[7] P. Mattavelli, L. Rossetto, G. Spiazzi, P. Tenti, "General-purpose sliding-mode controller for DC/DC converter applications", Proc. of IEEE Power. Electronics Specialists Conf. (PESC), Seattle, June 1993, pp.609-615

[8] S. Banerjee, C. George. "Nonlinear phenomena in power electronics'', ISBN 0-7803-5383-8. TK 7881.15 B36 2001.

Publication P[5]

M. Ahmed, M. Kuisma, O. Pyrhonen, P. Silventoinen. Sliding Mode Control for Buck-Boost Converter Using Control Desk dSPACE^{TM}**.** *Proceedings of the International Conference on Power Electronics and Drive systems (PEDS2003).* 17-20 November 2003, Singapore. Provisionally accepted for publication in *IEEE Transactions on Power Electronics*.

Sliding Mode Control for Buck-Boost Converter Using Control Desk dSPACE™

M. Ahmed, M. Kuisma, O. Pyrhonen, P. Silventoinen

Department of Electrical Engineering, Lappeenranta University of Technology, Finland
P.O.Box 20, FIN-53851 LPR, Finland

Abstract- **Switch mode power supplies have been controlled using different control algorithms like PID control, current mode programmed control etc. Many control tools were used to implement these control techniques e.g. analog operational amplifier, microprocessor. This paper focuses on using a new control tool called dSPACE™ for controlling the switch mode power supply. Programming the control circuit via MATLAB/Simulink™ can be made. The prototype of the basic three converters Buck, Boost, and Buck-Boost can be controlled by the simulation model via Real time hardware. Buck-Boost converter was chosen as our prototype converter. The sliding mode control (SMC) was chosen as a control algorithm in MATLAB/Simulink™ for controlling the Buck-Boost prototype model. The reason behind choosing SMC is that it is an efficient control and simple to implement in MATLAB/Simulink™. The paper shows that the control algorithm represented by SMC in MATLAB/Simulink™ and using the dSPACE™ as control toolbox is able to control the prototype model.**

Keywords— **Buck-Boost converter, dSPACE™, sliding mode control**

I. Introduction

The increasing complexity of the software, electronic prototype models and the way to control these prototypes obliged designers to look for new control tools for controlling prototype models with high efficiency and simple implementations. Using dSPACE Simulator, you can test your prototypes reliably. dSPACE™ Simulator replaces the real environment by a simulated scenario, largely avoiding high-cost or failed test that causes damage. Test automation makes tests systematic and reproducible, and many tests would not even be possible without simulation. dSPACE™ simulator is ready to use simulator for testing. dSPACE™ software and the control modeling tool MATLAB/Simulink™ from the Mathworks gives you reasonable possible test efficiency. The powerful, robust dSPACE ™ hardware and the integrated software use cutting-edge technology [1].

dSPACE™ Simulator is optimally prepared for integrating simulation models from MATLAB/Simulink™. The tools from Mathworks and dSPACE™ are tailored to each other. After developing the simulation model, you can test it with Simulink and Control Desk's Simulink interface and then in real time on dSPACE™ Simulator with the same layouts, test scripts and parameter sets.

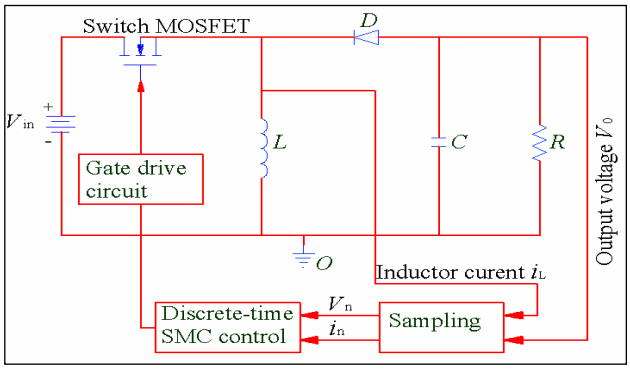

Fig.1. Buck-Boost Converter Circuit and its interface diagram, where V_n and i_n are the voltage and current in discreet mode.

The sliding mode control (SMC) is a control approach, which complies with the non-linear nature of switch-mode power supplies. This control technique offers several advantages compared to traditional control methods: Stability, even for large line and load variations, robustness, good dynamic response and simple implementation [2, 3].

II. Buck-Boost Converter

This paper constructs a Buck-Boost converter as a prototype model. This converter is controlled by SMC simulation model via I/O interface. The simulated control circuit is in discrete mode. A simplified diagram of Buck-Boost converter with an interface circuit is shown in Fig.1. The sampling frequency is 100 kHz, which will restrict the switching frequency to be not more than 30 kHz. A gate drive circuit is needed for *n*-channel MOSFET.

The prototype model of the converter circuit was constructed in the Laboratory of Applied Electronic at Lappeenranta University of Technology with the parameters specified in Table 1.

TABLE 1
THE BUCK CONVERTER MAIN CIRCUIT PARAMETERS

Parameter name	Symbol	Value
Input voltage	V_{in}	28 volts
Output voltage	V_o	-12 volts
Capacitor	C	220 µF
Load resistance	R	15 Ω
Nominal switching frequency	F_s	20 kHz

0-7803-7885-7/03/$17.00 ©2003 IEEE

III dSPACE™

One of the benefits that could be realized from dSPACE™ coupled with MATLAM/Simulink™ as a real time platform is that it can achieve an environment where a real time simulations and measurements can be performed together. The use of real time platform requires programming and implementation of the program in real time hardware. The real time platform could be classified to:

1. Real time software: In dSPACE™ platform the programming can be made via MATLAB/Simulink™. The connections to the I/O of the real time hardware are accessible via special real time blocks. After accomplishing the programming, that is building the control using the Simulink™, the model is converted to C-code by using RTI and C-compilers. The compiling and loading the code into real time hardware is fully automatiezd.

2. Real time hardware: Real time hardware consists of the processor card DS1103 and the I/O connector panel [1]. The processor card is physically a single card installed into ISA slot of the host pc. Detailed descriptions of used real time hardware can be found from reference [1].

One main problem in using this technique is the limitation of the I/O sampling frequency of the dSPACE™ which is limited to 100 kHz. To keep the simulation model running in MATLAB/ Simulink™ with the limited sampling frequency, the switching frequency is assumed to be one forth of 100 kHz otherwise the SMC model will be aborted during simulation.

The SMC described later was build with MATLAB/Simulink™ in discrete mode, keeping in mind that the controller sampling frequency should be higher than the switching frequency to keep track of events. To force the circuit to work with a desired switching frequency, usually we select the switching frequency to be for example 20 kHz and find the inductor value according to this frequency by some mathematical equations given bellow, where I_o denotes the output current, P_o is the output power, P_{in} is the input power, η indicates the efficiency, ΔI_L denotes the peak to peak inductor current, and finally L denotes the inductor value.

1. The output current I_o is

$$I_o = \frac{V_o}{R} = \frac{12}{15} = 0.8\ \text{A} \tag{1}$$

2. The output power P_o is

$$P_o = V_o I_o = 9.6\ \text{Watt} \tag{2}$$

3. Assuming the efficiency η to be 90%

$$\eta = \frac{P_o}{P_{in}} \Rightarrow P_{in} = 10.7\ \text{Watt} \tag{3}$$

4. The average input current I_{in} is

$$P_{in} = V_{in} I_{in} \Rightarrow I_{in} = 0.89\ \text{A} \tag{4}$$

5. The peak-to-peak input current I_{inpeak} is

$$I_{in\,peak}(\Delta I_L) = 2 I_{in} = 1.78\ \text{A} \tag{5}$$

6. Let us write the inductor voltage general law and for *switch on*, we obtain the inductor value that is used as the value for the prototype design

$$V_L = L \frac{\Delta I_L}{2\Delta t} \tag{6}$$
$$L = 1.6\ \text{mH}$$

IV. SLIDING MODE CONTROL

One effective control tool complies with the non-linear nature of switch mode power supply is represented by SMC, which is derived from the variable structure system theory (VSS) [4]. SMC for (VSS) offers an alternative way to implement a control action, which exploits the inherent variable structure nature of DC/DC converters. In practical, the converter switches are driven as a function of the instantaneous values of the state variables in such a way to force the system trajectory to stay on a suitable selected surface on the state space called the sliding surface.

To make it clearer let's take a look at Fig.2, which represent a trajectory for an equation $x_2 + cx_1 = 0$. The system structure changes whenever the system Representative point (P) enters a region defined by the switching boundaries. The immediate consequence of this property is that, once P hits the switching line, the control law ensures that P does not move away from the switching line $x_2 + cx_1 = 0$, which is called the sliding line. For more details of SMC refer to [3], [5], and [6].

Implementing of SMC for controlling switch mode power supply using dSPACE™ is explained as follow:

Fig.3 shows the control circuit diagram used in Matlab/Simulink™, which is used to control the prototype model of the Buck-Boost converter shown in Fig.1 via control desk dSPACE™. It could be shown from Fig.3 that the control circuit is in discrete mode.

For most DC/DC converters used in practice, the motion rate of the current is much faster than the motion rate of the output voltage. The control problem can be solved by using cascaded control structure with two control loops: an inner current control loop (represented by block in Fig.3) and an outer voltage control loop (PI control). The combined loops compose SMC, which in this paper is the control model used to drive the switch circuit of the DC/DC converter.

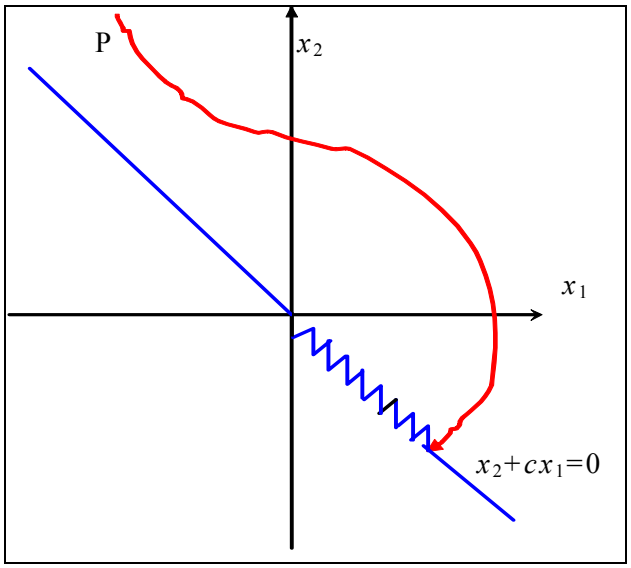

Fig.2. Sliding regimes in VSS, the Representative point P hits the switching line.

V. TEST SETUP

Buck-Boost converter was used as an experimental device. The parameter values were given earlier; dSPACE^{TM} DS1103 board was used as a real time system to control the converter. A picture of the test set-up is shown in Fig.4. The measured inductor current and output voltage are connected to ADC inputs of the dSPACE^{TM} system and scaled to 0-5 V for the DS1103 [1]. The switch control is done via digital output of dSPACE^{TM} using TTL voltage levels. Calculation time set-up of the simulation model and control time set-up is assigned to be 10 μs , and the instant switching frequency is to be 20 kH.

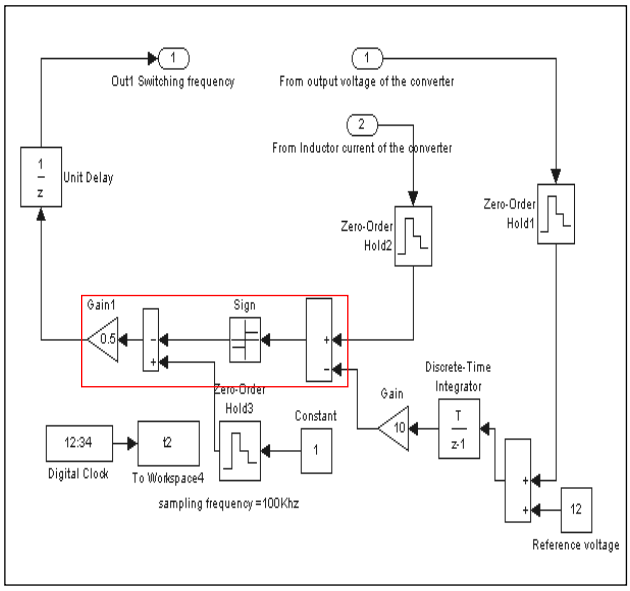

Fig.3. (PI+ current control in block) control in Matlab/Simulink^{TM}, that is used to control the prototype model of Buck-Boost converter through control desk dSPACE^{TM}.

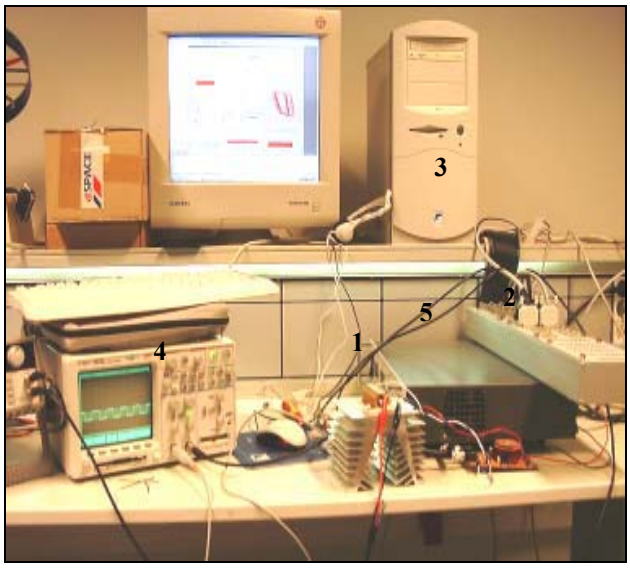

Fig.4. Test set-up consisting of the: Buck-Boost converter (1), connector panel (2), host pc with dSPACE^{TM} DS1103 card (3), oscilloscope (4), and input voltage source (5).

The processor technology is improving fast so that the calculation time steps even less than 1 μs may be achieved in near future.

VI. TEST RESULTS

To prove that a simulated SMC algorithm in MATLAB/Simulink^{TM} can control a real prototype Buck-Boost converter through control desk dSPACE^{TM} , the system was turned on. Fig. 5 shows the output voltage and inductor current together of the prototype model in steady state mode where the average output voltage is –12.6 and approximately 0.4-volt ripple (the additional 0.6 volt is due to non-optimized scaling calculation).

One important aspect which was done in the measurements, is that the output voltage was taken in the prototype model directly from load to oscilloscope while the inductor current was scaled in a way that every 3 A represents 5 volts, so in Fig.6 the average voltage that represent the current is 2.416 and by re-scaling it could be noticed that the actual inductor current is 1.45 A.

VII. CONCLUSION

It is worthwhile to concentrate on building the test setup as flexible as it can. A possibility to run simulations and to verify the simulation results with experimental device is a crucial part of the learning. The dSPACE^{TM} real time solution is one way to easy up the implementation of the simulation model to work as a part of the experimental devices.

One main disadvantage for using dSPACE^{TM} as a control tool for switch mode power supply is the limitation of the I/O sampling frequency of the dSPACE^{TM}, which is limited to 100 kHz. As a result and

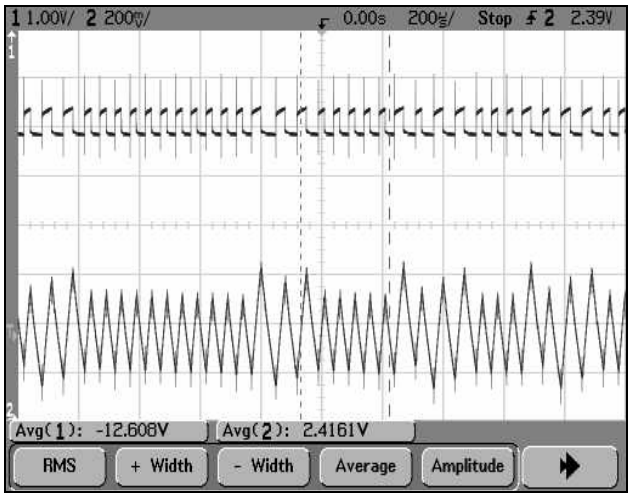

Fig.5. Output voltage and inductor current of Buck-Boost converter prototype model, where we can see high frequency switching noise in output voltage caused by non-ideal component.

an assumption for the switching frequency to not exceed one forth of 100 kHz is done. This disadvantage leads to high inductor value (in value and size), and more parasitic losses.

The processor technology is improving fast so that the calculation time steps even less than 1 μs may be achieved in near future, which will overcome these disadvantages.

The SMC is an efficient and easy control algorithm that could be implemented in Matlab/Simulink^{TM} and could be used in control desk dSPACE^{TM} to control a real prototype switch mode power supply.

SMC is gaining increasing importance as a universal design tool in Matlab/Simulink^{TM} for the robust control of linear and non-linear systems. Its strength results from the ease and flexibility of the methodology for its design and implementation.

REFERENCES

[1] H. Sarén, A. Parviainen "Real Time Simulation and Measurement Environment of DC Converters for Educational Purposes'', proc. SIMS 2002. University of Oulu, Finland, ISBN 952-5183-18-1. 273, pp 133-138.

[2] M. Ahmed, M. Kuisma, K. Tolsa, P. Silventoinen, " Implementing Sliding Mode Control for Buck Converter'', Power Electronic specialist conference (PESC) Proc. Mexico June, 2003, pp 634-637, Vol. 2.

[3] V. Utkin, J. Guldner, and J. Shi "Sliding Mode Control in Electromechanical Systems", ISBN 0-7484-0116-4(cased), Taylor & Francis 1999.

[4] J. VAN DE VEGET "FEEDBACK CONTROL SYSTEMS", 1986 by Prentice-Hall, Inc, USA.

[5] B. Nicolas, M. Fadel, Y. Cheron, "Sliding mode control with DC-DC converters with input filter based on Lyapunove-function approach" APEC Conf. Proc., 1995, pp. 1.338-1.343.

6] G. Spiazzi, P. Mattavelli, L. Rossetto, L. Malesani, "Application of Sliding Mode Control to Switch-Mode Computers'' (JCSC), Vol. 5, No. 3, September 1995, pp.337-354.

[7] R. W. Erickson "Fundamentals of Power Electronics", ISBN 0-412-08541-0, Chapman & Hall 1997.

Publication P [6]

M. Ahmed, M. Kuisma, P. Silventoinen. Comparison between PID Control and Sliding Mode Control for Buck Converter. *Proceedings of the Symposium on Power Electronics, Electrical Drives, Automation and Motion. SPEEDAM 2004*. CAPRI – ITALY, 16-18 June, 2004.

SPEEDAM 2004 June 16th - 18th, CAPRI (Italy)

COMPARISON BETWEEN PID CONTROL AND SLIDING MODE CONTROL FOR BUCK CONVERTER

M. Ahmed, M. Kuisma, P. Silventoinen

Lappeenranta University of Technology, Department of Electrical Engineering
P.O. Box 20, 53851 LPR, Finland,
fax: +358 5 6216799
E-Mail: ahmed@lut.fi. E-Mail: kuisma@lut.fi. E-Mail: pertti.silventoinen@lut.fi

Abstract

This paper studies the DC/DC Buck converter response controlled with two different control techniques. The first control technique is the traditional PID control, while the second control technique is the sliding mode control. A brief explanation of selecting the PID and sliding mode control parameters is given. The output voltage and the inductor current of both models are studied and compared in transient region (turn on), steady state region, under line variation, and load variation. The sliding mode control for DC/DC Buck converter shows to be: more effective than PID control especially when dynamic tests are applied. Also selecting the control parameters and implementing it in Matlab/Simulink™ is easier.

***Keywords*: Buck converter, PID control, sliding mode control**

1. - INTRODUCTION

The DC/DC Buck converter with PID control was designed and implemented with a prototype in [1]. The same DC/DC Buck converter with sliding mode control (SMC) was designed in [2], and implemented with a prototype in [3]. In both models in [1] and [3], the converter was tested in steady state and under different disturbances. Both models showed acceptable results. This paper considers the output voltage and inductor current of the Buck converter controlled with two different control techniques, traditional PID control and SMC. The results of both models are compared in steady state, transient region, and under line and load variations.

2. - CONVERTER PARAMETERS

The main DC/DC Buck converter parameters were given in [1], and [2], and are represented in Table.1. The Buck converter implemented in this paper is for low power applications. The Buck converter with both PID and SMC is implemented by Matlab/Simulink™. The value of the inductor was found in [1], and [2] to be 69µH, while the capacitor value was 220µF.

Table.1
THE CONVERTER MAIN CIRCUIT PARAMETERS

Parameter name	Symbol	Value
Input voltage	V_{in}	24volts
Output voltage	V_o	12volts
Capacitor	C	220µF
Inductor	L	69µH
Nominal load resistance value	R_L	13Ω
Nominal switching frequency	F_s	100kHz

3. – CONTROL PARAMETERS

This section is divided into two sub-sections. In first part a brief description of selection the PID control parameters control is given, while the second part briefly describes the selection of SMC parameters.

3.1 – PID control parameters

The detail analysis for selecting the PID control parameters were given in [1]. A brief explanation is given in this section. The Buck converter small signal AC model of control to output and line to output transfer function is given in equation (1)

$$\hat{v}(s)=G_{go}\frac{1}{1+\frac{s}{Q\omega_0}+\left(\frac{s}{\omega_0}\right)^2}\hat{v}_g(s)+G_{do}\frac{\left(1+\frac{s}{\omega_z}\right)}{1+\frac{s}{Q\omega_0}+\left(\frac{s}{\omega_0}\right)^2}\hat{d}(s) \quad , \quad (1)$$

where G_{go} is the line to output transfer function DC gain, and G_{do} represents the control to output transfer function DC gain.

The parameters given in Table.1 where compared to the Silent features of the small-signal CCM transfer function of some basic DC/DC converter given in Table.2

Table.2
SILENT FEATURES OF THE SMALL-SIGNAL CCM TRANSFER FUNCTION OF SOME BASIC DC/DC CONVERTERS [4].

Converter	G_{go}	G_{do}	W_o	Q (quality factor)	W_z
Buck	D	$\frac{V_o}{D'}$	$\frac{1}{\sqrt{LC}}$	$R_L\sqrt{\frac{C}{L}}$	∞
Boost	$\frac{1}{D'}$	$\frac{V_o}{D'}$	$\frac{D'}{\sqrt{LC}}$	$D'R\sqrt{\frac{C}{L}}$	$\frac{D'^2R_L}{L}$
Buck-Boost	$\frac{D}{D'}$	$\frac{V_o}{DD'^2}$	$\frac{D'}{\sqrt{LC}}$	$D'R\sqrt{\frac{C}{L}}$	$\frac{D'^2R_L}{DL}$

Matlab/Simulink™ was used for simulating the model with a unity feedback. The Bode diagram showed a poor phase margin and a low gain at low frequency, so a PID control was added with the following transfer function:

$$G_c=10\left(\frac{s+3142}{s}\right)\left(\frac{s+10681}{s+91106}\right), \quad (2)$$

where the constant represent the gain, the second term represent the integral action, and the third term is the derivative action. For more detail analysis reader should refer to [1]. Fig.1 shows the structure of the simulated PID control circuit in Matlab/Simulink™.

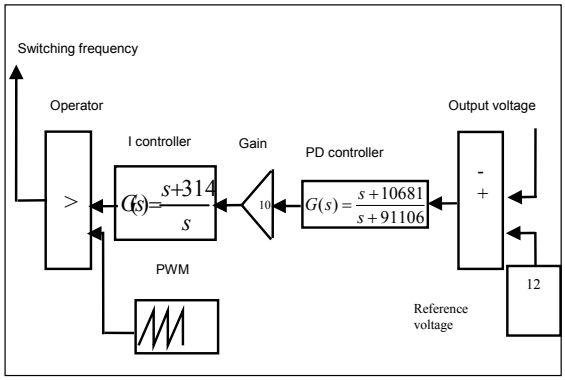

Fig.1 The simulation controller block diagram. Controller includes PID control parameters used in this paper. For derivation of the control parameters reader should refer to [1] and [4].

3.2 – Sliding mode control parameters

SMC is a non-linear control which complies with the non-linear structure of switch mode power supply. The control topology consists of a linear and non-linear part. The non-linear parameter can be selected, while it is left to the designer to tune the linear part and get the optimum values depending on the application.

Fig.2 shows the control structure of SMC. It consists of two control loops, the output voltage is subtracted from the reference voltage and the difference is passed through an integral action. The output of the integral is amplified through a gain and the result is subtracted from the inductor loop, the difference is passed through a hysteresis. One major drawback of this model is the lack of a standard procedure to select the gain. The hysteresis parameter can be selected by measuring the peak-to-peak inductor current and these are the limits for the hysteresis parameters. For more details of selecting the SMC parameters reader should refer to [2], while in [3] reader can find the prototype model design of SMC.

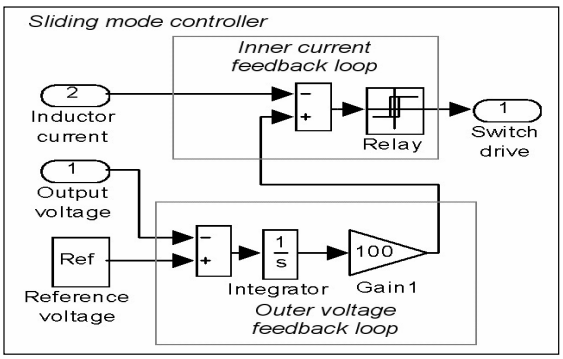

Fig.2 The simulation controller block diagram. Controller includes the current controller (inner loop) and the voltage control loop (PI-control), where together they present SMC. For more details reader should refer to [2] and [5].

4. - TEST RESULTS

The output voltage and inductor current were tested in the following regions: turn on region, steady state, line variation, and load variation. In each region a detailed analysis and comparison between the two models, Buck converter with PID and Buck converter with SMC are presented.

4.1 - Transient region

Fig.3 shows the output voltage and inductor current of DC/DC Buck converter with PID control, while Fig.4 shows the same graphs for DC/DC Buck converter with SMC. Both are in transient region. Table.3 shows the comparison between the two models in transient region. The output voltage of Buck converter with PID has no overshoot, while the output voltage of the same converter with SMC has 4.5 volt overshoot. The gain of the output voltage with SMC can be reduced by increasing the gain but it will increase the settling time. The graphs show that the settling time with PID is shorter, but on the other hand the inductor current has a very high overshoot. For Buck converter with SMC, the settling time is longer with some voltage overshoot but the inductor current has much less overshoot. It can be seen from Fig.3, Fig.4, and Table.3 that although the SMC has longer settling time in this region the inductor current has much less overshoot. This reduction in the inductor current overshoot is due to the additional inner inductor current loop.

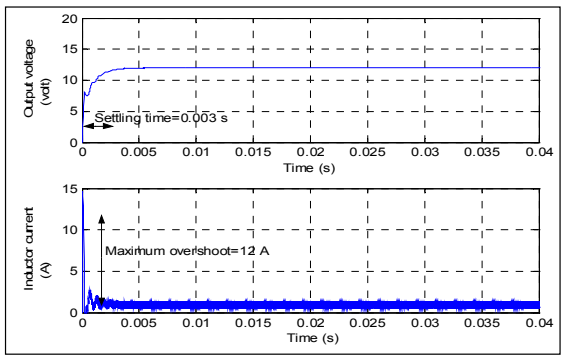

Fig.3 Output voltage and inductor current of Buck converter with PID control in transient region. The settling time is 3 ms, and the inductor current has a high overshoot.

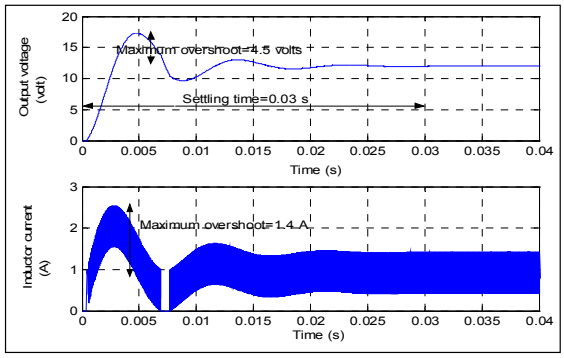

Fig.4 Output voltage and inductor current of Buck converter with SMC in transient region. The settling time is 30 ms. The voltage overshoot is 4.5 volt and the current overshoot is1.4 A.

Table.3
OUTPUT VOLTAGE AND INDUCTOR CURRENT OF BUCK CONVERTER PARAMETERS WITH BOTH PID AND SMC IN TRANSIENT REGION

	PID control		SMC	
	Settling time	Maximum overshoot	Settling time	Maximum overshoot
Output voltage	3 ms	No overshoot	30 ms	4.5 volt
Inductor current	3 ms	12 A	30 ms	1.4 A

4.2 - Steady state region

Fig.5 shows the converter output voltage and inductor current implemented with PID control, while Fig.6 shows the same graph when implemented with SMC. Both graphs are in steady state. In both cases the output ripple voltage value is 4 m volt and the peak-to-peak inductor current value is approximately 1A. These values

are close to the calculated values in equation (3) and (4).

$$i_c = c\frac{\Delta v_c}{(1-D)T_s} \Rightarrow \Delta v_c = 3.5 \text{ mV}, \quad (3)$$

$$v_L = L\frac{\Delta i_L}{DT_s} \Rightarrow \Delta i_L = 0.94 \text{ A}, \quad (4)$$

where $D = \frac{V_o}{V_{in}}$ is the duty cycle, $T_s = \frac{1}{F_s}$.

Table.4 shows the comparison between the two models in steady state. These results are obtained from Fig.5 and Fig.6. It can be said that both models have the same performance in the steady state. This shows that both PID and SMC are efficient in steady state region.

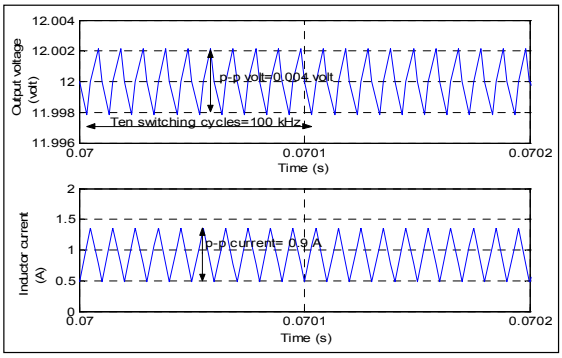

Fig.5 Output voltage and inductor current of Buck converter with PID control in steady state. The voltage ripple is 4 m volt and the peak-to-peak inductor current is approximately 0.9 A. the switching frequency is shown to be 100 kHz

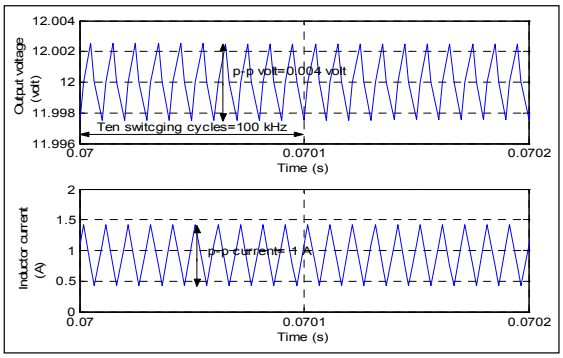

Fig.6 Output voltage and inductor current of Buck converter with sliding mode control (SMC) in steady state. The output voltage ripple is 4m volt and the peak-to-peak inductor current is approximately 1 A. The switching frequency is shown to be 100 kHz.

Table .4

OUTPUT VOLTAGE AND INDUCTOR CURRENT OF BUCK CONVERTER PARAMETERS WITH PID AND SMC IN STEADY STATE REGION

	PID control		SMC	
	Peak to peak	Average value	Peak to peak	Average value
Output voltage	4 m volt	12 volt	4 m volt	12 volt
Inductor current	0.9 A	0.87 A	1 A	0.85 A

4.3 - Line variation

To study the line variation, a step change of 20% from the input value is applied to both models. It is shown in Fig.7 that the converter with PID control is highly affected by line variation, while Fig.8 shows that the converter model with SMC has almost negligible effect. It shows that SMC has a strong immunity against line variation disturbances, and has better performance than PID control in this region. Table.5 shows the comparison between the two models in this region.

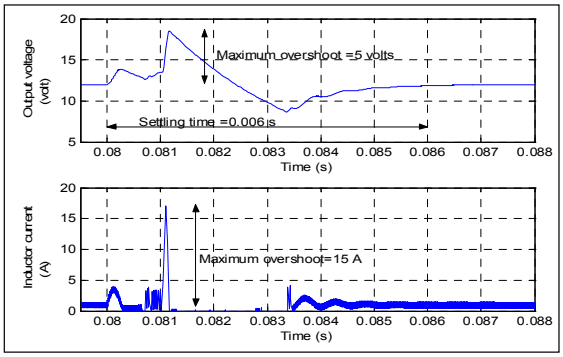

Fig.7 Output voltage and inductor current of Buck converter with PID control under line variation. The output voltage has a maximum overshoot of 5 volts, while the inductor current has a high overshoot of 15A. The settling time is 6ms.

Table.5

OUTPUT VOLTAGE AND INDUCTOR CURRENT OF BUCK CONVERTER UNDER LINE VARIATION

	PID control		SMC	
	Settling time	Maximum overshoot	Settling time	Maximum overshoot
Output voltage	6 ms	5 volt	Negligible ≈ 0	Negligible ≈ 0
Inductor current	6 ms	15 A	Negligible ≈ 0	Negligible ≈ 0

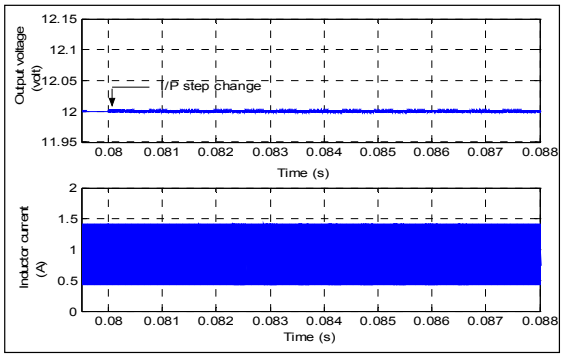

Fig.8 Output voltage and inductor current of Buck converter with SMC. It is shown that the converter is not affected by the line disturbance and that SMC has a strong immunity against this kind of variation.

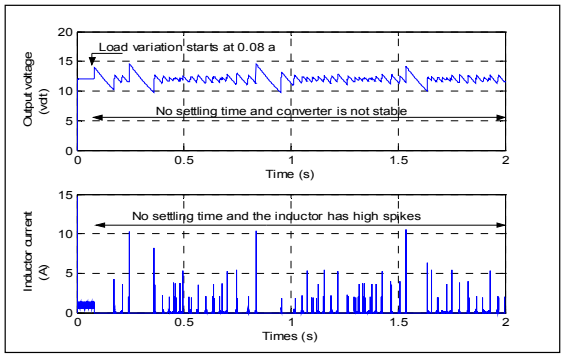

Fig.9 Output voltage and inductor current of Buck converter with PID control when the load changes from 13Ω to 1.3kΩ. The voltage and the current are unstable with no load value.

4.4 – Load variation

To study the effect of the load variation on the DC/DC Buck converter behavior, two tests should be done to both models. First the load changes from its nominal (13 Ω) value to no load (1.3kΩ) and secondly from its nominal value to full load (1.3Ω). These two tests are considered to be the worst case. Both cases are studied separately.

4.4.1 - From nominal value to no load

Fig.9 shows the output voltage and inductor current of the DC/DC Buck converter with PID control when the load changes from the nominal value to no load. The same graphs are shown in Fig.10 for converter with SMC. For PID control the converter will be unstable with a high output voltage ripple and the inductor current will have high spikes, instability continues if the converter still work with no load . For SMC model (Fig. 10) the settling time is approximately 1.4 s and a ripple of 0.5 volt appears if it continues to work with no load. The inductor current spikes are approximately 1 A. This means that SMC will force the Buck converter to be stable and work in discontinuous conduction mode DCM with a ripple voltage of 0.5 volts in the steady state when no load condition is applied. Table.6 shows the comparison between both models. It shows that SMC has more immunity (return to stability) than PID control when the converter load changes its value to no load.

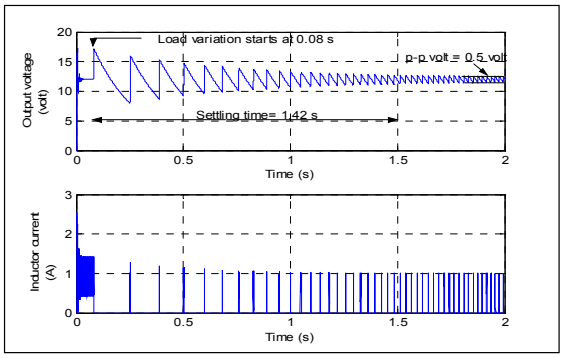

Fig.10 Output voltage and inductor current of Buck converter with SMC when the load changes from 13Ω to 1.3kΩ. The ripple voltage at 1.3kΩ is 0.5volt. The current has peaks of 1A.

Table.6
OUTPUT VOLTAGE AND INDUCTOR CURRENT OF BUCK CONVERTER WITH BOTH PID AND SMC WHEN LOAD CHANGES FROM 13 Ω to 1.3 kΩ

	PID control		SMC	
	Settling time	Peak to peak	Settling time	Peak to peak
Output voltage	No settling time (unstable)	5 volt	1.48 s	0.5 volt
Inductor current	No settling time (unstable)	10 A	1.48 s	1 A

4.4.2 - From nominal value to full load

Finally in this section the load switches from its nominal value to full load. Only in this section the PID has the advantage over the SMC in the output voltage response, but still the inductor current with PID has overshoot of 7 A. Fig.11 shows the output voltage and inductor current response of the converter with PID control. Fig.12 shows the same response with SMC, where the settling time is

longer but the current overshoot is negligible. Table.7 shows the comparison between the two models.

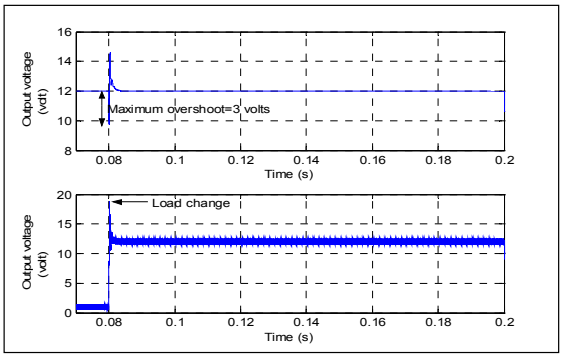

Fig.11 Output voltage and inductor current of Buck converter with PID control when the load changes from 13Ω to 1.3Ω. The voltage overshoot is 3 volts. The current overshoot is 5 A.

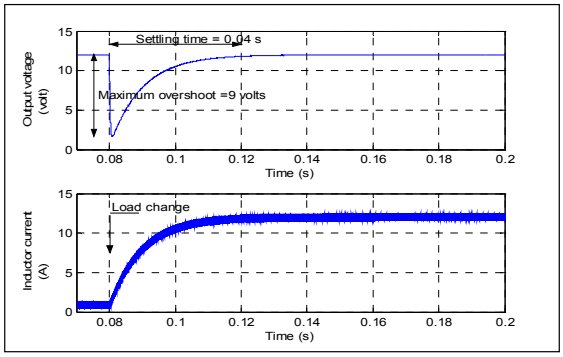

Fig.12 Output voltage and inductor current of Buck converter with SMC when the load changes from 13Ω to 1.3Ω. The voltage overshoot is 9 volts. The current has no overshoot.

Table.7

OUTPUT VOLTAGE AND INDUCTOR CURRENT OF BUCK CONVERTER PARAMETERS WITH BOTH PID AND SMC WHEN LOAD CHANGES FROM 13Ω to 1.3Ω

	PID control		SMC	
	Settling time	Maximum overshoot	Settling time	Maximum overshoot
Output voltage	Negligible ≈ 0	3 volt	40 ms	9 volt
Inductor current	Negligible ≈ 0	7 A	40 ms	Negligible ≈ 0

5. – CONCLUSIONS

The DC/DC Buck converter was tested in steady state region, transient region (turn on), under line variation, and under load variation. These tests where done for the Buck converter using two different control techniques, the traditional PID control and the SMC. In steady state both models showed similar characteristics. For dynamic tests the SMC showed to be more efficient against disturbances than the PID control. The settling time was longer in case of SMC also a higher output voltage overshoot. On the other hand, the inductor current didn't have high overshot while it had high inductor current overshoot with PID control. The reduced current overshoot is due to the additional inductor current feedback. The SMC is showing a promising future in the application of switch mode power supply because it is a non linear control and can evaluate the non linearity of the converter components. Second, it isn't operating at a constant switching frequency. Third, it's easer to design a converter with SMC than PID control.

REFERENCES

[1] M. Ahmed, M. Kuisma, P. Silventoinen, "*Standard Procedure for Modeling the Basic Three Converters (Buck, Boost, and Buck-boost) With PID Algorithm Applied*'', XIII-th International Symposium on Electrical Apparatus (Siela). May 2003. pp 15-20, Vol. 1.

[2] M. Ahmed, M. Kuisma, P. Silventoinen, "*Implementing Simple Procedure for Controlling Switch Mode Power Supply Using Sliding Mode Control as a Control Technique*'', XIII-th International Symposium on Electrical Apparatus and technologies (Siela).May 2003, pp 9-14, Vol.1

[3] M. Ahmed, M. Kuisma, K. Tolsa, P. Silventoinen, "*Implementing Sliding Mode Control for Buck Converter*'', Power Electronic specialist conference (PESC) Proc. Mexico June, 2003, pp 634-637, Vol. 2.

[4] R W. Erickson "*Fundamentals of Power Electronics*", ISBN 0-412-08541-0, Chapman & Hall 1997. pp 323-355.

[5] V. Utkin, J. Guldner, "*Sliding Mode Control in Electromechanical Systems*", ISBN0 7484-0116-4, Taylor & Francis 1999.pp231-236.

[6] G. Spiazzi, P. Mattavelli, L. Rossetto, "*Sliding Mode Control of DC-DC Converters*," 4 " Congresso Brasileiro de Elettronica de Potencia , BeloHorizonte, December 1997, pp.59-68.

Publication P [7]

M. Kuisma, M. Ahmed, P. Silventoinen**.** Comparison of Conducted RF-Emissions between PID and Sliding Mode Controlled DC-DC Converter. *Proccedings of the European Conference on Power Electronics and Applications EPE03*, September2003. Toulouse, France.

Comparison of Conducted RF-Emissions between PID and Sliding Mode Controlled DC-DC Converter

M. Kuisma, M. Ahmed, P. Silventoinen
LAPPEENRANTA UNIVERSITY OF TECHNOLOGY
Department of Electrical Engineering
Skinnarilankatu 34
Lappeenranta, Finland
Tel: +358(0)562111 / Fax:+358(0)56216799
Email: Mikko.Kuisma@lut.fi

Keywords

Converter control, EMC/EMI, harmonics, sliding mode control

Abstract

Traditional pulse width modulated (PWM) power converter operates on a constant switching frequency. This frequency is also presented in the electromagnetic interference (EMI) -spectrum of the converter. During the last decade, intensive study of EMI-reduction techniques, including spread spectrum technology, in the field of power electronics has been made. Selected control strategy also effects on the generated EMI spectrum. In this paper, a comparison between EMI-noise effects of fixed frequency, PID-controlled PWM and sliding mode –controlled (SMC) converter has been done. Both simulation and experimental results are presented.

Introduction

DC/DC, AC/DC and DC/AC power supplies are usually implemented with use of some constant clock frequency. For example, with pulse width modulation (PWM), the modulator clock and harmonic frequencies are present in both conducted and radiated electromagnetic interference EMI. With help of spread spectrum modulation techniques emissions can be reduced to meet the EMC-regulations. The spread spectrum techniques are under intensive research in power supply applications.

Main conducted radio frequency RF-energy emitted from converter into the supplying network is in the frequency range from few kilohertz to tens of megahertz. At this frequency range, the emitted electromagnetic energy spreads mainly by conduction. In addition to that, conducted emissions to the load circuit and RF -interference are generated.

Most commonly, EMI-reduction techniques presented in literature are based on modulating the clock signal, [1], [2], [3]. Some pseudo random clock generation schemes have also been proposed, [4], [5]. The control design of the switch mode converter affects also on the EMI-spectrum of the converter. Sigma-delta, hysteresis-control, chaotic peak current control and sliding mode control are most commonly used non-linear control techniques used in the field of power electronics. These non-linear control techniques generate non-harmonic switching spectrum when controller parameters are correctly chosen. This paper concentrates on EMI-properties of the sliding mode controlled Buck-converter. Conducted EMI-spectrum is compared to PID-controlled converter. Simulation and experimental results are presented.

Spread spectrum noise

The aim of use of spread spectrum techniques is to reduce the measurable and effectible noise content of switch mode power supply. The main idea of the spread spectrum generating technique is presented

in Fig. 1. Signal power from single frequency is spread over wide range of frequencies. Total power transferred has remained constant, but the peak values have been reduced. The main drawback in this scheme is that although the peak values have been reduced, the noise is spread at wider frequency range.

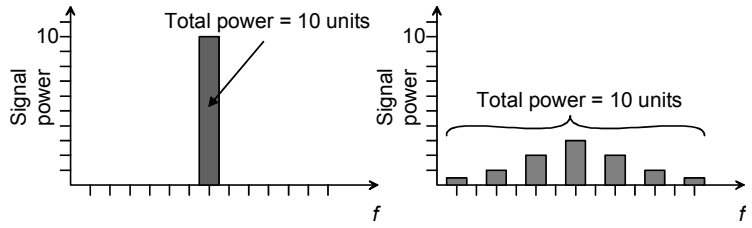

Fig. 1: The main idea in spread spectrum generation. Total transferred power remains constant when power from single frequency is spread over wide range of frequencies.

Spread spectrum noise, or *spread spectrum modulation* when speaking about switch mode power supplies (SMPS), can be generated in many different ways. One solution is using a programmable device that is programmed with some random or pseudo-random modulation sequence. This pseudo random sequence then interacts with the system clock of the power converter thus generating non-periodic drive signal to the power switch of the converter. Other approach is by using "intelligent" control system design. Some feedback control strategies (e.g. sigma-delta modulation, peak current control, sliding mode control) have inherent spread spectrum properties when applied to non-linear system like SMPS.

Advantage of the hardware-programmed method is that the modulation sequence can be tailored for maximum spectral performance. Some other design parameters can also be enhanced at the same time. Drawback of this solution is that it needs extra circuitry or application specific integrated circuit to generate the modulating signal. Advantage of the non-linear control design approach is the simplicity of the circuit: even basic switch mode power supply control circuits, made by many IC manufacturers, can be used with only few additional passive components. Main drawback of this approach is that the designer has to carefully study the circuit performance at all load conditions and parameter variations to ensure the spread spectrum operation and system overall stability in all cases.

Sliding mode control and chaos

The approach used in this paper utilizes the nonlinear dynamics and nonlinear effects of the control system to generate chaotically operating SMPS. When the system is in chaos, it can still be under control, although chaotic operation may sound disordered and non-controllable. Chaos can be loosely defined as an apparently random behavior in nonlinear system. Since all switch mode power electronic circuits are nonlinear, chaotic behavior can be expected in power electronic circuits with some specific component and parameter values. Usually this chaotic behavior is undesirable, but if the chaotic behavior can be controlled (or actually understood) it is very simple way to reduce measurable EMI-content of the SMPS.

Chaotic operation is deterministic but not predictable. This often misleads someone to think that chaotic operation is random process. Chaos is not random process, but it usually looks like random. If we don't know *exact* values of *all* system parameters, we cannot predict the exact operation of the chaotic system. Sometimes chaotic system (power converter) is not recognized as chaotic, and "weird looking operation" has been explained by sub-harmonic oscillations and instability of the converter.

There are four steady state behavior (solutions) associated with a non-linear system, [6]:

- Equilibrium points
- Periodic solutions
- Quasi-periodic solutions
- Chaos

Most solutions in power electronic circuits operate at stable equilibrium point or they may have periodic solution. With proper (or accidental) design, the operation of the power system can be chaotic. Usually practical power supply can mainly operate in (stable) equilibrium point, but with some parameter values (e.g. variation in input voltage or load), the system can go to chaos.

In our design, the sliding mode control is implemented with current hysteresis controller. The feedback controller consists of two control loops: inner current control and outer linear voltage control, Fig. 2. Outer control loop monitors the output voltage V_o and subtracts it from the reference voltage V_{ref}. The error signal is then fed to the linear voltage controller (PI-controller) generating the current reference signal I^*. Current feedback signal is then fed to the hysteresis comparator and compared to the current reference thus generating the switch drive signal u. This kind of non-linear control strategy applied to non-linear power converter can force the system to chaos.

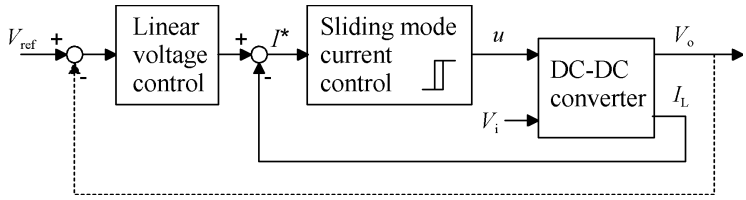

Fig. 2: Control loops of the sliding mode controlled converter. Outer voltage control loop is traditional PI-controller and inner loop is based on hysteresis comparator.

Sensibility of the system to parameter variations and tendency to chaotic operation can be studied with bifurcation diagram. In bifurcation diagram, one system parameter is varied and other system state is sampled. Bifurcation diagram illustrates the creation of sub-harmonic oscillations and chaos as function of selected system parameter. Varied system parameter in the test converter is the hysteresis width in current control block, which can be seen in bifurcation diagram, Fig. 3. Multiple-periodic operation of the converter can also be seen on time-domain waveform of the input current, Fig. 4. If more information about basic chaos theory is needed, refer to [6], [7], [8] and [9]. Calvente et al. [10] has also nice overview on the topic of chaos in sliding mode controlled Boost converter.

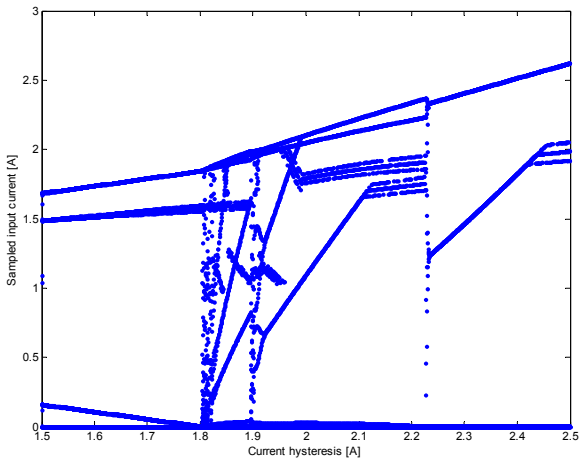

Fig. 3: Bifurcation diagram generated by sweeping the hysteresis width of the current controller from 1.5A to 2.5A. Chaotic operation regime is quite small (three regimes around 1.8 A, 1.9 A and 2.2 A) with selected parameter values. Multiple periodic operation and periodic doubling is clearly visible when the operation is not chaotic.

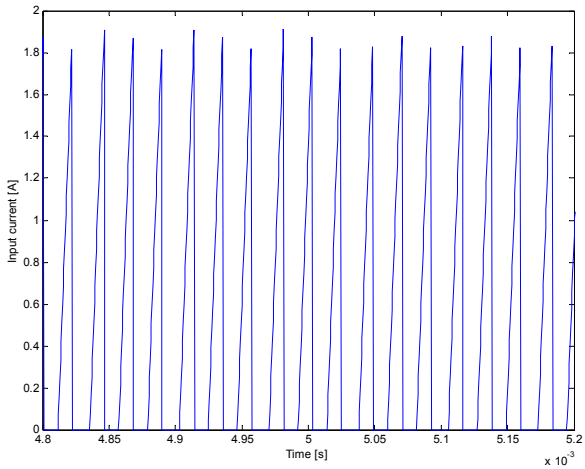

Fig. 4: Example of input current waveform in non-periodic operation point. Current fluctuation seems to almost have some period, but instant switching frequency actually changes continuously.

When SMPS operates on chaotic regime there is no constant switching frequency and the spectrum of the converter is spread over wide frequency range. Even periodic and quasi-periodic operation usually eases the EMI –problem compared to single frequency system clock, thus generating non-constant frequency for the power switch.

Simulations and experimental results

Simulation and prototype model for the Buck converter was constructed. Two different controllers were also constructed to compare differences in the EMI-performance. The main parameters used in the converter main circuit design are presented in Table I.

Table I. Parameters used in the converter main circuit.

Parameter	Value
Input voltage, V_{in}	24 V
Output voltage, V_o	12 V
Nominal switching frequency, F_s	100kHz
Load resistance, R_L	13 Ω
Output filter capacitor, C	220μF
Inductor, L	69 μH

The block diagram of the main circuit with the PWM-PID-controlled reference controller is presented in Fig. 5. Proposed sliding mode controlled Buck converter is presented in Fig. 6.

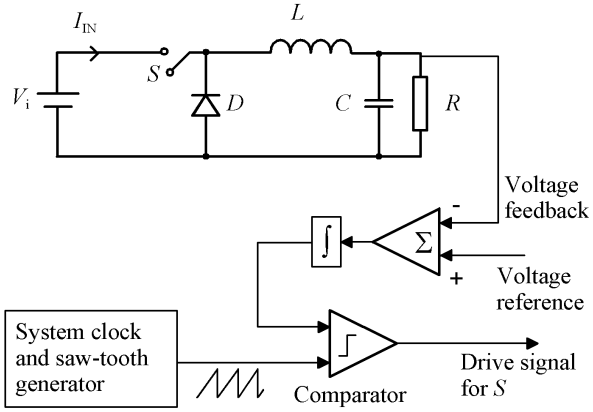

Fig. 5: Simplified block diagram of PWM-PID –controlled reference Buck converter. Output voltage of the converter is subtracted from the reference voltage and the resulting error signal is integrated. After the integration, the signal is compared to the saw-tooth wave to generate the switch drive signal.

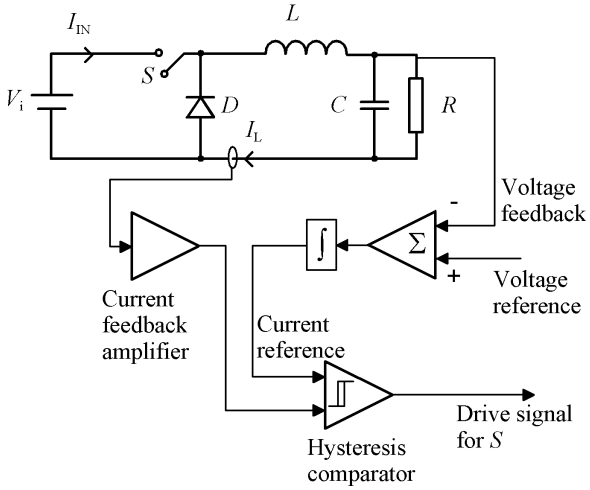

Fig. 6: Simplified block diagram of sliding mode -controlled Buck converter. Voltage feedback loop (PI) is used to generate the current reference signal. Feedback signal from the inductor current is then fed to the hysteresis comparator and compared to the current reference.

Simulation results

Simulink™ models of the Buck converter and two different control strategies were constructed for EMI-simulations. EMI input current spectrum was calculated with Matlab™ PSD-function, which estimates the power spectral density using Welch's method. Parameters for the spectrum estimation were selected so that the result is comparable to the results made with the EMI test receiver. In Fig. 7., the power spectral density of the PID –controlled reference converter is presented. Figures 8 to 10 show the simulated input current power spectral density of sliding mode controlled Buck converter with different current hysteresis widths in the sliding mode controller.

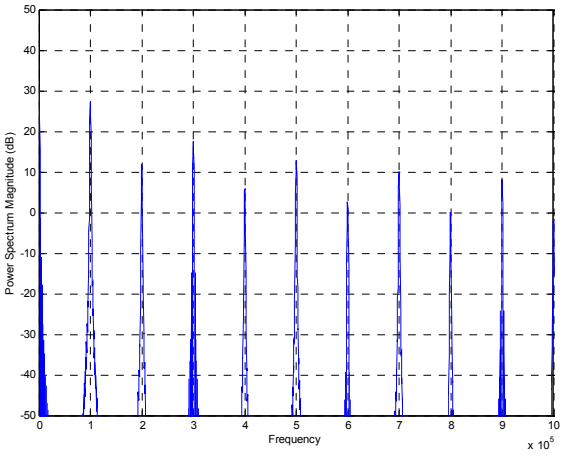

Fig. 7: Simulated input current spectrum of the PI-controlled, constant frequency reference converter. Constant, periodic operation causes discrete spikes on fundamental frequency and it's harmonics.

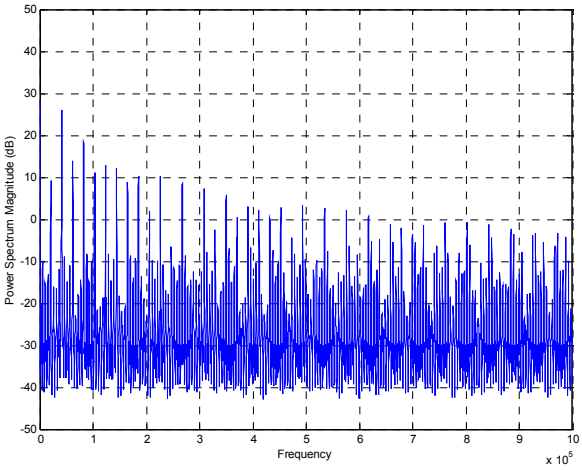

Fig. 8: Simulated input current spectrum, SMC, current hysteresis width set to 1.82 A, converter operating in chaotic mode. Spectral spikes have been lowered and noise floor has risen compared to the reference converter.

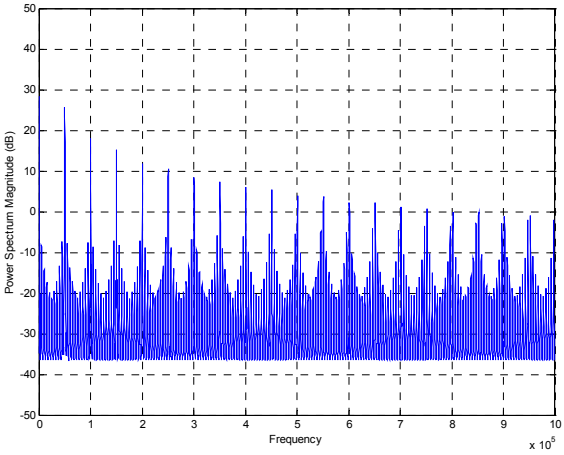

Fig. 9: Simulated input current spectrum, SMC, current hysteresis width set to 1.7 A. Converter is not in chaotic mode and periodic operation can be seen on the spectrum. However, spectral spikes have been lowered and noise floor has risen compared to the reference converter due to multi-periodic operation of the converter switch signal.

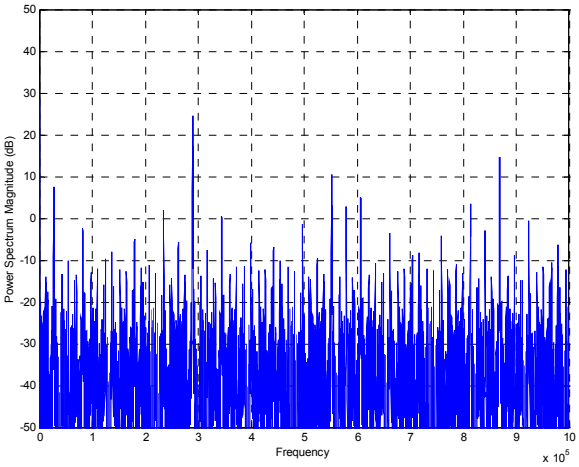

Fig. 10: Simulated input current spectrum, SMC, current hysteresis width set to 0.3 A. Small hysteresis width causes the converter to operate at high average switching frequency.

Simulation results show, that approximately 10-15 dB noise reduction can be achieved in Buck converter only by changing the control strategy of converter. 10 dB reduction has also commonly been reported in literature considering on the EMI-reduction techniques, for example in [3] and [11].

The spectra estimated here in Figures 8 – 10 are actually random variable itself: if the spectrum has been estimated from different time interval, the spectrum would look different. Of course, the shape of the graph will be approximately the same, but because the signal (current) is changing all the time, the resulted spectrum estimation will depend on the time when the signal is acquired.

Prototype converter and test results

The EMI-performance of the test converter was measured from the input current of the converter. Tests were made with Rohde&Schwarz ESHS 30 EMI test receiver and R&S EZ17 current clamp. Settings of the test receiver were: Linear scan from 9kHz to 1 MHz, peak detector, intermediate

frequency bandwidth (IFBW) 200 Hz, stepping 200 Hz, scan time for IFBW 20 ms. Constructed prototype of the converter is presented in Fig. 11. Test receiver with the current clamp is in Fig. 12. EMI spectrum of PI-controlled reference converter is presented in Fig. 13. Measured EMI spectra of SMC converter with different parameter values are presented in Figures 14 – 16.

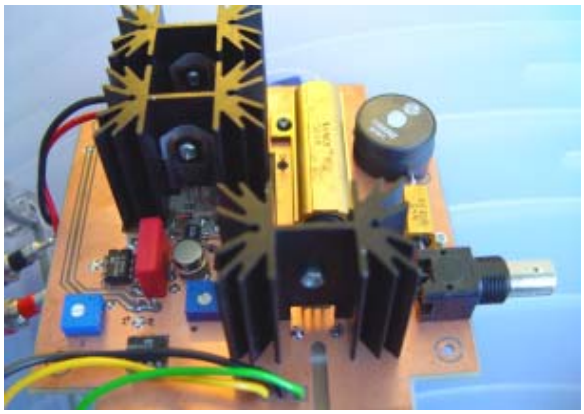

Fig. 11: Prototype converter for experimental tests built in our laboratory.

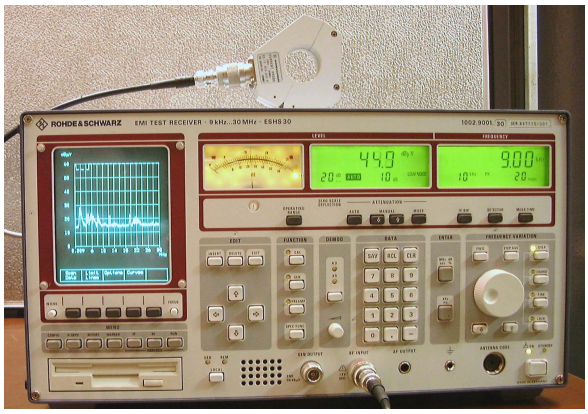

Fig. 12: Rohde&Schwarz EMI test receiver and the current clamp used in the measurements.

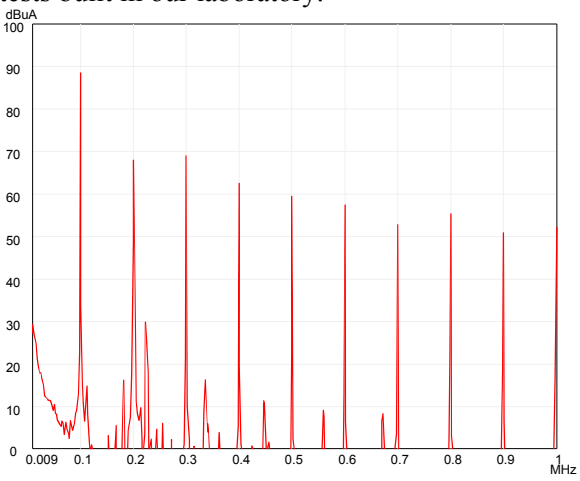

Fig. 13: Measured input current spectrum of the PI-controlled reference converter. Like in simulation, switching frequency and harmonic spikes are present.

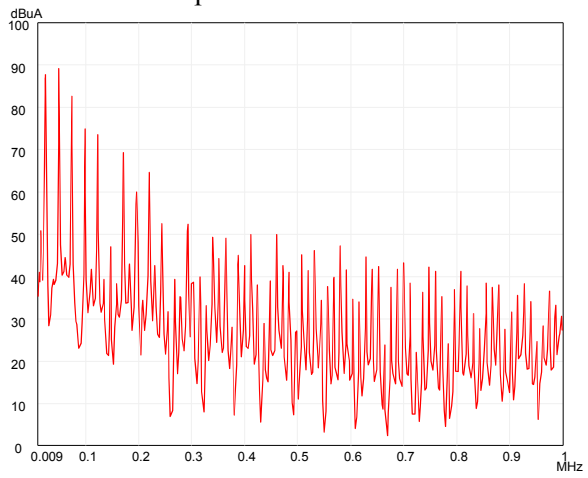

Fig. 14: Measured input current spectrum of the SMC converter, current hysteresis approximately 1.9 A.

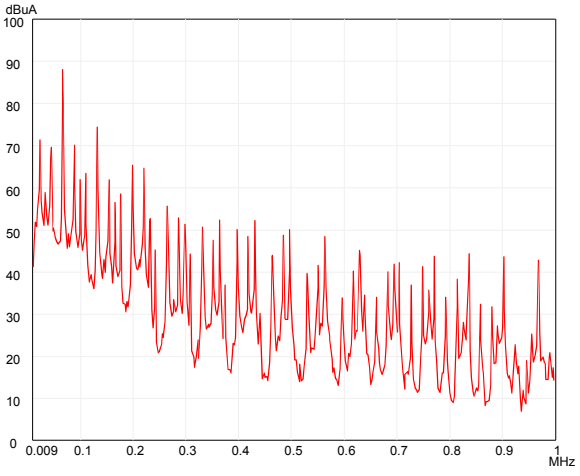

Fig. 15: Measured input current spectrum of the SMC converter, current hysteresis approximately 1.8 A.

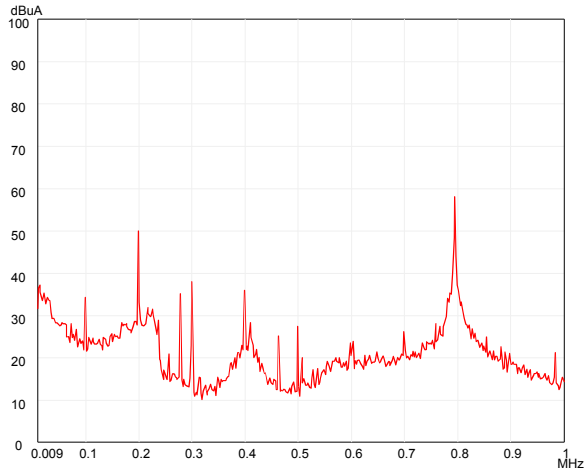

Fig. 16: Measured input current spectrum of the SMC converter, current hysteresis approximately 0.5 A. Small hysteresis width forces the converter to operate at high frequency.

In SMC converter, spectral spikes have been lowered and noise floor has risen compared to the reference converter. Measurements show that with proper parameter values the SMC converter can be forced to chaos, and the resulting EMI spectral noise can be reduced. Again, approximately 10 dB reduction can be achieved. The output voltage ripple was also measured and it has hardly noticeable difference in the peak-to-peak ripple when compared chaotically operating converter to the periodically operating converter.

Conclusions

This paper shows that proper selection of the control strategy has an effect on the EMI performance of the switch mode power converter. With non-linear control circuit, it is possible to achieve same results as achieved with more complicated spread spectrum modulation techniques proposed in the literature. Our tests show that this can be done more easily and the solution can be cost effective compared to more complicated spread spectrum generation schemes. In addition, robustness of the converter can be enhanced with non-linear control strategy. Tests and simulations also show, that non-linearly controlled system can be parameter sensitive and therefore the designer has to know and study non-linear effects of the converter system before adopting the technique on production.

References:

[1]. Vilathgamuwa M., Deng J., Tseng, K.J.: EMI Suppression with Switching Frequency Modulated dc-dc Converters, IEEE Industry Applications Magazine, vol. 5, No. 6, 1999.

[2]. Stankovic, A.M., Verghese, G.C., Perreault, D.J.: Analysis and synthesis of random modulation schemes for power converters. Power Electronics Specialists Conference, PESC '93, 1993.

[3]. Stone, D. A., Chambers B., Howe D.: Random Carrier Frequency Modulation of PWM Waveforms to Ease EMC Problems in Switched Mode Power Supplies, Proceedings of International Conference of Power Electronics and Drive Systems, 1995.

[4]. Stone, D. A, Chambers, B.: Easing radiated EMC problems with spread-spectrum modulation of computer clock signals. Electronics Letters, vol. 31, No 24, 1995.

[5]. Mihalic, F., Milanovic, M.: EMI reduction in randomized boost rectifier. Proceedings of the IEEE International Symposium on Industrial Electronics, vol. 2, ISIE '99. 1999.

[6] Hsiao-Dong Chiang, Chih-Wen Liu, Varaiya, P.P., Wu, F.F., Lauby, M.G.: Chaos in a simple power system. IEEE Transactions on Power Systems, vol. 8 Issue: 4, November 1993

[7]. Parker, T., Chua, L.: Chaos: A Tutorial for Engineers. Proceedings of the IEEE, vol. 75, No. 8, August, 1987.

[8]. Jefferies, D., Deane, J., Johnstone, G.: An Introduction to Chaos. Electronics & Communication Engineering Journal. May/June, 1989.

[9]. Deane, J., Hamill, D.: Instability, Subharmonics, and Chaos in Power Electronic Systems. IEEE Transactions on power electronics, vol. 5. No. 3. July, 1990.

[10]. Calvente, J., Guinjoan, F., Martinez, L., Poveda, A.: Subharmonics, bifurcations and chaos in a sliding-mode controlled boost switching regulator. 1996 IEEE International Symposium on Circuits and Systems, 1996. ISCAS '96. vol. 1, 12-15 May 1996

[11]. Tse, K.K., Chung, H.S.-H., Huo, S.Y., So, H.C.: Analysis and spectral characteristics of a spread-spectrum technique for conducted EMI suppression. IEEE Transactions on Power Electronics, vol. 15 No 2 , March 2000.

Publication P [8]

M. Ahmed, *Student member, IEEE*, M. Kuisma, P. Silventoinen. Sliding Mode Control for Half-Wave Zero Current Switching Quasi-Resonant Buck Converter. *Proceedings of Nordic Workshop on Power Industrial Electronics, NORPIE/2004,* Trondheim, Norway. June 2004.

Sliding Mode Control for Half-Wave Zero Current Switching Quasi-Resonant Buck Converter

M. Ahmed, *Student member, IEEE*, M. Kuisma, P. Silventoinen

Abstract— This paper focuses on the practical implementation of sliding mode control (SMC) in a half-wave zero current switching quasi-resonant Buck converter. SMC can manipulate efficiently the nonlinear phenomena that appear in switch mode power supplies, furthermore SMC is less affected by disturbances compared to other control techniques, and it is not operating at a constant switching frequency. Since half wave zero current switching quasi-resonant Buck converter is not operating at a constant switching frequency and it is sensitive to dynamic variation, SMC is selected in this paper as a control technique. An explanation of the implementation of SMC, and selecting its parameters is given. A detailed mathematical analysis is performed in order to select the appropriate values of the tank components elements. The tank inductor value is assumed to be small and constant, and a range of tank capacitor values is obtained. The prototype of an analog sliding mode control for the converter is constructed. In order to study the effect of SMC on the converter behavior, the system is tested in the steady state and under different load value conditions. The obtained graphs show that the performance of SMC is good, even under the worst load conditions, i.e. no load and full load.

***Index Terms*— half-wave zero current switching, quasi-resonant Buck converter, sliding mode control, tank inductor value, tank capacitor value.**

I. Introduction

SLIDING mode control (SMC) for switch mode power supplies has been studied in literature. Many papers and researches have shown that SMC is an effective control tool for switch mode power supply [1], [2], and [3]. Unfortunately, most of these researches depended on theories or simulation results that have no practical implementation. Previous researches have shown that SMC has good immunity against disturbances and component variations [2], [4], [5]. In this paper, an analog SMC circuit is constructed using operational amplifiers in such a way that the signals generated at each stage are shown in the control circuit. Following a detailed analysis of the selection of the tank component elements is given. A prototype model of the half-wave zero current switching quasi-resonant Buck converter with its control circuit is constructed. The elements of the main circuit of the converter are shown in TABLE 1.To prove that the circuit functions correctly the output voltage waveform, main inductor current waveform, tank inductor waveform, and tank capacitor waveform are studied in the steady state, under no load and under full load conditions.

M. Ahmed, *Student member, IEEE*., Department of Electrical Engineering, Lappeenranta University of Technology, P.O. Box 20, 53851 Lappeenranta, Finland. Phone: +358-407654841 Fax: +358-5-6216799. e-mail: mohammad.ahmed@lut.fi.

M. Kuisma, Department of Electrical Engineering, Lappeenranta University of Technology, P.O. Box 20, 53851 Lappeenranta, Finland, Phone: +358- 621 6711 Fax: +358-5-6216799. e-mail: Mikko.Kuisma@lut.fi.

P. Silventoinen, Department of Electrical Engineering, Lappeenranta University of Technology, P.O. Box 20, 53851 Lappeenranta, Finland. Phone: +358- 40 774 9930 Fax: +358-5-6216799. e-mail: Pertti.Silventoinen@lut.fi.

II. Sliding Mode Control and the Converter Circuit

Many researches have studied, analyzed, and designed the SMC to DC/DC converters [1], [2], [3], [4], and [5]. These researches concluded and showed great potential for the use of SMC in switch mode power supplies because it is a non-linear control and can manipulate the non-linear phenomena that appear in switch mode power supplies, it has a good immunity against disturbances, and is not operating at a constant switching frequency. Since half-wave zero current switching quasi-resonant Buck converter is not operating at a constant switching frequency and it is sensitive to dynamic variation [6], [7], [8], and [9], SMC is selected as a control technique.

The control circuit is represented by two control loops: an inner main inductor current control loop (represented in this paper by a hysteresis control) and an outer voltage control loop that is represented by proportional plus integral control (PI); the combined loops compose the SMC that is responsible for the zero current switching. Fig.1 shows a simple block diagram of the implementation of SMC in switch mode power supplies. The hysteresis parameters can be selected from the peak-to-peak main inductor current. It is difficult to find a standard procedure to determine the integral gain of the linear part. The reason for this difficulty is that the SMC is a non-linear control and can not be linarized. It is not possible to choose the linear part parameters based on the non-linear part. Choosing a low integral gain reduces the overshoot but the steady state error increases. It is left for the designer to choose the parameters depending on the application.

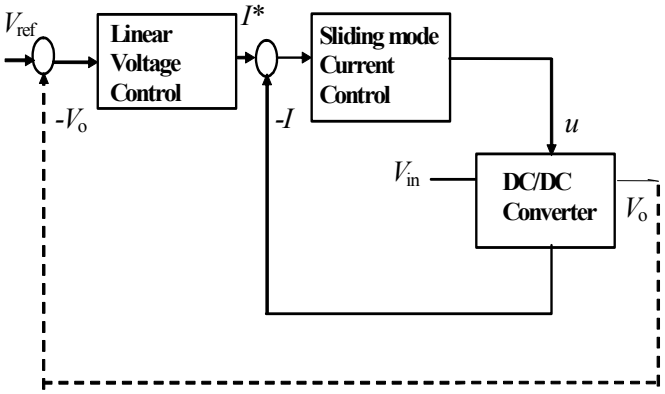

Fig. 1 A simple block diagram shows the implementation of SMC in switch mode power supply. The inner loop is the main inductor current loop, while the outer loop is the PI control. The combined loop is the SMC.

II. Circuit Design

A simplified circuit diagram of the prototype circuit for a half-wave zero current switching quasi-resonant Buck converter controlled by SMC is shown in Fig.2. Resonant converters contain resonant L_r, C_r networks where its voltage and current waveforms vary sinusoidally during one or more subintervals of each switching period. The main interest in resonant operation of the converters is the minimization of switching losses. Half-wave zero current switching quasi-resonant Buck converter, shown in Fig. 2, is a resonant converter, where the resonant tank capacitor (C_r) is placed in parallel with the main Buck converter diode D_2, while resonant tank inductor (L_r) is placed in series with the active switch. Diode D_1 is in series with active switch. The magnitude of the tank inductor current and hence also the DC load current can be controlled by variation of the switching frequency F_s [10].

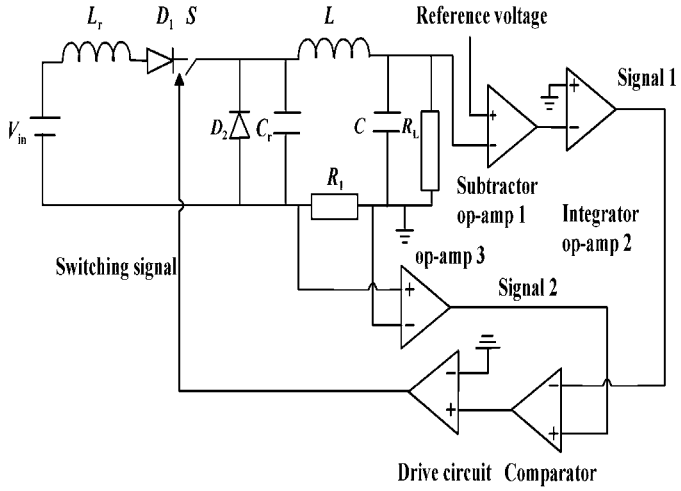

Fig.2. Half-wave zero current switching quasi-resonant Buck converter with a sliding mode control. Combination of PI and current hysteresis control circuits composes the SMC.

The operation of the prototype in Fig.2 can be described as follows: The output voltage is subtracted from the reference voltage using op-amp1. The voltage difference signal is integrated using op-amp2. The output of this amplifier generates signal 1. Op-amp3 is used to detect the inductor current with a shunt resistor R_1, generating signal 2. In the next stage, signals 1 and 2 are compared using a comparator (LM111), in which Hysteresis is used to control the switching frequency. The output level of the LM111 signal should be translated into the voltage difference between the gate-source of the switching device IRF530. A high-side MOSFET/IGBT driver IR2117 is used for this purpose.

The circuit was constructed in the Laboratory of Applied Electronic at Lappeenranta University of Technology. Fig.3 shows the constructed prototype for a half-wave zero current switching quasi-resonant Buck converter with SMC used in the Laboratory where the tests were performed.

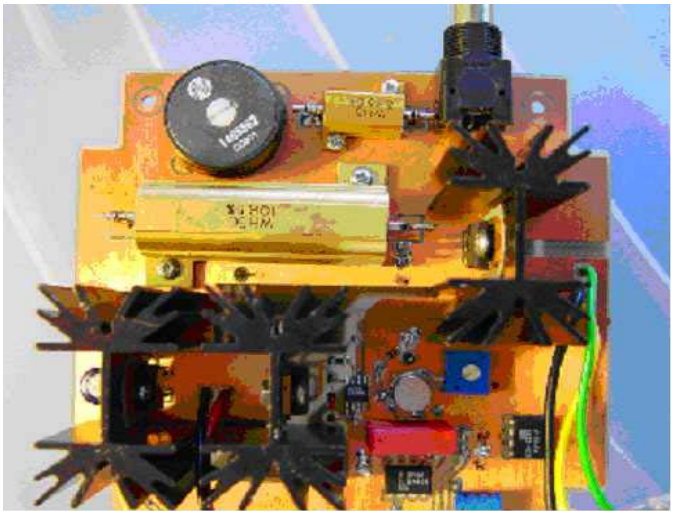

Fig.3 The prototype circuit of the half-wave zero current switching quasi-resonant Buck converter with SMC. The circuit was constructed and tested in the Laboratory of Applied Electronics at Lappeenranta University of Technology (Finland).

TABLE 1 shows the main Buck converter parameters used in the prototype model.

TABLE 1
CONVERTER MAIN CIRCUIT PARAMETERS

Parameter name	Symbol	Value
Input voltage	V_{in}	24 volts
Output voltage	V_o	12 volts
Capacitor	C	220 µF
Inductor	L	69 µH
Load resistance	R_L	13 Ω
Nominal switching frequency	F_s	100 kHz

III. Calculating and Selecting the Tank Component Elements Values

The resonant tank elements are selected by assuming a constant and small L_r value and obtaining C_r. There are two reasons for selecting small L_r value. First, a high L_r value stores a high amount of magnetic energy and since it is connected in series with switch, it may damage the switch MOSFET. Second, the tank resonant frequency should be greater than the nominal switching frequency.

$$F_o \geq F_s, \quad (1)$$

where $F_o = \frac{1}{2\pi\sqrt{L_r C_r}}$ denotes the tank resonant frequency.

If $F_o < F_s$, the tank elements respond more strongly to the harmonics of the input voltage than to its fundamental value. In order to obtain the range of C_r values, two conditions have to be fulfilled.

A. Condition 1

The tank resonant frequency should be greater than the nominal switching frequency, as given in equation (1). Using equation (1) and for $F_s = 100$ kHz, $L_r = 3\mu$H we get

$$C_r \leq 844\text{nF}. \quad (2)$$

B. Condition 2

the DC conversion ratio (μ) is less than one for Buck converter

$$\mu = \frac{V_o}{V_{in}} \leq 1. \quad (3)$$

To guarantee that the tank inductor current reach zero, the condition in equation (4) should be satisfied [1]

$$\frac{V_{in}}{Z_o} \leq I_L, \quad (4)$$

where $Z_o = \sqrt{\frac{L_r}{C_r}}$ denotes the tank characteristic impedance.

By substitute equation Z_0 into equation (4) and for $L_r = 3\mu$H, and $R_L = 13\ \Omega$, it can be obtained that

$$C_r \geq 4.5\text{nF}. \quad (5)$$

Equation (4) is the second condition for selecting C_r. From equation (2) and (5) the range of C_r is

$$4.5\text{nF} \leq C_r \leq 844\text{nF}. \quad (6)$$

TABLE 2 shows the effect of different C_r on the converter's response, provided that these values are within the tank capacitor range obtained from equation (6). Designers of switch mode power supplies prefer to work at high switching frequencies. TABLE 2 shows it is possible for a half-wave zero current switching quasi-resonant Buck converter to work at high switching frequencies by selecting small C_r values, but the two disadvantages recorded are the slow transient response and more tank waveform distortions. The value of C_r was selected in this paper to be 400nF and L_r is assumed to be 3µH in this paper. All the results obtained from the prototype model are based on $L_r = 3\mu$H, $C_r = 400$nF, and TABLE 1.

TABLE 2
HALF -WAVE ZERO CURRENT SWITCHING QUASI-RESONANT BUCK CONVERTER RESPONSE WITH CONSTANT L_R VALUE AND TWO DIFFERENT C_R VALUES

Constant and small L_r		
	Small C_r value	High C_r value
1	Operate at high switching frequency	Operate at low switching frequency
2	Slow transient response without overshoot	Fast transient response with overshoot
3	Low output voltage ripple	Low output voltage ripple
4	More tank waveform distortions	Less tank waveform distortions
5	Lower peak-to-peak tank inductor current	Higher peak-to-peak tank inductor current
6	Lower peak-to peak main inductor current	Higher peak-to peak main inductor current

IV. EXPERIMENTAL RESULTS OF THE PROTOTYPE

To prove that the constructed circuit functions properly and that SMC can be implemented with the prototype, as well as to show that SMC is resistant to load variations, the circuit was tested in steady state and under load variations (no load and full load). The output voltage, main inductor current, tank capacitor voltage and tank inductor current waveforms were tested, and the corresponding graphs are shown in Figs. 4 to 9. The main converter parameters were given in TABLE 1, assuming that $C_r = 400$nF, and $L_r = 3\mu$H.

A. Steady state region

Fig. 4 shows the output voltage waveform (ch1, upper waveform) has a 0.1-volt ripple and the main inductor current waveform (ch2, lower waveform) has 4.1A peak-to-peak value in steady state. The graph shows that in steady state the converter has a good response when controlled by SMC.

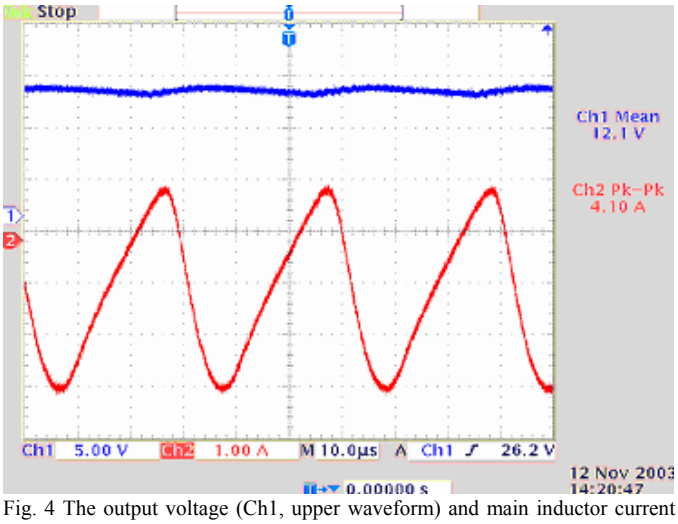

Fig. 4 The output voltage (Ch1, upper waveform) and main inductor current (Ch2, lower waveform) of the half-wave zero current switching quasi-resonant Buck converter controlled by SMC in steady state.

Fig. 5 shows in steady state the tank capacitor voltage waveform (ch1, upper waveform) with 57volt and the peak-to-peak tank inductor current waveform (ch2, lower waveform)

that is 5.16A with negative reverse recovery. It can be seen in Fig.5 that zero current switching occurs. The F_s is 32.46 kHz, (ch2 Freq). Reducing the tank capacitor value can increase the frequency, but more distortion occurs in the signals.

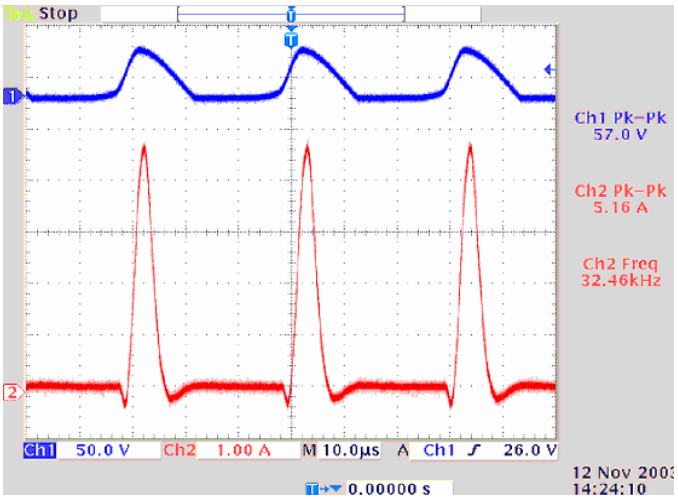

Fig.5 The tank capacitor voltage waveform (Ch1, upper waveform) and tank inductor current waveform (ch2, lower waveform) of the half-wave zero current switching quasi-resonant Buck controlled by SMC in steady state. (Ch2 Freq) shows the frequency of the converter

B. Load variation

To study the effect of SMC on the behavior of the converter under load variations, two tests were performed on the converter with different load values, which are considered to be the worst cases.

First case is when the converter is operating under no load (2kΩ). Fig. 6 shows the output voltage and main tank inductor current waveforms under no load condition. The mean output voltage is 12.1volts (Ch1 Mean, upper waveform). The peak-to-peak main inductor current is 3.68A (Ch2 PK-PK, lower waveform) and the frequency at which the converter operates under no load is 24.52 kHz (Ch2 Freq).

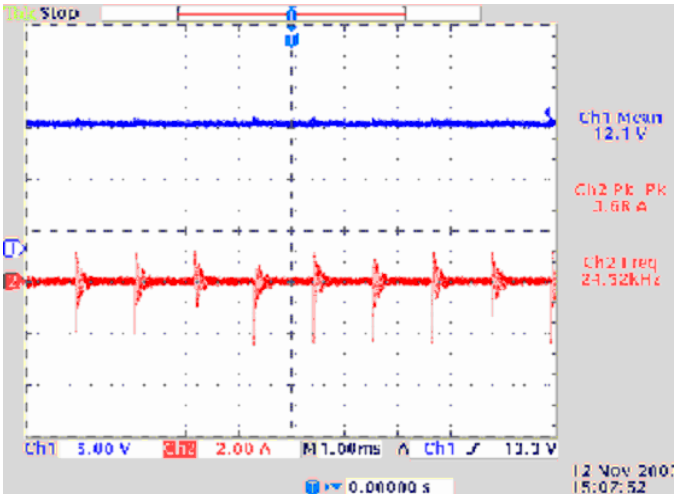

Fig. 6 The output voltage (Ch1, upper waveform) and main inductor current (Ch2, lower waveform) of the half-wave zero current switching quasi-resonant Buck converter controlled by SMC under no-load conditions. The switching frequency is 24.53 kHz, and SMC keeps the converter stable.

Fig. 7 shows the tank capacitor voltage waveform equal 44 volts (Ch1 PK-PK, upper waveform) and the tank inductor current waveform with a peak-to-peak value equal 3.56A (Ch2 PK-PK, lower waveform) under no load conditions.

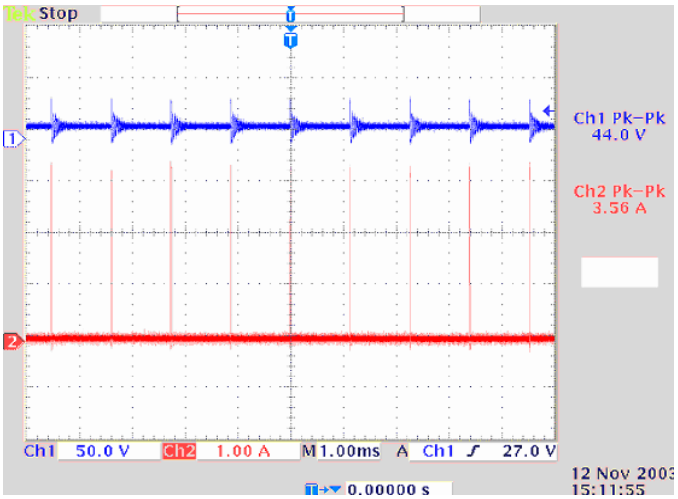

Fig. 7 The tank capacitor voltage waveform with 44volt (Ch1, upper waveform) and tank inductor current waveform = 3.56A (Ch2 peak-to-peak, lower waveform). The half-wave zero current switching quasi-resonant Buck converter is under no-load conditions.

The converter in this case is operating in discontinues conduction mode (DCM), and the SMC is functioning in a way that it keeps the converter stable with no load condition that is considered to be one of worst load variation cases.

Second case is when the load changes from its nominal value to full load (the full load value is 1Ω). Fig. 8 shows the output voltage waveform (upper waveform) and main tank inductor waveform (lower waveform). The mean output voltage is 12.3volts (Ch1 Mean) and a ripple voltage is equal to 3.6volts (Ch1 PK-PK). The peak-to-peak main inductor current is 3.12A (Ch2 PK-PK), while the switching frequency of the converter under full load is 48.22 kHz (Ch2 Freq).

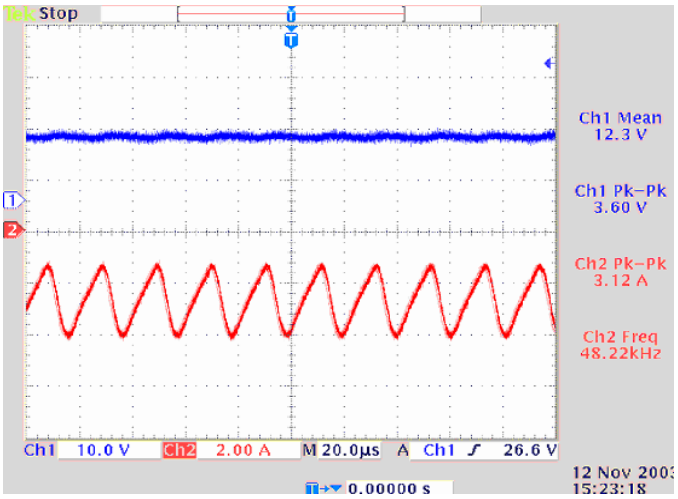

Fig. 8 The output voltage waveform (upper waveform) and main inductor current waveform (lower waveform) of the half-wave zero current switching quasi-resonant Buck converter controlled by SMC under full-load condition. The converter is stable but high output voltage ripple occurs.

Fig.9 shows the tank capacitor voltage waveform and tank inductor current waveform under full–load condition. The peak tank capacitor voltage is 58volts (Ch1, upper waveform), while the peak-to peak tank inductor current waveform is 8.9 A (Ch2 PK-PK, lower waveform). It can be said from Fig. 8 and Fig. 9 that although the converter is working under full load, the converter is still stable and SMC has an efficient influence against disturbances

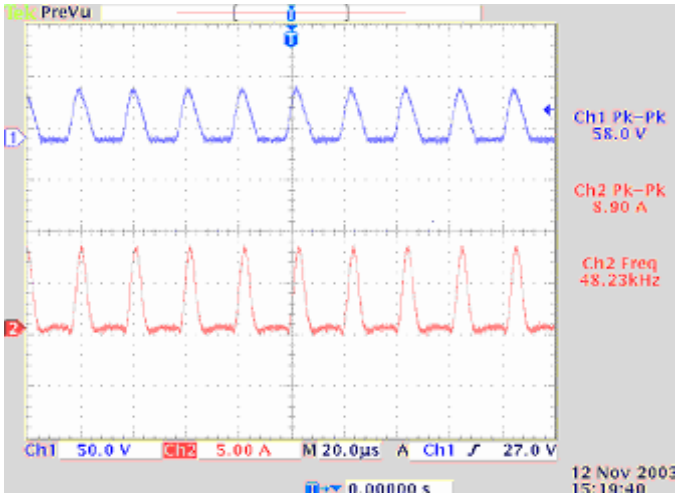

Fig. 9 The tank capacitor voltage waveform (Ch1, upper waveform) and tank inductor current waveform (Ch2, lower waveform) of the half-wave zero current switching quasi-resonant Buck converter controlled by SMC under full-load condition.

III. Conclusions

Sliding mode control (SMC) was implemented in a half-wave zero current switching quasi-resonant Buck converter. The reason behind the selection of SMC to this kind of converter was that: first, many researches studied theoretically the implementation of SMC to power supply and proved that it is an efficient control technique to switch mode power supply. Second, SMC is not operating at a constant switching frequency and resonant converters have a highly nonlinear and time-varying nature. Any change in operating conditions leads to significant changes in system dynamical model so that desired performance and even stability can be lost. Due to the reasons mentioned the paper linked the theoretical researches to a real prototype model.

SMC was implemented by dual control loops; an inner main inductor current loop represented by hysteresis control (non linear part) and an outer voltage loop represented by PI control (linear part).

A prototype of the controller with the converter was constructed and a detailed analysis performed to ascertain how the signals are generated by the operational amplifiers at each stage. The controller was designed using analog operational amplifiers.

The values of the main converter parameters were given and a mathematical analysis performed to select the tank inductor and tank capacitor values, where zero current switching occurs.

To prove that the prototype model is effective and that SMC can be implemented in real applications of a half-wave zero current switching quasi-resonant Buck converter, the circuit was tested in steady state and under load variations (no load and full load). Our analysis demonstrated that SMC gives acceptable results, not only from theoretical point of view but also in practical applications, and that SMC is an effective control tool for keeping the converter stable even in the worst cases (no load and full load).

References

[1] N. Vazquez, C. Hernandez, J. Alvarez, J Arau, “Sliding mode control for DC/DC converters: a new sliding surface’’ Industrial Electronics, 2003. ISIE '03. 2003 IEEE International Symposium on, Volume: 1, June9-11, 2003 Pages: 422 – 426.

[2] V. Utkin, J. Guldner, and J. Shi, “Sliding Mode Control in Electromechanical Systems’’, ISBN0-7484-0116-4(cased), Taylor & Francis 1999.

[3] K. Young, V. Utkin, U. Ozguner ,“Control Systems Technology’’, IEEE Transactions on ,Volume: 7 , Issue: 3 , May 1999 Pages:328 – 342

[4] M. Ahmed, M. Kuisma, K. Tolsa, P. Silventoinen, “ Implementing Sliding Mode Control for Buck Converter’’, Power Electronic specialist conference (PESC) Proc. Mexico June, 2003, pp 634-637, Vol. 2.

[5] M. Ahmed, M. Kuisma, P. Silventoinen, “Implementing Simple Procedure for Controlling Switch Mode Power Supply Using Sliding Mode Control as a Control Technique’’, XIII-th International Symposium on Electrical Apparatus and technologies (Siela). May 2003, pp 9-14, Vol. 1

[6] C. Chakraborty, S. Mukhopadhyay, “A novel compound type resonant rectifier topology’’ , The First IEEE International Workshop on Electronic Design, Test and Applications, 29- 31 Jan. 2002 Pages:428 – 430.

[7] A. Forsyth, G. War., V. Mollov, “Extended fundamental frequency analysis of the LCC resonant converter”, Power Electronics, IEEE Transactions on, Volume: 18, Issue: 6, Nov. 2003 Pages: 1286 – 1292.

[8] J. Lazar, R. Martinelli, “Steady-state analysis of the LLC series resonant converter”, Applied Power Electronics Conference and Exposition, 2001. APEC 2001. Sixteenth Annual IEEE , Volume: 2 , 4-8 March 2001 Pages:728 - 735 vol.2

[9] E. Lyshevski, “Resonant converters: nonlinear analysis and control” Industrial Electronics, IEEE Transactions on, Volume: 47, Issue: 4, Aug. 2000 Pages: 751 – 758.

[10] R. Erickson “Fundamentals of Power Electronics”, ISBN 0-412-08541-0, Chapman & Hall 1997.

[11] H. Bevrani, Y. Mitani; K. Tsuji; “Robust control design for a ZCS converter” ECON 02 , Industrial Electronics Society, IEEE 2002 28th Annual Conference , Volume: 1 , 5-8 Nov. 2002 Pages: 609 - 614 vol.1.

Publication P [9]

M. Ahmed, *Student member, IEE*, M. Kuisma, P. Silventoinen, J. Nerg, *Member, IEEE.* On the Design of Half-wave zero current switching DC/DC Buck converter.

M. Ahmed
Lappeenranta University of Technology
Department of Electrical Engineering
P.O.Box 20, LPR 53850, Finland
Email: mohammad.ahmed@lut.fi
Telephone: +358 (0) 407654841
Fax: +358 5 6216799

Mikko Kuisma
Lappeenranta University of Technology
Department of Electrical Engineering
P.O.Box 20, LPR 53850, Finland
Email: mikko.kuisma@lut.fi
Telephone: +358 (0) 400750403
Fax: +358 5 6216799

Janne.Nerg
Lappeenranta University of Technology
Department of Electrical Engineering
P.O.Box 20, LPR 53850, Finland
Email: Janne.Nerg@lut.fi
Telephone: +358 (0) 407749930
Fax: +358 5 6216799

Pertti Silventoinen
Lappeenranta University of Technology
Department of Electrical Engineering
P.O.Box 20, LPR 53850, Finland
Email: Pertti.Silventoinen@lut.fi
Telephone: +358 5 6216707
Fax: +358 5 6216799

ON THE DESIGN OF HALF-WAVE ZERO CURRENT SWITCING DC/DC BUCK CONVERTER

ABSTRACT

This paper focuses on the selection of the resonant tank component values of a half-wave zero current switching (HWZCS) DC/DC Buck converter. A general guideline for selecting the optimum tank component values is applied. To consider all the possible cases, a ± 10% tolerance from the optimum tank values is applied, which can be considered as the manufacture error tolerance. The relevance of the derived equations is confirmed with both simulation and prototype measurements, which ensures zero current switching (ZCS) in the defined boundary. The sliding mode control is implemented as a control method in controlling the HWZCS DC/DC Buck converter.

***Keyword*:** DC/DC power conversion, resonant power conversion, variable structure systems.

1. INTRODUCTION

Many authors have studied, analyzed and designed the half-wave zero current switching (HWZCS) DC/DC Buck converter, shown in Fig. 1, [1], [2], and [3]. These previous researches concluded that small tank inductor value (L_r) and small tank capacitor value (C_r) should be used in the converter without defining a clear algorithm what exactly these values should be and what effects these values have on the converter behavior.

This paper focuses on a mathematical algorithm that defines a range of L_r and C_r, where zero current switching (ZCS) occurs and selects the optimal L_r and C_r values in the design of a HWZCS DC/DC Buck converter. Two equations define the boundary of the L_r and C_r values, which assures ZCS.

Simulation and prototype results are obtained for the tank voltage and current waveforms. In both cases and to prove the analysis, values for L_r and C_r are taken in the defined range. Also ± 10% deviation from the selected L_r and C_r values, which is considered to be the error tolerance, is taken.

Values for L_r and C_r outside the defined range are taken and the results show that ZCS does note occur with these values.

This algorithm can be applied for any HWZCS DC/DC Buck converter that operates in: a defined input voltage range, defined output power range and defined maximum switching frequency.

Previous researches proved that sliding mode control (SMC) is a suitable control method for nonlinear systems like switched mode power supplies, and is not sensitive to component variations; furthermore SMC is less affected by disturbances compared to other control techniques[4], [5], [6], and [7].

Since HWZCS DC/DC Buck converter is parameter sensitive, i.e. a change in C_r and L_r can cause the converter not to operate in ZCS, therefore SMC is selected as a control method in this research work.

A simplified circuit diagram of the prototype for the converter with SMC is shown in Fig. 1, while Fig. 2 shows the prototype constructed.

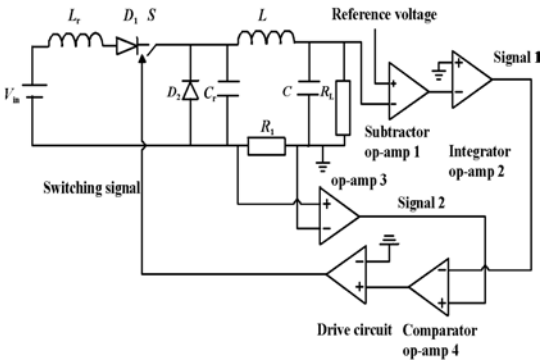

Fig. 1. Simplified prototype circuits of the HWZCS DC/DC converter with PI and current hysteresis control, the combined loops perform SMC. A gate drive circuit is used to provide isolation to the switch.

Fig. 2. The prototype of the HWZCS DC/DC Buck converter with the SMC constructed in the Laboratory of Applied Electronics at Lappeenranta University of Technology (Finland).

2. CIRCUIT DESIGN AND ANALYSIS

In this section two conditions, to obtain L_r and C_r values that ensure ZCS, are studied in detail.

Condition 1

The tank resonant frequency should be greater than the maximum switching frequency. This condition ensures that the tank inductor current reaches zero before the next switching period.

$$f_o > f_{s(max)}, \tag{1}$$

where $f_o = \frac{1}{2\pi\sqrt{L_r C_r}}$ denotes the tank resonant frequency, and $f_{s(max)}$ is the maximum switching frequency. Substituting f_o into equation (1) leads to:

$$L_r < \frac{1}{4(\pi)^2 (f_s)^2 C_r}. \tag{2}$$

Condition 2

The tank characteristic impedance must be low enough to provide large variations in the inductor current when resonant circuit is operating [8]:

$$\frac{V_{in}}{Z_o} > I_L, \tag{3}$$

where V_{in} is the DC input voltage, $Z_o = \sqrt{\frac{L_r}{C_r}}$ denotes the tank characteristic impedance, and $I_L = \frac{P_o}{V_o}$ is the average load current. Substituting Z_o, and I_L into equation (3) results in:

$$L_r < C_r (V_o)^2 \left(\frac{V_{in}}{P_o} \right)^2. \tag{4}$$

Substituting equation (4) into equation (2) leads to two solutions, one is not valid as the value of C_r converges to negative. The valid solution is given below:

$$C_r > \frac{P_o}{2\pi f_s V_{in} V_o}. \tag{5}$$

Equations (2) and (5) define the boundary of L_r and C_r values that ensure ZCS for a HWZCS DC/DC Buck converter. Substituting $I_L = \frac{P_o}{V_o}$ into equation (3) leads to the equation below:

$$Z_o < \frac{V_{in} V_o}{P_o}. \tag{6}$$

Equation (6) should be fulfilled to guarantee ZCS under all conditions and it can be seen that the worst case is a minimum input voltage $V_{in(min)}$ and a maximum output power $P_{o(max)}$.

From the equations given above, a design algorithm process to select the L_r and C_r values for any HWZCS DC/DC Buck converter can be obtained, and is given in Fig.3.

3. DESIGN EXAMPLE

A HWZCS DC/DC Buck converter has the parameters given in Table.1. Substituting the given values into equation 2, and equation 6 leads to

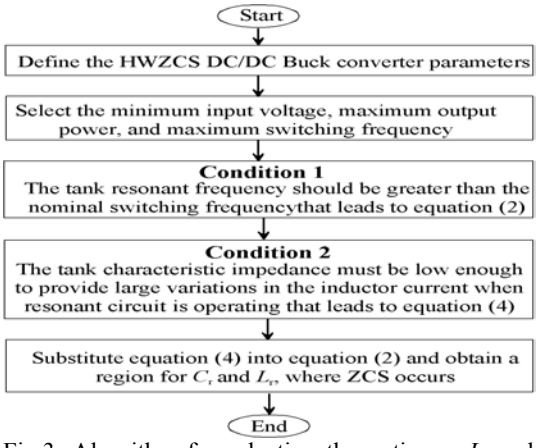

Fig.3. Algorithm for selecting the optimum L_r and C_r values in the design of a HWZCS DC/DC Buck converter.

Table.1 HWZCS DC/DC Buck Converter parameters. The output voltage ripple is < 2% .$L_{critical}$ and $C_{critical}$ can be measured [8]. The converter operates in CCM

V_{in}	16 V to 26 V
P_o	6 Watt to 30 watt
V_o	12 V_o
R_L	10 Ω
Output voltage ripple	< 2 %
$f_{s(max)}$	100 kHz
Circuit operation	CCM
$L_{critical}$	65 μH
$C_{critical}$	47 μF

$C_r > 248$ nF, and $L_r < 10\ \mu$H. (7)

Even in the defined region, a high L_r value may store a high amount of magnetic energy and therefore may damage the switch MOSFET. To avoid switch damaging, a varistor is added across the switch. The voltage dependent characteristic enables the varistor to protect the switch against high switch voltage spikes.

4. SIMULATION AND PROTOTYPE RESULTS

In order to prove the previous analysis $L_r = 3\ \mu$H and $C_r = 800$ nF are selected from equation (7) to be within the defined range, where ZCS occurs. Simulation and prototype results in Fig. 4 and Fig.5 respectively show to be compatible and that ZCS occurs in both models.

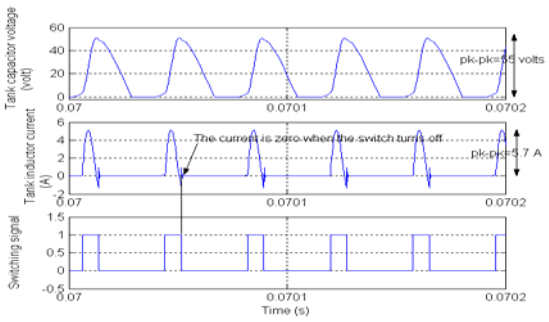

Fig. 4 Simulation results for tank capacitor voltage waveform with a peak value of 55 V, tank inductor current waveform with 5.8 A, and a switching signal with 30 kHz. It can be seen that ZCS occurs. $C_r = 800$ nF, and $L_r = 3\ \mu$H.

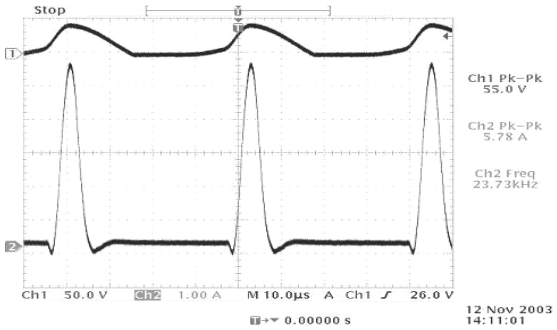

Fig.5 Prototype results, obtained from oscilloscope, for tank capacitor voltage waveform with a peak value of 55 V, tank inductor current waveform = 5.78 A, and f_s = 23.7 kHz. It can be seen that ZCS occurs. $C_r = 800$ nF, and $L_r = 3\ \mu$H.

In practice L_r and C_r values may deviate from their nominal values, which are considered to be the error tolerance. Fig.6 shows the simulated tank graphs when +10% changes are applied to L_r and C_r. Fig. 7 shows the same graphs when -10% changes are applied to L_r and C_r. The graphs guarantee that ZCS occurs even with these values. The obtained results coincide with the general algorithm in Fig.3.

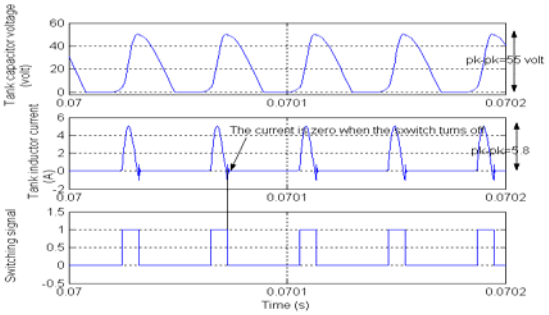

Fig. 6 Simulation results for tank capacitor voltage waveform, tank inductor current waveform, and a switching signal when C_r and L_r deviate +10% from the nominal value in Fig.4. It can be seen that ZCS occurs.

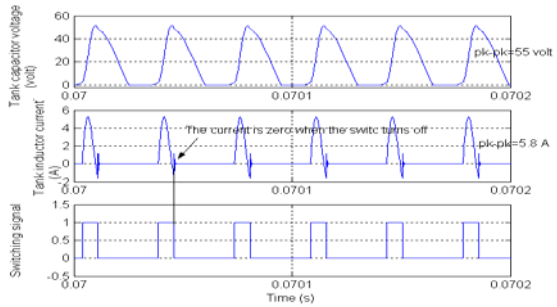

Fig. 7 Simulation results for tank capacitor voltage waveform, tank inductor current waveform, and a switching signal when C_r and L_r deviate -10% from the nominal value in Fig.4. It can be seen that ZCS occurs.

To analyze the effect of selecting L_r and C_r values outside the range defined in equation (7), a value of C_r = 50 nF is selected and keeping L_r = 3 μH. Fig.8 and Fig.9 show the simulation and prototype results respectively. It can be seen that ZCS does not occur anymore. This coincides with the previous statement that by selecting C_r outside the defined range ZCS will not occur.

The same thing can be said when selecting L_r outside the defined boundary and more results can be shown in the final paper.

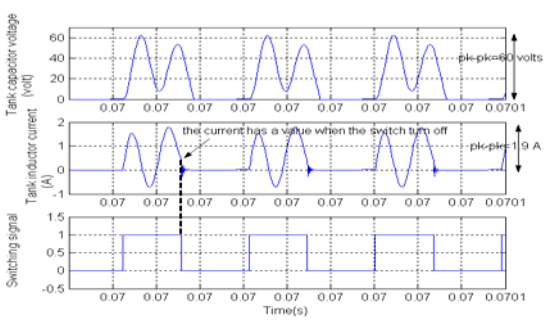

Fig. 8 Simulation results for tank capacitor voltage waveform with a peak value of 60 V, tank inductor current waveform with 1.9 A. It can be seen that the waveforms have oscillation and ZCS does not occur. C_r = 50 nF, and L_r = 3 μH. The switch turns off while the current is not in peak value.

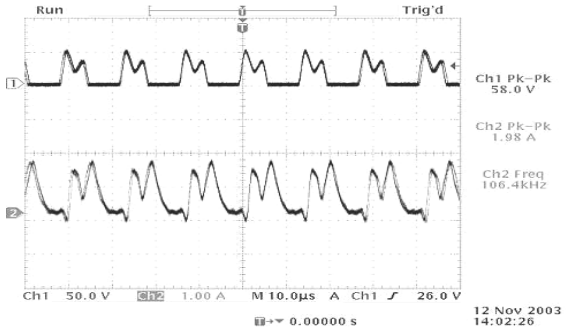

Fig. 9 Prototype results for tank capacitor voltage waveform with a peak value of 58 V, tank inductor current waveform with 1.98 A, and a switching signal with 106 kHz. It can be seen that the waveforms have oscillation and ZCS does not occur. C_r = 50 nF, and L_r = 3 μH.

5. CONCLUSIONS

This paper simplified a mathematical procedure obtained from previous studies to define the range of L_r and C_r values for a HWZCS DC/DC Buck converter, where ZCS occurs. Two mathematical conditions were applied and a range for C_r and L_r values were obtained. Values for C_r and L_r were selected within the range obtained. The analysis was proved by simulation and prototype results. To ensure the investigation for worst case, ± 10% deviation from the selected C_r and L_r values were taken. The results proved that ZCS occur even if the selected values have deviation from the nominal values. C_r and L_r were also selected outside the defined boundary and results showed that ZCS does not occur. The algorithm gives a good guideline for designers, when selecting C_r and L_r, provided that the converter operates in defined input voltage range, output power range, and desired maximum switching frequency.

SMC was selected to control the converter and the reason for selecting SMC as a control method was explained.

REFRENCES

[1] J. Chen, A. Ioinovici. “Switched-capacitor-based quasi-resonant converter operating at constant switching frequency’’. International Telecommunications Energy Conference. INTELEC ‘95, 29 Oct.-1 Nov. 1995 Page(s): 315 –321.

[2] H. Bevrani, Y. Mitani; K. Tsuji. “Robust control design for a ZCS converter” ECON 02, Industrial Electronics Society, IEEE 2002 28th Annual Conference, Volume: 1, 5-8 Nov. 2002 Pages: 609 - 614 vol.1.

[3] R. Lin, F. Lee. “Novel zero-current-switching-zero-voltage-switching converters”. Proceedings of the IEEE Power Electronics Specialists Conference, 1996. PESC '96 Record, 27thAnnual IEEE, Volume: 1, 23-27 June 1996 Pages: 438 - 442 vol.1.

[4] M. Ahmed, M. Kuisma, K. Tolsa, P. Silventoinen, “Implementing Sliding Mode Control for Buck Converter’’ Proceedings of the IEEE Power Electronic specialist conference (PESC) Proc. Mexico June, 2003, pp 634-637, Vol. 2.

[5] M. Ahmed, M. Kuisma, P. Silventoinen, “Implementing Simple Procedure for Controlling Switch Mode Power Supply Using Sliding Mode Control as a Control Technique’’**,** XIII-th International Symposium on Electrical Apparatus and technologies (Siela). May 2003, pp 9-14, Vol. 1.

[6] V. Utkin, J. Guldner, and J. Shi, “Sliding Mode Control in Electromechanical Systems’’, ISBN0-7484-0116-4(cased), Taylor & Francis 1999.

[7] G. Spiazzi, P. Mattavelli, L. Rossetto, L. Malesani, "Application of Sliding Mode Control to Switch-Mode Power Supplies," Journal of Circuits, Systems and Computers(JCSC), Vol.5, No.3, September 1995, pp.337-354.

[8] Philip, T. 1998. Elements of Power Electronics. Oxford University press. ISBN 0-19-511701-8. 0-766 pages.

[9] W. Ho, M. Pong, “Power loss and efficiency analysis of quasi-resonant converters’’ Industrial Electronics, Control, and Instrumentation, 1993. Proceedings of the IEEE IECON 93, 15-19Nov.1993 Page(s): 842 -847 vol.2.

[10] N. Pereira, B. Borges, V. Anunciada, “Supra resonant fixed frequency full bridge DC-DC resonant converter with reduced switching losses’’ Telecommunications Energy Conference, 1996. INTELEC '96, 18th International, 6-10 Oct. 1996.

[11] C. Chakraborty, S. Mukhopadhyay, “A novel compound type resonant rectifier topology’’, The First IEEE International Workshop on Electronic Design, Test and Applications, 29-31 Jan. 2002 Pages:428 – 430.